GOODYEAR AEROSPACE
CORPORATION

AKRON 15, OHIO

Copy No. ____

STATE-OF-THE-ART STUDY FOR HIGH-SPEED DECELERATION AND STABILIZATION DEVICES

GER-12616 10 September 1966

William C. Alexander Richard A. Lau

Goodyear Aerospace Corporation, Akron, Ohio

for

National Aeronautics and Space Administration

Washington, D. C.

ABSTRACT

Documented aerodynamic deployable decelerator performance data above Mach 1.0 is presented. The state of the art of drag and stability characteristics for reentry and recovery applications is defined for a wide range of decelerator configurations. Structural and material data and other design information also are presented. Emphasis is given to presentation of basic aero, thermal, and structural design data, which points out basic problem areas and voids in existing technology.

The basic problems and voids include supersonic "buzzing" of towed porous decelerators in the wake of the forebody, the complete lack of dynamic stability data, and the general lack of aerothermal data at speeds above Mach 5.

SUMMARY

Available documented supersonic and hypersonic data (thermodynamic, structures, and materials) have been surveyed and summarized to indicate the state of the art of deceleration and stabilization devices.

Supersonic parachutes that have been successfully flight tested indicate a performance limit of approximately Mach 3. Although parachutes have performed between Mach 3 and 6 in isolated tests, which demonstrates feasibility, the conclusion cannot be made that they can perform satisfactorily throughout the supersonic Mach number range during deceleration. During wind tunnel tests, all parachutes experienced some canopy breathing, even behind payload bodies of revolution, while operating above Mach 2.5. Until a basic aerodynamic supersonic inlet problem, which is further complicated by the payload complex wake, is solved, the possibility of successful parachute operation at high Mach numbers (above supersonic speed) appears remote.

Inflatable decelerators up to five feet in diameter have been successfully flight tested up to approximately Mach 3.8 and dynamic pressures up to approximately 200 psf. Metal cloth decelerators have been tested in the wind tunnel up to Mach 10 and fabric models up to Mach 6. These nonporous, nearly gas-tight towed decelerators were found to be the least sensitive to a forebody wake and therefore performed in a stable and satisfactory manner.

Materials development programs have resulted in finding lighter weight nylon and Nomex woven cloths and webbing for a given structural strength. Flexible coatings also have been developed that not only protect the decelerators from heat but also make a decelerator gas tight at a minimum of weight. Woven stranded wire metal also has been developed. Large gaps exist in the operational temperature ranges due to the lack of proved materials. Higher-strength, more flexible cloths are still needed as well as higher temperature impermeable coatings.

There is very little experimental or analytical aerodynamic, thermodynamic, or structural data available in the supersonic and hypersonic speed range. A general lack of analytical methods exists to describe basic phenomena, including lack of aerodynamic data over a range of Reynolds numbers; a complete lack of quantitative experimental dynamic stability data; and a basic lack of understanding of a forebody wake flow when influenced by a towed decelerator.

FOREWORD

This report was prepared by Goodyear Aerospace Corporation, Akron, Ohio, under Contract NASW-1288 and under the cognizance of J. E. Greene, Office of Advanced Research and Technology (OART), NASA Headquarters, Washington, D. C. J. T. McShera, Jr., Full Scale Divsion, NASA Langley Station, Hampton, Va., served as contract technical monitor.

Project engineer was W. C. Alexander; assistant project engineer was R. A. Lau - both from Goodyear Aerospace. Other contributing personnel from Goodyear Aerospace were F. R. Nebiker, manager, Recovery Systems Engineering; W. V. Arnold, assistant manager, Recovery Systems Engineering; F. Bloetscher, consultant; I. M. Jaremenko, aerodynamic wakes; H. H. Sheeter, aerodynamic stability; W. W. Sowa, thermodynamics; J. F. Werner, structures; and P. F. Myers, materials. The data gathering cut-off date was 1 April 1966.

TABLE OF CONTENTS

LIST OF ILLUSTRATIONS

LIST OF TABLES

SECTION I - INTRODUCTION

1. GENERAL

a. Program Objective

Under Contract NASW-1288 with the National Aeronautics and Space Administration, Washington, D.C., Goodyear Aerospace Corporation has conducted a study program of deployable aerodynamic decelerators for re-entry and recovery applications from Mach 1 to Mach 25. The objective of this program was to survey and summarize available documented supersonic and hypersonic analytical and experimental data to determine the latest state of the art of deceleration and stabilization devices. The findings of this study, presented in this report, summarize the status of high-speed recovery techniques and supplement Reference 1 and other handbook-type reports.

b. Background and Problem Statement

With the advent of the space age, and the general need to provide for successful entry, re-entry, and descent into the atmosphere of the earth and other planets, new and efficient (lightweight, low cost) methods of deceleration and stabilization must be developed to recover payloads such as manned space capsules, emergency escape capsules, instrument data packages, rocket boosters, and nose cones. Before such devices can be developed, additional basic and applied research will be required. This study program was conducted to provide data for an overall "in-house" NASA evaluation study to determine the state of the art of supersonic decelerator systems.

c. Scope and Constraints

The study was performed so system design criteria could be established

for providing supplemental drag area to best meet the needs of the following supersonic-sample, general-recovery applications:

1. Payload stabilization and deceleration to conditions necessary for a satisfactory deployment of a final-stage landing device (conventional parachute, gliding parachute, inflatable wings, paragliders)
2. Payload re-entry to minimize temperature and deceleration environment
3. Initial high-speed stabilization of spacecraft or booster, or both
4. Emergency escape from any flight vehicle (aircraft, space capsule)
5. Highly stable low supersonic descent of instrumented payloads operating at a high altitude in the atmosphere (high-altitude air sampling, infrared payload tracking)

The performance data for these recovery applications include aerodynamic drag and stability characteristics for both steady and unsteady conditions; performance data for both free-stream operations and operations in the wake of a forebody; structural and material design-support data; and basic aerothermodynamic design parameters and their effect on the stowage, deployment, and operation of the decelerator. The study-spectrum limits were as follows:

1. Mach number - 1 to 25 (emphasis on Mach 1.5 to Mach 10)
2. Altitude - below 600,000 ft (emphasis below 200,000 ft)
3. Temperature - below 3000 F (emphasis below 1000 F)

d. Description of Search

The program was initiated with a library search, during which a bibliography of applicable documents (see Appendix A) was obtained from:

1. DDC (Defense Documentation Center)
2. NASA STAR
3. Goodyear Aerospace Library

From these bibliographies applicable reports and other documents were ordered, and their abstracts, results, and conclusions were reviewed. The detailed data presented in this report are based on the list of references on pages 195 through 201. The bibliography of this report groups related publications according to the issuing or authorizing government agencies and other sources.

e. Historical Summary

The concept of aerodynamic decelerators in the form of parachutes dates back at least to DaVinci and probably earlier. Until the balloon flights of the nineteenth century and the heavier-than-air flights of the twentieth, parachutes were of little more than scientific interest. World War I demonstrated their practicality, as had the earlier balloon flights, for safe descent from a disabled aircraft. At that time, development headed toward the modern small packaged canopy and attaching body harness from the noncollapsible canopies and trapeze or open-basket containers of the balloonists. With packaging came the complication of deployment, and various methods were utilized - static lines, pilot chutes, etc. From 1945 to 1955, higher speed (transonic and low supersonic) and higher altitude (up to 100,000 ft) military applications arose.

Between 1955 and 1960, the space-age arrived, bringing with it still higher speed (high supersonic and hypersonic) and higher altitude (orbital and superorbital) applications. The new applications consisted of recovering all types of payloads over a broader flight spectrum. Because of these new recovery requirements, supersonic tests were

conducted; the initial formal documented results of these tests became available about 1960. Goodyear Aerospace Corporation's search revealed that, since 1960, the number and type of experimental tests were greatly increased, and most of the available experimental data presented in this report were generated during this period.

SECTION II - STATE OF THE ART OF AERODYNAMIC DEPLOYABLE DECELERATORS

1. GENERAL

This section provides a summary and analysis of available data on aerodynamic decelerators that are deployable in the supersonic and hypersonic speed ranges. The various decelerators are categorized into aerodynamic shape configurations. Appropriate information on design, aerodynamic performance, structures and materials, and logistics sequencing is presented.

2. DESIGN AND PERFORMANCE REQUIREMENTS

The scope and limitations of deceleration devices included in this study in terms of the flight regime are presented in Figure 1. This figure depicts the desired flight-study spectrum of altitude versus Mach number for general recovery-system applications. The cross-hatched area shows the main emphasis of this study.

Since the main function of a deployable decelerator is to generate a specific amount of aerodynamic drag for deceleration and stabilization with a minimum of weight and bulk, the key design goal is to obtain a maximum value of the square feet of drag area per pound of weight. To predict that a given configuration (a given geometric shape or a composite arrangement of various shapes) will obtain certain values of drag area and hence will perform in a prescribed manner, the effects of high-speed aerothermodynamics and space mechanics performance parameters must be known and understood.

The deployment of a decelerator during a re-entry or recovery operation leads to an increase in the drag forces acting on the vehicle system. As

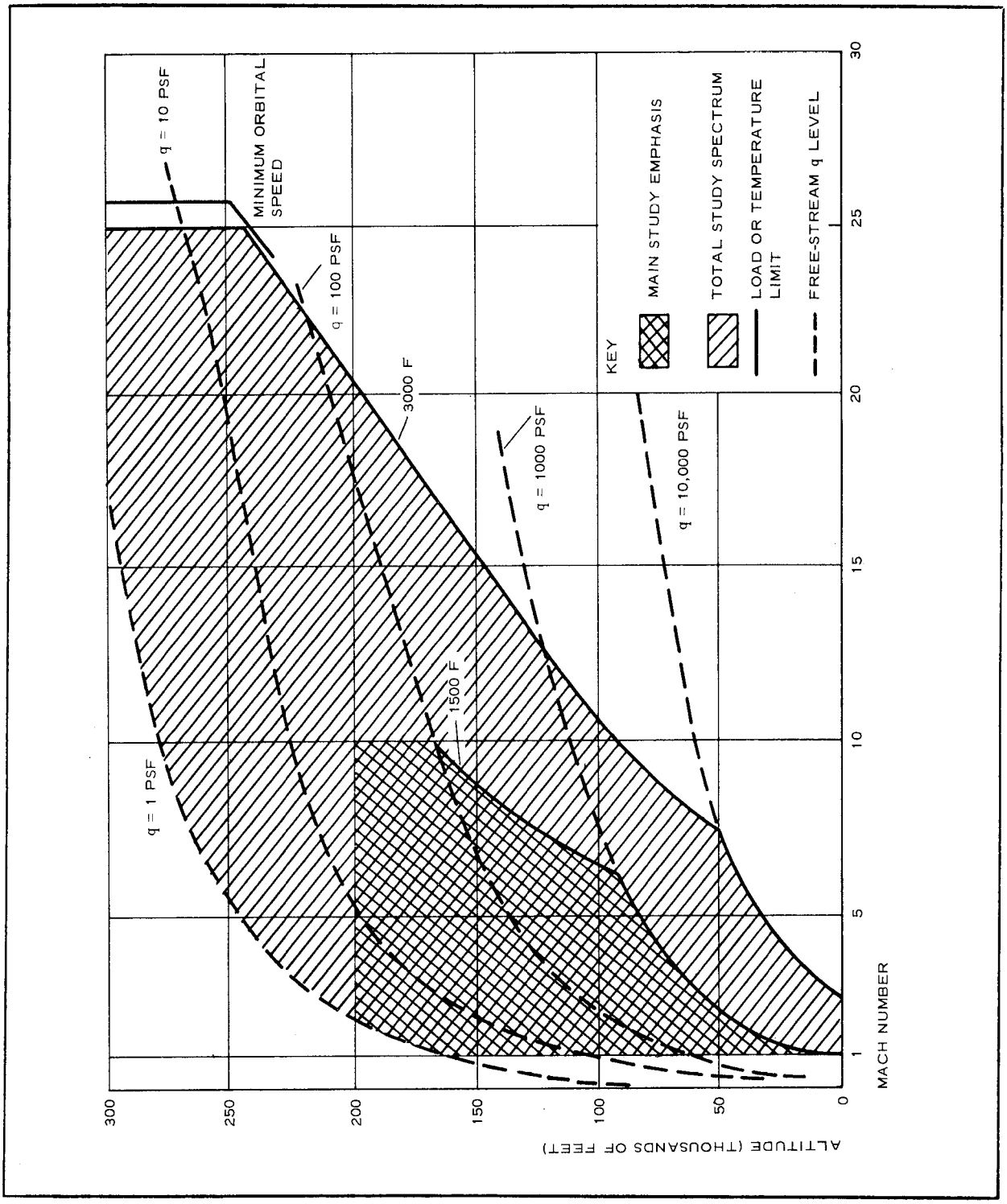

Figure 1 - Study Spectrum

the drag forces increase and the deceleration rate becomes more acute, the possibility of aerodynamically heating the decelerator also increases. The effect of this aerodynamic heating can be seen more readily by referring to the thermal-performance parameters in Figure 2. Since the major emphasis in this study was on an altitude range from sea level to about 200,000 ft and a Mach range from 1.5 to 10, the parameters in Figure 2 cover only this range. In this figure, lines of constant dynamic pressure and adiabatic wall temperature for turbulent flow are plotted as a function of altitude and Mach number. The lines form boundary conditions for material strength requirements, while the lines of adiabatic wall temperature foretell approximate expectations of material temperature. Thus, decelerators deployed in the Mach 1 to Mach 3 flight regime can sustain a temperature rise of up to 700 F as the deployment Mach number approaches about 3, while those deployed above Mach 3 can expect a temperature rise to above 700 F. Lowering the deployment altitude or increasing the dynamic pressure decreases the time over which deceleration occurs, and thus hastens the temperature rise of the decelerator material toward the appropriate adiabatic wall-temperature line.

3. DESIGN CONCEPTS

To meet the requirements of space-age recovery, various deployable decelerator designs have been proposed, each of which suggests some potential competitive advantage or advantages. Various programs have been conducted to advance the state of the art, and valuable data have been obtained. Some applicable data, especially for configurations of a basic geometrical shape, have been obtained from programs with nonrelated objectives.

By definition, deployable decelerators are devices that are packageable and are capable of being extended or inflated to an enlarged blunt shape. From this definition and based on the degree of completeness of the experimental investigations previously conducted, the main decelerator

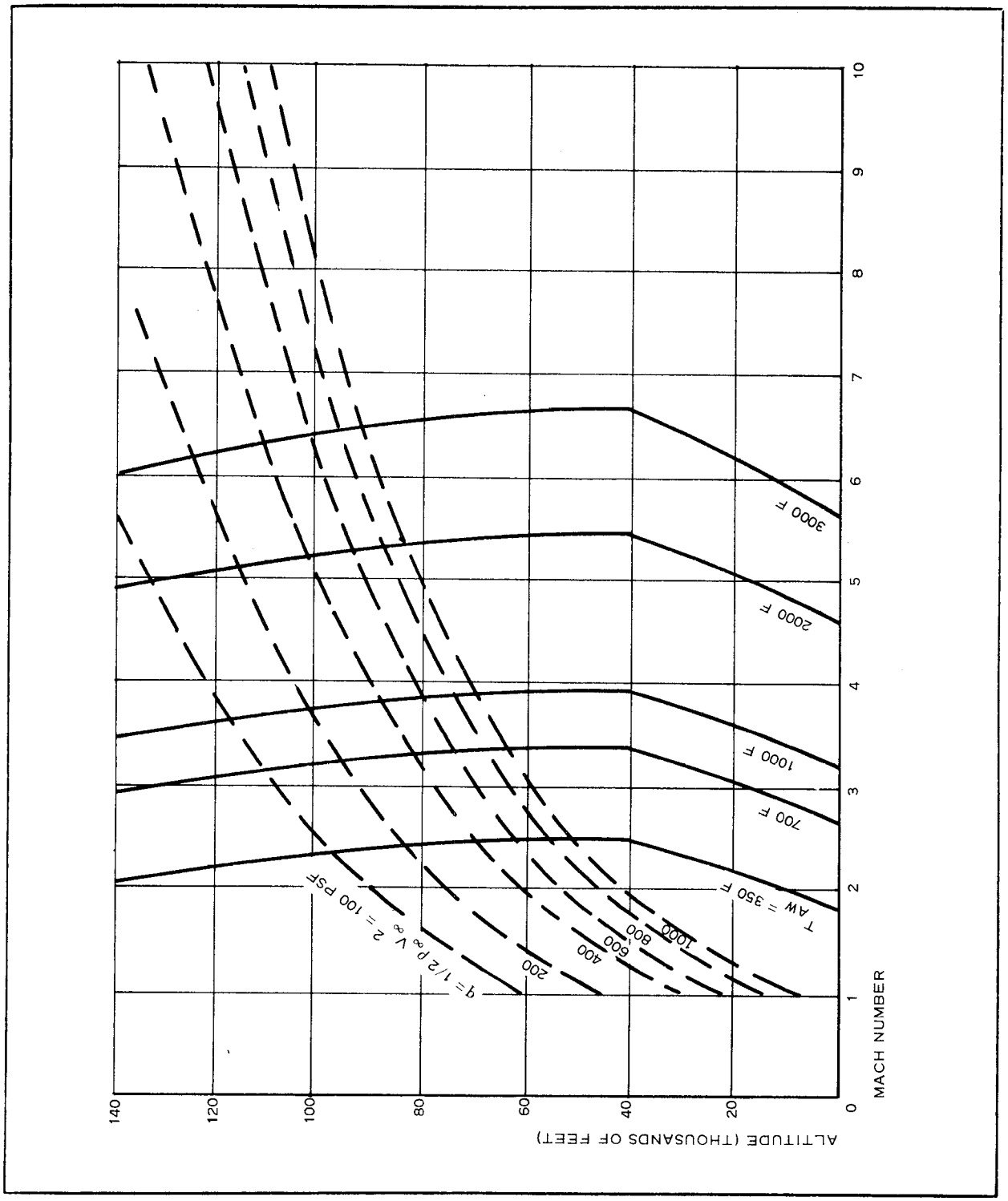

Figure 2 - Thermal Performance Spectrum

candidates are shown in Figure 3. For purposes of terminology, the types of decelerator configurations are further broken down as follows:

1. Two body (towed)
   a. Nonporous
      Forced inflation
      Ram-air inflation
   b. Porous
      Designed for supersonic operation
      Subsonic modified
2. Single body (attached) - nonporous
   a. Basic single shape
   b. Composite shape

In the discussion that follows, the various configuration construction details are presented. The apparent performance and design advantages of each concept in terms of why they are likely decelerator candidates are given.

Of the ten concepts, presented in Figure 3, the cone, sphere, Ballute,[a] and flared skirt are all nonporous types that either can be attached to or towed by a payload. These four concepts have certain desirable performance characteristics in common:

1. They are blunt-body, high drag-producing shapes.
2. They can be inflated to a close, coupled position behind the payload.
3. Since they are nonporous, these decelerators act as pressure vessels and remain fairly rigid when inflated.

In the past the cone, sphere, and flared skirt have been inflated with compressed air or nitrogen. Ballutes have been inflated either with

[a]TM, Goodyear Aerospace Corporation, Akron, Ohio.

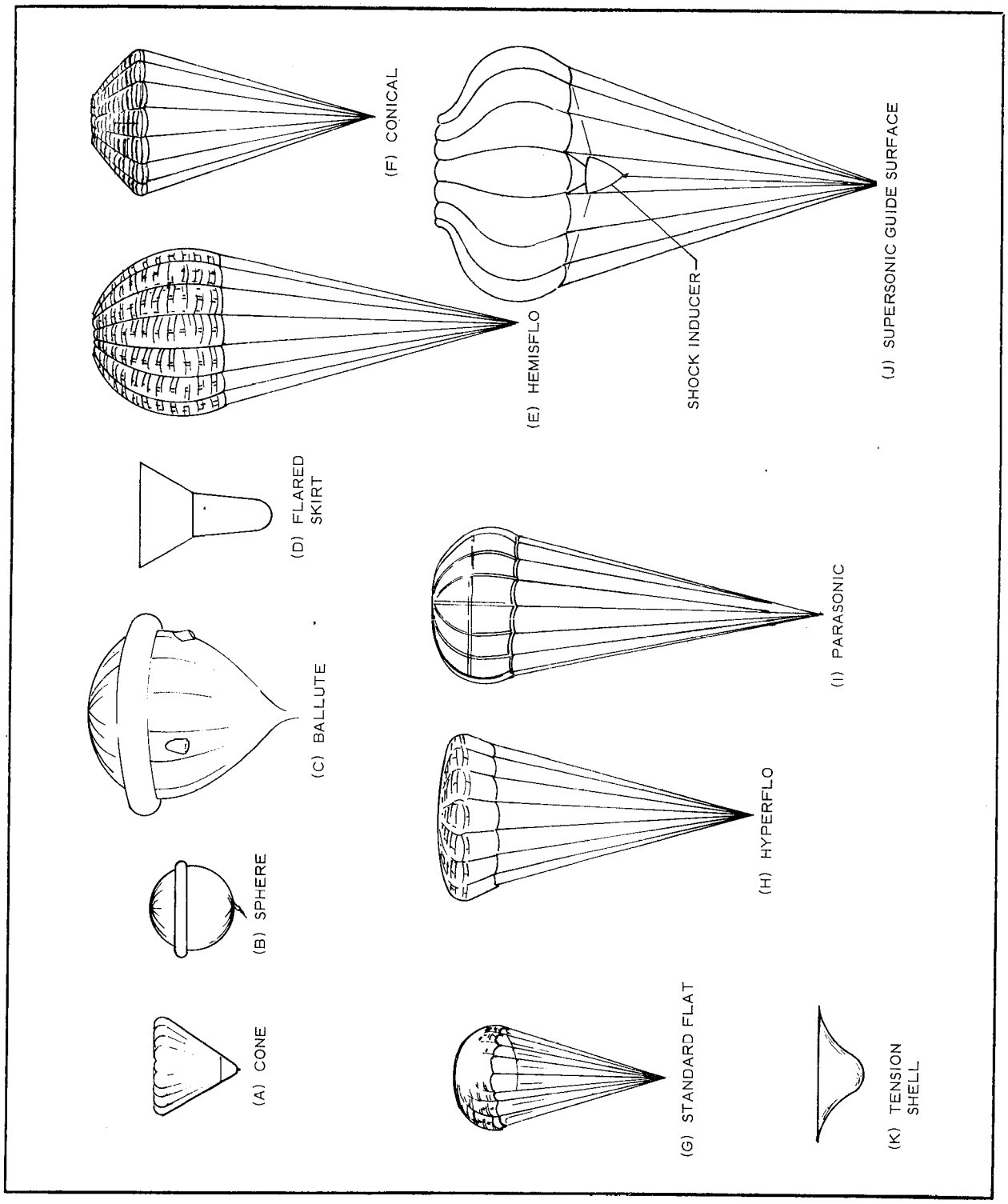

Figure 3 - Decelerator Configurations

compressed gas or with ram-air. Note the ram-air inlets on the Ballute in Figure 3.

The sphere and Ballute can be made from fabric gores similar to those on the parachute. These gores not only can be sewn together to form the decelerator shape but also can be cemented or welded together, depending on the type of fabric required.

The above-mentioned concepts are coated with various elastomers to obtain gas-tight integrity. In addition, the coating protects the cloth and is less susceptible to temperature, water, and abrasion. The remaining concepts shown in Figure 3 are the porous-type decelerators; namely, parachutes. In all cases, the canopy geometric openness - that is, the porosity - is the prime factor for satisfactory performance (a stable, high drag-producing canopy).

The three ribbon parachutes are named for their shapes: standard flat, conical, and hemisflo. All three chutes are made from fabric gores. Each gore is composed of a given amount of horizontal and vertical ribbons plus radial webs. As the name implies, a standard flat ribbon canopy is made from a number of triangular gores sewn together into a circular constructed shape and is capable of lying "flat" on a work table. The conical ribbon chute is similar to the standard flat with triangular gores, except that a few gores are excluded and thus a constructed shape results in a frustrum of the cone. The hemisflo type is made from "shaped" gores, and the resulting inflated shape is a near hemisphere. The advantage of the conical over the standard flat is that the same C_D's are attainable with less canopy fabric. The advantage of the hemisflo over the standard flat or the conical is that the portion of the canopy ahead of the canopy equator acts as an extended skirt. Based on test results in general, canopies with skirts have less coning instability. These parachutes were designed originally for subsonic operation and were limited in performance when carried to supersonic speeds.

The final three parachutes, the Hyperflo,[a] the Parasonic,[b] and the Supersonic Guide Surface,[c] are configurations designed for supersonic operation. All of these types in essence have extended skirts. These skirts are essentially nonporous to aid the inflation retention capability. The Hyperflo has a constructed flat top called the canopy roof. This roof can be made either from ribbons or from a mesh or net type cloth structure. With shaped gores, the Parasonic is an evolved canopy configuration that most nearly meets the membrane shape requirements of an isotensoid design from predicted supersonic pressure loadings. Coating of the canopy mesh-type crown provides for not only the proper choked flow but also for thermal protection. The Supersonic Guide Surface configuration is shaped like a supersonic-subsonic diffuser (flow converter). In addition to this convergent, divergent shape canopy (which has a large vent in the crown), a small conical body is suspended ahead of the canopy lip to induce the formation of an oblique shock.

Tables I through X summarize the known pertinent documented analytical and experimental investigations conducted on the candidate configurations. The information is presented with the report (or test) dates in chronologically descending order to indicate the evolution of the various configurations and to suggest the present status of each. The tabulated historical information indicates the type of documented data that is available.

Figure 4 depicts the miscellaneous configurations. These concepts are labeled miscellaneous since little or no experimental programs have been conducted. While some theoretical work has been done, the majority of these concepts are at best only ideas.

Concepts of interest are listed in the following tables:

---

[a] Registered, U.S. Patent Office, Cook Electric Co., Chicago, Illinois.

[b] TM, Goodyear Aerospace Corporation, Akron, Ohio.

[c] Registered, U.S. Patent Office, University of Minnesota, Minneapolis, Minn.

TABLE I - R AND D - CONE DECELERATORS IN FREE STREAM

Reference	Report date	Cone configuration: Semiapex angle, θ_s (deg)	Cone configuration: Nose	Theory	Experimental Mach no.	Type of data obtained: Pressure	Type of data obtained: Force and moment	Type of data obtained: Stability	Purpose and remarks
SC-R-64-1311 (Ref 2)	1/65	5 to 50	Sharp and blunt	Newtonian	1 to 6.9	None	C_A, C_N, C_M	Static	Obtain experimental results and compare with theory; determine effects of bluntness
JPL-TR-32-677 (Ref 3)	11/64	10 to 60	Sharp and blunt	Modified Newtonian	1 to 5, 9	None	C_D	Static	Obtain experimental results and compare with theory; determine effects of bluntness
NASA TN D-2283 (Ref 4)	5/64	5 to 50	Sharp	Newtonian	6.8	None	C_A, C_N, C_M	Static	Obtain experimental results and compare with theory
NASA TN D-840 (Ref 5)	6/61	6 to 50	Sharp	Newtonian	6.8	None	C_A, C_N, C_M	Static	Obtain experimental results and compare with theory
MSFC-MTP-AERO-61.38 (Ref 6)	5/61	10, 13.3, 25, 50	Sharp (1) and blunt (2)	Newtonian	0.5 to 4.4	None	C_A, C_N, C_M	Static	Obtain experimental results and compare with theory
U of C: HE-150-190 (Ref 7)	1961	9 and 45	Sharp	None	6	None	C_A, C_N, C_M	Static and dynamic	Determine experimental hypersonic force and stability data
NAA/MD-59-453 (Ref 8)	1960	0 to 35	Sharp	None	Transonic	None	C_D	None	Obtain experimental drag and pressure data
NASA TN D-176 (Ref 9)	1959	0 to 90	Sharp	Newtonian	None	C_P	C_A, C_N, C_M	None	Presentation of theoretical aerodynamic data
Hoerner (Ref 10)	1958	All	Sharp	None	1 to 10	C_P	C_D	None	Presentation of drag and pressure data
NACA TN 3788 (Ref 11)	1956	30 to 40	Sharp	Potential, Newtonian	None	C_P	C_A, C_N, C_M	Static and dynamic	Development of analytical techniques; presentation of the indicated data; and comparison of theoretical methods
Convair: ZA-7-017 (Ref 12)	1955	20 to 40	Sharp and blunt	Modified Newtonian	Subsonic, 1 to 4	None	C_D	Static	Development of theory and comparison with experimental results
J. Aeron. Sci., Vol 19 (Ref 13)	1952		Sharp	Second-order theory (revised)	None	None	None	None	Development of theory
J. Math and Phys., Vol 30 (Ref 14)	1952		Sharp	Second-order theory	None	None	None	None	Development of theory
NACA Report 1081 (Ref 15)	1952		Sharp	Second-order theory	None	None	None	None	Development of theory
NACA Report 1045 (Ref 16)	1951		Sharp	Corrected first order	6.86 and 16	C_P	None	None	Development of theory and comparison of theoretical and experimental results
J. Aeron. Sci., Vol 18 (Ref 17)	1951		Sharp	Second-order theory	None	C_P	None	None	Development of theory and tabulation of results
MIT TR-5 (Ref 18)	1949		Sharp	Stone's and second order	None	None	None	None	Development of theory and tabulation of results (θ_s = 5 to 25 deg)
Rand T-8 (Ref 19)	7/48		Sharp	Stone's and first order	None	None	None	None	Development of theory
J. Math and Phys., Vol 27 (Ref 20)	1948		Sharp	Stone's second order (revised)	None	None	None	None	Development of theory
MIT TR-3 (Ref 21)	1947		Sharp	Stone's second order	None	None	None	None	Development of theory and tabulation of results (θ_s = 5 to 50 deg)
MIT TR-1 (Ref 22)	1947		Sharp	Stone's second order	None	Pressure	None	None	Development of theory and tabulation of results (θ_s = 5 to 50 deg)

TABLE II - R AND D - TOWED-CONE DECELERATORS

Reference	Report date	Configuration				Test Mach number (wind-tunnel) data	Type of data obtained			Test purpose and remarks
		θ_s	x/d	D/d	Forebody		Pressure	Force and moment	Stability	
RTD-TDR-63-4023 (Ref 23)	1/65	45	2, 4, 7.89	1, 2	Ogive cylinder (F.R. = 4.5)	0.85 to .2	C_{P_B}, C_{P_o}, C_{P_L} (forebody with and without decelerator)	C_D	None	Obtain experimental aerodynamic data; solid sting-mounted model used
RTD-TDR-63-4242 (Ref 24)	12/64	45	2 to 8	1, 2	Hemisphere-cylinder, flare (F.R. = 1.06)	0.85 to .25	Same	C_D	None	Obtain experimental aerodynamic data; solid sting-mounted model used
RTD-TDR-63-4242		45	4 to 8	1, 2	Ogive cylinder (F.R. = 4.5)	4.35	None	C_D	None	Obtain experimental aerodynamic data; solid sting-mounted model used
RTD-TDR-63-4246 (Ref 25)	12/64	45	2 to 8	1, 2	Hemisphere-cylinder, flare (F.R. = 1.06)	0.85 to .25	C_{P_B}, C_{P_o} (decelerator and forebody)	C_D	None	Obtain experimental aerodynamic data; solid sting-mounted model used
RTD-TDR-63-4226		45	4 to 8	1, 2	Ogive cylinder (F.R. = 4.5)	4.35	C_{P_B}, C_{P_o} (decelerator and forebody)	C_D	None	Obtain experimental aerodynamic data; solid sting-mounted model used
NASA TN D-1789 (Ref 26)	4/63	40	2 to 15.9	2.05	Cone-cylinder (F.R. = 10.7)	2 to 4.65	None	C_D	*	Obtain experimental aerodynamic data for solid cones on flexible towlines; three of four cones had disk extensions
NASA TN D-1789		40	2 to 15	0.89	Cone-cylinder, flare (F.R. = 4.34)	2 to 4.65	None	C_D	*	
ASD-TDR-62-702 Part II (Ref 27)	12/62	40	1 to 13	2.92	Cone-cylinder (F.R. = 4.5)	2 to 4.65	None	C_D	*	Obtain experimental aerodynamic data using an inflatable fabric Airmat cone on a flexible towline
NASA TN D-994 (Ref 28)	12/61	30, 35 40, 45	2 to 7	0.89	Cone-cylinder, flare (F.R. = 4.34)	2.3, 2.96, 3.83, 4.65	None	C_D	*	Obtain experimental aerodynamic data using a sting-mounted (at base) decelerator
NASA TN D-994		30	2 to 6	0.86	Biconical (F.R. = 4.75)	1.57, 2, 2.87	C_{P_B} (decelerator)	C_D	None	Obtain experimental aerodynamic data using a sting-mounted (at base) decelerator

*Visual coning observation

Preceding page blank

TABLE III - R AND D - SPHERE DECELERATORS IN FREE STREAM

Reference	Report date	Sphere diam. (in.)	Experimental parameters			Type of test	Type of data	Test purpose and remarks
			Mach no.	Knudson no.	Reynolds no.			
JPL-TR 34-160 (Ref 29)	6/61	1/16 to 1/2	3.8 to 4.3	0.25 to 0.107	50 to 1000	Wind tunnel	C_D	Obtain drag in low-density supersonic flow
Rand RM 2678 (Ref 30)	11/61	0.09 to 1.5	11 to 64.7	0.002 to 4	3×10^5 to 2×10^6	Hotshot tunnel	C_D	(Data in air and helium) to obtain drag at very high velocities in continuum and near-free molecular flow
Fl. Dyn. Drag - Hoerner (Ref 10)	1958	. . .	1 to 10	. . .	. . .	Wind tunnel and ballistic	C_D	Presentation of experimental data
J. Aeron. Sci., Vol 24 (Ref 31)	1957	3/8	2.2 to 9.7	. . .	. . .	Ballistic range	C_D	Obtain supersonic and hypersonic drag data
J. Aeron. Sci., Vol 20; NavOrd Report 2352 (Ref 32)	1953	1/4, 9/32, 5/16,	0.8 to 4.7	. . .	1.14×10^3 to 8.4×10^5	Ballistic range	C_D	Investigate Mach no. and Reynolds no. effects on drag
J. Aeron. Sci., Vol 18 (Ref 33)	1951	1/4, 1/2, 1	2.1 to 2.8	. . .	15 to 800	Wind tunnel	C_D	Investigate Reynolds no. effects in a very low density flow
J. Aeron. Sci., Vol 12 (Ref 34)	1945	9/32, 9/16, 1-1/2	0.29 to 3.96	. . .	9.3×10^4 to 1.3×10^6	Ballistic range	C_D	Investigate Mach no. effects on drag

Preceding page blank

TABLE IV - R AND D - TOWED-SPHERE DECELERATORS

Reference	Report date	Configuration				Test Mach no.	Type of data obtained			Type of test	Test purpose and remarks
		X/d	D/d	Fence (percent)	Forebody		Pressure	Force and moment	Stability		
RTD-TDR-63-4023 (Ref 23)	1/65	2, 4, 7.89	1, 2	None	Ogive-cylinder (F.R. = 4.5)	0.85 to 1.2	C_{P_B}, C_{P_o}, C_{P_L} (forebody with and without decel.)	C_D	None	Wind tunnel	Obtain aerodynamic data; solid sting-mounted models (0.8- and 1.6-in. diam) used
RTD-TDR-63-4242 (Ref 24)	12/64	2 to 8	1, 2	None	Hemisphere-cylinder, flare (F.R. = 1.06)	0.85 to 1.25	C_{P_B}, C_{P_o}, C_{P_L} (forebody with and without decel.)	C_D	None	Wind tunnel	Obtain aerodynamic data; solid sting-mounted models (9/16- and 1-1/8-in. diam) used
RTD-TDR-63-4242		4 to 8	1, 2	None	Ogive-cylinder (F.R. = 4.5)	4.35	None	C_D	None	Wind tunnel	Obtain aerodynamic data; solid sting-mounted models (9/16- and 1-1/8-in. diam) used
RTD-TDR-63-4226 (Ref 25)	12/64	2 to 8	1, 2	None	Hemisphere-cylinder, flare (F.R. = 1.06)	0.85 to 1.25	C_{P_B}, C_{P_c} (decelerator and forebody)	C_D	None	Wind tunnel	Obtain aerodynamic data; solid sting-mounted models (9/16- and 1-1/8-in. diam) used
RTD-TDR-63-4226		4 to 8	1, 2	None	Ogive-cylinder (F.R. = 4.5)	4.35	C_{P_B}, C_{P_c} (decelerator and forebody)	C_D	None	Wind tunnel	Obtain aerodynamic data; solid sting-mounted models (9/16- and 1-1/8-in. diam) used
NASA TN D-1789 (Ref 26)	4/63	2 to 12	1.69, 2.53, 3.37	39	Cone-cylinder (F.R. = 18.7)	2 to 4.65	None	C_D	*	Wind tunnel	Obtain aerodynamic data; solid spheres on flexible towline (4-, 6-, and 8-in. diam) used
NASA TN D-1789		2 to 12	0.73, 1.09, 1.45		Cone-cylinder, flare (F.R. = 4.34)	2 to 4.65	None	C_D	*	Wind tunnel	Obtain aerodynamic data; solid spheres on flexible towline (4-, 6-, and 8-in. diam) used
NASA TN D-1789		2 to 12			Eggers body with flaps	2 to 4.65	None	C_D	*	Wind tunnel	Obtain aerodynamic data, solid spheres on flexible towline (4-, 6-, and 8-in. diam) used
NASA TN D-1601 and ASD-TDR-62-702, Pt. II (Ref 27 and 35)	3/63	1 to 9	3.37	6.25	Cone-cylinder (F.R. = 10.7)	2 to 3.96	None	C_D	*	Wind tunnel	Obtain aerodynamic data; inflatable fabric sphere on flexible towline (8-in. diam) used
ASD-TDR-62-702 (Pt. II) and ASD-TR-60-182 (Ref 27 and 36)	9/62 11/61	8	12	3.9	Spiked cone-cylinder	1.4 to 2.1	None	C_D	*	Free flight	Obtain data and investigate free flight capabilities; 9-ft-diam pressurized fabric models used
NASA TN D-919 and ASD-TR-60-182 (Ref 36 and 37)	8/61 11/61	0 to 10	3, 32	None	None, unsymmetrical capsule, attached spike	1.5 to 2.87	C_P	C_D	None	Wind tunnel	Obtain aerodynamic data; all 8-in.-diam models, some inflatable, some fabric-covered solid models used
		0 to 10	2.37 to 3	3.9	Symmetrical and unsymmetrical capsule, sphere, disk	1.5 to 2.87	. . .	C_D	None	Wind tunnel	
NASA TN D-919 and ASD-TR-60-182		0 to 10	2.37 to 3	3.9	Symmetrical and unsymmetrical capsule, sphere, disk	1.5 to 2.87	. . .	C_D	*	Wind tunnel	Obtain aerodynamic data; all 8-in.-diam models, some inflatable, some fabric-covered solid models used
ASD-TR-60-182 (Ref 36)	11/61	6	2.34	3.9	Symmetrical capsule (strut-mounted)	2 to 3.5	None	C_D	*	Wind tunnel	Obtain aerodynamic data; 26.1-in. fabric sphere (pressurized); first supersonic-deployment demonstration

* Visual Coning Observation

TABLE V - R AND D - FREE-STREAM AND TOWED-BALLUTE DECELERATORS

Reference	Report date	Test date	Test configuration: Forebody	Test configuration: Decelerator	Apex angle (deg)	Diameter	Fence (percent)	Test conditions: Mach no.	Test conditions: q (psi)	Test conditions: X/d	Test conditions: D/d	Type of data obtained: Pressure	Type of data obtained: Force and moment	Type of data obtained: Stability	Type test	Test purpose and remarks
AEDC-TR-65-218 (Ref 38)	10/65	8/65	Blunted ogive (F.R. = 2.39), strut-mounted	Small rigid model (isotensoid) aft-sting mounted	80	6.3, 7.65, 10.6 in.	10	1.98 to 3.98	158	2, 3	1.06, 1.3, 1.8	None	C_D	None	Wind tunnel	Obtain aerodynamic drag in near-forebody wake
Unpublished data (Ref 39)		9/65	Unsymmetrical forebody	Ram-air-inflated coated nylon model (isotensoid)	80	4 ft	10	2.6, 3.0	120	6	1.23	None	C_D	*	Wind tunnel	Obtain aerodynamic drag and visual stability in wake of unsymmetrical forebody
AEDC-TDR-65-110 (Ref 41)	6/65	2/65	Cone-cylinder, flare-cylinder (F.R. = 7.8)	Nylon ram-air cone-balloon	75	7 in.	6.30	4 to 6	144 to 245	9	3.5	None	C_D	*	Wind tunnel	Obtain high Mach no. towed drag data and visual stability
Unpublished (Ref 41)		12/64	Cone-cylinder, flare-cylinder (F.R. = 5.82)	Ram-air Nomex model (isotensoid)	80	5 ft	0	3	120	10.2	3.4	None	C_D	*	Wind tunnel	Obtain towed drag data and visual stability for relatively large model
Unpublished data (Ref 42)		11/64	Unsymmetrical sled	Nylon ram-air		3.75 ft	10	1.36 (deploy)	2380	7.2	3	None	C_D	*	Track	Obtain high-q drag and stability data
GER-11665 S/3 (Ref 43)	2/65	8/64	Cone-cylinder, flare-cylinder (F.R. = 6)	Nomex ram-air model (isotensoid)	80	5 ft	0	2.4 to 3.15 (deploy M = 3.25)	50 to 208	7	3.4	Internal	C_D	*	Free flight	Obtain towed free-flight test performance characteristics and aerodynamic data
GER-11665 S/2 (Ref 44)	2/65	7/64	Cone-cylinder, flare-cylinder (F.R. = 6)	Nylon ram-air model (isotensoid)	80	5 ft	10	1.0 to 1.88 (deploy M = 2.17)	32.5 to 240	7	3.4	Internal	C_D	*	Free flight	
GER-11665 S/1 (Ref 45)	2/65	6/64	Cone-cylinder, flare-cylinder (F.R. = 6)	Nylon ram-air model (isotensoid)	80	5 ft	10	1.1 to 2.1 (deploy M = 2.5)	36 to 144	7	3.4	None	C_D	*	Free flight	
AEDC-TDR-64-131 (Ref 46)		6/64	Tow-strut used (no forebody)	Nylon ram-air model (isotensoid)	80	4 ft	10	1.92	. . .	. . .		None	C_D	*	Wind tunnel	Demonstrate Ballute deployment and obtain drag and stability data
Unpublished data (Ref 47)		4/64	Cone-cylinder, flare-cylinder (F.R. = 5.82)	Nylon ram-air model (isotensoid)	80	3 ft	10	2.53, 2.79, and 3	121	3.07	1.7	None	C_D	*	Wind tunnel	Obtain towed drag and stability data
AEDC-TDR-64-65 (Ref 48)	4/64	12/63	Cone-cylinder, flare-cylinder (F.R. = 7.8), and connecting shaft	Small rigid isotensoid model; aft-sting mounted	80	7.5 in.	10	1.5 to 6	. . .	6 to 12	3.75	C_{P_L} and internal	None	None	Wind tunnel	Obtain drag and pressure data over a wide Mach no. range
GER-11538 (Ref 49)	1/65	5/63	Not towed (no forebody)	Rigid isotenoid model; aft-sting mounted	80	9 in.	10	1 to 2.5	. . .	. . .		None	C_D	None	Wind tunnel	Obtain free-stream drag data
AEDC-TDR-63-119 (Ref 50)	7/63	2/63	Biconic (F.R. = 5)	Nylon ram-air isotensoid model	80	7.5 in.	10	4 to 5.5		8.0	2.0	None	C_D	*	Wind tunnel	Obtain towed drag data up to Mach 5.5 and visual stability
ASD-TDR-62-702, Part II (Ref 27)	12/62	6/61-6/62	Cone-cylinder (F.R. = 10.7)	Nylon ram-air cone-balloon	75	7 in.	6.3	2.0 to 4.65	. . .	2 to 9	2.92	Internal	C_D	*	Wind tunnel	Initial feasibility tests to demonstrate ram-air inflation (free of "buzzing") of textile inflatable models and obtain towed drag data and visual stability
ASD-TDR-62-702, Part II	12/62	6/61-6/62	Cone-cylinder (F.R. = 10.7)	Dacron ram-air isotensoid model	80	8 in.	3.9	2.5 to 4.65	. . .	2 to 9	3.33	None	C_D	*		
ASD-TDR-62-702, Part II	12/62	11/61	Hemisphere-cylinder, boattail	Metal cloth, flexible, ram-air isotensoid model	80	10 in.	0	10	. . .	0 to 11		None	C_D	*	Wind tunnel	Mach 10 performance tests (same as above) of coated metal-cloth models
ASD-TDR-62-702, Part II	12/62	11/61	Hemisphere-cylinder, boattail	Rigid isotensoid model	80	10 in.	0	10	. . .	4 to 18		C_P	None	None	Wind tunnel	Obtain towed-model temperature and pressure data
ASD-TDR-62-702 (Part I), ASD-TR-60-182 (Ref 27, 36)	9/62, 11/61		Spiked cone-cylinder	Pressurized fabric spherical models	. . .	9 ft	3.9	1.4 to 2.1	. . .	8	12	None	C_D	*	Free flight	Demonstrate feasibility and obtain data during flight of nonporous inflatable model

*Visual coning observation.

TABLE VI - R AND D - FLARED-SKIRT DECELERATORS

Reference	Date	Flare configuration			Theory	Experimental Mach No.	Type of data obtained		
		θ_s (deg)	D/d	Forebody			Pressure	Force and moment	Stability
NASA TN D-2854 (Ref 51)	6/65	0, 10, 20, 30	1 to 2.896	45-deg cone-cylinder (F.R. = 2.21 and 5.21) Hemisphere-cylinder (F.R. = 1.6 and 4.5)	Modified Newtonian	6	None	C_A, C_N, C_M	Static
WADC-TR-59-324, Part II (Ref 52)	12/60	30, 50, 70	6	Hemisphere-cylinder (l/d = 6)	None	8	C_P	C_A, C_N, C_M	Static
OML Report 6R2P (Ref 53)	6/55	6, 14, 22	3	45-deg cone-cylinder (cylinder: 1, 3, 5 cal.)	1.3, 1.8, 2.5 (linearized theory)	None	None	None	Static

Preceding page blank

TABLE VII - R AND D - HEMISFLO, CONICAL, AND STANDARD FLAT RIBBON PARACHUTES

Reference	Report date	Test date	Test configuration		Geometric porosity (percent)	Reefed to 'x' percent of D_o	Mach no.	Type of data obtained			Type of test	Test purpose and remarks
			Forebody	Decelerator				Pressure	Force and moment	Stability		
AEDC-TR-65-110 (Ref 40)	6/65		Cone-cylinder (F.R. = 6.16)	Reefed hemisflo, 13 and 21.3 in. D_o	14 (13 in.), 17 to 9 (21.3 in.)	. . .	1.5 to 3	None	C_{D_o}	*	Wind tunnel	Demonstrate supersonic feasibility of reefed chutes
FDL-TDR-64-35 (Ref 54)	7/64		Spiked cone-cylinder	Hemisflo, 4.12-ft D_o	14.3	None	0.18 to 2.35 (deploy M = 2.4)	None	C_{D_o}	*	Free flight	Free-flight demonstration and free-flight results
FDL-TDR-64-35	7/64		Spiked cone-cylinder	Hemisflo, 4.12-ft D_o	14.3	None	2 to 3.39 (deploy M = 3.44)	None	C_{D_o}	*	Free flight	Free-flight demonstration and free-flight results
AEDC-TDR-64-120 (Ref 55)	6/64	4/64	Cone-cylinder flare-cylinder (F.R. = 5.82)	Hemisflo, 10-ft D_o	14	20	1.8 to 3.0	None	C_{D_o}	*	Wind tunnel	Demonstrate supersonic feasibility of reefed chutes
AEDC-TDR-64-120	6/64	4/64	Cone-cylinder flare-cylinder (F.R. = 5.82)	Conical, 10-ft D_o	14	20	1.8 to 3.0	None	C_{D_o}	*	Wind tunnel	Demonstrate supersonic feasibility of reefed chutes
FDL-TDR-64-66 (Ref 65)	5/64		Unsymmetrical test sled	Hemisflo, 4.2-, 5.54-, 6.77-ft D_o	25 to 27	None	1.29 to 1.46 (deployment)	None	C_{D_o}	*	Track	Obtain transonic, high-q performance data
AEDC-TDR-63-263 (Ref 57)	1/64	8/63	Cone-cylinder flare-cylinder (F.R. = 7.8)	Hemisflo, 19.3-in. D_o	14	20.7, 23.4	1.48 to 2.98	None	C_{D_o}	*	Wind tunnel	Demonstrate supersonic feasibility of reefed chutes
AEDC-TDR-63-263			Cone-cylinder flare-cylinder (F.R. = 7.8)	Conical, 19.3-in. D_o	14	20	1.48 to 2.98	None	C_{D_o}	*	Wind tunnel	Demonstrate supersonic feasibility of reefed chutes
AEDC-TDR-62-234 (Ref 58)	12/62		Biconic (F.R. = 5)	Conical, 1-ft D_o	20	None	1.48 to 2.98	None	C_{D_o}	*	Wind tunnel	Obtain supersonic-performance data
NASA TN D-752 (Ref 59)	5/61		Mercury capsule	Standard flat, 9.6 in.	19	None	1.82 to 2.5	None	C_{D_o}	*	Wind tunnel	Mercury program: first-stage drogue feasibility
NASA TM X-448 (Ref 60)	11/60		Spiked cone-cylinder	Conical, 6 ft; standard flat, 6 ft	23 to 30	None	1 to 1.5	None	C_{D_o}	*	Free-flight drop	To obtain flight-test data
AEDC-TN-59-107 (Ref 61)	9/59		B-58 unsymmetrical capsule	Equiflo, 1-ft D_o	Not recorded	None	0.8 to 1.6	None	C_{D_o}	*	Wind tunnel	B-58 escape-capsule stabilization test

*Visual coning and inflation observation.

TABLE VIII - R AND D - HYPERFLO, PARASONIC, AND SUPERSONIC GUIDE-SURFACE PARACHUTES

Reference	Report date	Test date	Test configuration: Forebody	Test configuration: Decelerator	Geometric porosity (percent)	Ai/Ae	Mach no.	Type of data obtained: Pressure	Type of data obtained: Force and moment	Type of data obtained: Stability	Type test	Test purpose and remarks
Unpublished data	. . .	9/65	Cone-cylinder, flare-cylinder (F.R. = 5.82)	Mesh-roof parasonic (isotensoid), 4 ft D_o	. . .	3.5	3	None	C_{D_o}	*	Wind tunnel	Obtain drag and stability data from deployment
Unpublished data	. . .	9/65	Unsymmetrical forebody	Nomex mesh-roof parasonic (isotensoid), 5.5 ft D_o	. . .	6.57	3	None	C_{D_o}	*	Wind tunnel	Determine effects of unsymmetrical body on the parachute performance
AEDC-TR-65-110 (Ref 40)	6/65	. . .	Cone-cylinder, blunted; cone-cylinder, flare-rounded-nose cylinder	Hyperflo (17 config., in size roof mesh, susp. lines) 308.2 in. D_o	5 to 20	None	.2 to 5.5	None	C_D	*	Wind tunnel	Obtain model drag and stability with combinations of porosity, material, and size
AEDC-TR-65-57 (Ref 62)	3/65	12/64	Blunted cone-cylinder, flare-cylinder (F.R. = 5.8)	Mesh-roof hyperflo, (one metal configuration)	9, 9.6	. . .	2.6 to 3	None	C_{D_o}	*	Wind tunnel	Determine Mach no. effects on drag, stability, and inflation characteristics
AEDC-TR-65-57	. . .	12/64	Blunted cone-cylinder, flare-cylinder (F.R. = 5.8)	Mesh-roof parasonic (isotensoid), 4 ft D_o (one 3 ft D_o configuration)	7 to 10.9	. . .	2.2, 2.6 to 3	None	C_{D_o}	*	Wind tunnel	Determine Mach. no. effects on drag, stability, and inflation characteristcs
FDL-TDR-64-35 Vol 1 (Ref 54)	7/64	. . .	Spiked cone-cylinder, flare-cylinder	Hyperflo 2.71 ft and 4.12 ft D_o (5 perlon mesh, 2 steel mesh)	. . .	. . .	2.1, 2.98, 4.4 (deployment)	None	C_{D_o}	Angular displacement	Free flight	Evaluate ribbon and mesh roof canopies in free-flight at various Mach no.
FDL-TDR-64-35 (Vol 1)	7/64	. . .	Spiked cone-cylinder, flare-cylinder	Ribbon hyperflo (4), 2.71 and 4.12 ft D_o	. . .	. . .	2.84, 3.22, 3.98 (deployment)	None	C_{D_o}	Angular displacement	Free flight	Evaluate ribbon and mesh roof canopies in free-flight at various Mach no.
AEDC-TDR-64-120 (Ref 55)	6/64	. . .	Blunted cone-cylinder, flare-cylinder (F.R. = 5.8)	Mesh-roof (3 Perlon, 2 HT-1, 1 stainless steel) hyperflo, 2.72, 3.69 and 4.0 ft D_o	9 to 14	. . .	1.80 to 3.01	None	C_{D_o}	*	Wind tunnel	Mach no. effects on the drag, stability, and inflation characteristics
AEDC-TDR-64-120	6/64	. . .	Blunted cone-cylinder, flare-cylinder (F.R. = 5.8)	Mesh-roof (3 HT-1 and 1 Perlon) parasonics (isotensoid), 4 ft D_o	9 to 17	. . .	1.80 to 2.73	None	C_{D_o}	*	Wind tunnel	Mach no. effects on the drag, stability, and inflation characteristics
AEDC-TDR-64-120	6/64	. . .	Blunted cone-cylinder, flare-cylinder (F.R. = 5.8)	Supersonic guide-surface (cone cup), 4 ft D_o	. . .	. . .	2.01, 2.2, 2.6	None	C_{D_o}	*	Wind tunnel	Mach no. effects on the drag, stability, and inflation characteristics
AEDC-TDR-64-120	6/64	. . .	Blunted cone-cylinder, flare-cylinder (F.R. = 5.8)	Ribbon-roof hyperflo (nylon and HT-1 skirts) 2.68, 3.69 ft D_o	7.5, 13.7, 14.14.6	. . .	1.8 to 3.01	None	C_{D_o}	*	Wind tunnel	Mach no. effects on the drag, stability, and inflation characteristics
FDL-TDR-64-66 (Ref 56)	5/64	. . .	Unsymmetrical test, sled	Ribbon-roof hyperflo, 3.69, 4.95, 6.06 ft D_o	13.3 to 14.8	. . .	1.3 to 1.5 (deployment)	None	C_{D_o}	Angular displacement	Track	Obtain transonic and low supersonic data; one hyperflo cluster test also performed; three S-G-S parachute test attempted but no meaningful data obtained
FDL-TDR-64-66	5/64	. . .	Unsymmetrical test, sled	Mesh-roof hyperflo, 10.67 and 19.22 ft D_o	13.3, 14.3 14.5	. . .	1.08 to 1.34	None	C_{D_o}	Angular displacement	Track	Obtain transonic and low supersonic data; one hyperflo cluster test also performed; three S-G-S parachute test attempted but no meaningful data obtained
FDL-TDR-64-66	5/64	. . .	Unsymmetrical test, sled	Supersonic guide-surface (cone cup) 2 ft D_o	. . .	. . .	1.1, 1.3	None	None	None	Track	Obtain transonic and low supersonic data; one hyperflo cluster test also performed; three S-G-S parachute tests attempted but no meaningful data obtained
AEDC-TDR-63-263 (Ref 57)	1/64	. . .	Spiked cone-flare, cone-cylinder; spiked cone-flare, flare (F.R. = 7.8, 3.14)	Ribbon- or mesh-roof (steel or Perlon) hyperflo, 7.5, 8, 9.4 ft	. . .	. . .	4 to 5	None	C_{D_c}	*	Wind tunnel	Further development of Supersonic parachutes
AEDC-TDR-63-119 (Ref 50)	7/63	. . .	Biconic (F.R. = 5)	Reefed ribbon-roof hyperflo, 8 in. D_c	. . .	. . .	1.5 to 2.98	None	C_{D_c}	*	Wind tunnel	Further develop and evaluate Supersonic decelerator
ASD-TDR-62-844 (Ref 63)	2/63	. . .	Cone-cylinder (F.R. = 10.7)	Mesh- and ribbon-roof hyperflo, 6 and 8 in. D_c	2.3 to 18, 2 to 4	. . .	2.3 to 4.65	None	C_{D_c}	*	Wind tunnel	Investigate supersonic-parachute performance
AEDC-TDR-62-234 (Ref 58)	12/62	. . .	Biconic (F.R. = 5)	Reefed and unreefed ribbon-roof hyperflo, 8 in. D_c	. . .	. . .	1.48 to 4.0	None	C_{D_c}	*	Wind tunnel	Compare and further develop Supersonic-parachute configurations
AEDC-TDR-62-185 (Ref 64)	10/62	. . .	Biconic (F.R. = 5)	Ribbon- and mesh-roof hyperflo (one reefed configuration) 8 in. D_c	. . .	. . .	1.5 to 6	None	C_{D_c}	*	Wind tunnel	Compare and further develop Supersonic-parachute configurations
AEDC-TDR-63-119 (Ref 50)	7/63	. . .	Biconic (F.R. = 5)	Mesh- and ribbon-roof hyperflo, 9.4 in. D_c	. . .	. . .	1.5 to 6	None	C_{D_c}	*	Wind tunnel	Further develop and evaluate Supersonic decelerator

*Visual coning and inflation observation.

TABLE IX - R AND D - TENSION-SHELL

Test date	Report date	Configuration	Theory	Test mach no.	Type of data obtained			Type of test	Reference	Test purpose and remarks
					Pressure	Force and moment	Stability			
	7/65	Tension shells, β = 15.4 to 47 deg ($\approx$semiapex angle), Ref 65	Newtonian	3, 7	Local pressure	C_D	None	Wind tunnel	AIAA paper, presented 7/26-29/65	Study performed to ascertain aerodynamic characteristics and structural efficiency
	3/65	Newtonian tension shell, Ref 66	Newtonian	None	C_p	C_D	None	None	NASA TN D-2675	Theoretical study to evaluate high-drag low-weight characteristics
8/64		25-deg (β) towed tension shell behind X-15 aircraft, Ref 67	None	4.65	None	C_D	None	Wind tunnel	Unpublished data (NASA/Langley Unitary W. T.)	Obtain performance characteristics behind unsymmetrical forebody
6/61	12/62	Flexible tension shell (aluminum torus and fabric catenary curtain nose section), Ref 27	None	1.82	None	C_D	Coning and fabric flutter	Wind tunnel	ASD-TDR-62-702 (Pt. II)	Evaluate potential high-drag low-weight characteristics and qualitatively ascertain stability

29-A

Preceding page blank

29-B

TABLE X - MISCELLANEOUS CONFIGURATIONS

Reference	Date	Configuration	Theory	Test mach no.	Type of data obtained			Type of test	Test purpose and remarks
					Pressure	Force and moment	Stability		
ASD-TR-61-348, AEDC-TN-61-4 (Ref 68 and 69)	1/62	O. M.* Mark III-A (launch position) drag brake	Newtonian	Subsonic to 6.0	C_P	C_A, C_N, C_M	Static and dynamic	Wind tunnel	Obtain performance data of orbital models at various angles of attack and various environmental conditions
Same	(Also Phase I Report, 1/61)	0, 10, 20, and 40 deg (rib angle) I. S.† Mark I-B drag brake	Newtonian	2, 4, 6, 8	C_P	C_A, C_N, C_M	Static and dynamic	Wind tunnel	As above with I. S. models
		10 deg O. M. Mark III-A drag brake	Newtonian	5, 8	C_P	C_A, C_N, C_M	Static and dynamic	Wind tunnel	As above with orbital models
		F.S.‡ Mark I (fully opened) drag brake	Newtonian	0.3 to 8.0	C_P	C_A, C_N, C_M	Static and dynamic	Wind tunnel	As above with F.S. models
Astro Research Reports ARC-R-177 and ARC-R-176 (Ref 70 and 71)	2/65	Rotor net	. . .	. . .	. .	. . .	. . .	. . .	Analytical studies - no tests
AFOSR-104 (Ref 72)	3/61	Flexibrake, inverted drag cone, drag ring, paraflap, paraskirt	. . .	. . .	. . .	. . .	. . .	. . .	Feasibility studies - no tests

*O. M. - Orbital model

†I. S. - Instrumented satellite (model)

‡F. S. - Full scale

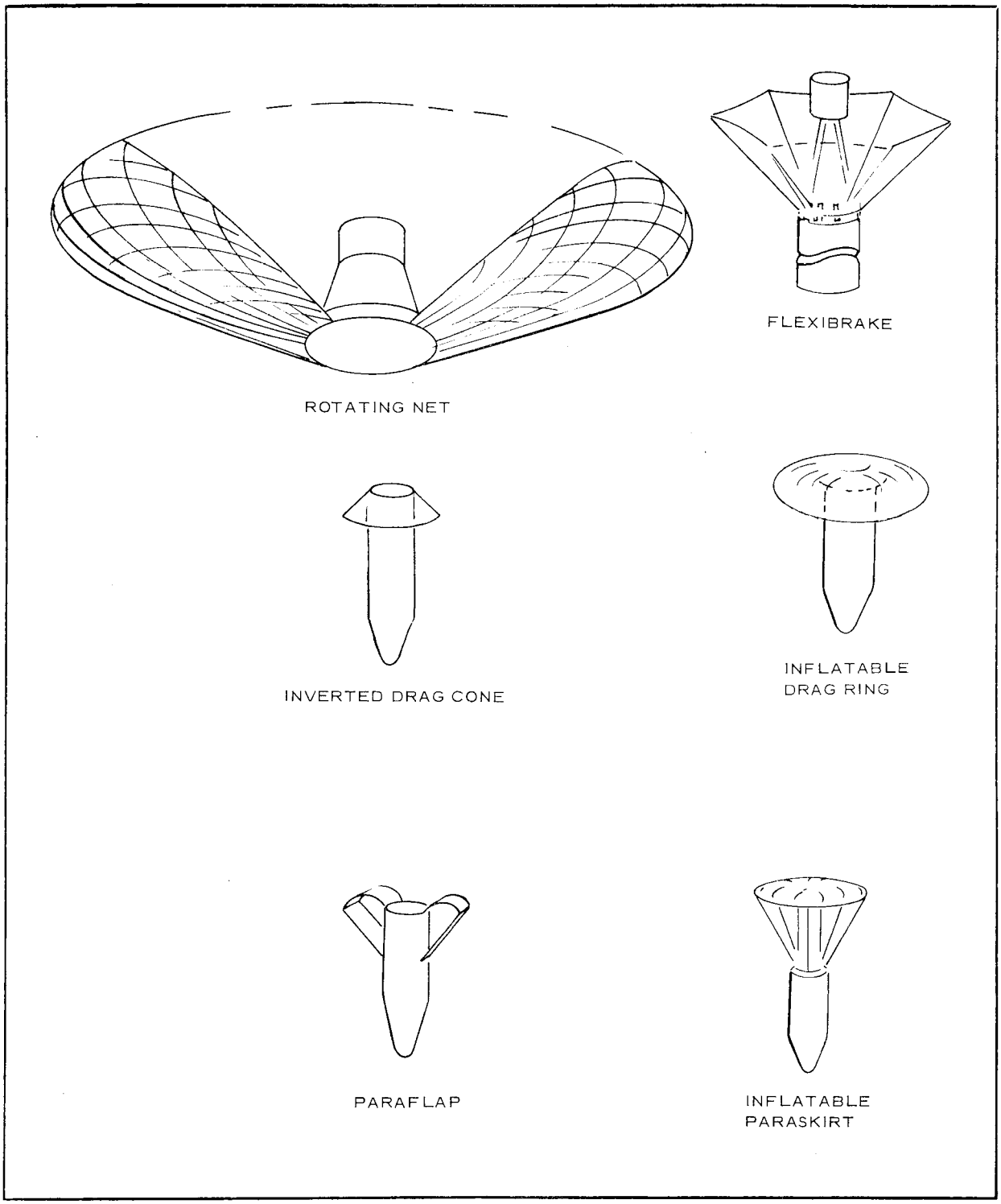

Figure 4 - Miscellaneous Decelerator Concepts

1. Blunted and shape free-stream cone configuration, Table I
2. Towed-cone configurations, Table II
3. Free-stream sphere configurations, Table III
4. Towed-sphere configurations, Table IV
5. Free-stream and towed Ballute configurations, Table V
6. Flared-skirt configuration, Table VI
7. Hemisflo-type ribbon parachute configurations, Table VII
8. Conical ribbon parachute configurations, Table VII
9. Standard flat ribbon parachute configurations, Table VII
10. Hyperflo parachute configurations, Table VIII
11. Parasonic parachute configurations, Table VIII
12. Supersonic Guide-Surface parachute configurations, Table VIII
13. Free-stream tension shell (tension shape) configurations, Table IX
14. Towed tension shell (tension shape) configuration, Table IX
15. Miscellaneous configurations, Table X

4. AERODYNAMICS

a. General

A review of the historical data obtained on the type of investigations conducted reveals, as an initial problem area, the general lack of data concerning blunt-body supersonic aerodynamic performance. Previous efforts to obtain performance data of slender bodies emphasized a reduction of drag for supersonic lifting-flight application. Therefore, the basic R and D philosophy for decelerators was to reverse the procedure completely

and conduct investigations on blunt bodies, using methods to increase the drag.

Research and development programs in the past have relied upon one of two methods to effect recovery and to obtain data in the development of supersonic high-drag devices.

One method was the "evolution approach," in which existing subsonic parachute designs were modified slightly, models were built (rigid and flexible), and tests above Mach 1 were made in small increasing velocity steps. Based on the results of these tests, additional design modifications were made, models were built and tested at slightly higher Mach numbers, and the cycle was repeated. A significant advantage of this method is that a considerable backlog of knowledge is used to enhance the chance of success. Past experience indicates that this technique has been applied with limited success. Unfortunately, since basic problem areas are not always defined completely, the solutions that are obtained may be unique to a particular operational situation. Hence a "fix" is made, but the general problems often remain unsolved.

The second method initially incorporates performance characteristics of basic blunt-body geometric shapes in the development of supersonic decelerators. Small rigid models (solid or rigidized by internal pressurization) are built and tested without concern, initially, for the method of construction. Once satisfactory performance characteristics have been obtained, subsequent detailed work is warranted to obtain an efficient light weight deployable system. In addition, desirable characteristics of a wider variety of basic shapes can be incorporated into a design.

The results of the two approaches show the second to be more efficient. This is because, when basic aerodynamic performance problems are solved, subsequent successful, large-scale structure and design investigations are more readily attainable since they clearly are dependent on an accurate definition of the aerodynamic performance. Items b through d, below, present the aerodynamic performance data, interpreted in terms of the knowledge that has been gained, the problems that have been solved, and the problems that remain to be solved.

b. Steady-State Drag of Towed Porous Decelerators

The drag of a towed decelerator depends on the type of flow environment that surrounds it. Since the decelerator is being towed, it must operate in the wake of the towing forebody. In addition, the drag-producing capabilities are dependent on its own size and shape. Because of these facts, dimensionless "towed-condition" parameters x/d and D/d were established to aid in evaluating comparative decelerator test data. x/d (the number of payload calipers aft) describes the decelerator-trailing distance (longitudinal position in the wake); D/d (the ratio of decelerator-to-payload size) indicates the transverse wake size, which - in turn - influences the flow around a given size and shaped decelerator.

Figure 5 indicates the Mach-number limits and the sizes and types of parachutes that have been flight tested. In addition, the track-test Mach number limits are shown. Results of hemisflo and Hyperflo track and wind-tunnel tests are presented to show the limited amount of data for correlation between ground and flight tests of the same configurations. Of all the chute tests, one available data point was found showing wind-tunnel drag results at Mach 2.5 for a 4.12-ft D_o hemisflo parachute, compared with flight-test results for the same parachute. Significant aspects of the Figure 5 plots are the C_D dispersion between configurations and the apparent inconsistency in drag trends. Physical interpretation of these results cannot be substantiated completely from this limited data. However, the effects of performance due to configuration and test-condition difference can be explained as follows.

It is generally recognized that performance of parachutes operating in the subsonic speed regime is influenced by the degree of canopy porosity. Ribbon parachutes with a known amount of geometric porosity have been used successfully for a wide variety of subsonic applications and at high subsonic and transonic speeds. These parachutes have performed effectively up to a free-stream Mach number of nearly 2; this is because the local flow behind the normal detached-canopy bow shock is still subsonic, and at about Mach 2 portions of the flow in the canopy do become supersonic.

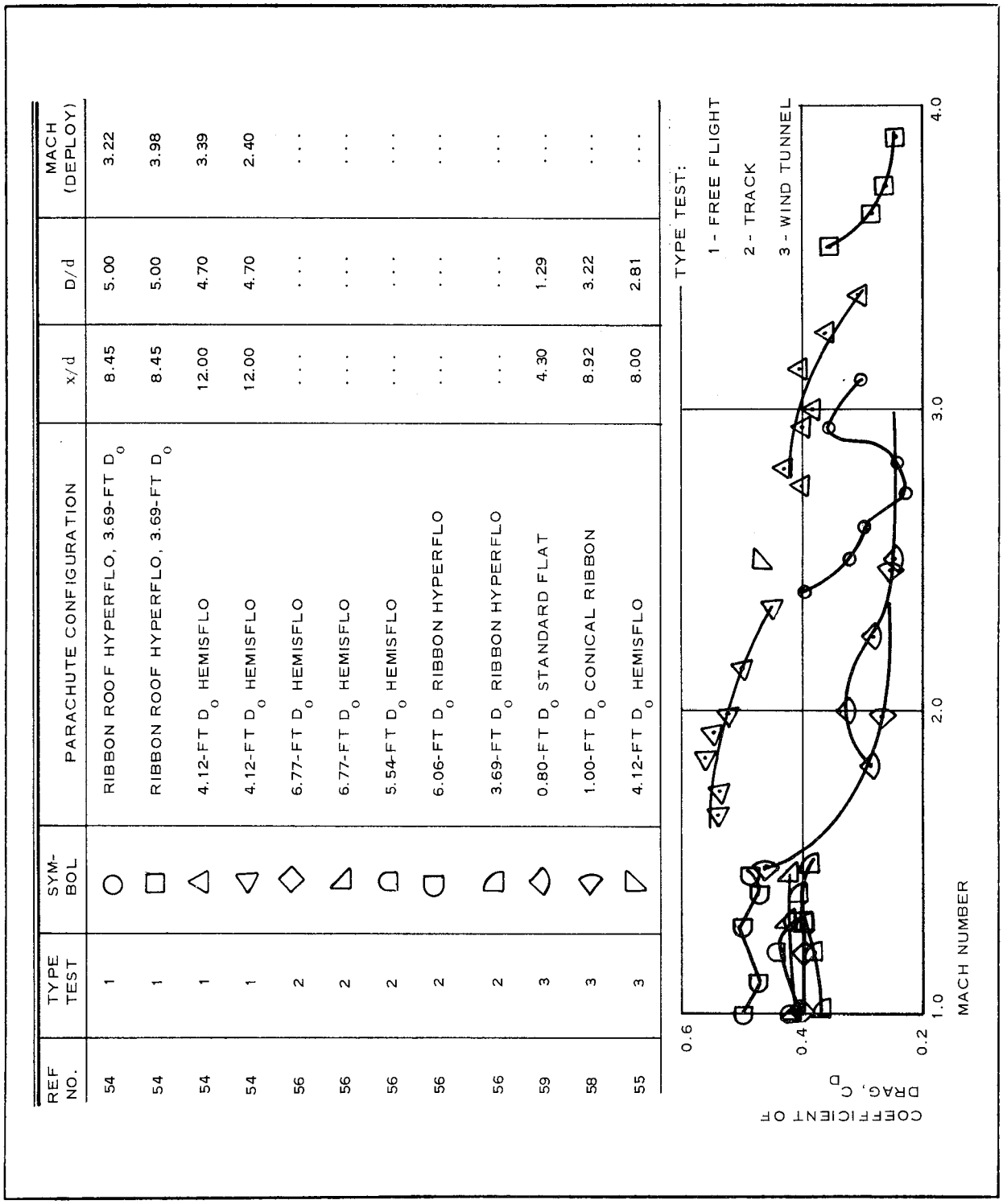

REF NO.	TYPE TEST	SYM-BOL	PARACHUTE CONFIGURATION	x/d	D/d	MACH (DEPLOY)
54	1	○	RIBBON ROOF HYPERFLO, 3.69-FT D_o	8.45	5.00	3.22
54	1	□	RIBBON ROOF HYPERFLO, 3.69-FT D_o	8.45	5.00	3.98
54	1	◁	4.12-FT D_o HEMISFLO	12.00	4.70	3.39
54	1	▽	4.12-FT D_o HEMISFLO	12.00	4.70	2.40
56	2	◇	6.77-FT D_o HEMISFLO	...	...	...
56	2	◺	6.77-FT D_o HEMISFLO	...	...	...
56	2	⊏	5.54-FT D_o HEMISFLO	...	...	...
56	2	⊐	6.06-FT D_o RIBBON HYPERFLO	...	...	...
56	2	◧	3.69-FT D_o RIBBON HYPERFLO	...	...	...
59	3	◇	0.80-FT D_o STANDARD FLAT	4.30	1.29	...
58	3	◇	1.00-FT D_o CONICAL RIBBON	8.92	3.22	...
55	3	◺	4.12-FT D_o HEMISFLO	8.00	2.81	...

Figure 5 - Coefficient of Drag vs Mach Number

During the review of the small-scale parachute wind-tunnel tests, the higher-porosity parachutes tested between Mach 1 and 2 had both good coning stability and good inflation stability, while low-porosity parachutes generally had good inflation stability but poor coning stability.

As soon as the local flow into the canopy becomes supersonic, the influence of the amount of geometric porosity (and other factors) on the performance is amplified, since a system of unsteady shock waves results when little or no mass air flow is allowed through the canopy. Under this condition of very low porosity, good inflation and high drag might be obtained, except that the canopy experiences adverse coning oscillation since the low-porosity canopies have basically unstable static-moment derivatives. This coning is considered adverse, because the cyclic breathing that is already present due to the cyclic "source" (high-pressure outer-wake air) and "sink" (low-pressure inner-wake air) phenomenon is amplified by spillage of the canopy captured air.

On the other hand, canopies with higher values of geometric porosity (between 20 and 30 percent) have improved stability characteristics but lower drag-producing characteristics. In this situation a system of more stable shock waves exists. It is further noted, however, that this lower restriction of mass flow will result eventually in the bow shock being attached to the canopy lip with increasing Mach number operation and subsequently being swallowed in the canopy. This shock attachment and swallowing causes the inflated canopy to assume a shape resembling that of a reefed parachute. The drag characteristics are then reduced substantially. Hence, there is a basic mismatch of a number of aerodynamic parameters.

In the specific parachute performance tests documented in Figure 5, some of the above general performance tendencies did occur. It is important to note, however, from the tabular model description and test condition data accompanying the plotted performance data that a straightforward evaluation of the meaning of the steady-state drag variation cannot or should not

be made. This is because (1) the different size parachutes were towed at different locations in the payload wake and (2) the structural integrity of the model, performing for various lengths of time prior to obtaining measured data, was uncertain.

The parachutes (hemisflo and Hyperflo) had extended skirts coned less than the standard flat and conical chutes; since their geometric porosities were less than those of the standard flat and conical ribbon parachutes, their drag-producing characteristics were higher and remained higher at higher Mach numbers.

Figures 6 and 7 present supersonic wind-tunnel data, the test conditions of which are presented in Table XI, for the larger parachutes (2.72 to 5.5 ft in diameter, D_o) when the amount of canopy choking was known and recorded. The configurations tested (specifically designed for supersonic velocity) were the Parasonic and the Hyperflo-type canopies. Table XI presents the test conditions and the type parachute for each data point shown in Figures 6 and 7.

Figure 6 shows the model choking ratio versus the Mach number at which the model was tested; the theoretical isentropic (A/A^*) area ratio for increasing supersonic Mach numbers is superimposed. Figure 7 presents the supersonic drag coefficient versus A_i/A_e (canopy inlet area over canopy exit area) of the models tested. There was an apparent trend that the C_D's (coefficients of drag) were larger values when the A_i/A_e was greater than the isentropic A/A^*; when the A_i/A_e was less than A/A^*, the C_D's were smaller values - that is, the parachute did not take a full-inflated design shape. Figure 6 shows that, to meet the requirement that a parachute have choking greater than its isentropic area ratio, the design of a given parachute for operation at higher Mach numbers would require a decreased porosity. At Mach 5,

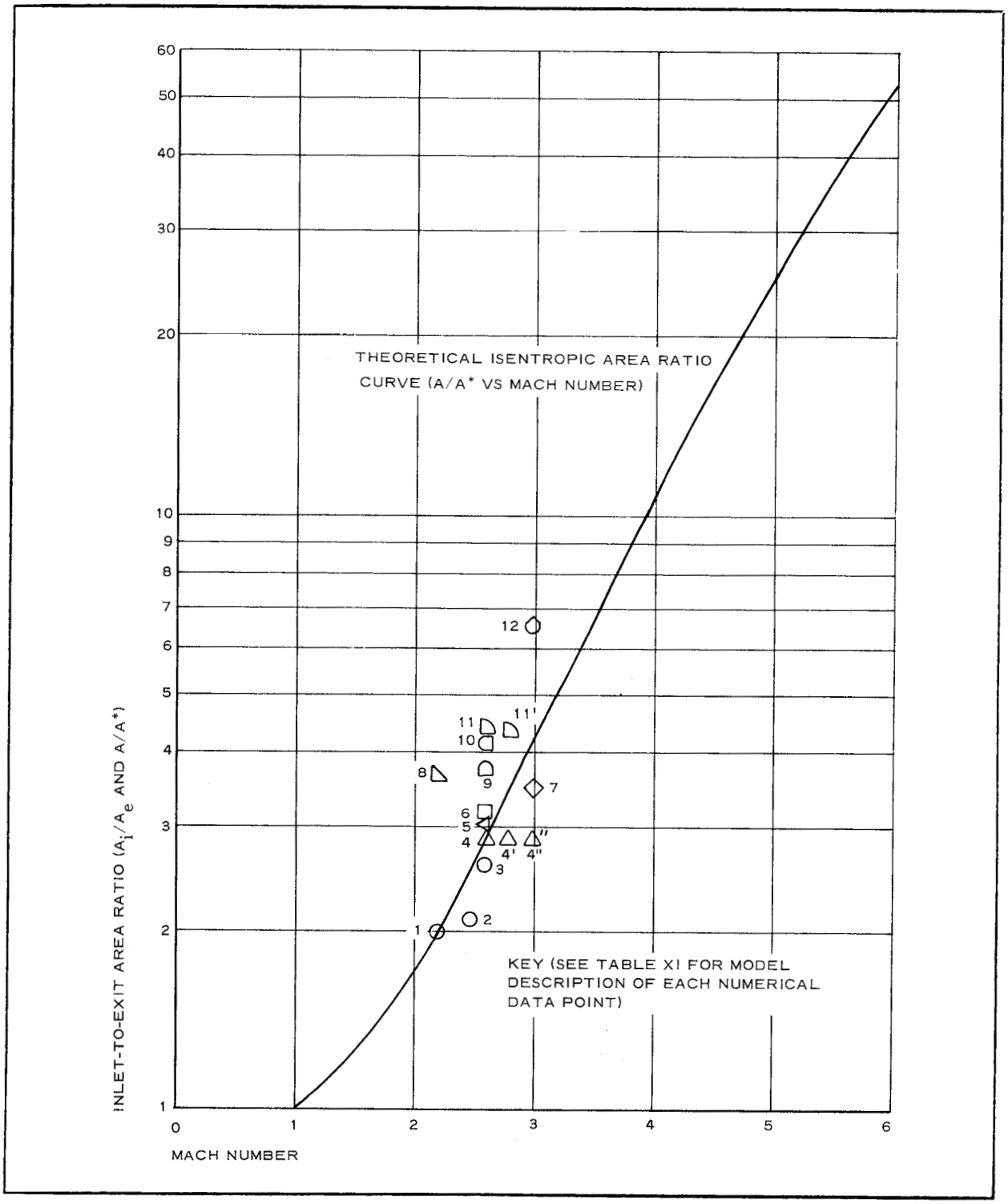

Figure 6 - Area Ratio vs Mach Number for Large Supersonic Parachutes

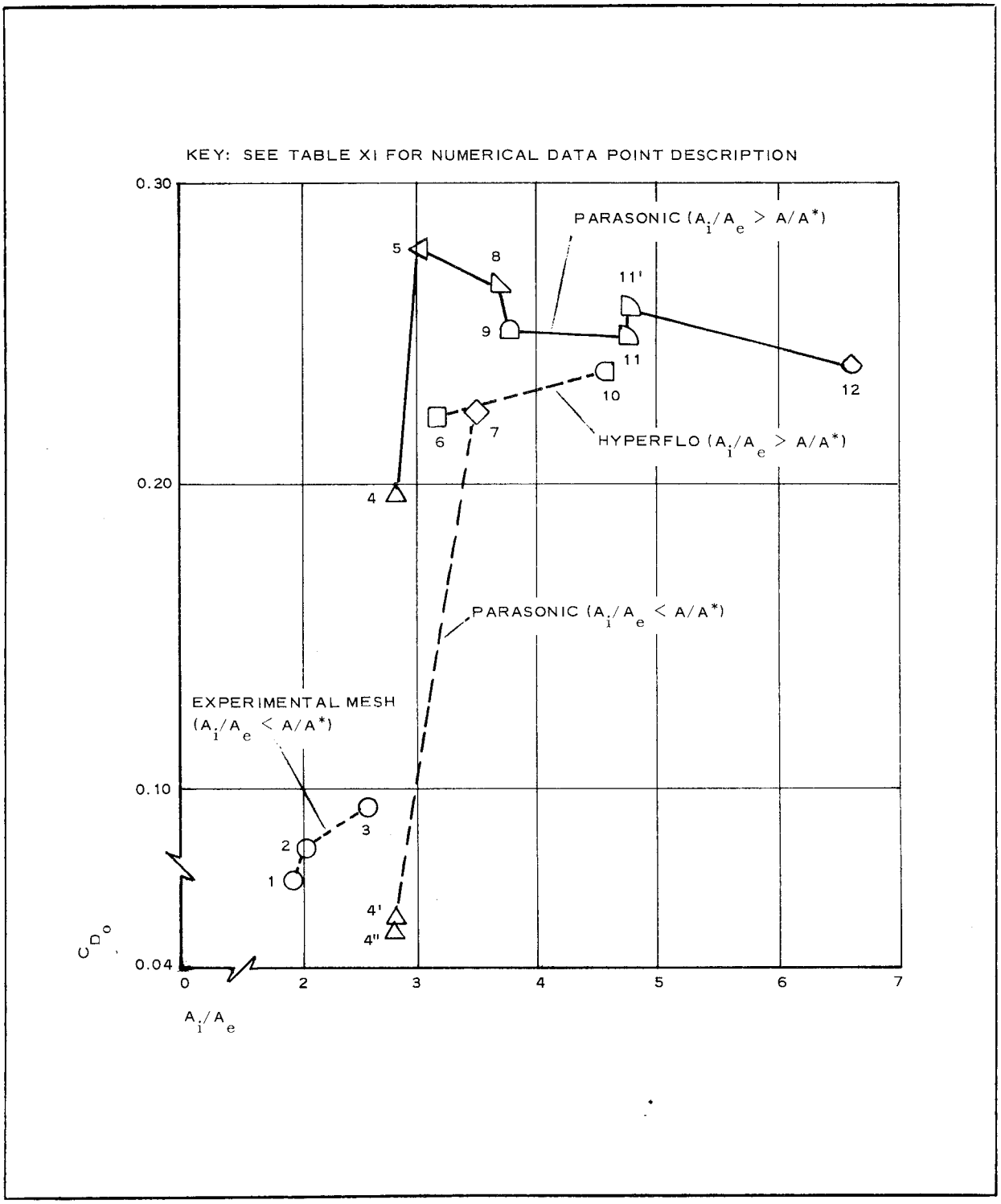

Figure 7 - C_D vs Area Ratio for Large Supersonic Parachutes

TABLE XI - FIGURES 6 AND 7 DATA POINT TEST CONDITIONS

Data point	Reference number	q	x/d	D_o/d	Type model
1 ○	55	121	8.51	2.72	*
2 ○	55	119	8.51	2.72	*
3 ○	55	120	8.51	2.72	*
4 △	62	119	9.75	2.72	Parasonic
4' △	62	120	9.75	2.72	Parasonic
4" △	62	120	9.75	2.72	Parasonic
5 ◁	62	120	5.80	2.04	Parasonic
6 □	55	120	8.51	2.72	Hyperflo
7 ◇	73	119	8.51	2.72	Parasonic
8 ◺	62	120	9.75	2.72	Parasonic
9 ⌂	55	121	7.16	2.72	Parasonic
10 ⊐	55	121	8.51	2.72	Hyperflo
11 ◺	62	120	9.75	2.72	Parasonic
11' ◺	62	120	9.75	2.72	Parasonic
12 ◊	73	120	8.51	3.70	Parasonic

*Exploratory mesh roof models.

for example, the canopy porosity would approach a solid canopy, which would probably develop stability problems when carried to a low Mach number.

Figure 8 presents C_{D_c} versus Mach number results for both small- and large-scale Hyperflo parachute wind-tunnel model tests. The plots are presented mainly to show the available documented data; a straightforward analysis of the meaning of the drag variation with Mach number cannot be made since design and performance parameters - such as the type of model (line length, canopy porosity), the type of model setup

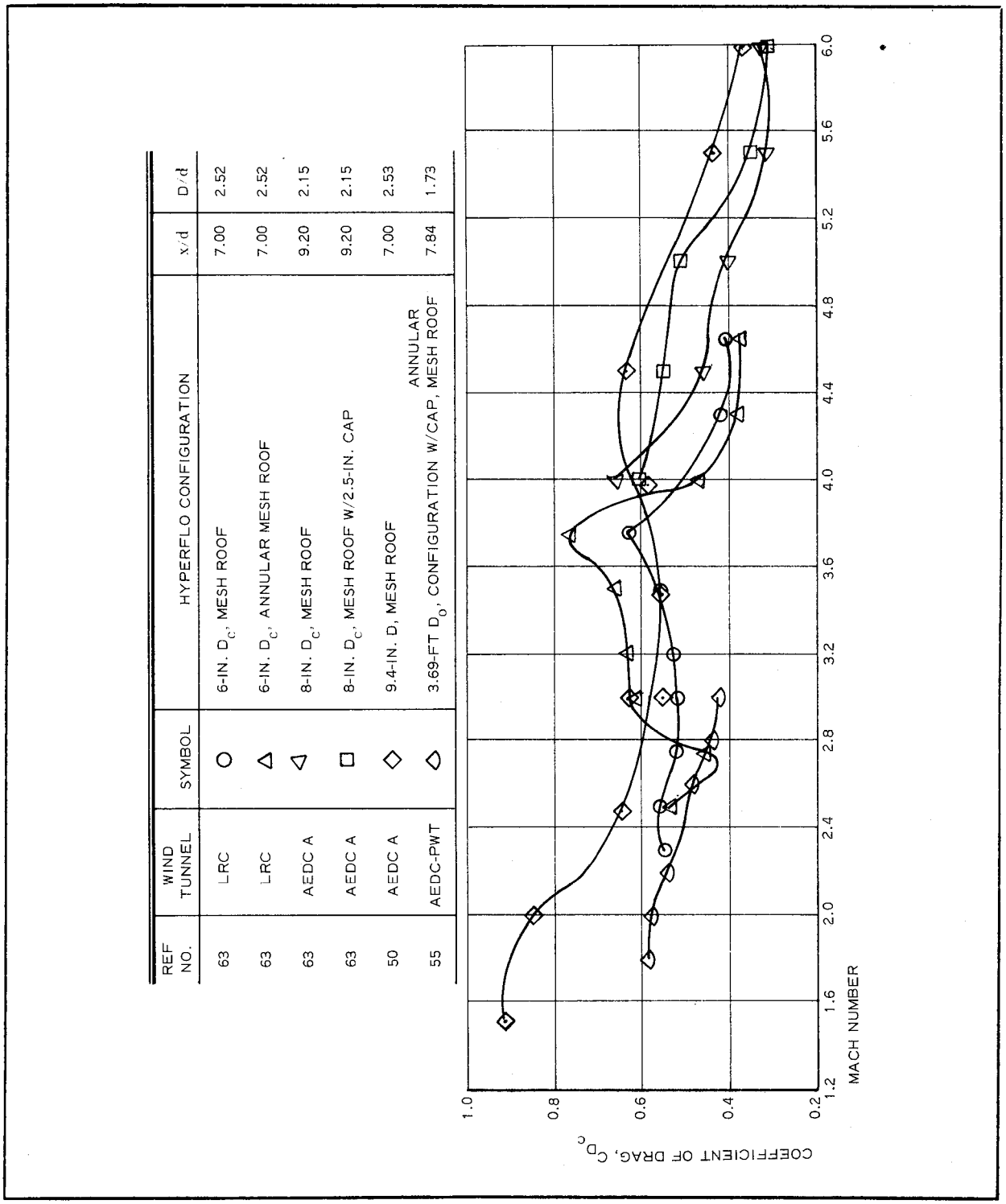

Figure 8 - Wind-Tunnel Tested C_D vs Mach Number for Hyperflo Parachutes

(towline length, use of a swivel), and the actual test conditions (dynamic pressure, Reynolds number) vary widely. From a review of the data, the following might be postulated:

1. High C_D's from Mach 1.5 to 2.0 occur because the local flow is subsonic.
2. Peaks in the C_D curves at Mach 3.6 to 4.4 occur because the dynamic pressures are minimum and hence the stiffness of the small models aids in keeping them in their fully inflated shapes.

However, to attribute the higher drag values to material stiffness only is probably not completely valid, since a low q (dynamic pressure) at a given Mach number results in a lower Reynolds number. A change in Reynolds number reflects a change in forebody wake and hence a change in the performance of the parachute. In addition, material fatigue causes deterioration in performance with time in the wind tunnel, and wind-tunnel tests at various temperatures affect performance. Not only does the Reynolds number change, but the material becomes stiffer; this added stiffness influences its inflated shape and hence its performance. Figure 9 gives the average drag results at various towline lengths during Mach 2 to Mach 2.6 wind-tunnel tests of a 4-ft diameter Supersonic Guide-Surface parachute. The plots also show the variation in drag readings, which is believed to be due to canopy breathing. Variation is reduced with increased x/d.

Figure 10 shows the C_D of the guide-surface parachute at three Mach numbers for a towline length that had the least amount of C_D variation. This variation varies between ±7 to ±16.5 percent of average value.

Not enough documented data on supersonic tests of solid extended skirt-type parachutes are available to make a data-correlation evaluation between wind tunnel tests and flight tests, since two of the three configurations have not been flight-tested. The only available supersonic flight-test data (above Mach 2) were for the "ribbon-roof" Hyperflo parachute; unfortunately, this parachute did not perform in a similar manner in a wind

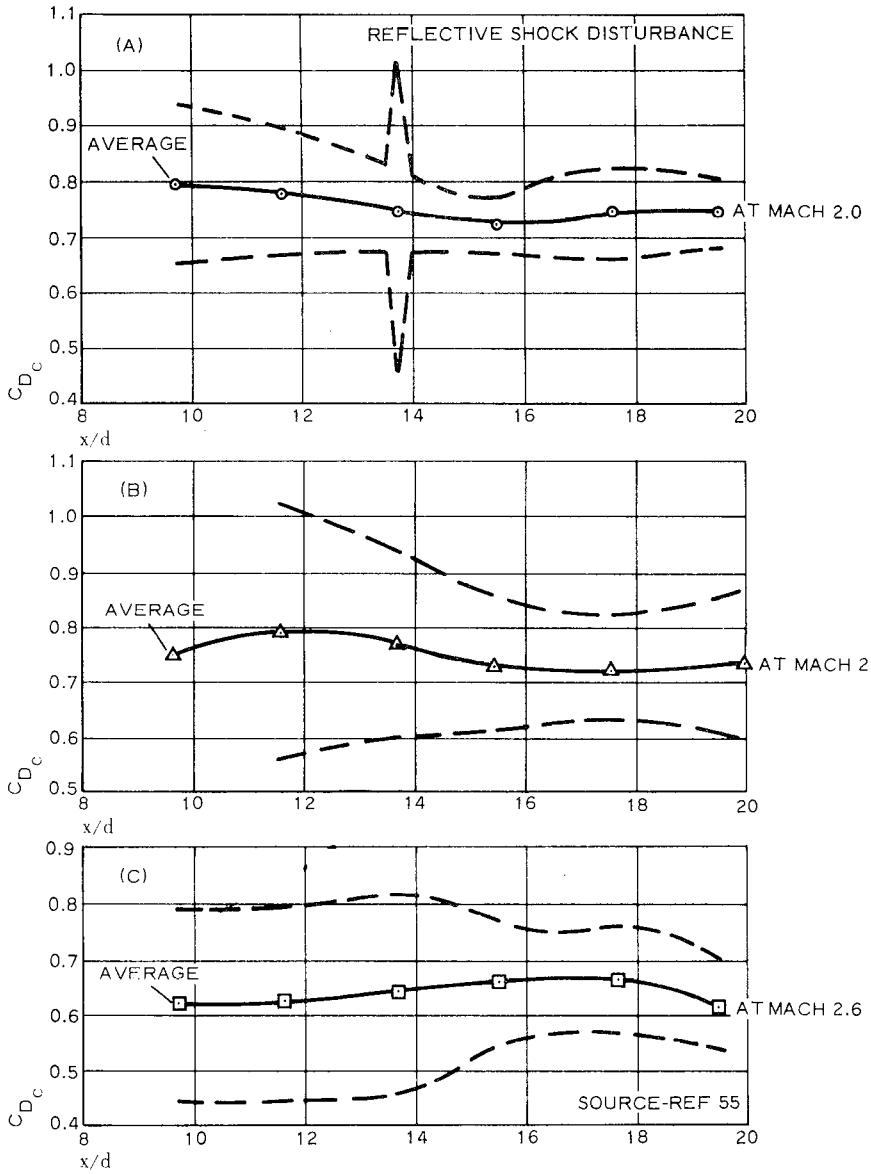

Figure 9 - Guide-Surface Parachute C_{D_c} vs x/d

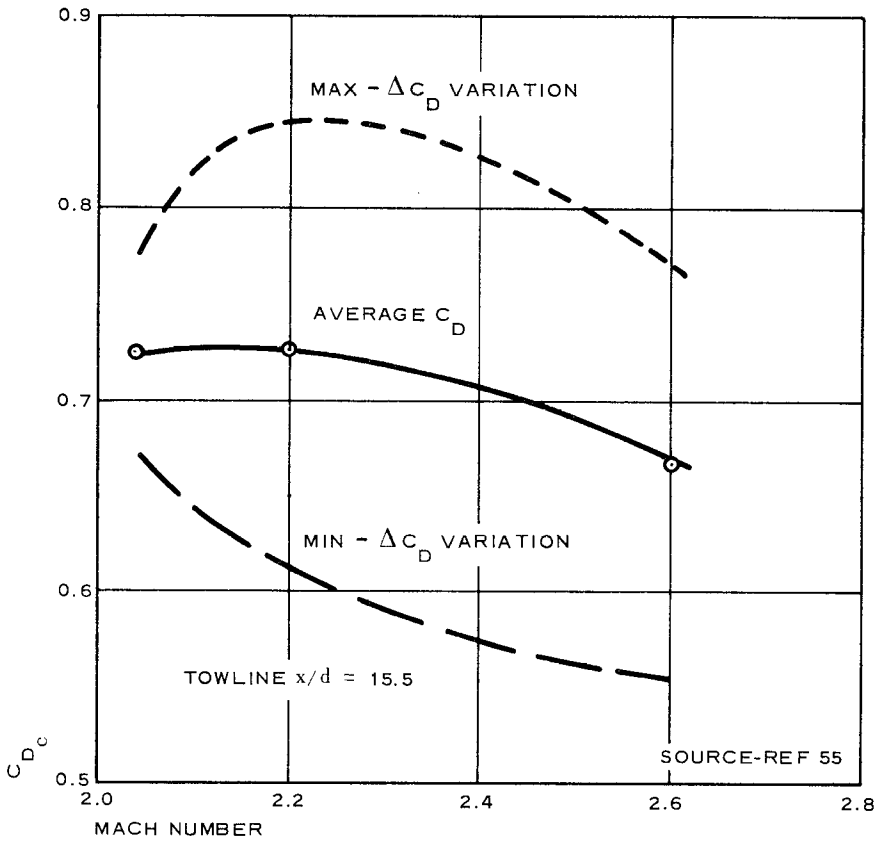

Figure 10 - Guide-Surface Parachute C_{D_c} vs Mach Number at One Towed Condition (with Minimum C_D Variation)

tunnel, as evidenced by extremely heavy canopy breathing and the resulting very low drag coefficients in all tests. The "mesh-roof" Hyperflo wind-tunnel tests were more successful than those of the ribbon-roof parachute; however, because of structural failures of the mesh roof during flight tests, no significant flight-test data were available for data correlation. Therefore, the lack of parachute flight-test data must be considered a major void.

Based on available data with respect to porosity conditions (A_i/A_e), no one parachute apparently can be designed to operate successfully over a wide range of supersonic Mach numbers. In addition the amount of breathing that can be tolerated for successful operation remains a void.

c. Steady-State Drag of Towed Nonporous Decelerators

Ballute decelerator representative supersonic drag data are presented in Figure 11. The data are for the largest decelerators tested. Part of the data shows the variation in drag obtained while decelerating during a flight test. Another part shows the drag obtained at the highest Mach number during deceleration in a track test. The remaining data show the drag obtained in wind-tunnel tests during a number of constant Mach-number runs. In summary, the meaning of these data is as follows:

1. A drag coefficient above 1 can be obtained between Mach 1 and Mach 2.

2. At a given set of design conditions, a conventional 10 percent fence model can obtain a drag coefficient from 0.8 to 1.2 between Mach 2 and 3.

The most significant fact concerning the performance results of the Figure 11 data is that the drag coefficient values remain high as the Mach number is increased to 2.5 and higher. This is because the isotensoid design (1) essentially does not change shape, (2) is free of coning instability, and (3) experiences little or no "canopy breathing" as the Mach

REF NO.	TYPE TEST	SYM-BOL	CONFIGURATION	M, DE-PLOY	FENCE HEIGHT (PERCENT)	x/d	D/d
42	1	⌂	3.75-FT DIAM 80-DEG BALLUTE	. . .	10	7.2	3.00
39	2	◇	4-FT DIAM GEMINI BALLUTE	. . .	10	. . .	. . .
44	3	○	5-FT DIAM ADDPEP TB-1B	2.17	10	7.0	3.40
47	2	□	3-FT DIAM GEMINI BALLUTE	. . .	10	3.0	2.04
43	3	◁	5-FT DIAM ADDPEP TB-2	3.25	0	7.0	3.40
41	2	⊐	5-FT DIAM ADDPEP TB-3	. . .	NONE	10.2	3.40
39	2	◺	4-FT DIAM GEMINI BALLUTE	. . .	10	6.0	1.23
38	2	△	22-IN. DIAM ALARR BALLUTE	. . .	10	6.0	1.23

TYPE TEST

1 - TRACK

2 - WIND TUNNEL

3 - FREE FLIGHT

NOTE:

ALL C_D'S ARE BASED ON BALLUTE EQUATOR DIAMETER WITHOUT FENCE. FENCE HEIGHT (PERCENT) EQUALS HEIGHT OF FENCE DIVIDED BY BALLUTE EQUATOR DIAMETER × 100.

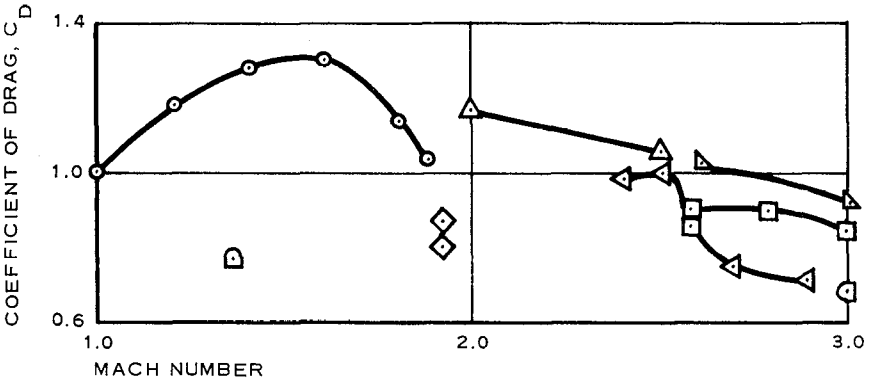

Figure 11 - C_D vs Mach Number for Large-Size Ballutes

number approaches Mach 2.5 or higher and with the subsequent attachment of the main bow shock to the decelerator.

The plots are presented primarily to show the available documented data and to give a brief description of their meaning. Here again, as with the parachute data, a straightforward analysis of the drag variation at a given Mach number cannot be made, since design and performance parameters such as type of model (with various fence sizes and locations), various towline lengths, and the actual test conditions vary widely. Other reasons for drag variation are that Reference 42 data present drag results behind an unsymmetrical sled, and Reference 38 data present drag results behind an unsymmetrical lifting body. It is concluded, therefore, that additional study or testing, or both, will be required to define more completely the effects of the various performance parameters.

However, based on the present available small-size wind tunnel model data presented in Figure 12, a partial description of how some of the parameters affect the supersonic and hypersonic performances can be given as follows:

1. The C_D level (see Reference 49) in free stream between Mach 1.5 and Mach 2.5 varies between 1.3 and 1.35. (These results give useful control-type data and, coupled with the towed decelerator data, indicate payload wake effects that lower the C_D values of an 80 deg Ballute to between 0.8 and 1.0.)

2. Theoretical 70-deg and 80-deg apex angle cone-wave drag values are superimposed on the experimental data to show the general drag trend with increasing Mach number. (The general trend of all data can be seen. Note the rapid decay from Mach 1 to Mach 3 - the upper side of the transonic hump - where the detached bow wave becomes an attached and more oblique shock wave with increasing Mach number.)

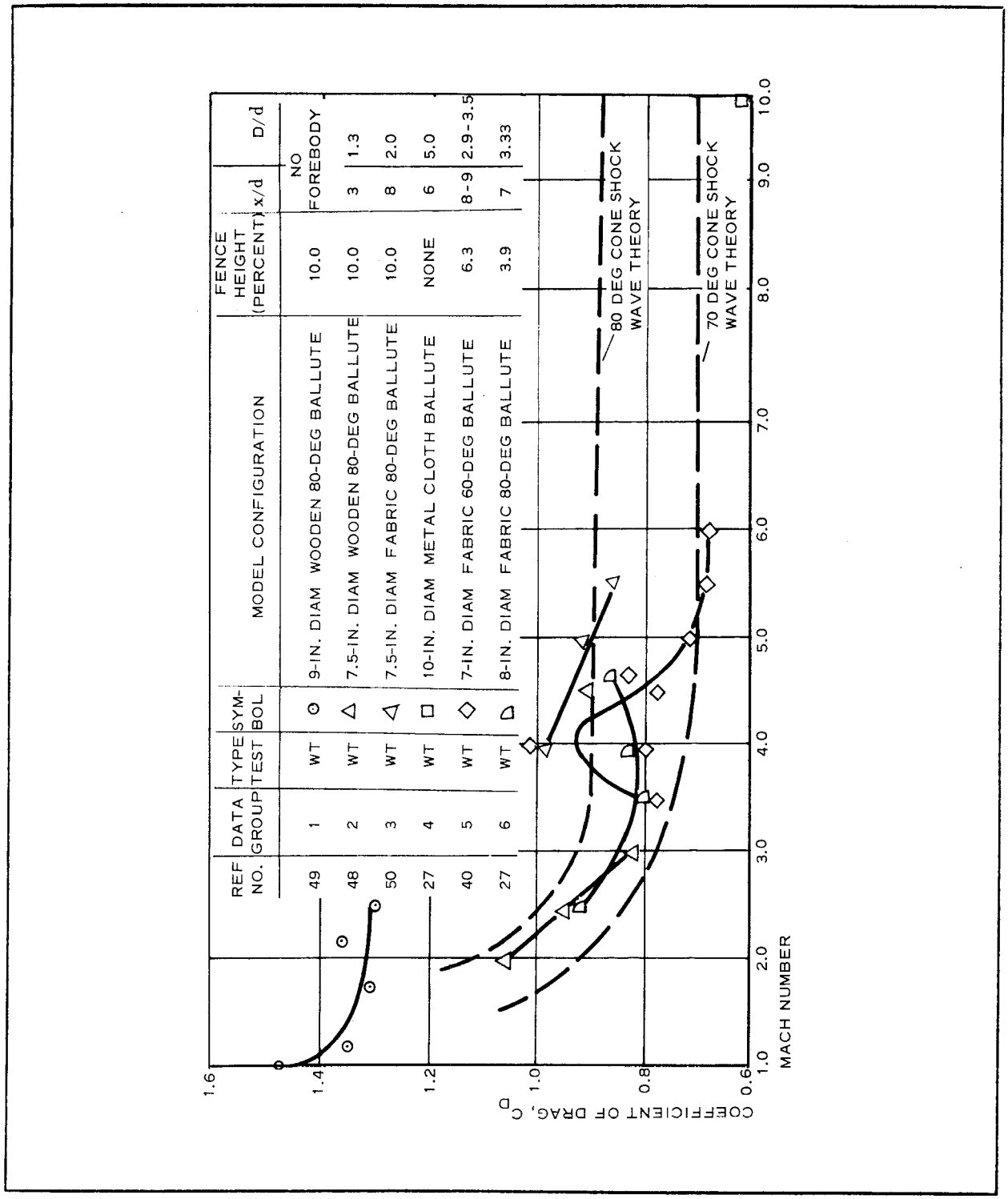

Figure 12 - C_D vs Mach Number for Small-Size Wind-Tunnel Test Ballutes

3. Data point 4 shows the C_D of the flexible, coated, metal-cloth, 80-deg Ballute without a burble fence to be 0.62 at Mach 10.

Since no explanation of the reverse trend (increasing C_D with increasing Mach number) of the C_D of data groups 5 and 6 is known, this should be a void area for further consideration. Furthermore, the reason for the wide dispersion of the drag values of the (group 5) 60-deg Ballute is not clearly understood. It was clear that at a given Mach number a low q value resulted in higher C_D's than at a high q. This would suggest a shape change, which is supported by the fact that this particular decelerator configuration was not an isotensoid design. While the experimental data obtained to date utilizing Ballute decelerators have been the most extensive, there are still voids in the available data. These voids consist of not completely understanding the effects of varying forebody diameter ratios, of varying towline lengths, and of varying apex angle and fence size (for optimization) over a range of Mach numbers and Reynolds numbers.

Figures 13 through 20 from References 2, 3, 26, and 27 present representative results of wind-tunnel drag tests of basic blunt-body geometric shaped decelerators. This type of data is extremely useful since it is generally for basic shapes (cone and sphere), and other experimental data and analytical work are available to aid in an aerodynamic evaluation. Because of the rigidity and stability of these basic shapes, real steady-state flow conditions exist; therefore, more constant and valid drag level measurements can be obtained. (Validity, here, means that these drag data can be used with a higher level of confidence in evaluating the type of flow that did occur for a given set of test conditions, since such varying parameters as model change in shape or model instability are not present to complicate further an already complex flow pattern.)

Figure 13 shows C_D variation with Mach numbers at various towline lengths

for the same 4.88-in. diameter, 80-deg apex angle cone behind two differently shaped forebodies. Based on drag values in Figure 13B, Schlieren photographs, and NACA 1135 flow tables, the following postulation is presented as an example of how the local flow affects decelerator performance:

1. The general C_D decrease (at any of the three towline lengths) with increasing Mach number between Mach 2 and Mach 3.5 occurs primarily because the decelerator bow shock becomes attached and more oblique as the Mach number increases. The net result is a lower pressure rise across the shock and hence lower C_D values.
2. At a given Mach number between 2 and 3.5, the C_D's increase with increasing towline length. This can be explained since (1) the cone is positioned in the far wake (from 8D to 12D); (2) the inner viscous core has the same diameter moving aft; and (3) the inner wake is gradually mixing with the outer wake, the farther aft the decelerator is positioned (the closer to free stream conditions exist), the higher the C_D.
3. The general level of drag values in Figure 13 was approximately the same; even though the payload size and shapes were different, the x/d and D/d's were different. The D/d in Curve B was more than twice the D/d of Curve A. An anticipated higher C_D riser with increasing D/d did not occur. However, the physical distance aft of the payload was approximately the same, and the size and shape of the decelerator were identical in each case, which suggests a wake change with payload shape change.

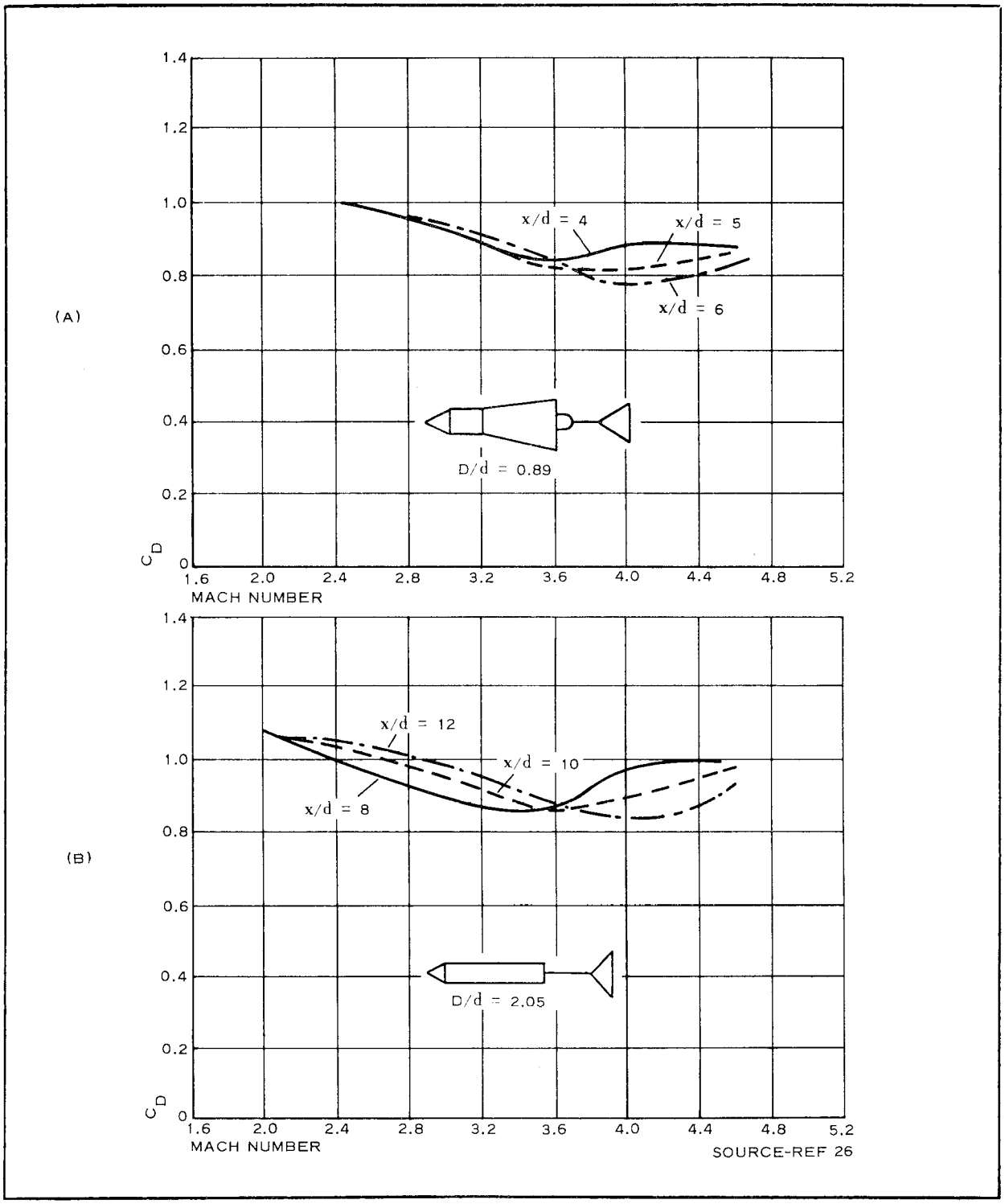

Figure 13 - C_D vs Mach Number for 80-Deg Cone

NOTE

The 8D to 12D location is defined as the "far wake," since at this Mach number range (2 to 3.5), the near wake is between 3D and 5D, which is the portion of the wake immediately aft of the neck and trailing shock location. To complete the definition of the longitudinal wake regions, the base-flow portion of the wake is defined as that region ahead of the trailing shock (in this case, between 0 and 3D aft of the forebody).

Above Mach 3.5, a reverse trend in C_D variation with Mach number and x/d occurs. In fact, at Mach 4.2 and at an x/d of 8, the C_D of 1.0 is obtained, which is the same as the drag of an 80-deg cone in free stream. From a review of the Schlieren movies, the increasing drag with increasing Mach number can be attributed to the following:

1. As the main decelerator bow shock moves aft, the higher local pressure immediately aft of the shock is nearer the cone sides; hence, the higher C_D values are obtained.

2. Boundary layer thickness increases with increasing Mach number; this implies lower local velocities along the cone sides, resulting in higher local pressures and hence increased C_D values. (A quantitative discussion of the boundary layer thickness is not possible because of the complexity of the forebody wake flow that affects decelerator performance. However, qualitatively the combined effects at a high Mach number, which consist of (1) higher energy flow, (2) varying flow angles (which vary

local Reynolds and Mach numbers) and (3) complex shock-boundary layer interaction (which suggests turbulent boundary-layer conditions along the cone sides) result in higher C_D values.

The lower C_D values with increasing towline length above 8D at Mach numbers above 3.5 can be attributed to the divergence of the inner viscous core aft of the near wake region. Although mixing of the inner and outer wake tends to increase the local pressures moving aft, the final result is a decrease in local pressure. One explanation for the lowering of the energy level moving aft is the effect of the core diameter squared. Hence, the transverse growth $\pi(y)^2$ of the inner core (with the resulting decreasing local pressures) is a squared function compared to the linear increase in longitudinal position aft (x) - resulting in increasing pressure and the subsequent mixing of the inner and outer wake.

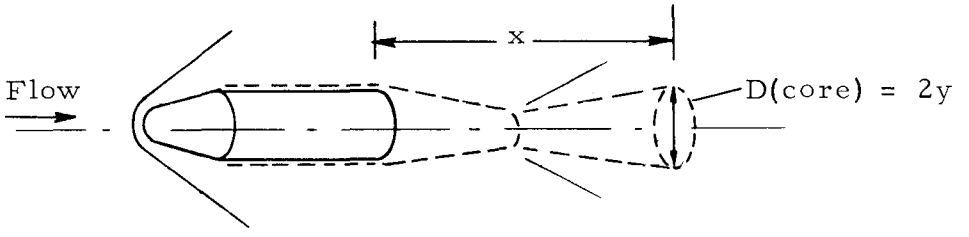

Figure 14 shows the effect of towline length on the C_D for a greater range of x/d's. The sharp drop in the C_D (see Figure 14) at x/d's less than 4 is due to the divergence of the base-flow portion of the forebody wake because of the presence of the decelerator near the forebody. A $C_D = 0.6$ is obtained as close as an x/d of only 1. This was because the diameter of the decelerator was almost three times the diameter of the forebody base, causing the flow over the forebody and decelerator to be approximately the same as a single forebody-flare combination. Unfortunately, since the experimental data in Figures 13 and 14 are limited to one size of rigid cone, experimental data on the effect of size is a void that will require future work. In spite of the data shortage, a review of Figures 13 and 14 reveals that when the diameter ratio is small and the towline length

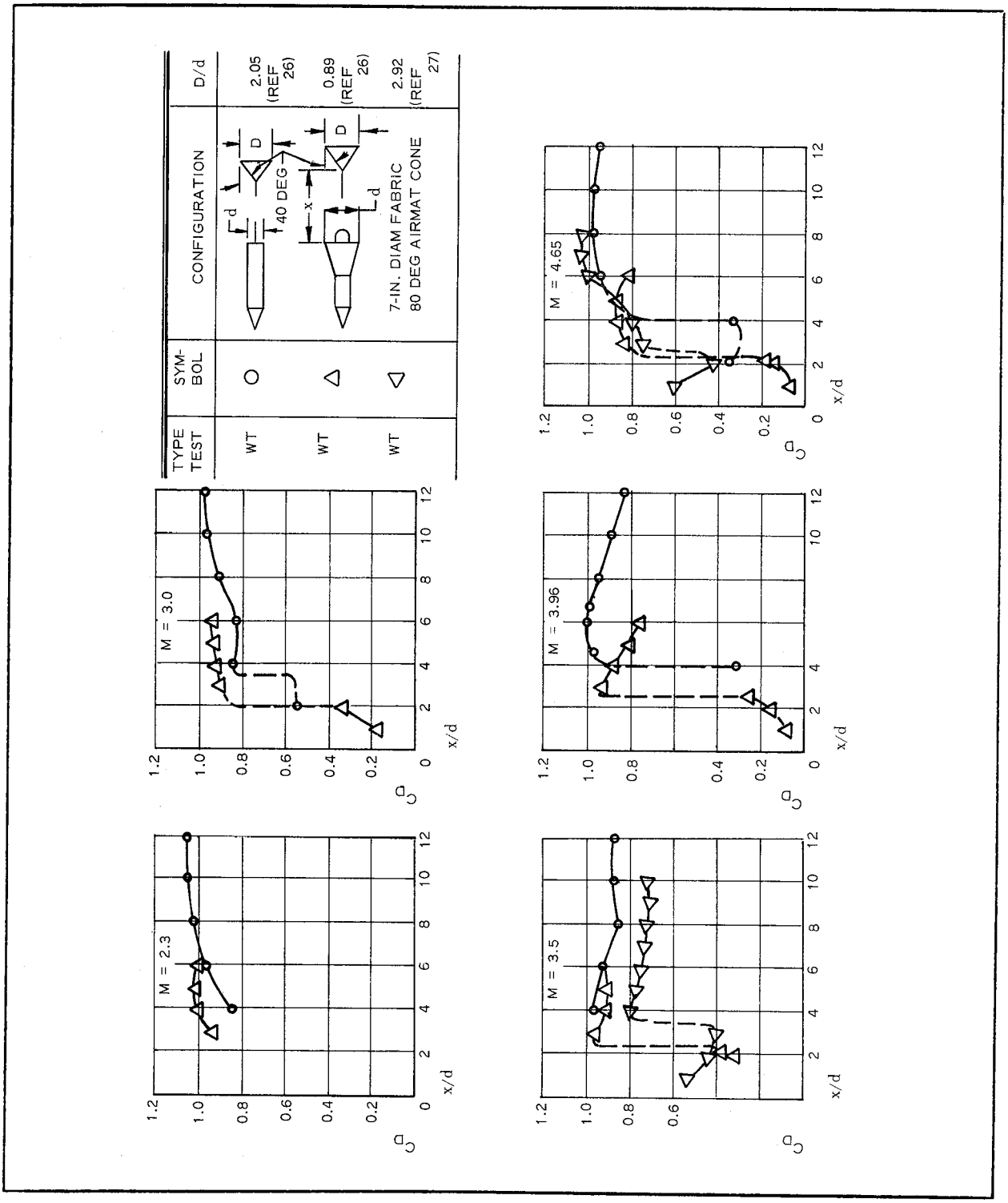

Figure 14 - C_D vs x/d for 80-Deg Rigid Cone

is short the drag drops off as wake effects of the reverse flow regions appear. Anticipated higher C_D's with larger diameter ratios did not occur consistently, which substantiates the need for more experimental testing.

Figure 15 presents available C_D versus Mach-number data for various half-angle cones in the free stream. These wind-tunnel drag results represent only the nose-pressure portion of the total drag. Superimposed on this figure are the C_D levels obtained from the Newtonian flow theory. These experimental data clearly show the amount of increase in C_D with increasing apex-angle geometry. Here again, the void of data above Mach 5 is evident. Comparing this data with total drag values clearly reveals that the major portion of the total drag is obtained from bow-wave nose drag during operation above Mach 1.

In addition to their academic value, these basic cone data can be used to evaluate the performance of various decelerator concepts (see Table I) as follows:

1. To forecast the performance of the basic single body attached system
2. To serve as "control" data for towed cones

Figure 16 presents additional C_D data similar to the Figure 15 free-stream cone data, with the added parameter of spherical nose-bluntness variation. The data show the nose radius of between 1/2 and 1.0 of that of the cone base radius. The variation in C_D with nose bluntness is negligible.

One of the obvious uses of these data is to exploit a more rounded decelerator to lower the aerodynamic heating level at a minimum expense of aerodynamic drag and stability. With the exception of a few points of data at Mach 9, the void of hypersonic data in Figure 16 is evident.

Figures 17 and 18 present towed sphere drag data similar to the Figure 13 towed cone data for 8- and 4-in.-diameter spheres. Figures 19 and 20 show the increase in C_D with increasing sphere size versus Mach number

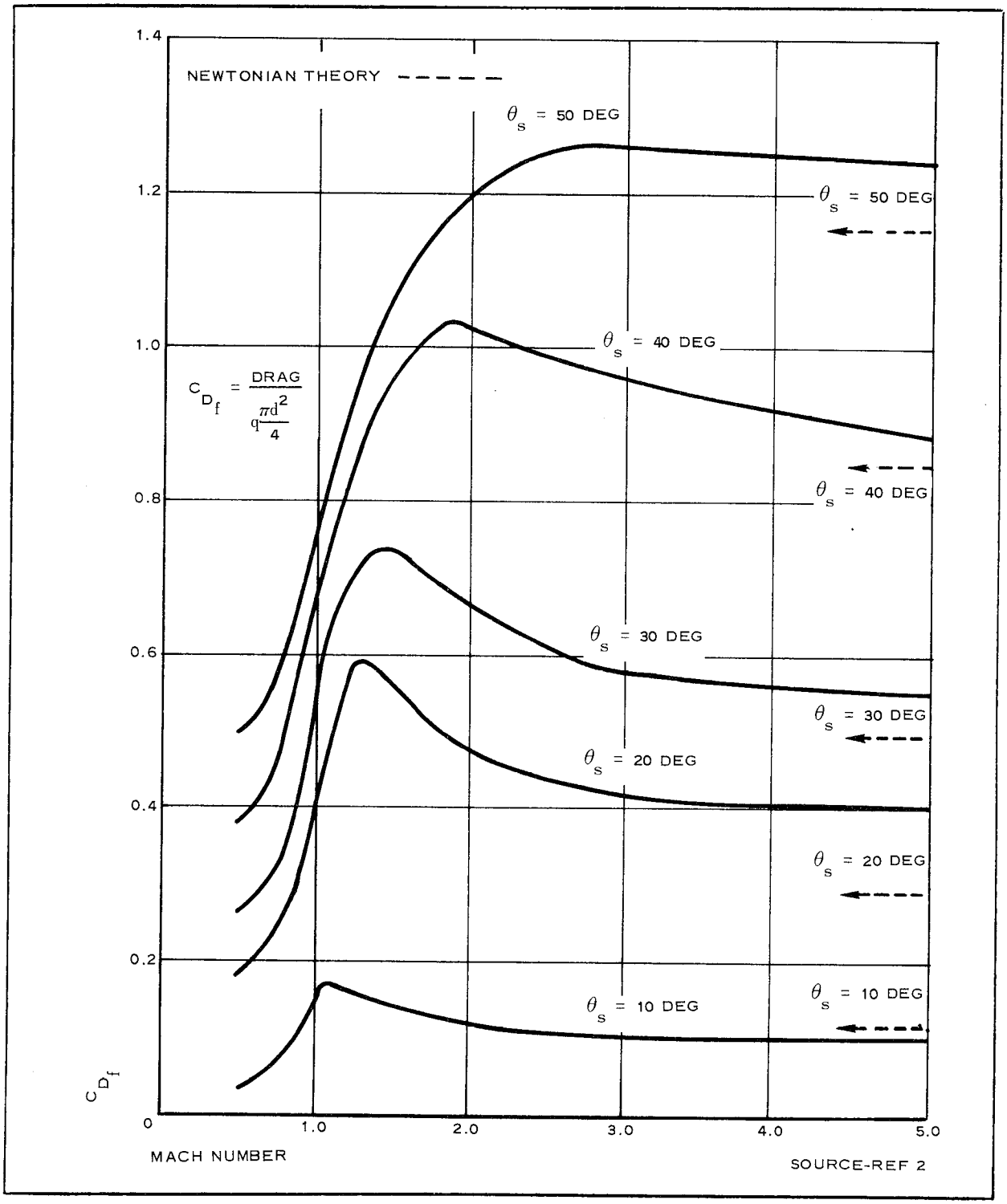

Figure 15 - Free-Stream Cone Data vs Mach Number

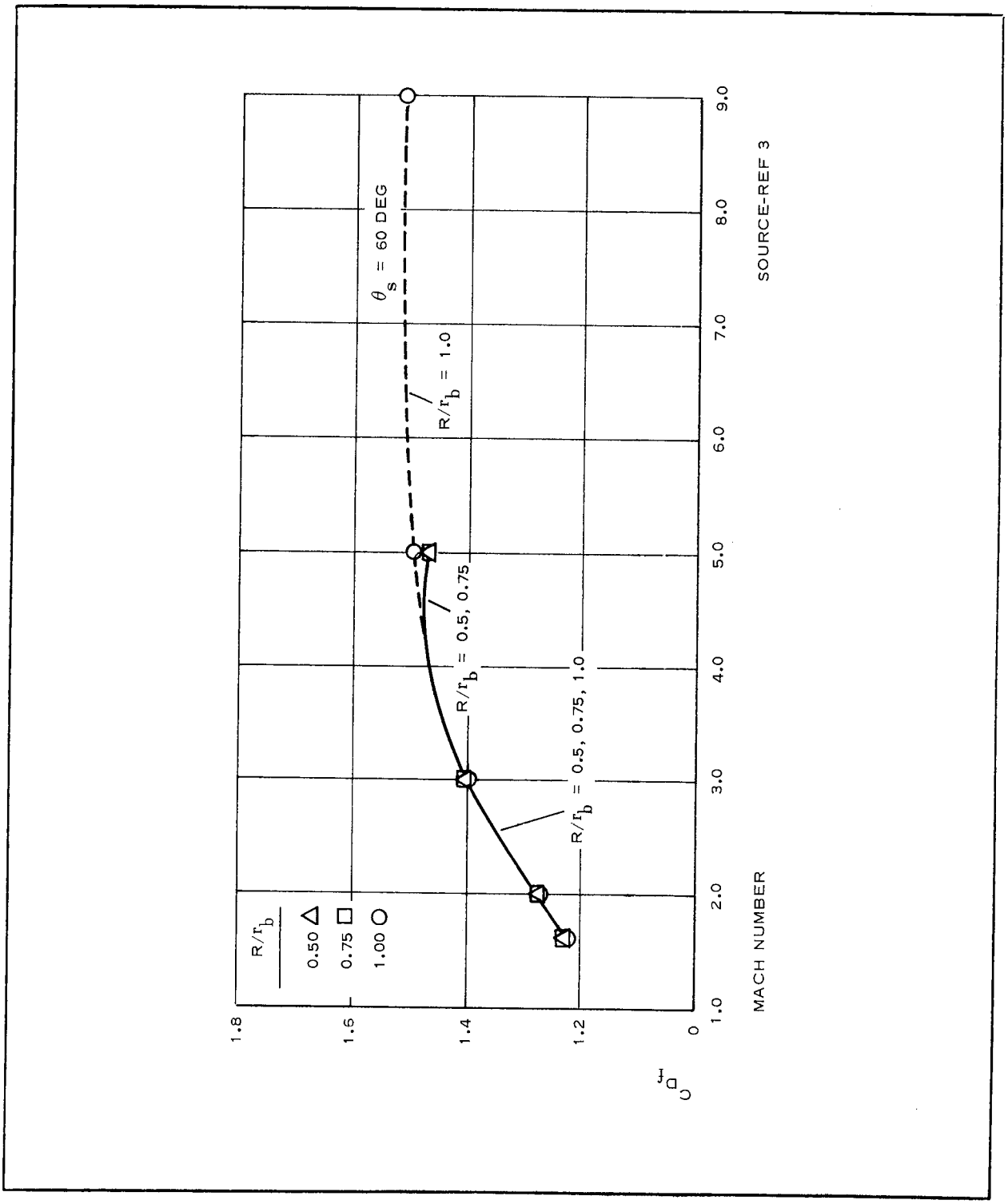

Figure 16 - Axial Nose Drag Coefficient vs Mach Number

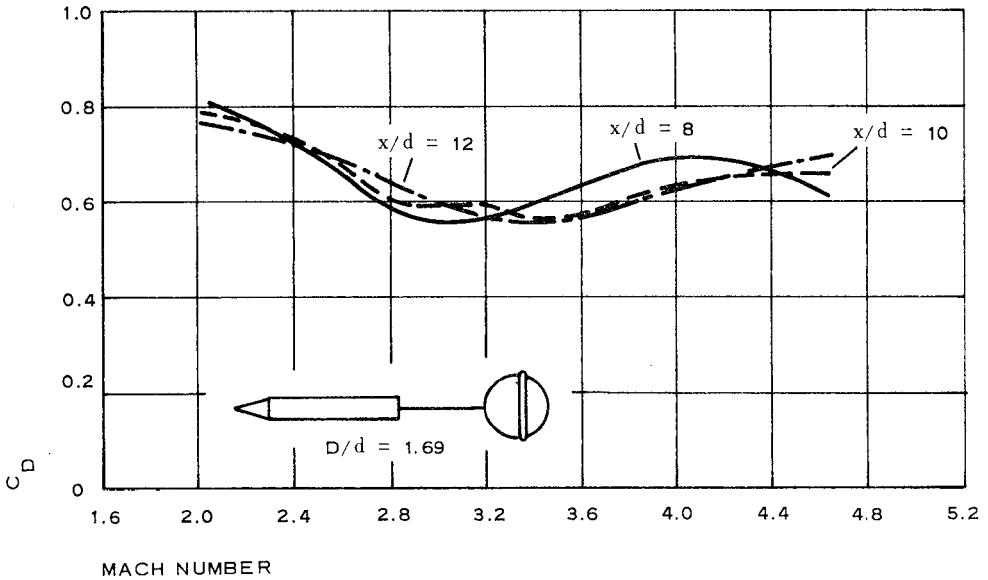

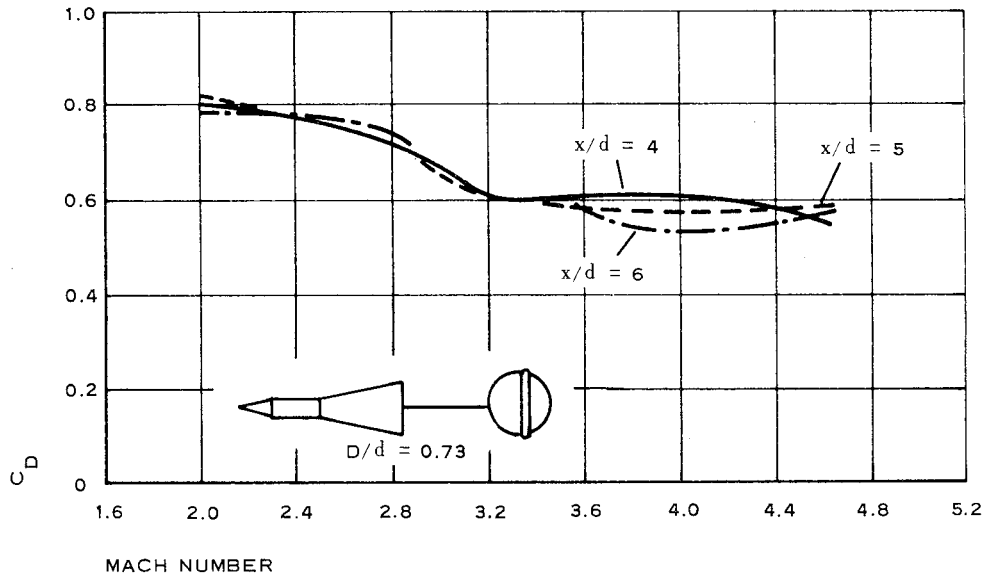

SOURCE-REF 26

Figure 17 - Sphere C_D vs Mach Number (8-In. Model)

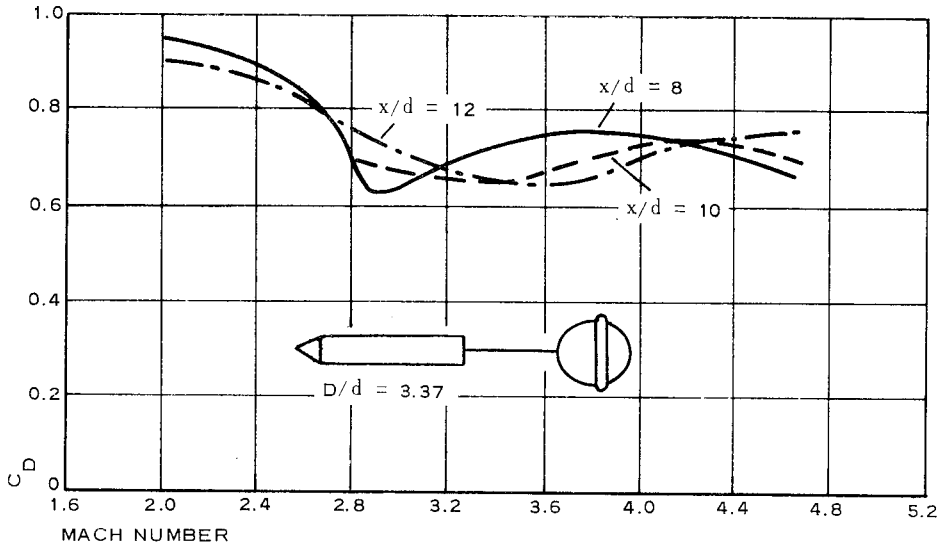

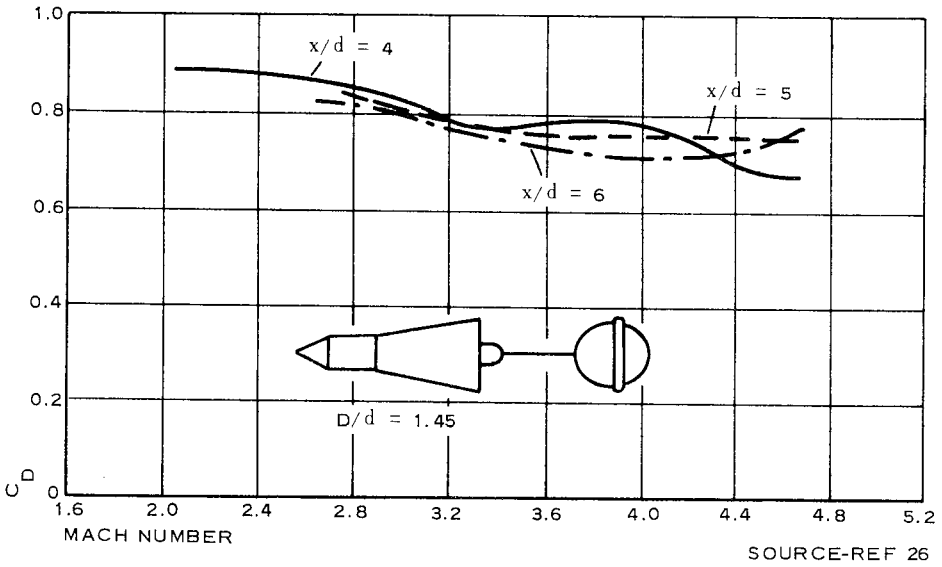

Figure 18 - Sphere C_D vs Mach Number (4-In. Model)

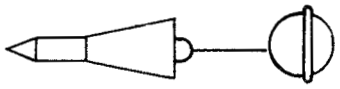

TYPE TEST	SYM-BOL	MODEL CONFIGURATION	x/d	D/d
WT	○	4-IN. DIAM SPHERE, 3.9 PERCENT FENCE	6	0.73
WT	△	6-IN. DIAM SPHERE, 3.9 PERCENT FENCE	6	1.09
WT	◁	8-IN. DIAM SPHERE, 3.9 PERCENT FENCE	6	1.45

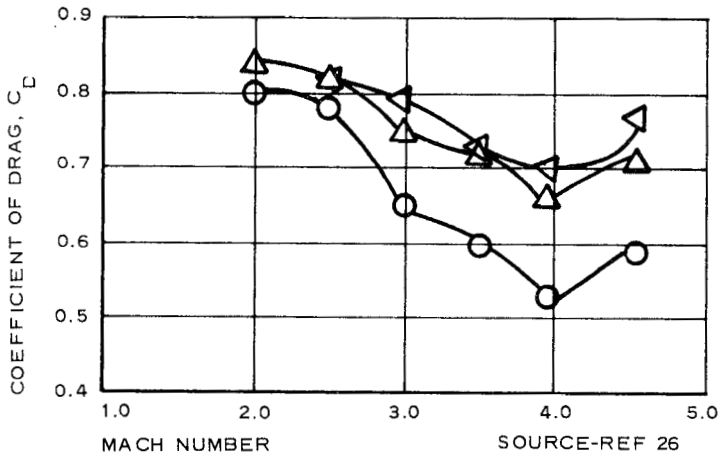

Figure 19 - C_D vs Mach Number for Sphere behind Flared Body

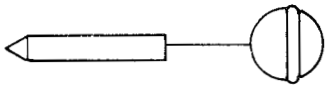

TYPE TEST	SYM-BOL	MODEL CONFIGURATION	x/d	D/d
WT	○	4-IN. DIAM SPHERE, 3.9 PERCENT FENCE	6	1.69
WT	△	6-IN. DIAM SPHERE, 3.9 PERCENT FENCE	6	2.53
WT	◁	8-IN. DIAM SPHERE, 3.9 PERCENT FENCE	6	3.37

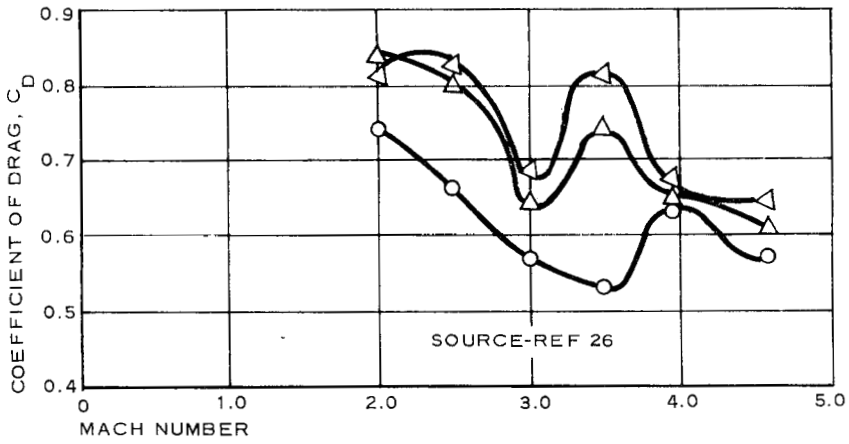

Figure 20 - C_D vs Mach Number for Sphere behind Cylindrical Body

at an x/d of 6. In each figure the expected increase in C_D with increasing D/d did occur. However, the similar C_D levels in each figure, in spite of Figure 20 D/d values being over twice the Figure 19 values, suggest the payload shape also affects the drag-producing capabilities of a given decelerator (see Figure 13). Here again, more detailed work is required on a number of payload and decelerator shapes (cones, spheres, Ballutes) to understand fully how these parameters affect performance.

Figure 21 presents C_D versus Mach-number data for a free-stream sphere. These results were obtained in ballistic-range tests reported in Reference 30, which are in good agreement with wind-tunnel tests reported in Reference 10. The free-stream C_D level in Figure 21 is higher than the towed-sphere C_D level given in Figures 17 through 20.

Figure 22 presents the only C_D data found from the survey of experiments above Mach 10. These super-hyper free-stream sphere drag data were obtained during wind-tunnel tests between Mach 11 and Mach 65. Tests at increasing Mach numbers showed increasing C_D in the transition regime

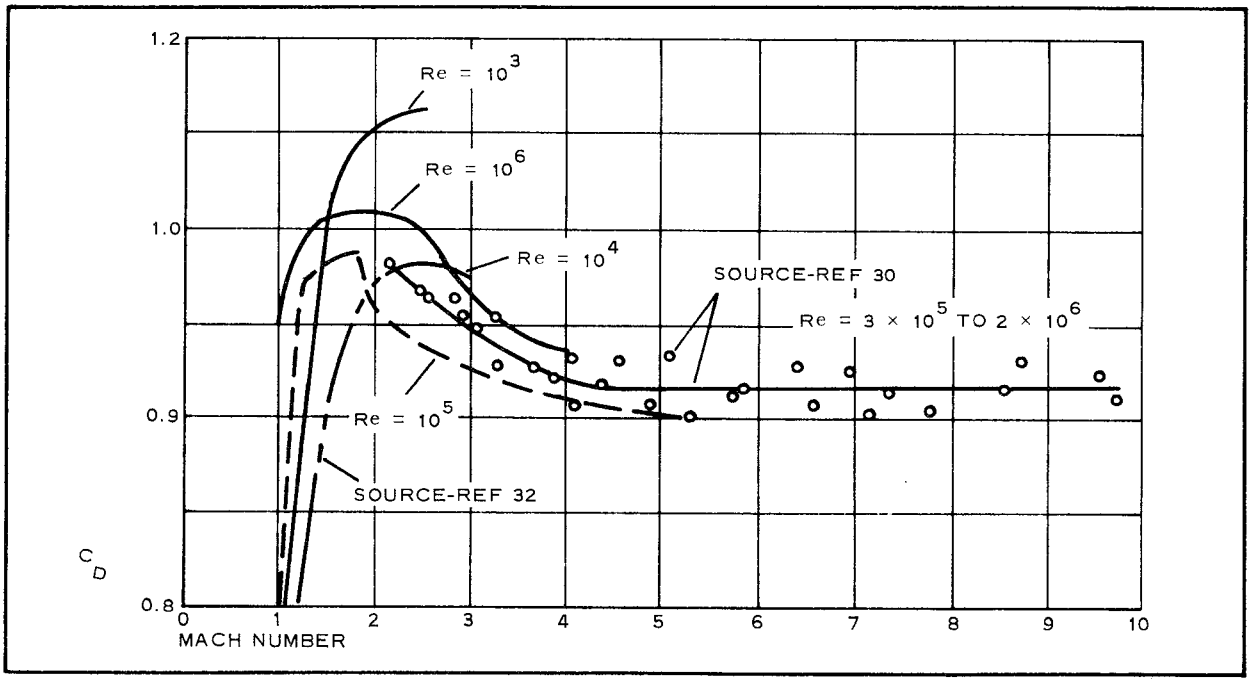

Figure 21 - C_D vs Mach-Number for Spheres at Various High Reynolds Numbers

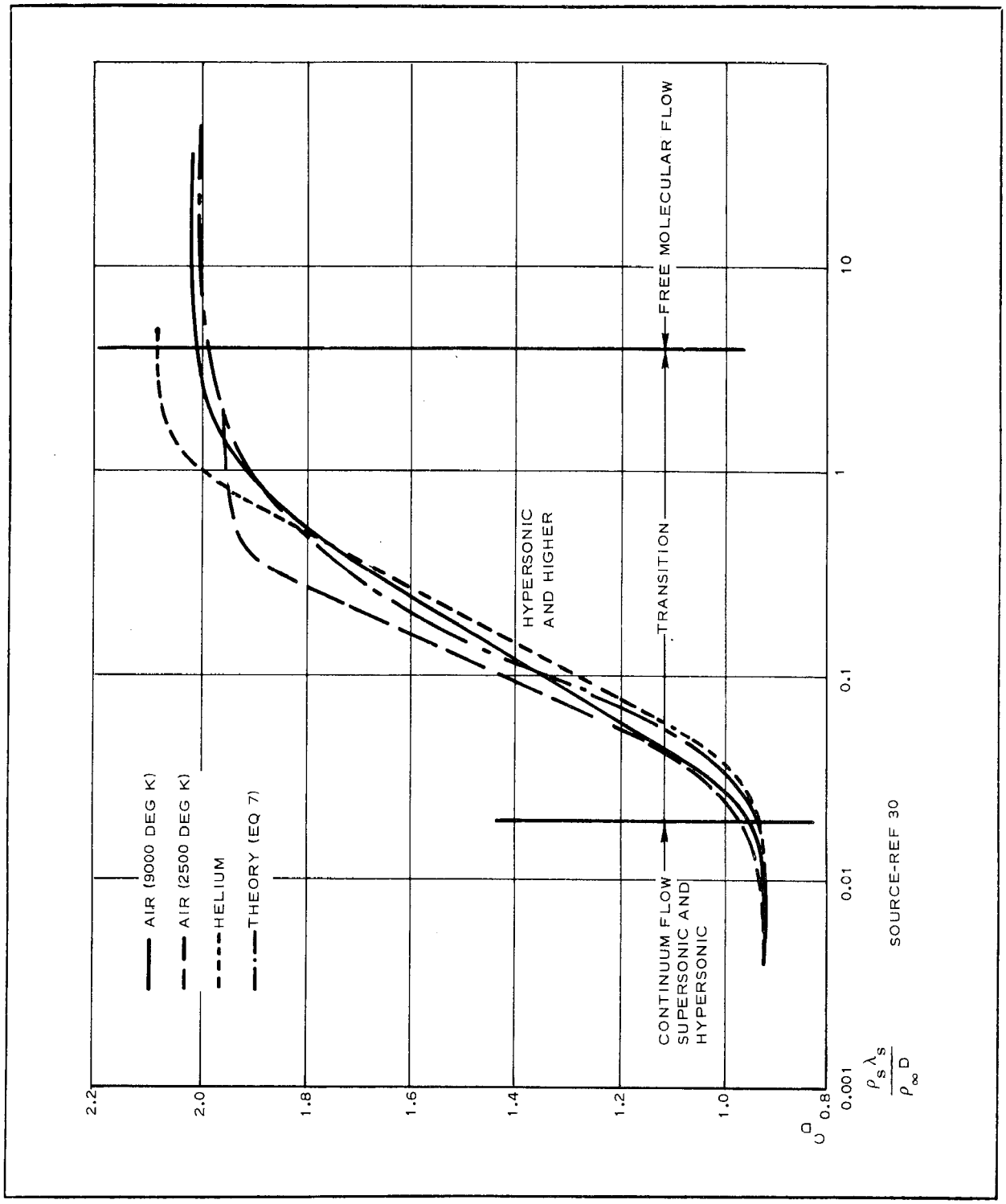

Figure 22 - Correlation of Sphere Drag Coefficients

between continuum flow and free molecular flow. The C_D value of more than twice that of a sphere below Mach 10 is significant. This phenomenon should be exploited, not only to forecast a more accurate re-entry trajectory but also to show either a weight saving due to a smaller-size decelerator or improved performance for the same size.

d. Attached Nonporous Decelerators

Figure 23 presents available hypersonic C_D data versus flare angle from wind-tunnel tests of a basic flared-skirt decelerator configuration. The significance of these data can be summarized as follows:

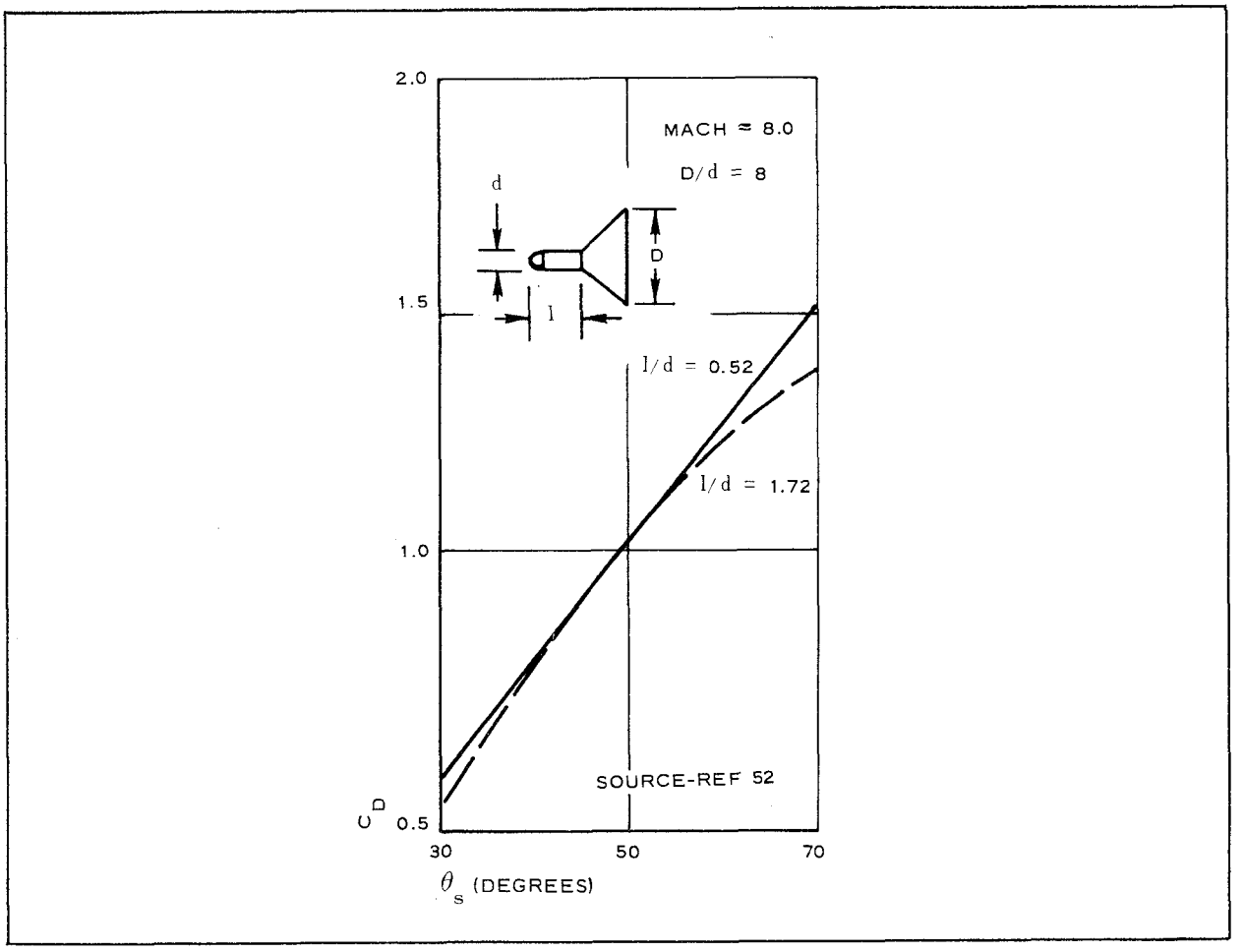

Figure 23 - C_D vs θ_s for Flared Body

1. It is for a decelerator configuration that has a large base diameter in relation to the payload diameter, which is directly applicable for high drag and stable re-entry and recovery.

2. It can be considered to apply for a zero towline-length decelerator.

The available data found in this survey of the flared-skirt configuration are limited to Mach 8 and to aerodynamic models. Since these data are limited to only one Mach number, three flare angles, and two forebody sizes, additional effort clearly is required over a wider range of flight conditions and configuration sizes.

e. Transient and Fluctuating Loads

Compared with the data presented in Figures 5 through 23, considerably less supersonic experimental data are available to document transient loads during decelerator deployment. This data void can be attributed to a basic lack of understanding of the dynamics of the system as well as to instrumentation limitations. In the past few years, the operation of test facilities has improved because of new equipment and improved operating procedures. Table XI presents data for representative porous and nonporous decelerator transient loads during deployment, inflation loads, and the fluctuating loads after decelerator inflation. The data in Table XI were limited to results of decelerator tests that were representative and performed satisfactorily. Results considered unsatisfactory were those for tests in which the models failed before data could be obtained or the measured oscillating-load variation was near or more than 100 percent of the mean load.

All tests used a tensiometer, located in the riser line between the payload and the towed decelerator, to measure the instantaneous transient and steady-state loads. In each of the 15 tests shown in Table XII, the decelerator was forcibly deployed from its stowed position in a payload by either a pyrotechnic or a spring-thrusting mechanism. For such tests,

the stowed decelerator is held in its packed condition in a deployment bag as it moves aft to the "line-stretch" condition. At this time, the "snatch load" occurs as the fully extended riser line causes the decelerator to slow down to the speed of the payload; the deployment bag is released from the decelerator, and the decelerator being to inflate. Usually at the instant of full inflation, the opening-shock load occurs. If the system operates as designed, the opening-shock load is the peak load that decelerator feels during its operating life. Since this opening-shock load must be known so that structural strength can be designed into a decelerator system, the lack of this type of experimental data is a major void in the state of the art of decelerators.

Table XI shows that the peak load during deployment was the opening-shock inflation load in all but two tests. Of these exceptions (test items 6 and 10), line-first deployment did not occur since the deployment bag inadvertently was released from the decelerator and the decelerator began to inflate before line stretch occurred. This resulted in loads due to snatch that were higher than the opening shock loads.

The significant results of the Table XII test data can be summarized as follows:

1. The Ballutes are essentially free of breathing and coning.
2. The parachutes experience breathing and coning.
3. The decelerators that had longer filling times experienced lower opening-shock loads.
4. Data are available that demonstrate successful deployment and inflation of both textile and metal cloth models.

Wind-tunnel test examples of the levels of parachute and Ballute breathing and coning or the lack of it are given in Figures 24 through 27. Figures 24 and 25 present data obtained with two types of recording equipment.

TABLE XII - DECELERATOR TEST RESULTS

Model and test condition				Transient opening conditions								Steady-state loads				Reference	Model reference designation	Remarks
				Snatch load			Opening load											
Description	Type of test*	M	q (psf)	Load (lb)	Time (sec)	Type of reading	Shock factor	Load (lb)	Time (sec)	Filling time (sec)	Type reading	Average load (lb)	Load fluctuation from average, Δ (lb)	Fluttering frequency (cps)	Coning frequency (cps)			
Hyperflo, 4-ft D_o	WT	2.6	120.4	. . .	. . .	Oscillograph	2.13	700	. . .	. . .	Oscillograph	328	. . .			AEDC-TDR-64-120	H-1	A_i/A_e = 3.20; suspension line failed after 3 min
Hyperflo, 4-ft D_o	WT	2.6	120.6	. . .	. . .	Oscillograph	. . .	. . .	. . .	. . .	Oscillograph		. . .	50		AEDC-TDR-64-120	H-2	A_i/A_e = 4.20; suspension line failed after 2 min
Hyperflo, 4-ft D_o	WT	2.5	119.7	550	0.02	Oscillograph	2.42	800	0.07	. . .	Oscillograph	331	. . .			AEDC-TDR-64-120	H-3	
Parasonic, 4-ft D_o	WT	2.6	120.0	500	0.008	Oscillograph	1.46	562	. . .	. . .	Oscillograph	385	. . .			AEDC-TDR-64-120	H-7 (SP-3)	At t = 0.21 sec, load = 440 lb + 250; at t = 0.55 sec, load = 440 lb + 100. Configuration failed at t = 4^+ min (A_i/A_e = 3.75)
Hyperflo, 2.72-ft D_o	WT	2.6	120.0	120	0.05	Oscillograph	5.00	930	0.1	. . .	Oscillograph	186	± 30 to ± 60			AEDC-TDR-64-120	H-8	Model in tunnel 22 min
Hyperflo, 3.69 D_o	WT	2.2	249.0	2100	0.02	Oscillograph	1.78	1250	0.19	0.17	Oscillograph	702	± 192 to ± 375			AEDC-TDR-64-120	H-12	Model in tunnel 28 min
Gemini Ballute 3-ft diam	WT	2.59	120.7	450	0.02	Oscillograph	1.37	1000	0.21	0.19	Oscillograph	729	± 50		0	AEDC-TDR-64-120	. . .	Model spinning occurred after inlet cord failed; model in tunnel 23 min; no coning
Parasonic, 4-ft D_o	WT	2.2	120.0	470	0.02	Beckman	1.62	650	0.11	0.09	Beckman	401	± 120 to ± 270	80	8.9	AEDC-TR-65-57	H-1 (SP-3A)	A_i/A_e = 3.62 Roof failed
Hyperflo, 4-ft D_o	WT	2.6	120.3	1110	0.0075	Beckman	2.74	746	0.075	0.0675	Beckman	241 to 306	± 120 to ± 240	80	8.0		H-3	A_i/A_e = 4.3
Parasonic, 4-ft D_o	WT	2.6	120.1	600	0.055	Beckman	2.13	815	0.18	0.125	Beckman	383	± 36 to ± 216	80	8.95		H-5 (SP-7)	A_i/A_e = 4.7
ADDPEP Ballute 5-ft diam	WT	3.01	120.5	1340 890	0.11 0.235	Beckman Oscillograph	. . .	1600	1.34	1.0	Oscillograph	1042	± 36	80	0			Ballute TB-3 (unpublished PWT tests 12/64, no coning
ADDPEP Ballute 5-ft diam	FF			1200	0.2	Telemetry	0.66	4880	. . .	1.0						GER-11665	TB-1B	
Hemisflo, 4.12 D_o	FFT	3.42	140.0	. . .			2.35	. . .	. . .	. . .								
Parasonic, 5.5 D_o	WT											720	± 180					
ADDPEP 5-Ft diam Ballute	WT	2.8	120	2175		Oscillo.				$0.65^\dagger$		1675						No failure during test of high-temperature, metal-cloth Ballute

*Types of test: FF = free flight; WT = wind tunnel.

†Filling time accelerated by alcohol and water vapor.

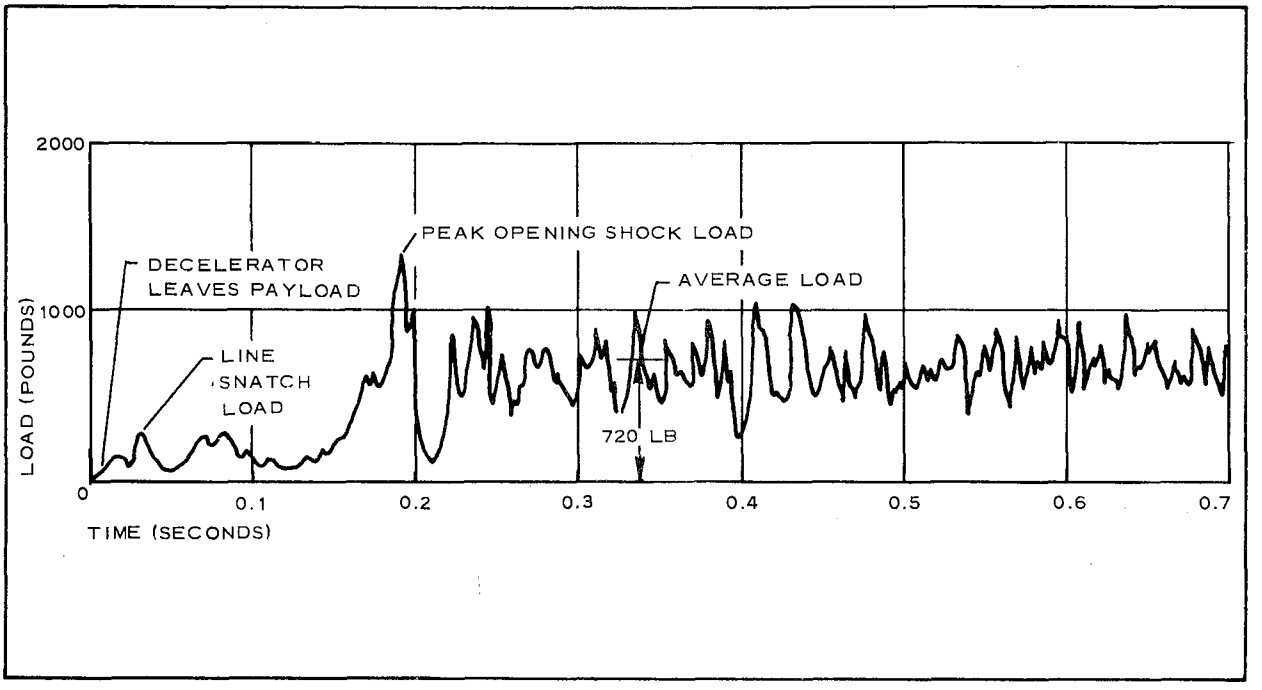

Figure 24 - 5.5-Ft D_o Parasonic (Oscillograph - Instantaneous Load vs Time); See Table XI, Item 14

Figure 24 data was obtained with an oscillograph record and Figure 25 data obtained with a Beckman instrument. Beckman instruments are more accurate for measuring near instantaneous load values than the oscillograph. However, the Beckman records data for very short periods. The oscillograph can record the data continuously and also indicate such sequences as deployment initiation and movie camera start. The oscillograph record also can be read immediately after it records, while the Beckman data must be reduced. This data reduction takes hours.

These traces of the actual records indicate the degree canopy breathing (amplitude and frequency). In addition, the high peaks that occur every 0.2 sec indicate the relative degree (amplitude) of coning. This data is supposedly "steady-state" data. Figure 26 presents Beckman results of a 4-ft D_o Hyperflo.

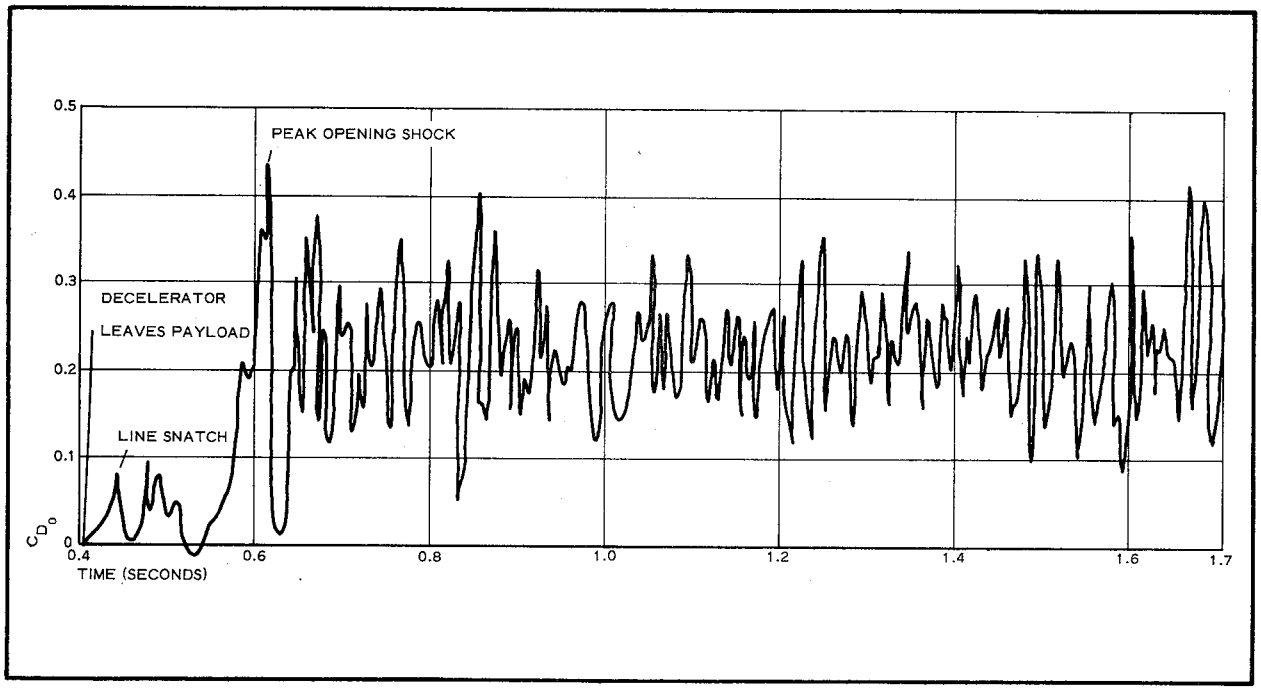

Figure 25 - 5.5-Ft D_o Parasonic (Instantaneous C_{D_o} vs Time); See Table XI, Item 14

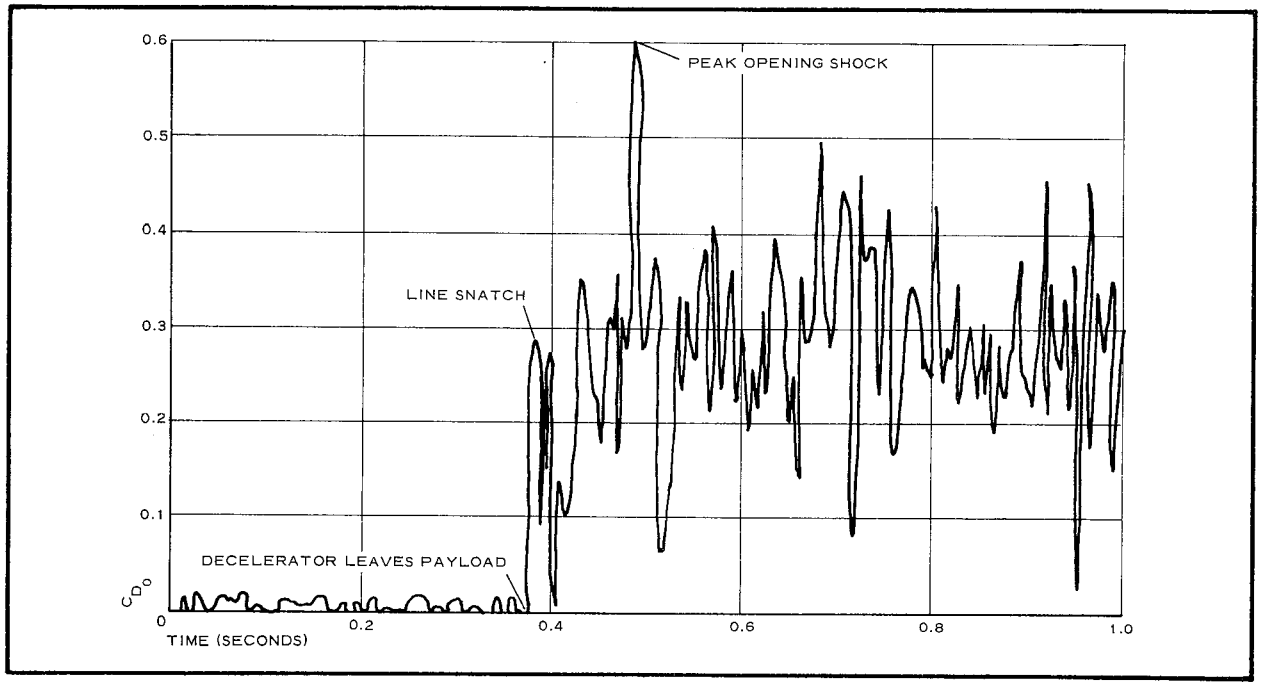

Figure 26 - 4-Ft D_o Hyperflo (Instantaneous C_{D_o} vs Time); See Table XI, Item 9

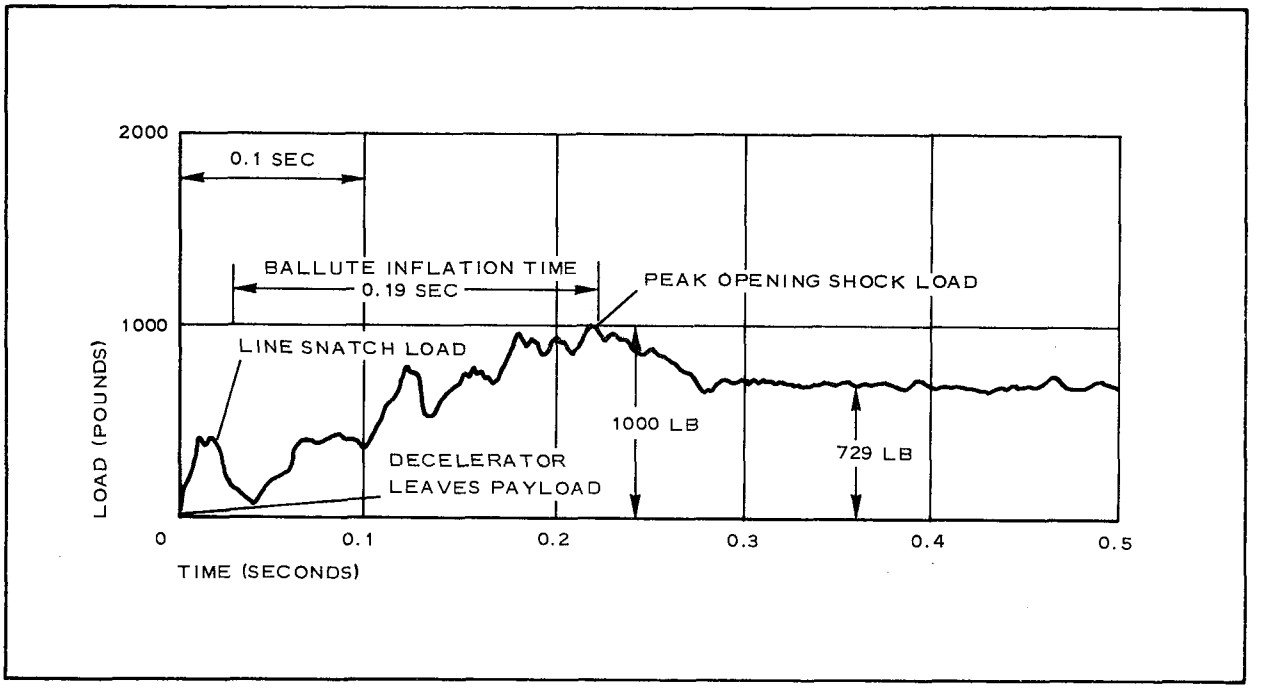

Figure 27 - 3-Ft Diameter Ballute, Load vs Time (See Table XI, Item 7)

Figure 27 also presents a trace of the actual oscillograph record of Ballute test loading variation encountered. Note the relatively smooth trace after model inflation indicating negligible breathing and coning. After model inflation, the relatively smooth trace is under a steady-state condition.

5. AERODYNAMIC STABILITY

a. General

For the purpose of determining stability, aerodynamic decelerators can be broadly classified into two categories. The first category includes those that are attached to the payload, the second includes those that are towed behind the payload. For an attached decelerator (flares, extended flaps, etc.), the current airplane-type static and dynamic coefficients are adequate for determining stability; however, these coefficients do

not appear adequate for a towed decelerator, because of the complex flow field that it separates and the towline influence.

b. Attached Decelerator System

Goodyear Aerospace's survey determined that there is no documented, quantitative, experimental dynamic-stability data available for any concept shown in Figure 3. The only stability data found were static stability data for a cone or flared skirt.

Extensive wind-tunnel tests have been run on flared bodies; however, most of the data from these tests are applicable only to flares with small flare angles, which are intended to be used to stabilize re-entry bodies and missiles. Most of these experimental data were considered unrelated to flared skirts used as decelerators. Only three wind-tunnel tests (see References 51, 52, and 53) present data for flares of sufficiently large flare angles and frontal area.

Reference 52 shows that static stability is reduced with flare-angle increase and that stability rises with forebody-length increase, as flare-to-forebody frontal area is held constant.

Reference 51 shows that static stability is reduced as flare angle increases, with flare length held constant, for both conical and hemispheric nose forebodies; stability is increased with forebody elongation and flare-angle increase, as flare length is held constant.

Apparently, there is a complete void in experimental dynamic stability data of flared bodies.

c. Towed Decelerator System

Information previously has been limited to visual observations of decelerators under towed conditions. The only data available to date on devices that might be considered towed decelerators are dynamic and static coefficients of these devices sting mounted under free-stream conditions (see Figures 28 and 29).

Static stability variation with Mach number for cone semiapex angles from 20 deg to 50 deg is shown in Figures 28 and 29. These curves are based completely on experimental data at small angles of attack from References 2, 4, 5, 6, 11, 12, and 74 through 77. C_{N_α} is shown to be positive and increases with the cone half angle; the static center of pressure moves rearward, indicating that cones with large apex angles are very stable statically. The distance from the cone apex to the static center of pressure from Newtonian theory (see References 11 and 74) is

$$X_{cp} = \frac{2}{3}(1 + \tan^2 \theta_s)\ell, \text{ where } \ell \text{ is the cone length .}$$

The damping capability of either a ballistic or lifting vehicle is greatly affected by C_{L_α}, which is important to the damping of the longitudinal short-period mode (see Reference 5). Both theory and experiment show that, as cones become shorter (high θ_s), the lift-curve slope decreases until it reaches zero at θ_s = 45 deg. At higher semiapex angles, C_{L_α} is negative.

Although stability is well defined statically, little is known from dynamic-stability tests. References 4, 74, and 77 present damping characteristics for cones at very low speeds and at Mach 6.8 (hypersonic).

Reference 74 presents results of comprehensive stability wind-tunnel tests on a cone of θ_s = 12.5 deg at Mach 6.8 and the damping moment coefficient derivative transfer equation

$$(C_{M_q} + C_{M_{\dot\alpha}})_1 = (C_{M_q} + C_{M_{\dot\alpha}})_2 + (C_{N_q} + C_{N_{\dot\alpha}})_2 \frac{X_{1-2}}{\ell} - C_{M_{\alpha_2}} \frac{X_{1-2}}{\ell} - C_{N_{\alpha_2}} \frac{X_{1-2}}{\ell}^2$$

where subscript 1 refers to the longitudinal position about which the damping coefficient derivative is desired, subscript 2 refers to the longitudinal position about which all of the above coefficient derivatives are known, and subscript 1-2 refers to the longitudinal distance between the respective points.

Where

C_M = pitching moment coefficient, $M/q_\infty Sd$

$C_{M_q} = \partial C_M / \partial (\frac{2V}{q'd})$

$C_{M_\alpha} = \partial C_M / \partial \alpha$

$C_{M_{\dot\alpha}} = \partial C_M / \partial \dot\alpha$

C_N = force coefficient normal to body axis, $N/q_\infty S$

$C_{N_q} = \partial C_N / \partial (\frac{2V}{q'd})$

$C_{N_\alpha} = \partial C_N / \partial \alpha$

$C_{N_{\dot\alpha}} = \partial C_N / \partial \alpha$

X = longitudinal distance

ℓ = body length and/or reference length

q = pitch rate

q_∞ = free-stream dynamic pressure

V = velocity

S = projected area ($\pi/4\ d^2$)

d = reference diameter.

Three sets of data were taken about three different centers of moment. Since data from two centers of moment are required, this test provides three sets of moment data for equation (2) for transferring $C_{M_q} + C_{M_{\dot\alpha}}$ to any other moment center.

These were used to make a triple check of $C_{M_q} + C_{M_{\dot\alpha}}$ about the cone base. Correlation was very poor and is not presented here. Either small errors in the test data are magnified by the transfer equation (2) or, as is suspected, the equation is incorrect for large moment-transfer distances because of the assumption that C_{N_q} is invariant with moment center. A

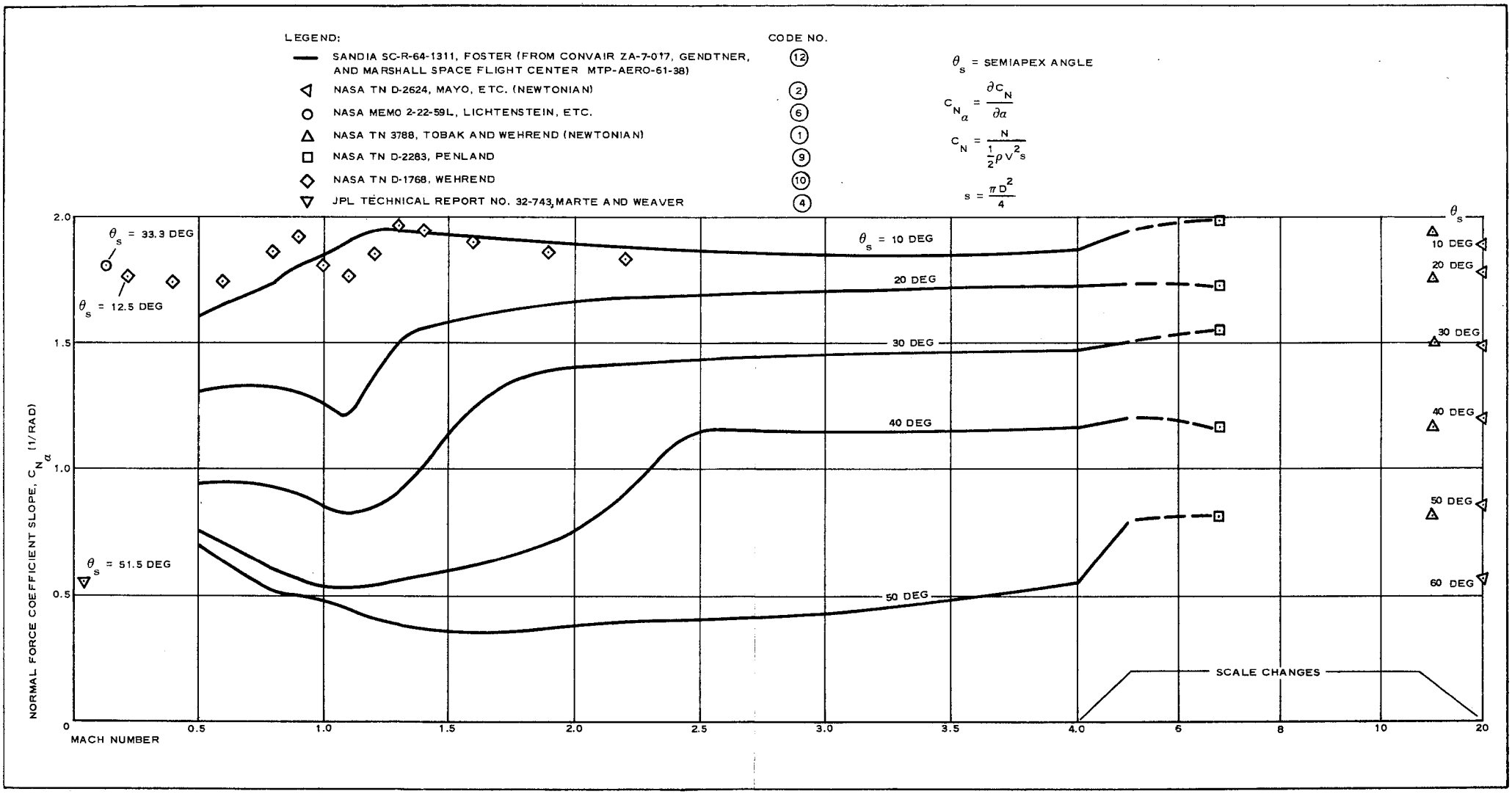

Figure 28 - C_N vs Mach Number for Cones

77-A

77-B

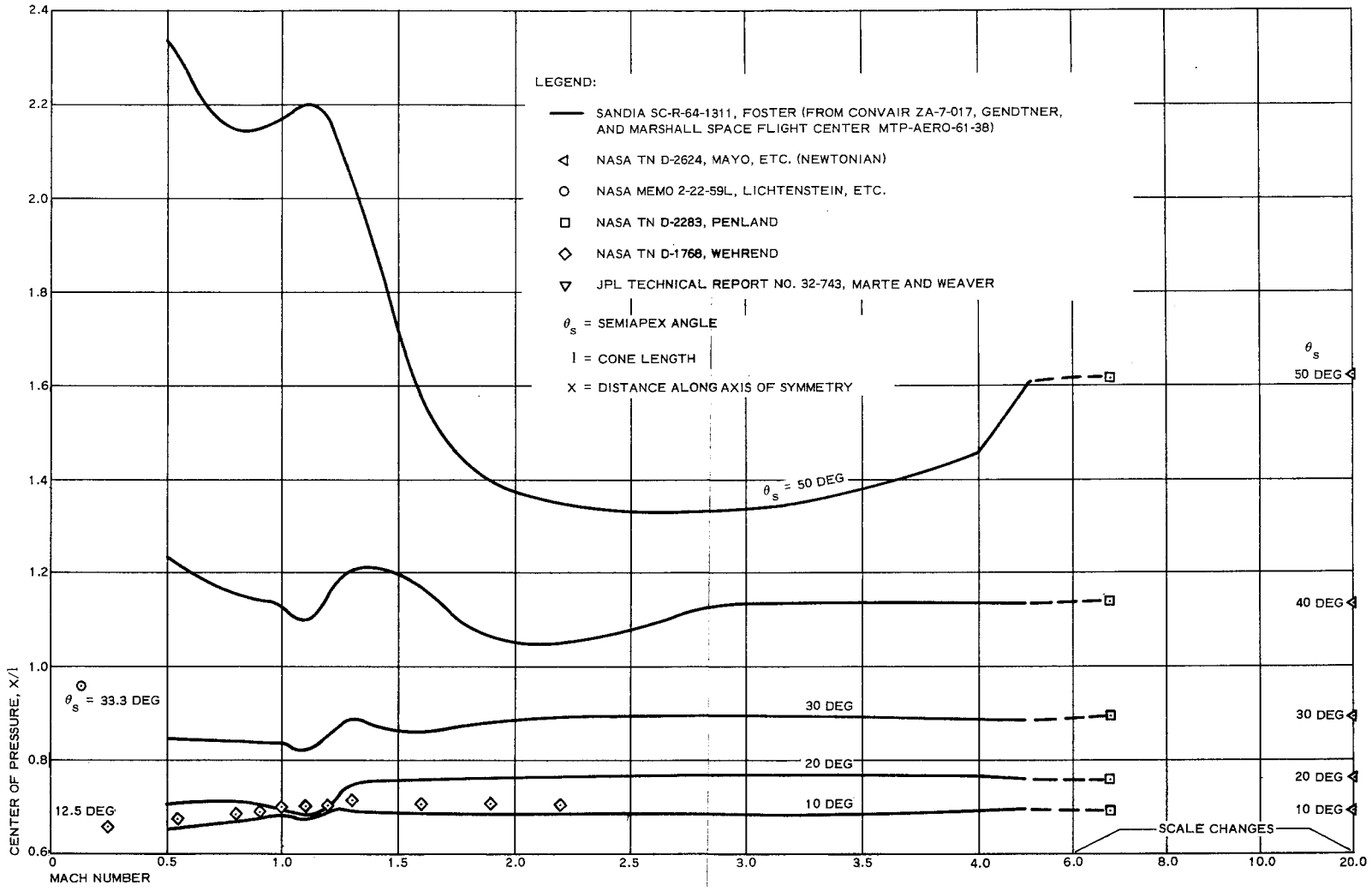

Figure 29 - cp vs Mach Number for Cones

Preceding page blank 79-A

79-B

brief attempt to verify this latter suspicion failed. The test data derivatives from Reference 5 and the Newtonian expressions for C_{N_q} and C_{N_α} from Reference 11 were used to calculate three values for $C_{M_q} + C_{M_{\dot{\alpha}}}$ about the base. Correlation was poor.

Reference 11 is a collection of various theories for estimating static- and dynamic-stability derivatives of simple axisymmetric bodies. Potential flow theory, first-order and/or second-order linear theory, slender-body theory, and Newtonian impact theory were all used to determine the stability derivatives.

The cone free-stream static- and dynamic-stability data presented are not representative when the decelerator is trailing the payload and is operating in the flow regime that is generally classified as a wake. The decelerator, being placed in this flow regime, becomes an object of its environment and at the same time by its physical presence influences this very regime. Qualitative and quantitative properties of this regime will completely define the performance and subsequently the design of a decelerator if it is immersed in the flow downstream of the payload. Tests have indicated, for example, that when a towed cone has an apex angle of more than 90 deg, it becomes unstable.

d. Wake Effect on the Decelerator

Essentially, the problem of determining the interaction effects between the wake and a decelerator immersed within it would be no different from any problem of a body immersed in a flow, provided the flow properties are known. Unfortunately, this is not the case, since the wake flow has specific complicated properties. In addition, the proximity to the body creating the wake, plus the fact that the body and decelerator are connected by means that are subject to the laws of rigid mechanics, introduces complexities that require sophisticated and rigorous analysis.

As previously indicated, lack of experimental data make it impossible to verify theoretical wake models by experiment. Thus, the interaction can

at best be described in hypothetical terms. If interaction is approached by the principle of the momentum defect, and the initial conditions at the forebody base are known, it can be postulated that the growth of the wake depends on the skin friction of connector and riser lines.

In accordance with Prandtl's concept of viscous flow, and assuming that local acceleration in the inner wake is more pronounced than acceleration due to an external pressure gradient, the momentum integral equation can be expressed by (see Reference 78)

$$\rho_1 u_1^2 \pi \theta_1^2 = 2\pi \int_o^\sigma \rho\, u(u_1 - u) r\, dr$$

$$= C_x ,$$

where

ρ = air density,

θ_1 = momentum thickness,

σ = wake thickness,

r = radial coordinate,

u = velocity in x direction,

C_x = constant with respect to x, and

1 = wake edge location.

To satisfy the conservation of momentum:

$$\rho_B u_B^2 (\pi \theta_B d_B) = \rho_1 u_1^2 (\pi \theta_1^2) ,$$

where B equals conditions at the base, and d equals the body diameter.

If the above postulate is true, a particular decelerator configuration and a particular forebody will exhibit only slight variations in drag coefficient at certain x/d locations and a constant Mach number. If Figure 30 is considered representative, this concept is apparently valid for

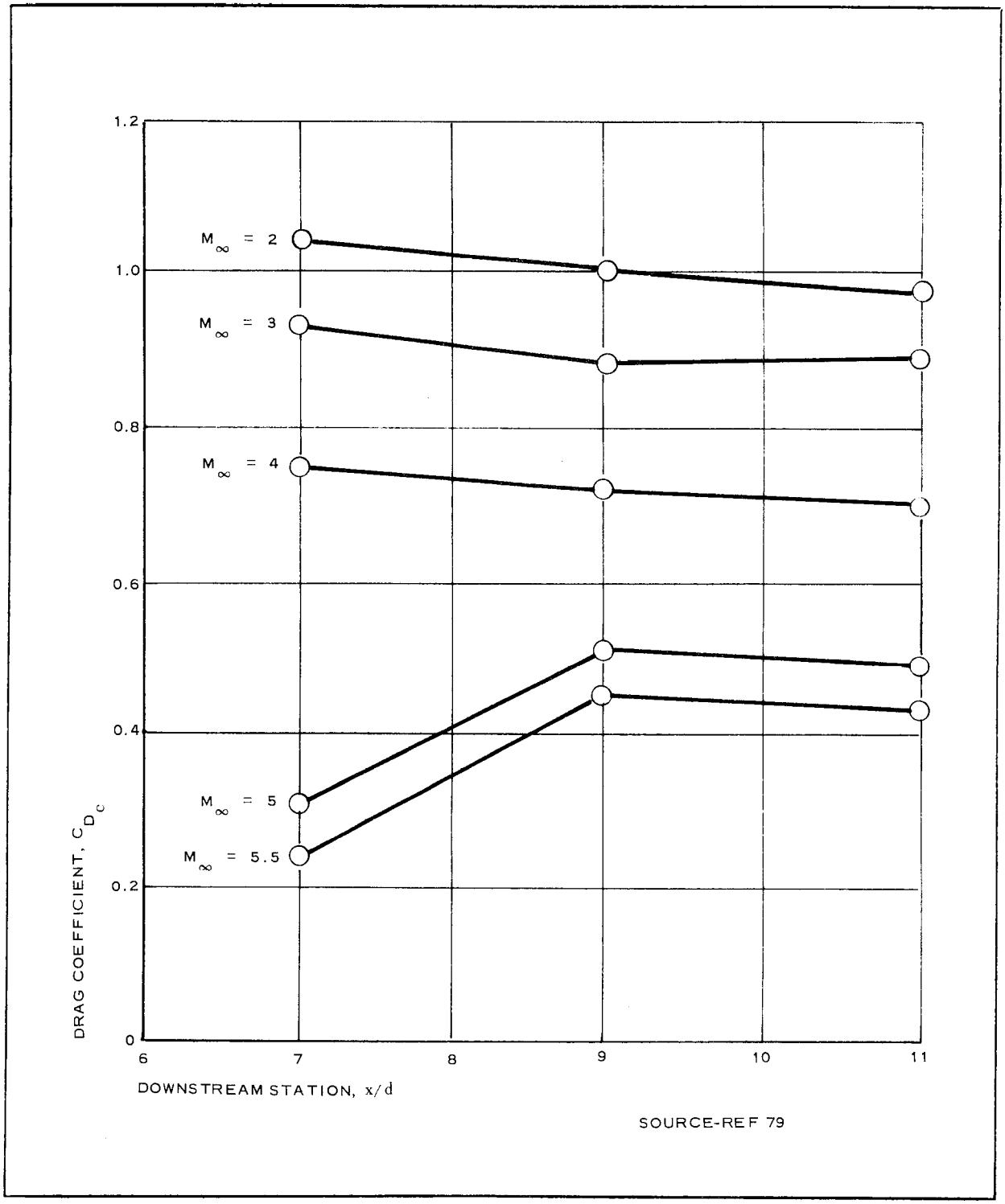

Figure 30 - Drag vs x/d, Hyperflo Model 1 behind Forebody Type I

$$2 \leqq M_\infty \leqq 4$$

at

$$7 \leqq \frac{x}{d} \leqq 11 ,$$

and for

$$M_\infty = 5 \text{ to } 5.5 ,$$

at

$$\frac{x}{d} = 9 \text{ to } 11 .$$

Figure 31 shows the C_D variation versus parachute downstream location x/d at three Mach numbers, due to the momentum "defect" influence of two different forebody shapes.

Figure 32 is representative drag data of another parachute model in a wake that is arranged to show the effects of Mach number on the C_D at two downstream decelerator locations.

In general, further and more detailed evaluations of the flow field, pressure distribution, etc., are clearly required. Specifically, evaluations of the fluid dynamics properties such as shock-wave/wake interaction, shock/boundary larger interaction (in the wake behind the payload and in front of the decelerator), and separated flow due to the presence of the riser line and attachments in the wake are required.

A detailed discussion of wake data found during the survey is given in Reference 80.

Because of the dynamic time-dependent properties of the forebody wake acting on the towed decelerator in this wake, current acceptable dynamic- and static-stability coefficients do not appear adequate to describe the motion of the decelerator. The only information on stability of towed decelerators is from visual observation of the degree of stability.

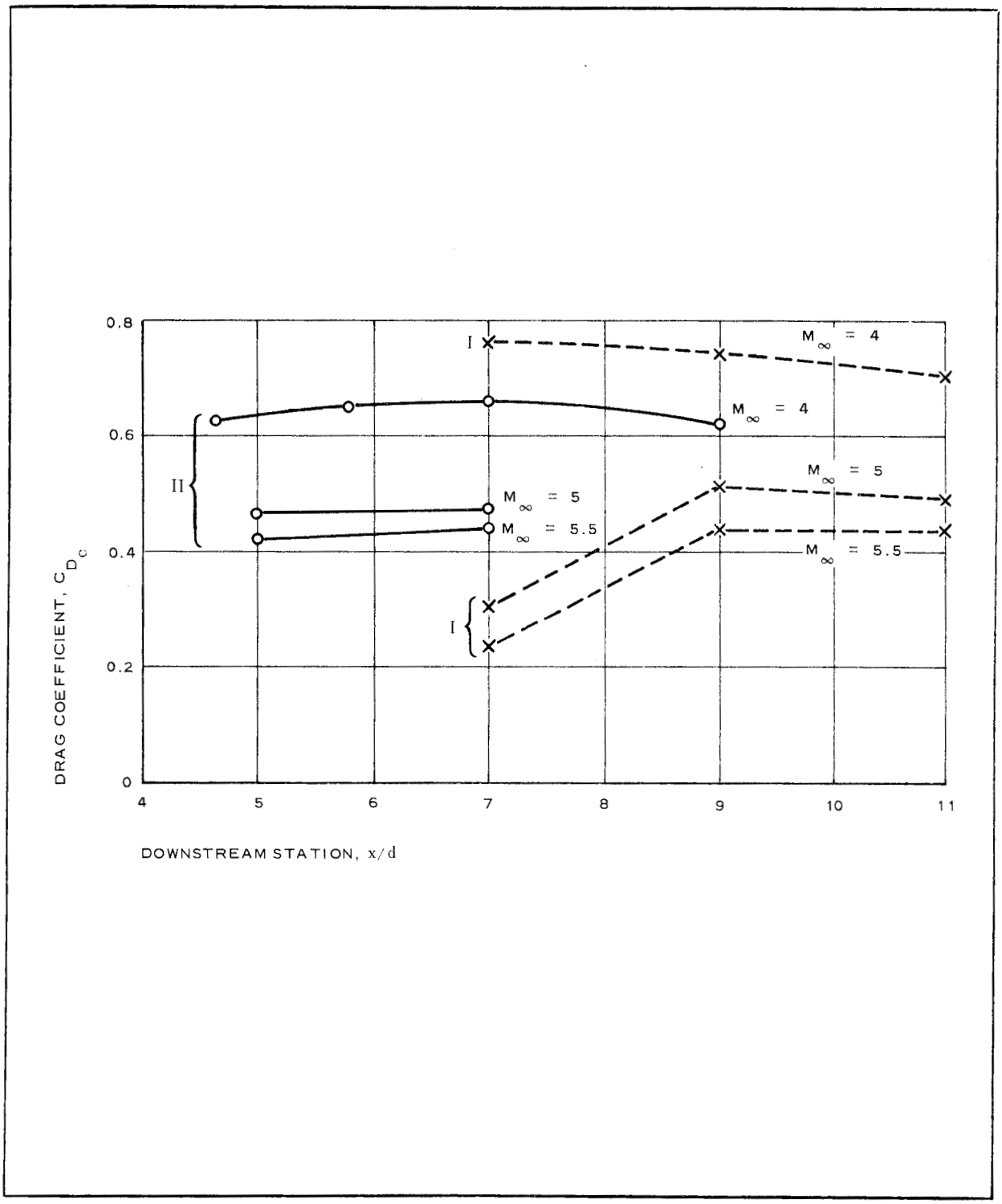

Figure 31 - Drag vs x/d, Hyperflo Model 1 behind Forebody Types I and II

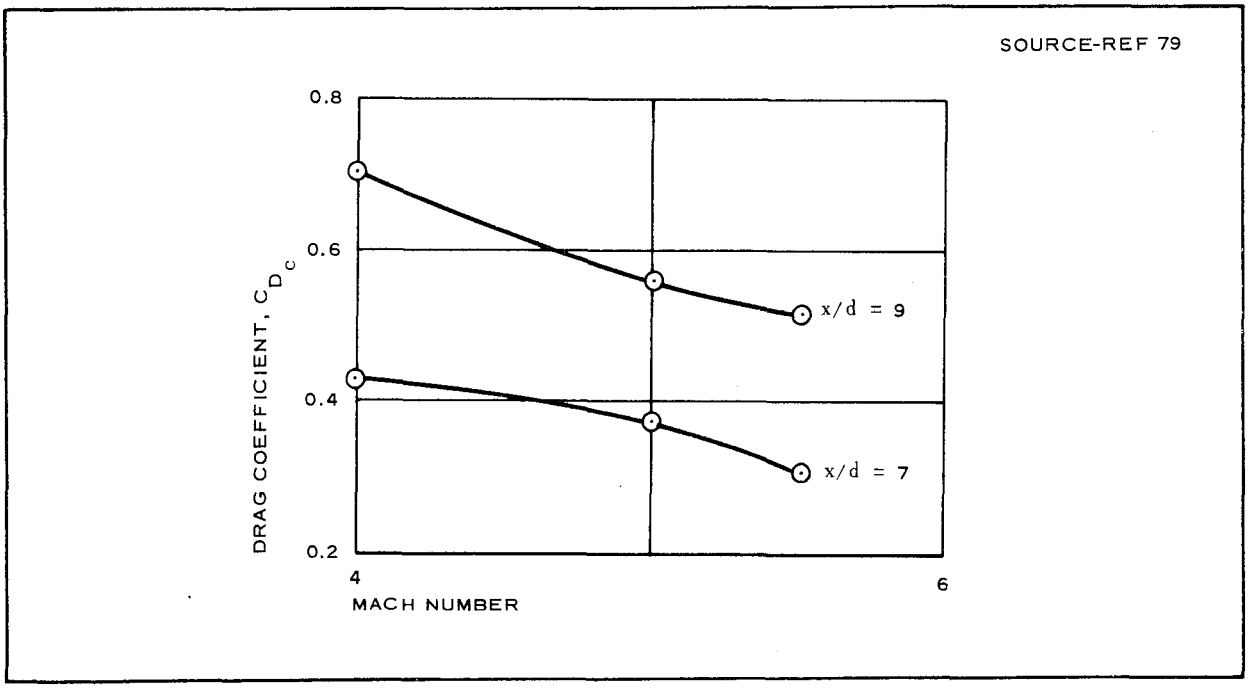

Figure 32 - Drag vs Mach Number, Hyperflo Model 2 behind Forebody Type I

References 27, 40, and 57 use relative descriptive terms such as excellent, good, fair, and poor. Since this type of reporting does not describe adequately the motions that define stability characteristics, more vigorous future test-condition criteria and test-reporting procedures are needed to acquire this necessary experimental information.

The following are examples of the motions that need to be described and have criteria applied to them:

1. Single-mode pendulum motion (rigid towline)
   a. Pitch-angle displacement and pitch rate about attachment point
   b. Roving-angle magnitude (pitch and yaw) and roving rate
   c. Roll angle and roll rate
2. Two-mode motion - combined inflation-shape change and single-pendulum mode (amplitude and frequency)
3. Multimode motion - superimposing flexible towline motion on Items 1 and 2, above

6. AEROTHERMODYNAMIC LOADING

a. General

The types of aerothermodynamic loading and some methods for estimating the heat load are described below.

In general, the use of a decelerator during re-entry or recovery of a system in the flight regime of interest requires a near-instantaneous deployment to augment the system drag characteristics. This deployment usually leads to the exposure of surfaces that are subjected to sudden aerodynamic heating, leading to an immediate buildup of the local heating rates with either (1) a rapid decay from the instantaneous maximum local heating rate or (2) a more gradual decay, depending on the type of device used and the altitude, velocity, and direction of motion at which deployment was initiated. The problem of defining these local heating rates is compounded because some of the more basic decelerators such as parachutes, Ballutes, and inflated skirts generate flow fields that are inherently characteristic of the device itself. Therefore, the determination of the local heating rates and the degree of temperature rise to determine material applicability become a function of the system operation and its deployment requirements, as well as the aerodynamics of the flow field.

The following suggested methods can be and have been used to calculate the local heating loads. For example, the heat-transfer characteristics of an inflatable skirt or flare can be evaluated if the type of flow over these can be predicted. For attached flow, heat-transfer rates for either laminar or turbulent flow can be calculated by using established heat-transfer theory; flat-plate heat-transfer equations using local flow conditions can be used. However, for separated flow, the calculation of the heat transfer rates becomes more complex. In the past, the data in References 52 and 81 have been used to estimate the heat-transfer characteristics for separated flow. When the decelerator is attached or forms an integral part of the re-entry or recovery system, the

prediction of the local heating rates consists of applying usually reliable heat-transfer theory to estimate heat transfer coefficient.

Other common types of decelerators are the parachute and, more recently, the Ballute. These devices are usually deployed in the wake of a leading body. The prediction of the heating loads requires an understanding of the wake and its formation. The determination of the properties of the wake behind an object moving in a fluid medium is one of the oldest and most basic problems of fluid mechanics. Although theoretical solutions exist for both laminar and turbulent incompressible wakes, the extension of these solutions to high Mach-number compressible-wake phenomena has not been completely successful. As a consequence, little attention has been given to the wake phenomena with regard to aerodynamic deployable decelerators trailing in the wake of a leading body.

Although considerable exploratory work has been performed and documented dealing with the aerodynamic performance of decelerators trailing in the wake of a leading body and associated component performance, such as in References 26, 27, 54, and 82, only limited effort has been initiated to evaluate the thermal limitations and performance of such devices. The data contained in these reports were oriented primarily toward evaluating parachutes and balloon-type aerodynamic decelerators, with emphasis on drag characteristics. In particular, Reference 27 documents the initial effort devoted to both theoretical and experimental analysis of the heat-transfer characteristics of a decelerator trailing in the wake of a leading body. This initial effort terminated with the compilation of a series of design curves (see Figures 33 through 36) that aided in determining heat-flux-rate distribution over two different decelerator configurations and the corresponding radiation equilibrium-temperature distribution over these bodies. The design curves published in Reference 1 were based on a single experimentally determined heat-transfer distribution over

S - DISTANCE FROM STAGNATION POINT, FT

R_0 - RADIUS, FT

$\dot{q}$ - LOCAL HEAT FLUX, BTU/HR-SQ FT

$\dot{q}_0$ - HEAT FLUX AT STAGNATION POINT WITHOUT FOREBODY, BTU/HR-SQ FT

T - LOCAL TEMPERATURE, DEG R

T_0 - TEMPERATURE AT STAGNATION POINT WITHOUT FOREBODY OR INTERNAL RADIATION, DEG R

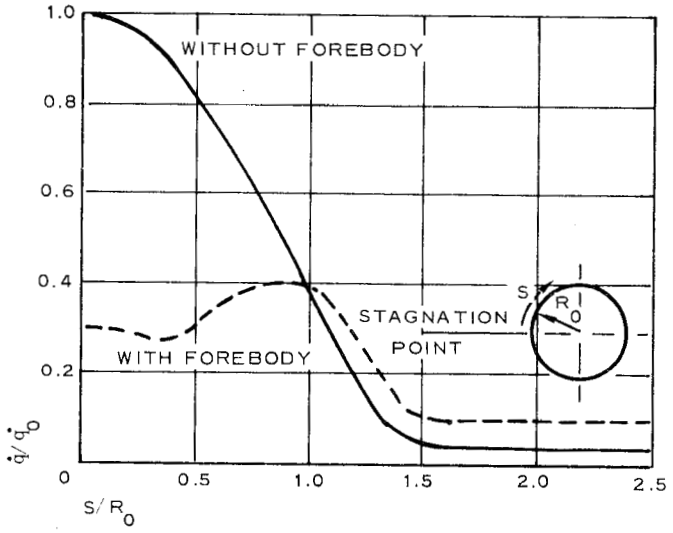

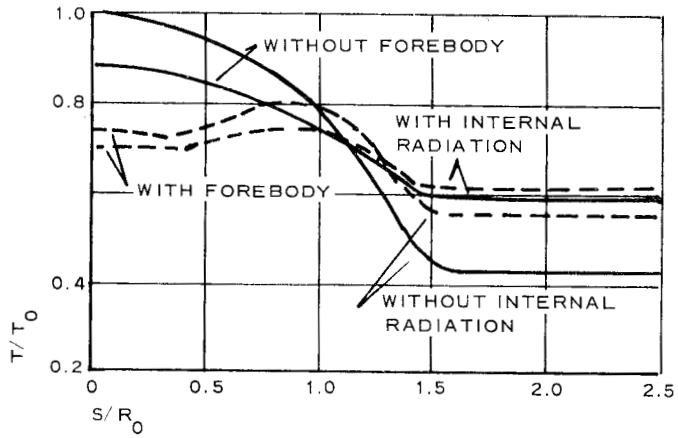

Figure 33 - Heat Flux and Temperature Distribution on a Sphere Laminar Flow

S - DISTANCE FROM STAGNATION POINT, FT

R_0 - RADIUS, FT

$\dot{q}$ - LOCAL HEAT FLUX, BTU/HR-SQ FT

$\dot{q}_C$ - HEAT FLUX AT $S/R_0 = 1$ WITHOUT FOREBODY, BTU/HR-SQ FT

T - LOCAL TEMPERATURE, DEG R

T_C - TEMPERATURE AT $S/R_0 = 1$ WITHOUT FOREBODY, DEG R

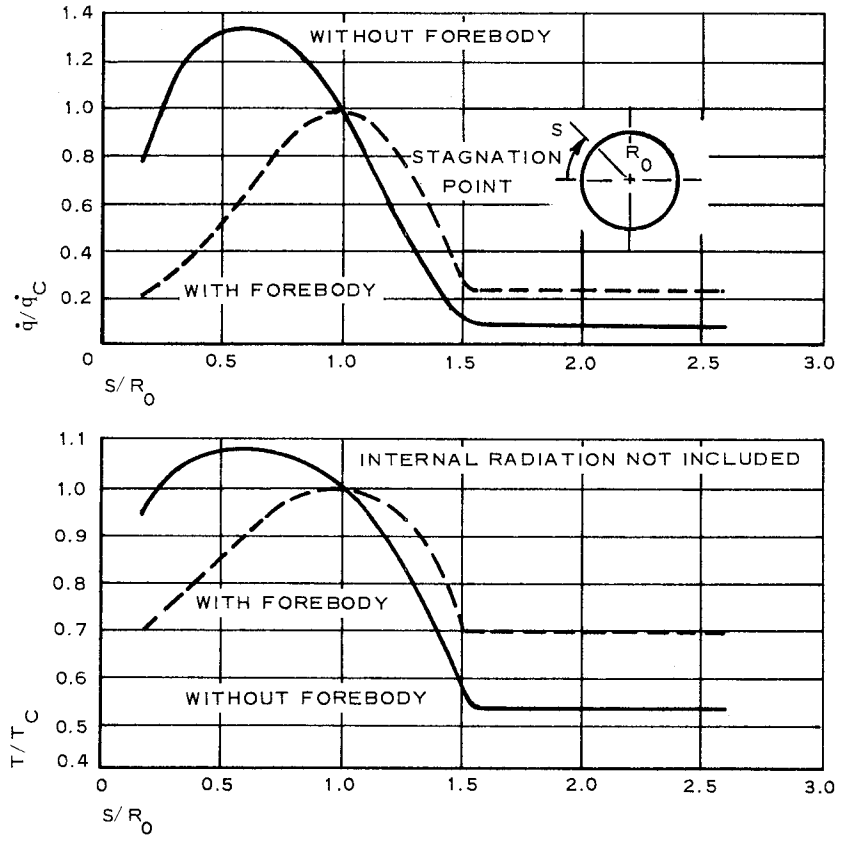

Figure 34 - Heat Flux and Temperature Distribution on a Sphere Turbulent Flow

S - DISTANCE FROM STAGNATION POINT, FT

R_0 - NOSE RADIUS, FT

$\dot{q}$ - LOCAL HEAT FLUX, BTU/HR-SQ FT

q_0 - HEAT FLUX AT STAGNATION POINT WITHOUT FOREBODY, BTU/HR-SQ FT

T - LOCAL TEMPERATURE, DEG R

T_0 - TEMPERATURE AT STAGNATION POINT WITHOUT FOREBODY, DEG R

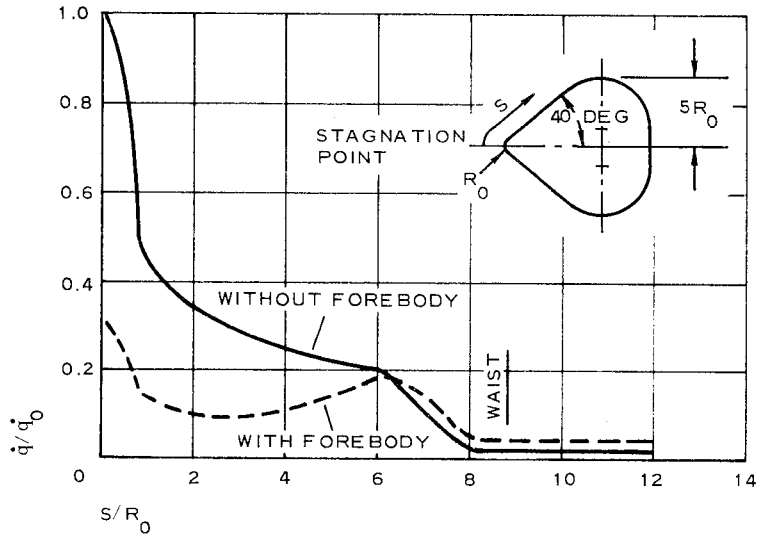

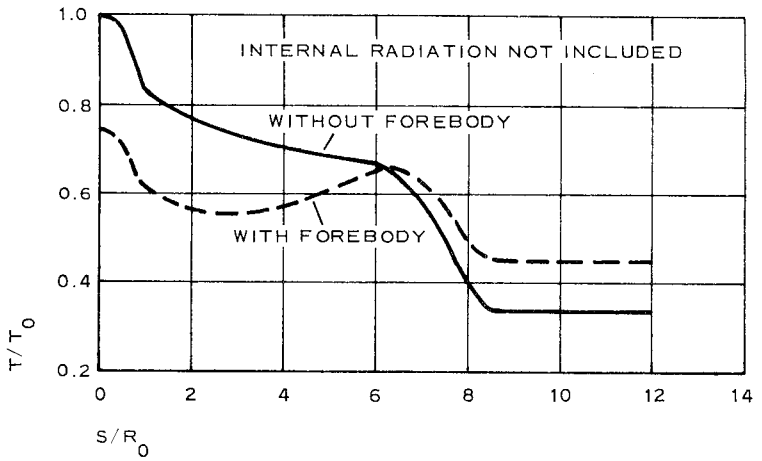

Figure 35 - Laminar Heat Flux and Temperature Distribution on a Blunted Cone

S - DISTANCE FROM STAGNATION POINT, FT

R_0 - NOSE RADIUS, FT

$\dot{q}$ - LOCAL HEAT FLUX, BTU/HR-SQ FT

$\dot{q}_C$ - HEAT FLUX AT $S/R_0 = 2$ WITHOUT FOREBODY, BTU/HR-SQ FT

T - LOCAL TEMPERATURE, DEG R

T_C - TEMPERATURE AT $S/R_0 = 2$ WITHOUT FOREBODY, DEG R

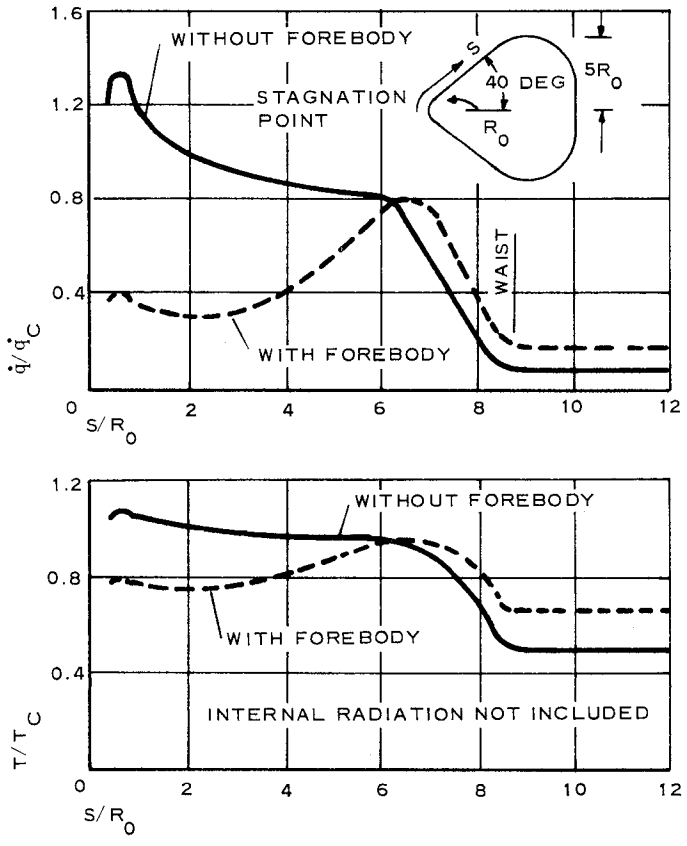

Figure 36 - Turbulent Heat Flux and Temperature Distribution on a Blunted Cone

a Ballute body at Mach 10. Apparently, these curves can serve as preliminary design guides for use in recovery-system applications such as those considered in this study.

Additional flight-test data and theoretical approaches were outlined in Reference 80 with limited thermal correlation correspondence. The results of the latter were directed primarily toward decelerators operating in the supersonic flow regime. To gain a better understanding of wake formations and their effect on trailing decelerators, Goodyear Aerospace conducted an in-house study of supersonic wake phenomena associated with Ballute-type decelerators. These studies were primarily concerned with correlating the experimental Mach 10 wind-tunnel results with a theoretical approach of a more exact nature than that used in estimating the design curves shown in Figures 33 through 36. The results of these studies were published in References 83 and 84. In these studies, a simple model of a wake flow based on the interaction between the leading body and the trailing decelerator was formulated, and engineering methods were developed for predicting pressure and heat-transfer distribution over Ballute decelerator surfaces. Both laminar- and turbulent-flow wake phenomena were considered.

b. Equations

At present, the type of wake can be estimated by using the transition data formulated in Reference 85. For laminar flow, a generalized equation developed in Reference 83 for the ratio of the heat-transfer coefficient on a decelerator immersed in a wake to a heat-transfer coefficient for a cone without the presence of a leading body was derived as follows:

$$\frac{h}{h_{cone}} = \frac{\left(\frac{P'}{P_\infty}\right)\left(\frac{r'}{D}\right)\left(\frac{S}{D}\right)^{0.5}}{\sqrt{3}\,\frac{P_{cone}}{P_\infty}^{1/2}\left[\int_0^S \left(\frac{P'}{P_\infty}\right)\left(\frac{r'}{D}\right)^2 d\left(\frac{S}{D}\right)\right]^{0.5}} \qquad (1)$$

where

h = heat transfer coefficient, Btu/hr-sq ft-deg F, or

h_{cone} = equivalent cone heat transfer coefficient, Btu/hr-sq ft-deg F,

c_p = specific heat of air (24 Btu/lb/deg)

P' = local pressure, psf

P_{cone} = equivalent cone pressure, psf,

P_∞ = free-stream pressure, psf,

r' = local radial coordinate, ft,

S = local distance from apex, ft,

S' = local distance along Ballute meridian surface from equator diameter, and

D = decelerator diameter, ft.

This expression was found generally to be in good agreement with the only experimental data available - that contained in Reference 27. A typical correlation is shown in Figure 37.

The turbulent heat-transfer distribution over a Ballute-type decelerator immersed in the wake of a leading vehicle also was formulated in Reference 83 in a manner similar to that used for the laminar-flow case. The resulting generalized heat transfer coefficient equation was formulated as:

$$h = \rho' u' c_p Pr^{-2/3}\left(\frac{C_f'}{2}\right)\left[G(S)\right]^{1/5} \qquad (2)$$

where

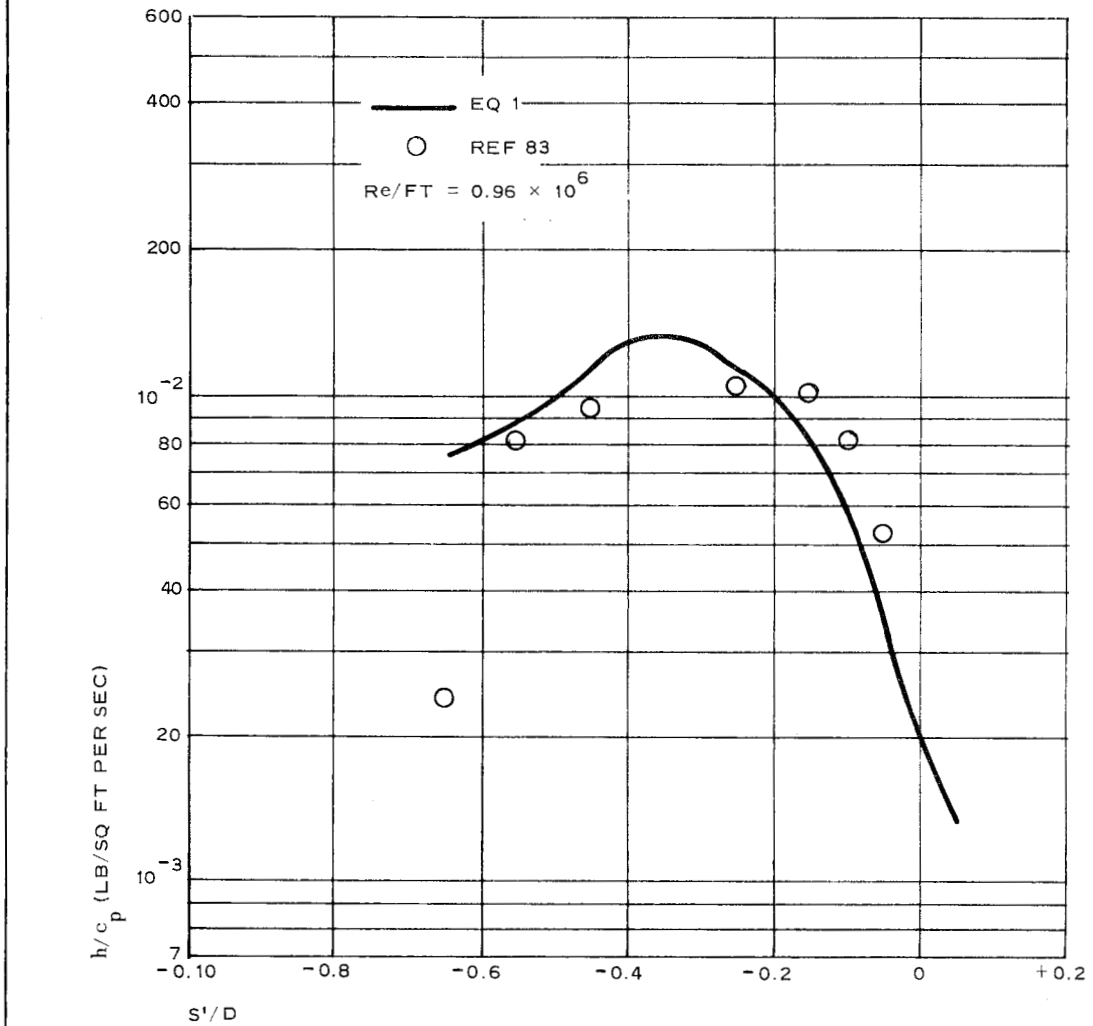

Figure 37 - Mach 10 Ballute Heat-Transfer Results

ρ' = local density, pcf,

u' = local velocity, fps,

c_p = specific heat at constant pressure, Btu/lb-deg F,

Pr = Prandtl number,

C_f' = local friction coefficient,

(S) = local form factor, dimensionless, and

h = heat transfer coefficient, Btu/sq ft-sec-deg F.

The primes in this equation indicate that the properties of the flow must be evaluated at the decelerator surface or at the edge of the decelerator boundary layer.

Practically no experimental or flight-test data exist to compare with the theoretically derived expressions. Thus, this largely unexplored area suffers greatly from the lack of high-quality experimental data to verify the prediction methods described in References 83 and 84. However, the use of the developed expressions appears to be justifiable since the flight test data obtained thus far, although of an exploratory nature, have not indicated severe or underpredicted aerodynamic-heating problems.

The expected temperature rise of parachute decelerators in the high supersonic-speed regime is another situation that will require an exploration of the wake and its interaction with the flow field before a prediction can be made. The use of a porous roof, either of a fine mesh or ribbon construction, has presented a flow-prediction problem that has not been resolved in the parachute-design field. Since the individual components of such parachutes can be composed of materials of relatively low mass (and hence, low heat capacity), they are subjected to severe aerodynamic heating. The exploratory flight-test data presented in Reference 54 shows that surface temperatures

of 600 F and above may be encountered by textile materials at medium altitudes at about Mach 4.

Analyzing the aerodynamic heating characteristics of parachute-type trailing decelerators has up to the present time been based on more intuitive principles than actual flow data. One procedure used now is outlined in Reference 82. A short description of this procedure follows. A schematic of a typical trailing-parachute decelerator is shown in Figure 38. The trailing parachute is assumed to be preceded by a bow-type shock at the inlet face, and constant stagnation conditions, which are functions of the free-stream flow properties, are assumed to exist inside the canopy. The pressure ratio across the roof panel also is assumed to be greater than critical so the sonic flow exists in the many openings of the roof panel. Using Bartz's equation for turbulent flow in a nozzle, the heat transfer coefficient in a typical orifice can be estimated using the following:

$$h = \left[\frac{0.026}{D_t^{0.2}}\left(\frac{\mu_o^{0.2} c_p}{Pr^{0.6}}\right)_0\left(\frac{P_t g}{c^*}\right)^{0.8}\left(\frac{D_t}{r_e}\right)^{0.1}\right]\left(\frac{A^*}{A}\right)^{0.9} \qquad (3)$$

where

D_t = orifice throat diameter, ft,

μ_o = viscosity at total temperature, lb/ft-sec,

c_p = specific heat, Btu/lb-deg F,

Pr = Prandtl number,

P_t = total pressure, psf,

g = gravitational constant, 32.2 ft/sec^2,

c^* = characteristic orifice velocity, fps,

r_e = radius of roof element, ft,

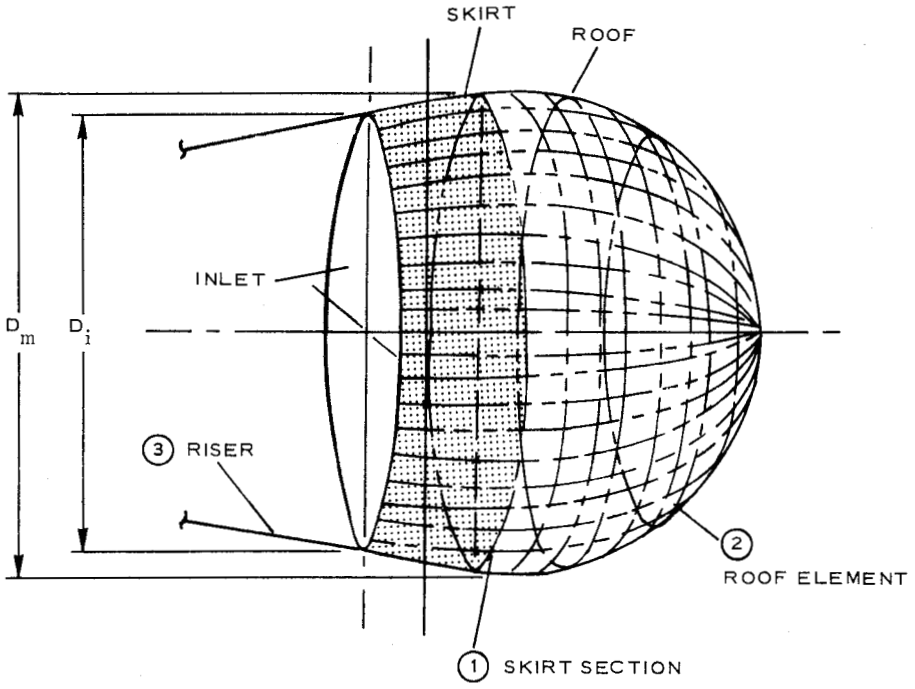

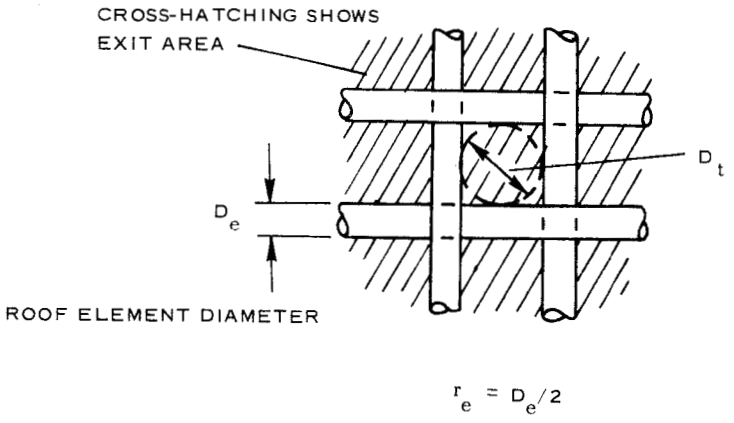

$r_e = D_e/2$

Figure 38 - Parachute Configuration

A^* = orifice throat area, sq ft.

A = orifice station cross-sectional area, sq ft, and

σ = dimensionless factor accounting for density and viscosity variation in boundary layer.

The heat transfer cocfficient and heat flux rates can be estimated to determine the temperature rise in duration of the heating. Once the heat transfer coefficients have been estimated, the variation in the heat flux rate into the fabric as a function of deceleration time can be calculated using trajectory data for the particular application. In some cases where the decelerator material is of thin gage, it is sufficient to calculate the temperature rise rate using a heat sink type of heat balance such as:

$$h\left(T_{aw}-T\right) = \dot{q} = \rho c\delta\left(\frac{\Delta T}{\Delta \tau}\right) + \epsilon\sigma T_w{}^4 \qquad (4)$$

where

h = heat transfer coefficient, Btu/hr-sq ft,

T_{aw} = adiabatic wall temperature, deg F,

T_w = material temperature, deg F,

τ = time,

ρ = density of material, pcf,

c = specific heat of material, Btu/lb -deg F,

δ = thickness, ft,

ϵ = emissivity,

σ = Stefan-Boltzmann constant, and

$\dot{q}$ = heat flux rate, Btu/hr-sq ft.

In other cases where a generous amount of heating is applied to the load carrying material, it is necessary to use a transient heat conduction type of solution.

For such a case, the decelerator materials usually form a nonhomogeneous layer that can be classed as a poor conductor. It is then appropriate to consider the heating of this type of material based on transient, one-dimensional heat conduction. The partial differential equation for heat conduction in a one-dimensional slab is

$$\frac{\partial T}{\partial \tau} = \alpha \frac{\partial^2 T}{\partial y^2} \tag{5}$$

where (for Equations 5 through 8)

τ = time, sec,

y = depth, ft,

k = thermal conductivity, Btu/ft-hr-deg F,

α = thermal diffusivity, sq ft/hr,

h_{aw} = adiabatic wall enthalpy, Btu/lb,

h_{cw} = cold wall enthalpy, Btu/lb,

h_w = wall enthalpy, Btu/lb,

$\dot{q}_w$ = wall heat flux rate, Btu/sq ft per sec, and

$\dot{q}_{cw}$ = cold wall heat flux rate, Btu/sq ft per sec.

Additional equations for the outer and inner surface boundary conditions must also be stated to augment the solution of equation (3). The outer surface boundary equation can be written as

$$h(T_{aw} - T_w) - \varepsilon \sigma T_w^4 = -k \left\{ \frac{\partial}{\partial y} \left[T(0,\tau) \right] \right\} \tag{6}$$

At the inner wall, the surface will be assumed to be an adiabatic wall

$$\left(\frac{\partial T}{\partial y} \right)_{y = \delta} = 0 \tag{7}$$

These equations were then converted to finite-difference form and solved on a digital computer as a function of the heat flux rates evaluated and presented previously. The cold wall aerodynamic heating rates presented earlier were coupled to the transient heat conduction solution by the following relationship:

$$h(T_{aw} - T_w) = \dot{q}_w = \dot{q}_{cw}\left(\frac{h_{aw} - h_w}{h_{aw} - h_{cw}}\right) \qquad (8)$$

Thus, the decrease in the heating rates is compensated for by the enthalpy ratio.

7. STRUCTURES

a. General

Present-day high-speed recovery operations are generally quite severe in weight and stowage-space requirements and in the hostile aerothermodynamic environment in which the decelerator must operate. It is usually of primary interest to design the lightest decelerator that can fulfill the system requirements. From this general specification, it is necessary to choose a material that can sustain the aerodynamic load at the potential temperature level. In terms of deployment conditions in the flight regime of interest, this type of criteria is available in the form of the data presented in Figure 2. For instance, the particular adiabatic wall-temperature lines have been drawn to correlate with the nominal maximum working temperature level of state-of-the-art fabric materials. Thus, a nylon fabric usually can operate up to about 350 F, a Nomex fabric up to about 700 F, and metal fabrics like stainless steel and René 41 up to 1200 F. Material capabilities can be extended by using heat-resistant coating. Coatings and their effects are discussed in more detail in Item 8, below.

Several different decelerator configurations (see Figures 39 through 42) have been investigated experimentally; applicable structural design parameters generally have been established. Configurations for which documented structural design data are available include Ballutes, spheres, parachutes, cones, inflated skirts, and tension shells. Each of these structural types is discussed in more detail in Items b through f, below.

b. Ballute and Spheres

(1) Description

Ballutes illustrated in Figure 43 are woven-fabric ram-air-inflated pressure vessels of isotensoid design. The inflated structure is primarily pear-shaped, except for the large circumferential burble fence at, or just aft of, the maximum diameter. Ram air enters through a series of symmetrically located side inlets or through a single large nose inlet. The fence is inflated through numerous small ports located around the decelerator proper and beneath the envelope of the fabric fence. The inflated height of the fence is up to 10 percent

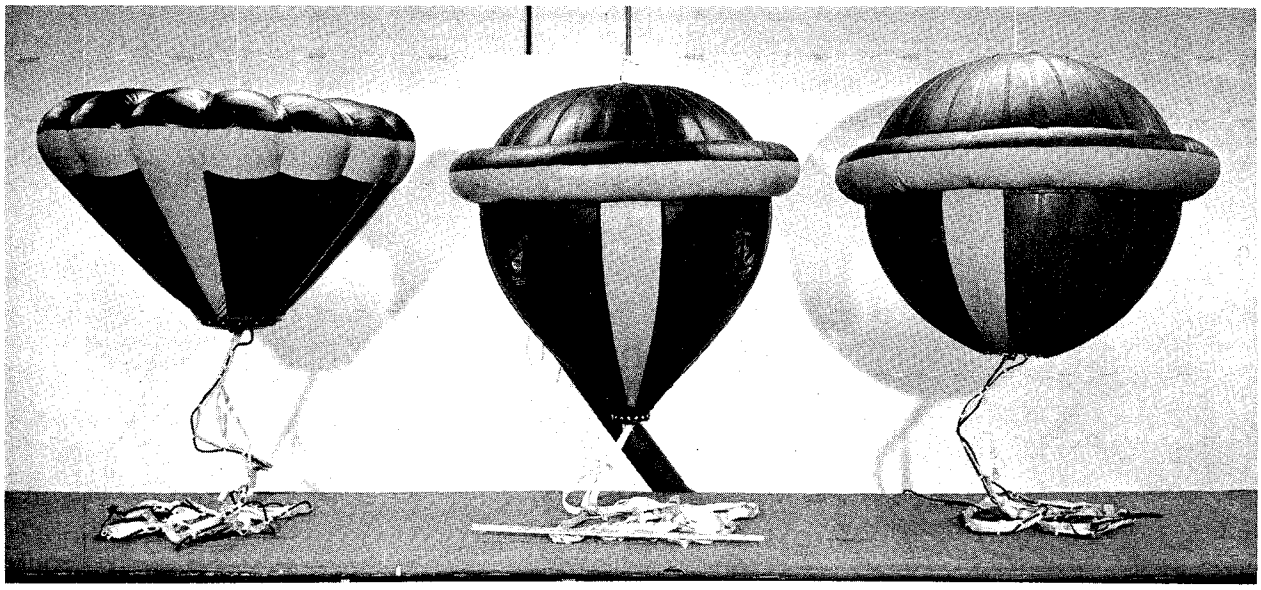

Figure 39 - 4-Ft-Diameter Decelerators To Be Flight Tested at Mach 5

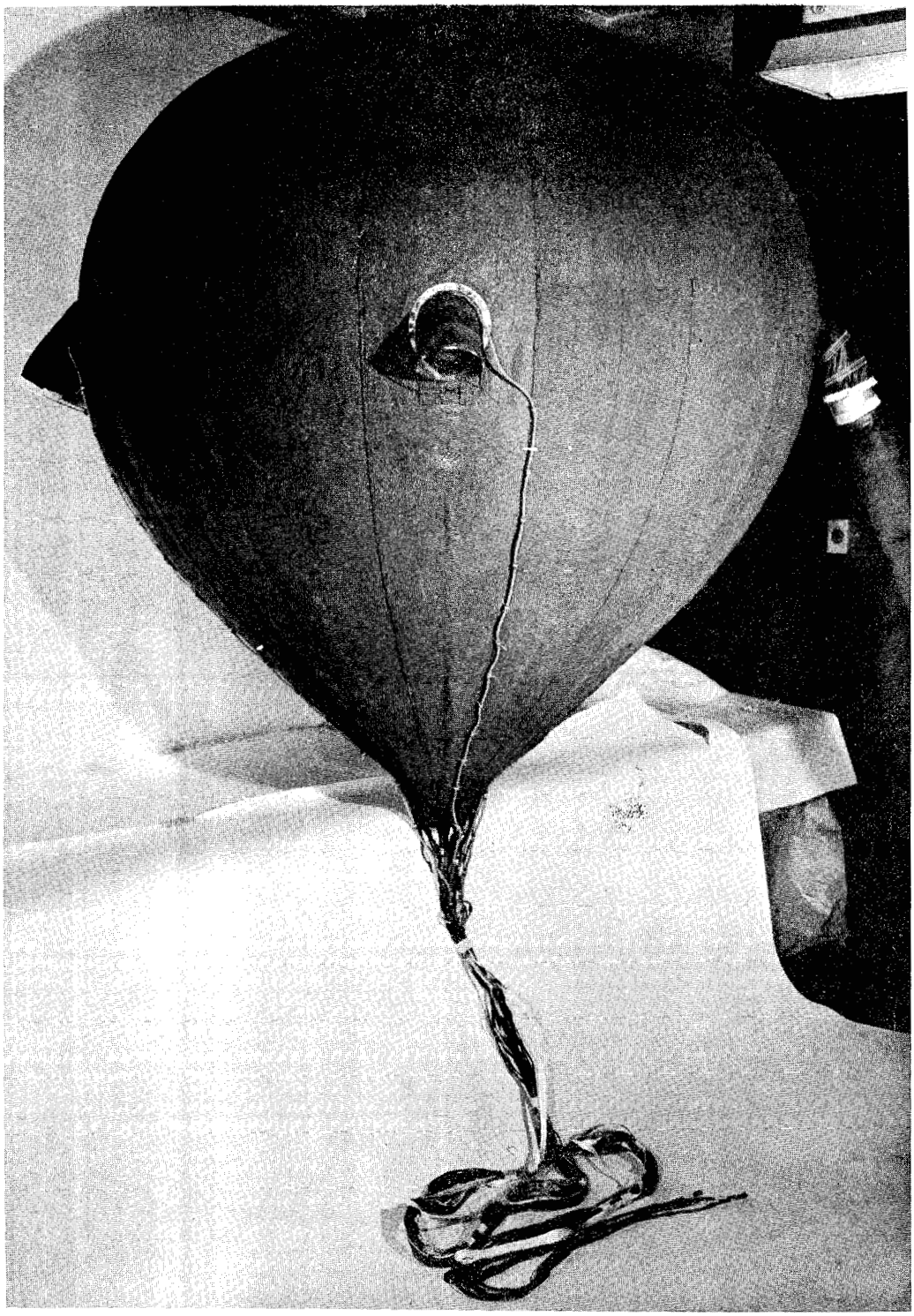

Figure 40 - Coated Metal-Cloth, 5-Ft-Diameter Ballute

of the maximum inflated diameter of the model. This conical model is a gore construction, fabricated from base materials such as nylon or Dacron or from heat-resistant materials such as Nomex.

Reference 27 considers a fabric sphere as one limiting case; thus, the discussions below can be applied to that configuration as indicated.

(2) Components

The principal components of the Ballute include the fabric covering, the meridional webs, and the fabric coating. The fabric covering is a high-strength material that forms the envelope of the structure. The meridional webs help to support the load by continuing around the structure and passing through the apex at the back. The webs may terminate on a nose fixture at the front of the model, or they may extend out to become the suspension lines. The heat-resistant coating applied to the envelope makes it nonporous and helps to provide thermal protection for the structure.

(3) Weights and Volume

The weight of a Ballute, W_B, is the sum of the weight of its components. Therefore,

$$W_B = W_f + W_m + W_c,$$

where

W_f = fabric weight,

W_m = meridian weight, and

W_c = coating weight.

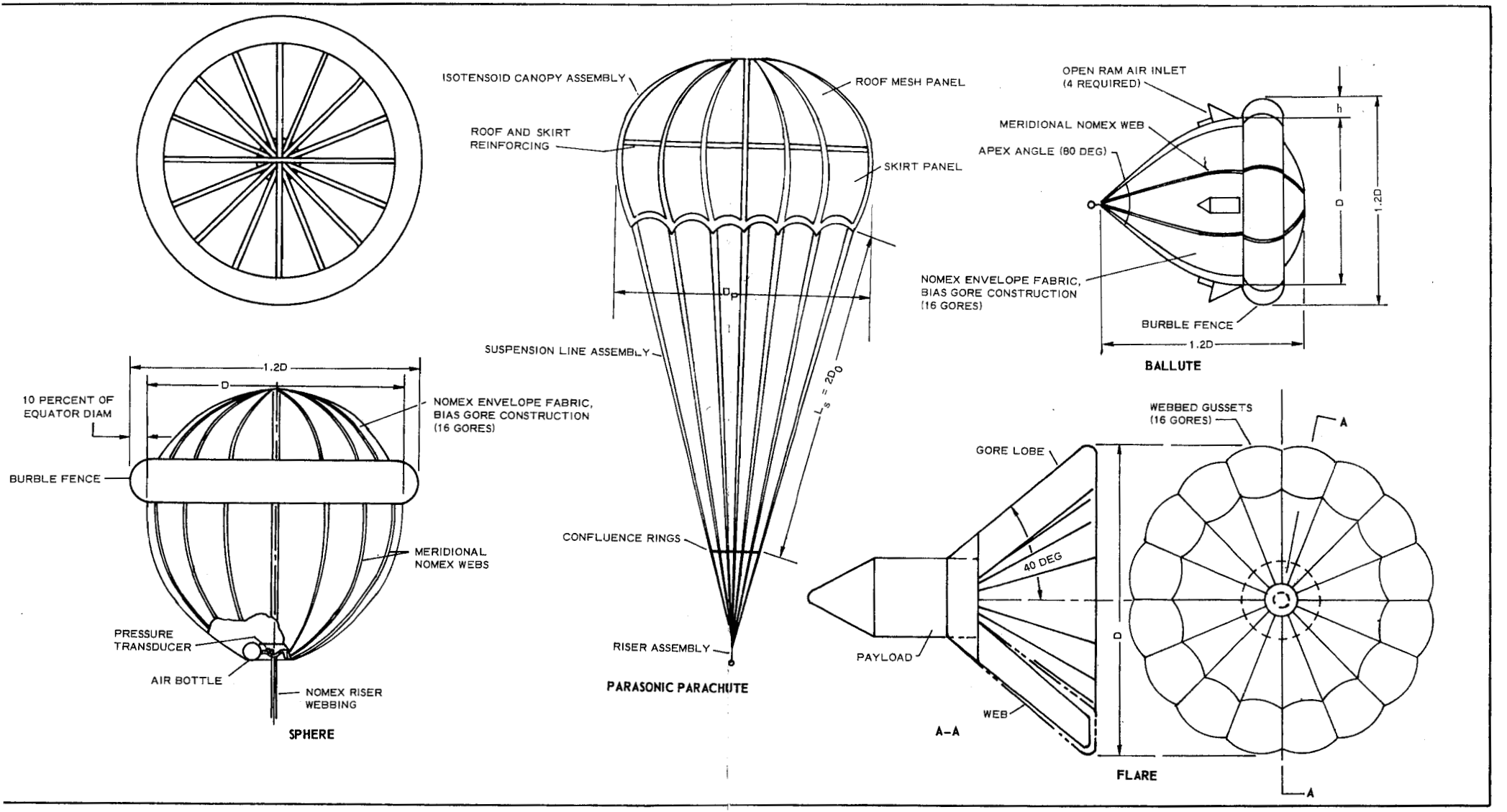

Figure 41 - Sketches of Sphere, Parachute, Ballute, and Flare

105-A

105-B

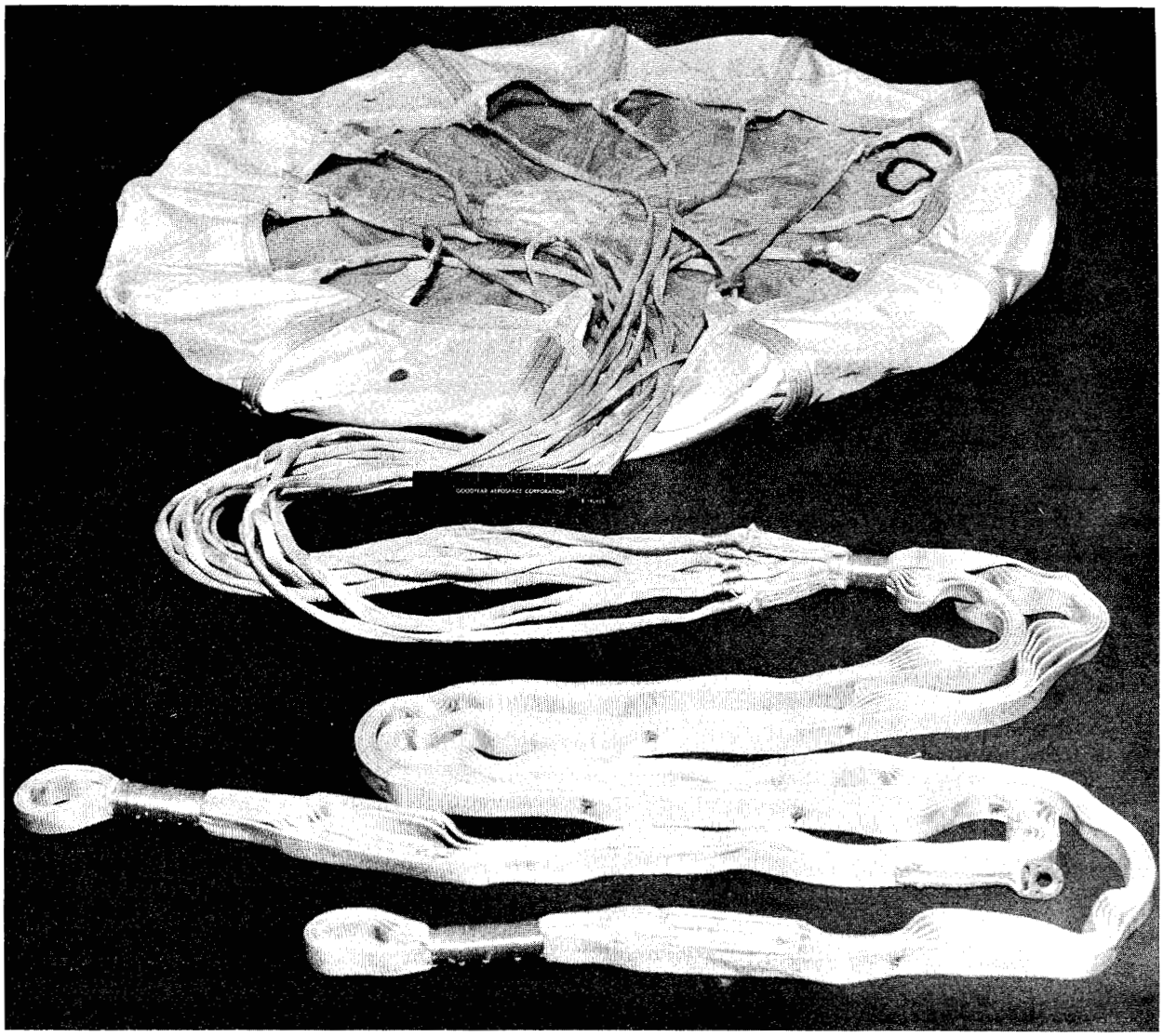

Figure 42 - 4-Ft-D_o Parasonic Parachute

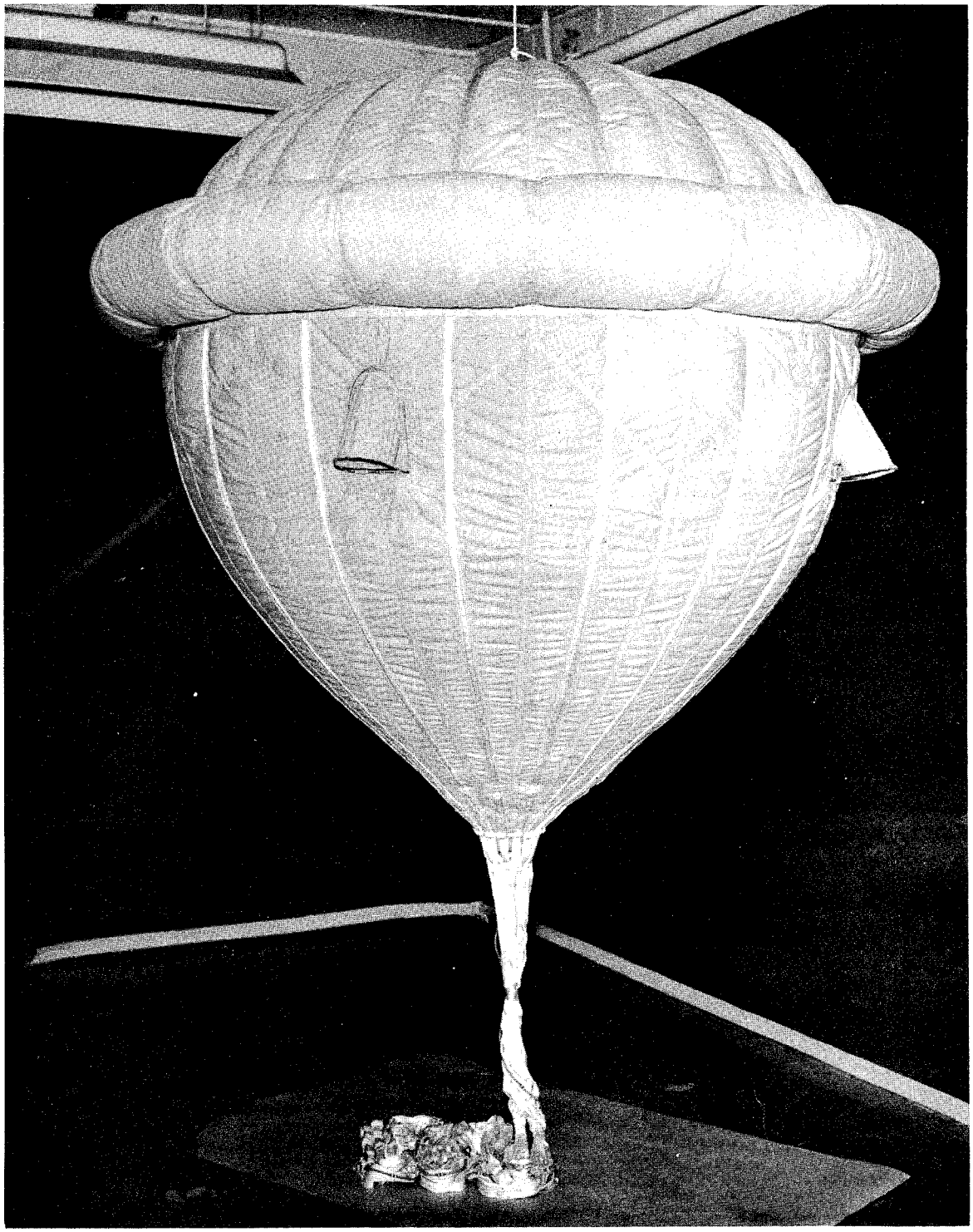

Figure 43 - TB-1 Ballute Configuration

The weight then becomes

$$W_B = \frac{A_f f_f (D.F.)}{K_f} + \frac{hLT(D.F.')}{K_m} + A_f(C.F.),$$

where

A_f = surface area of the decelerator,

f_f = design stress due to the design inflation pressure and the decelerator radius,

D.F. = total fabric design factor, which is the product of safety factor, dynamic loading, seam efficiency, temperature, etc.,

K_f = envelope fabric strength-to-weight ratio,

h = number of meridians (webs),

L = length of each meridian,

T = meridian design tension load,

D.F.' = total meridian design factor,

K_m = meridian strength-to-weight ratio, and

C.F. = unit coating weight (weight/area).

Since the Ballute is an isotensoid structure, the discussion of Reference 27 applies and can be used to determine the necessary values. For preliminary considerations, the required weight for a steady-state (ram-air inflated) condition is approximated by

$$W_B = \Delta P_R \pi R^3 \left[\frac{4(1-K-\rho)}{K_f} + 2\,\frac{(1.2\rho + \pi K)}{K_c}\right] + 4\pi R^2 (C.F.).$$

This equation uses a safety factor of two and does not include the weight of the burble fence or the riser line. The meridian length and fabric area are approximately $2\pi R$ and $4\pi R^2$, respectively.

For a 10-percent fence, the fabric weight is increased by approximately 30 percent.

Figure 44 presents the results of the above equation for various values of

$$\frac{\Delta P_R}{q} .$$

The following has been determined experimentally.

1. $\Delta P_{R/q}$ = 1 was sufficient for full decelerator inflation.

2. $\Delta P_{R/q}$ = 2 to 4 was obtained in the supersonic speed regime.

Hence, the weight of a presently designed Ballute is based on a $\Delta P_{R/q}$ of between two and four. However, subsequent effort to lower the resulting internal pressure for design optimization is feasible. One method is to relocate the ram-air inlets to a location of lower local pressures.

Ballute stowage-volume requirements are dependent on its weight and packing density. Typical packing-density values range from 20 to 30 pcf for handpack and 30 to 40 pcf for a pressure pack.

c. Parachutes

(1) Description

The basic parachute is a well-known configuration used almost exclusively in subsonic recovery operations. The tendency toward an evolution of supersonic-type decelerators resulted in the early consideration of parachutes for high-speed applications. To date, various configurations have been tested supersonically, including some comparatively recent high-speed designs. Subsonic canopies tested supersonically include the hemisflo, the

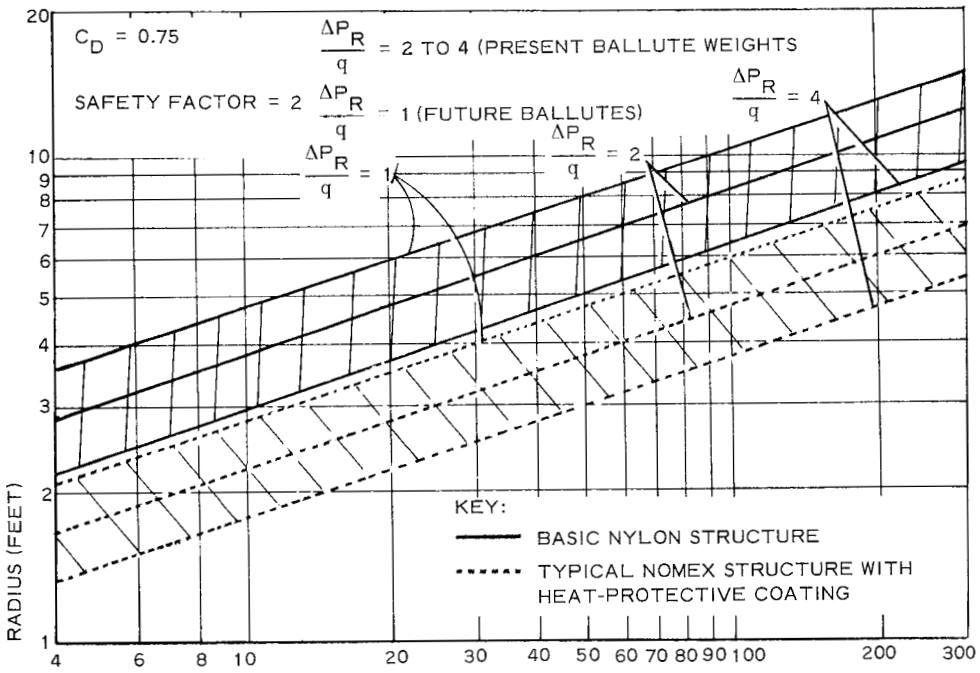

WEIGHTS BASED ON $W_B = \Delta P_R \pi R^3 \left[\frac{4(1-K)}{K_f} + \frac{2\pi K}{K_c}\right]$,

WHERE $K_f = 1.37 \times 10^4$ FT (600 FT COATED FABRIC VALUE), $K_c = 2.3 \times 10^4$ FT, K = 0.865, AND $\rho = 0$.

Figure 44 - Ballute Weight vs Radius

standard flat, the conical, and the equiflo. Notable supersonic canopy designs are the hyperflo, the Parasonic, and the supersonic guide surface.

(2) Components

The basic components of a parachute are its drag-producing canopy and suspension lines. The former can be further subdivided, for most supersonic configurations, into a crown, a roof, and a skirt. Each section may be either porous or nonporous, but generally the crown and roof are porous (either mesh or ribbon) and the skirt is relatively nonporous.

(3) Weights and Volume

Past reliance on parachute-type recovery has resulted in the documentation of various methods of weight and volume analysis. Reference 1 indicates several of these methods including the one discussed below, which is frequently used for preliminary calculations. The principles applied are applicable, in theory, at any Mach number. The desired maximum loading, F_o, is determined from overall program requirements, usually a maximum g-load specification. The equation on page 378 of Reference 1 gives

$$\text{individual line strength} = \frac{F_o \times J \times c}{Z \times u \times o \times e \times k},$$

where F_o is maximum opening shock, J is a safety factor, Z is the number of suspension lines, c is a factor related to suspension-line confluence angle, u is a factor for strength loss at connection points, o is a factor related to strength loss in material from water and water-vapor absorption, e is a factor related to strength loss from abrasion, and k is a factor related to strength loss from fatigue. Once the F_o axial design load level has been established (F_o = opening shock factor times C_D Aq, the strength of each line is obtained with the above equation.

The strength requirements of the invididual lines can be determined by the judicious selection of these factors. In general, Z (the minimum number of suspension lines extending from the canopy) is picked to be numerically equal to $D_o + 4$); however, more lines are usually selected since a number divisible by four should be used for loading attachment symmetry.

To determine the suspension-line weight, a material weight per unit of length corresponding to the strength requirement of the lines and the suspension-line length must be found. In supersonic operations, the length of each line from the canopy to the confluence point is approximately $2D_o$. Thus, the length of each line loop (Z/2), accounting for its continuation on around the canopy through the apex at the back, is $5D_o$. The weight of the suspension lines then becomes

$$W_M = \left(\frac{\text{line weight}}{\text{unit length}}\right)\frac{(Z)}{(2)} \times (5D_o) .$$

The strength requirements of the canopy material are found from the relative suspension-line strength requirements by using the tables on page 376 of Reference 1. The canopy weight can then be estimated by

$$W_{surf} = \left(\frac{\text{weight surf material}}{\text{unit area}}\right) \times (A - \lambda A) ,$$

where λ is the geometry porosity (openness) and A is determined from terminal-velocity requirements using the equation

$$A = \frac{W}{qC_D} ,$$

where W = D. The parachute weight then becomes

$$W_f = W_{surf} + W_M .$$

An approximation of the parachute weight, which has been obtained empirically from many tests, is given by the equation

$$W_f = \left(\frac{\text{line weight}}{\text{unit length}}\right) \frac{(Z)}{(2)} \frac{(5D_o)}{0.4}$$

That is, the suspension line weight comprises approximately 40 percent of the parachute weight. For isotensoid designed parachutes, the methods of Reference 81 can be used for more accurate results.

Example weights of these drogue-type parachutes can be obtained from Reference 1. For example, on page 89 of Reference 1, the weights of ribbon drogue parachutes from two feet to seven feet in diameter that are capable of withstanding "q's" between 135 to 794 psf (below Mach 2) vary from 2 to 20 lb. These ribbons weigh between 0.5 to 1.0 oz per linear yard. It is important to note that these weights are based on nylon material that is designed to take the "q" load but not capable of withstanding temperatures above 250 F. Based on this survey, there was no documented data found of high-speed (above Mach 2.5) parachutes that were capable of withstanding 600 F, as was the case of the coated, nonporous decelerators.

d. Airmat Cone

(1) Description

The Airmat cones shown in Figures 45 and 46 are composed primarily of two cone-shaped layers of fabric, between which are many thin fibrous strands called drop threads. When the volume enclosed by the fabric layers is pressurized, the fabric is constrained by the drop threads to form the desired shape. The cone thickness (depth between layers) increases with the distance from the apex; this is done to maintain structural rigidity while the diameter increases.

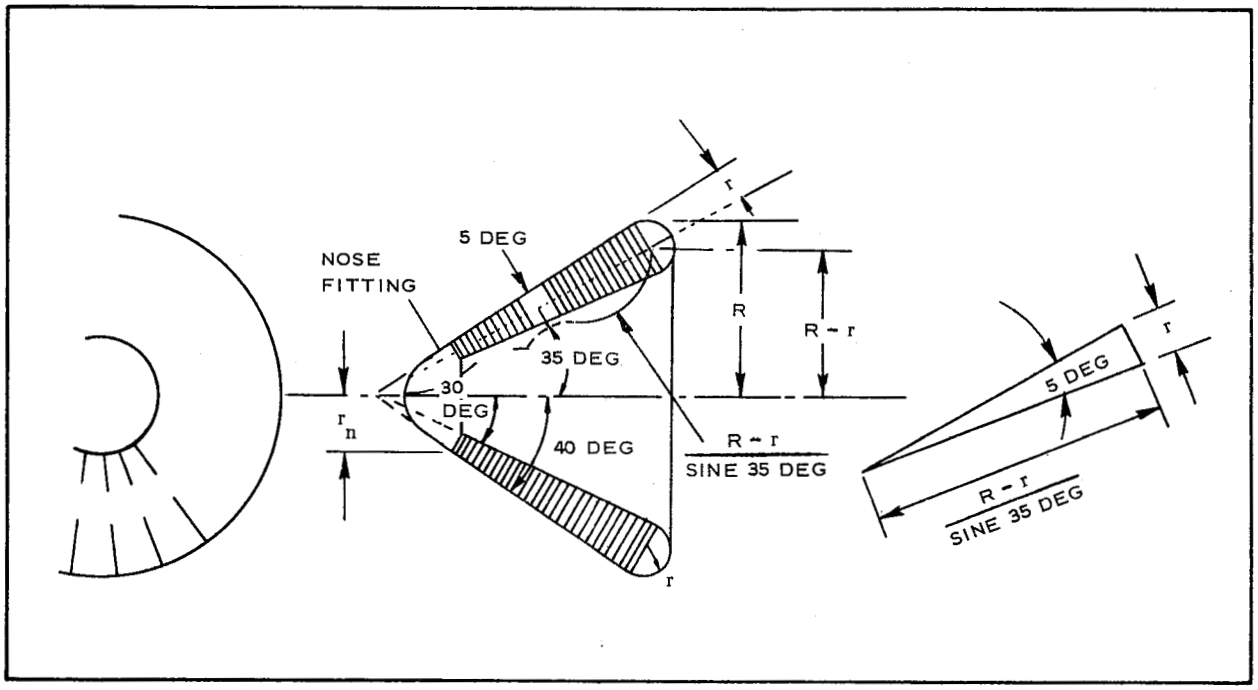

Figure 45 - Airmat Cone Dimensions

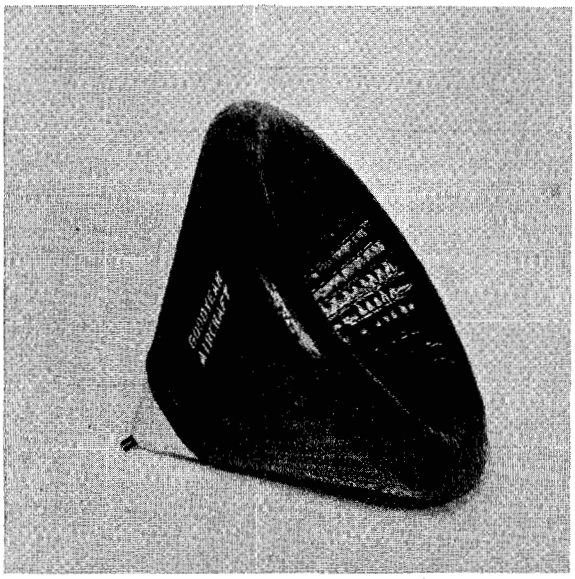

Figure 46 - 80-Deg Airmat Cone (Preinflated)

Since fabric is not effective in compression, the internal pressure must be sufficient to ensure only tension loadings. Reference 27 shows that the theoretical internal pressure must be at least 4.52 times the free-stream dynamic pressure to obtain tension loadings in the fabric. Wind tunnel tests (see References 27 and 48) supported this theory. It is important to note that this configuration requires pressurization from an additional source such as an air bottle. There is no documented evidence clearly showing ram-air inflation design feasibility, although this type of inflation method would indeed reduce the overall system weight.

(2) *Weight and Volume*

An analytical method of predicting the weight of the Airmat cone is given in Reference 27. This method is predicated on the assumption that the net external pressure over the face of the cone is constant and is given by $P = C_D q$. The internal pressure must be sufficient to counter the compressive loading of this external pressure. Accounting for both meridional and hoop stresses, the total cone weight, with an included safety factor of 2, is given as

$$W = \frac{17.4 C_D q R^3}{K_f} .$$

This does not include the weight of the drop threads, which is approximately an additional 30 percent by comparison. A plot of weight versus radius for various values of q is given in Figure 47.

e. Inflated Skirts (Flares)

At present, inflated skirts that have been built are comprised of coated fabric compartments formed by several right circular cone frustums with a common theoretical apex as shown in Figure 41. Each adjacent

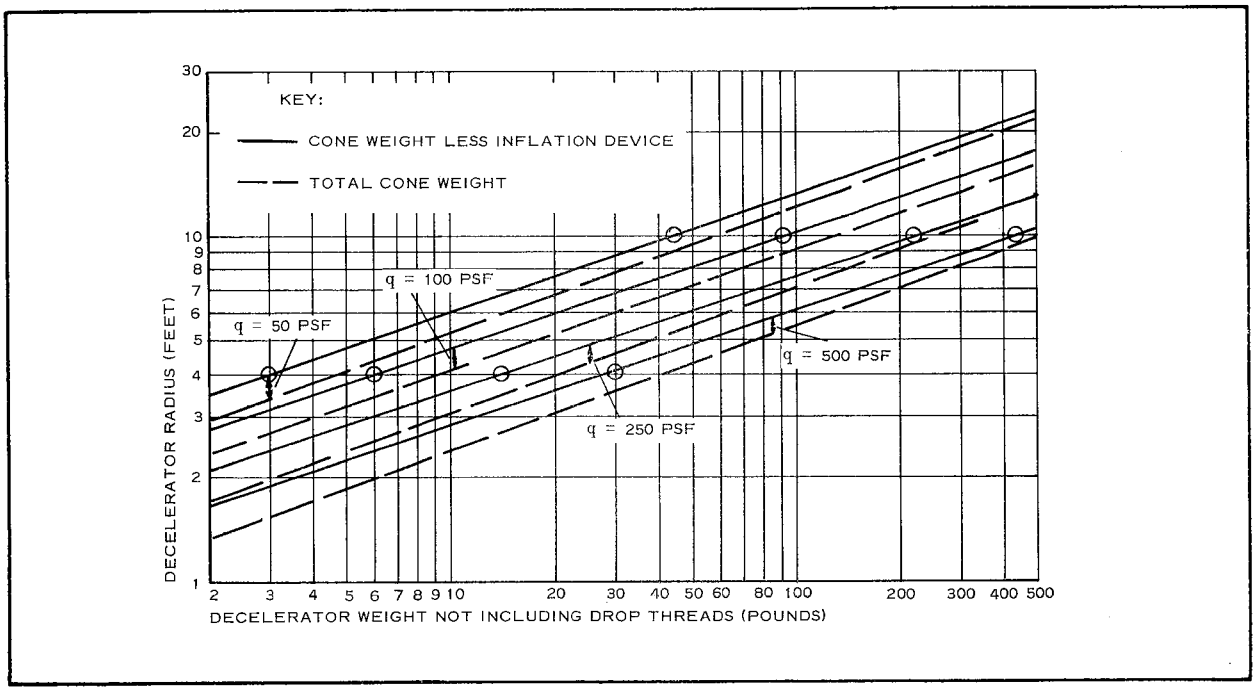

Figure 47 - Airmat Cone Weight vs Radius for Various Values of q

pair of cone frustrums intersects along two straight lines that must be connected by an internal fabric web to satisfy equilibrium of the hoop stresses at the intersection. Longitudinal meridian straps are placed along the outside intersection (gore seam) to withstand the longitudinal reaction forces. In addition to the fabric structure, a metal retaining ring connects the inner and outer surfaces of the compartments. While no single weight equation has been derived, procedures shown in Reference 27 can be used to determine weight.

f. Tension Shells

(1) Description

A tension-shell configuration (see Reference 66) is shown in Figure 48. The tension shell or tension shape is a concept in which aerodynamic surface loads are carried in tension. Since compression and buckling effects are eliminated, the full strength of the construction material can be utilized, and decelerators of

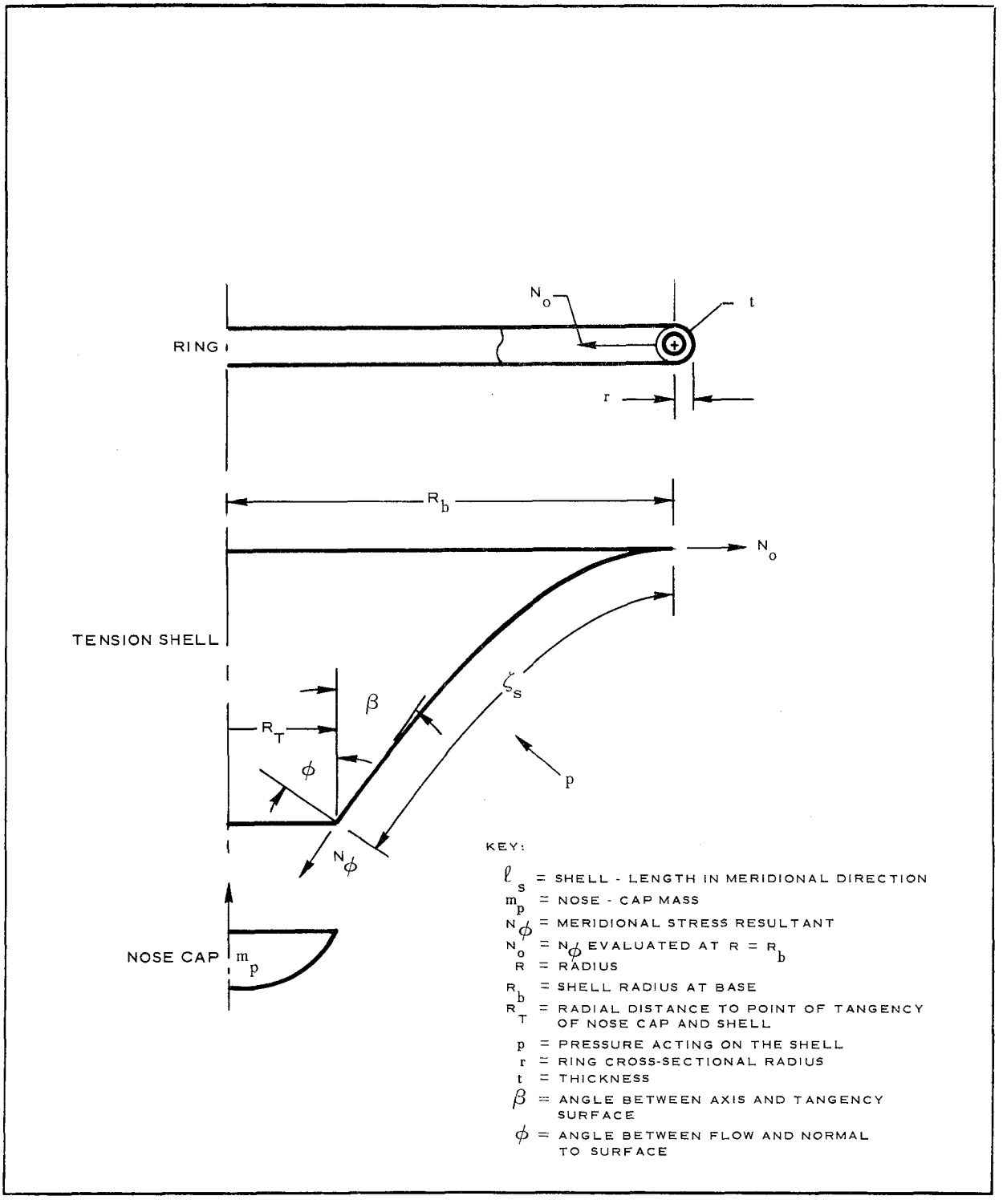

Figure 48 - Tension Shell Loading System, Assumed

potentially high structural efficiency are possible. The candidate deployable configuration can be either a semirigid or inflatable structure.

The tension shell, shown in Figure 48, is basically a cone-shaped structure with a blunted nose. The generated shell surface, however, is a concave surface of revolution. To eliminate hoops stresses, a catenary of revolution was chosen for analysis in Reference 65. It is feasible that this inflated base ring (torus) can be an inflated structure.

(3) Weight and Volume

Reference 65 presents a method for estimating the weight of the individual components and the total weight of the tension shell. This method assumes a variable thickness in the material, so that the membrane stress is constant and equal to the allowable value. Circumferential stresses are assumed to be negligible. For the upper shell and nose cap, the mass is estimated to be

$$m_{SH} = \frac{2\pi\rho}{\sigma_a} R_b^3 \frac{(q)}{(K^2)} \frac{l_s}{R_b} .$$

where

$$\frac{l_s}{R_b} = \frac{e^{K^2}\sqrt{\pi}}{4K}\left[\operatorname{erf}(K) - \operatorname{erf}\left(\frac{KR_T}{R_b}\right)\right] \frac{e^{-K^2}}{2K}\left[\phi(K) - \phi\left(\frac{KR_T}{R_b}\right)\right] .$$

For the ring, a uniformly distributed load is assumed. The mass of the ring is estimated in Reference 66 to be

$$m_R = 18 \times 27\rho R_b^3 \left(\frac{N_o}{ER_b}\right)^{\frac{2}{3}} ,$$

where

σ_a = allowable stress,

ρ = material density,

q = dynamic pressure,

K^2 = shape parameter associated with Newtonian pressure, $\frac{qR_b}{N_o}$,

l_s = shell length in meridional direction,

R = radius perpendicular to axis,

R_b = radius of model base,

R_T = radial distance to point of tangency of nose cap and tension shell,

N_ϕ = meridional stress resultant, positive in tension,

N_o = N_ϕ evaluated at $R = R_b$,

$$\text{erf}(K) = \frac{2}{\sqrt{\pi}} \int_o^A e^{-x^2} dx \text{ - error function,}$$

E = modulus of elasticity, and

$$\phi(K) = \int_o^A e^{x^2} dx .$$

Stowage and deployment of this configuration have not been documented.

8. MATERIALS

a. General

Material information in this report is limited essentially to (1) woven fabrics of synthetic fibers and metal filaments and (2) a variety of coating materials for porosity reduction and heat protection of woven

fabrics. Decelerator structure requirements of small predeployment volume, low weight, and high strength indicate that flexible structures are the most feasible. Of the flexible materials, woven fabrics are the most applicable for the majority of the decelerator performance requirements.

In general, the evaluation of woven fabrics is most conveniently accomplished by the analysis of the basic unit of fabrication - that is, fibers, yarns, or filaments. This is due to the myriad of variables involved in the direct analysis of a woven fabric, including those of the same basic units arising from the various weave patterns, fabrication techniques, cloth variations, nonhomogeneity of the cloth, etc. Thus, to provide a comparatively easy yet relatively effective method of woven cloth evaluation, attention is given to the basic units from which the characteristics of the fabric material (woven cloth) are largely dependent.

In addition, experimental data of various types of woven fabric (unit weights and strengths) tests over a wide range of loading conditions (and at various temperatures) are not available. Hence, material test data descriptions and discussions that follow are limited to the basic fibers, yarns, or filaments.

Important fiber qualities or characteristics for deployable decelerator materials include the following: (1) high strength, (2) temperature resistance, (3) high modulus of elasticity, (4) flexibility, (5) abrasion resistance and (6) chemical stability. A review of these basic properties as related to use in flexible structures shows that the desired high modulus of elasticity and flexibility characteristics are contradictory and are difficult problems for textile technology and production. Currently available fibers with good temperature-resistance qualities also tend to have high modulus characteristics, making temperature resistance and flexibility difficult to attain in a single fabric.

Table XIII summarizes the effects of various environmental conditions on the manmade and natural textiles that have been used in aerodynamic decelerators. Table XIV gives the modulus of elasticity and filament size relative to nylon and fiberglass for organic, synthetic, and metallic materials.

b. Textile Yarns and Fibers

(1) General

To date, most decelerator applications are filled by woven fabrics of nylon, Dacron, or Nomex. Thus, the proponderance of data available, appropriate for decelerators, are associated with these three yarns. In the following discussion, various properties of these yarns will be described and their use in terms of environmental and manmade conditions will be analyzed.

As is the custom with all engineering materials, fiber-breaking strengths can be listed on a psi basis. More commonly, however, the textile trade uses the term "tenacity" to describe strength on gram per denier[a] (gpd) basis since (1) a fiber's or yarn's weight per length can be determined easier than its cross-sectional area and since (2) yarn weight is an important textile physical and economic factor. Since denier is based upon weight per unit length, tenacity obviously is influenced by the specific gravity of the fiber, while strength per unit area is not. Relationship between these two properties is:

$$\text{Tensile strength (psi)} = 12,800 \times \text{specific gravity} \times \text{tenacity (gpd)}$$

Consequently, strength relationships of the yarns will, in the following discussion, often be measured in terms of tenacity. Fiber tenacity for various textiles is listed in Table XV.

[a]Denier is defined as the weight in grams of 9000 m of yarn.

TABLE XIII - EFFECTS OF ENVIRONMENT ON NATURAL AND MANMADE TEXTILES*

Environment	Cotton	Silk	Viscose Rayon	Fortisan	Nylon	Orlon
Heat	Highly resistant to dry heat; yellows at 248 F; decomposes at 302 F; burns readily	Begins to decompose at 270 F; rapid disintegration above 300 F; burns readily	Loses strength above 300 F; decomposes at 350 F to 400 F; burns readily	Scorches in ironing at about 20 C higher than cotton, otherwise like cotton, viscose rayon	Yellow slightly at 300 F when exposed for 5 hr; melts at 482 F	Sticks at 455 F; slight loss in strength after 32 days in air at 275 F melts at 480 F
Age	Little or none	Slight yellowing and loss of tensile strength	Slight	Little or none	Virtually none	Virtually none
Sunlight	Loses strength; formation of oxycellulose; tendency to yellowing	Loses tensile strength; affected more than cotton	Loses tensile strength after prolonged exposure; very little discoloration	Loses strength, tends to color	Loses strength on prolonged exposure; no discoloration; bright yarn more resistant than semi-dull	Very resistant to degradation by ultraviolet light and atmosphere
Chemicals	Disintegrated by hot dilute acids or cold conc. acids. Shells (mercerization) in caustics damaged by prolonged exposure in presence of air. Bleached by hypochlorites and peroxides, oxidized into oxycellulose by strong oxidizing agents.	Fairly resistant to weak acids; dissolved by strong acids except nitric. Insensitive to dilute alkali unless hot; dissolves in strong alkalis. Above pH11 and below pH3 stability decreases rapidly	Strong alkali causes swelling and reduces strength. Attached by strong oxidizing agents; not damaged by hypochlorite or peroxide bleaches	Disintegrates in hot dilute or cold concentrated acids. Strong caustic shrinks, as in mercerizing. Resistant to bleaches, phenols, and dyehouse reagents	Boiling in 5% HCl ultimately causes disintegration; dissolves in cold conc. sulfuric or nitric acids. Substantially inert to alkali. Generally good resistance to other chemicals	Good to excellent resistance to mineral acids. Fair to good resistance to weak alkalis. Not harmed by oils, greases, neutral salts and some acid salts
Organic solvents	Resistant	Resistant	Generally insoluble; soluble in cuprammonium	Unaffected	Insoluble except in some phenolic compounds and conc. formic acid	Unaffected by common solvents
Moths	Not attacked	Attacked slightly	Not attacked	Not attacked	Not attacked	Not attacked
Mildew	Poor resistance unless	Attacked	Attacked	Same as for cotton	Good resistance	Good resistance (coating may be attacked)

Environment	Dacron	Glass Fiber	Polyethylene	Mylar	Nomex HT-1	
Heat	Highly resistant to degradation and discoloration; melts at 480 F	Will not burn; strength loss starts at 600 F, continues to limiting temp. of 1000-1500 F, softens 1500 F	5% shrinkage at 165 F; softens at 225 to 235 F; melts at 230 to 250 F; slow burning	Strength reduced above 200 F, useful to 300 F, melts 482 F	Degrades above 700 F to friable char at 482 F; has 60 % room temp. structural strength	
Age	Virtually none	None	Virtually none under normal conditions	Virtually none	Virtually none	
Sunlight	Loses strength on prolonged exposure; no discoloration	None	Prolonged exposure decreases tensile strength	Moderate resistance	Loses strength on prolonged exposure; surface turns bronze	
Chemicals	Good resistance to mineral acids except conc. sulfuric. Good resistance to weak alkali, moderate to strong alkali at room temp.; dissolves in hot strong alkali. General good resistance to other chemicals; excellent to bleaches and oxidizing agents.	Good resistance to all but hot strong acids. Attacked by hot solutions of weak alkalis and cold solutions of strong alkalis. Generally good resistance.	Very resistant to acids. Generally good resistance to caustics and other chemicals.	Good resistance to cold dilute acids and alkalis. Becomes brittle in hot mineral acids and alkalis. Generally resistant to common chemicals	Acid resistance better than nylon 6-6; not as good as Dacron or Orlon; degraded by strong alkali at elevated temperature	
Organic solvents	Generally insoluble; soluble in some phenolic compounds	Insoluble	Insoluble, but swells in chlorinated hydrocarbons, aromatics	Insoluble; degraded by phenols and cresols	Highly resistant to most hydrocarbons	
Moths	Not attacked	Not attacked	Not attacked	Not attacked	Not attacked	
Mildew	Good resistance	Wholly resistant (binder may be attacked)	Good resistance	Good resistance	Good resistance	

* Source - Reference 1.

123-A

123-B

TABLE XIV - FILAMENT DIAMETERS REQUIRED FOR FLEXIBILITY EQUIVALENT TO NYLON AND FIBERGLASS*

Material	Modulus of elasticity (psi × 10^{-6})	Diameter required for same flexibility	
		19 u nylon	15 u fiberglass
Nylon	0.4	19.0	31.7
Silk	2.1	12.8	21.0
Carbon	0.7	16.8	27.5
Viscose rayon	1.6	13.7	22.4
Fiberfrax	6.8	9.5	15.7
Fiberglass	8.0	9.1	15.0
Fused silica	10.0	8.6	14.2
Gold	12.0	8.2	13.5
Columbium	22.7	7.1	11.2
Platinum	25.0	6.9	11.2
Iron, nickel, copper	30.0	6.6	10.8
Aluminum oxide	34.0	6.4	10.4
Tungsten, molybdenum	50.0	5.8	9.5
Iridium	75.0	4.8	8.6

*Source - Reference 86.

Preceding page blank

TABLE XV - FIBER TENACITIES*

Material	Dry tenacity		Wet tenacity
	Grams per denier (gpd)	Pounds per square inch (psi)	Percent of dry tenacity
Asbestos	2.5 to 3.1	80,000 to 300,000	. . .
Cotton, raw	3.0 to 4.9	59,500 to 97,000	100.0 to 110.0
Cotton, mercerized+	3.4	67,000	. . .
Flax	2.6 to 7.7	50,000 to 148,000	. . .
Hemp	5.8 to 6.8	110,000 to 129,000	. . .
Henequen	3.0 to 3.5	57,000 to 72,000	83.0 to 86.0
Jute	3.0 to 5.8	57,000 to 110,000	. . .
Manila abaca	6.0 to 7.5	115,000 to 155,000	100.0 to 113.0
Ramie	5.5	106,000	. . .
Silk	2.4 to 5.1	38,500 to 88,000	71.0 to 74.0
Sisal	4.0 to 5.0	64,000 to 89,000	92.0 to 100.0
Wool	1.0 to 1.7	16,500 to 28,000	76.0 to 97.0
Acrilan acrylic	2.0 to 2.7	30,000 to 40,500	80.0
Creslan acrylic	2.5	38,000	100.0
Orlon acrylic	2.2 to 2.6	32,000 to 39,000	80.0
Zefran acrylic	3.5	53,000	89.0
Acetate	1.3 to 1.5	20,500 to 26,000	61.5 to 80.0
Arnel triacetate	1.2 to 1.4	20,000 to 23,000	71.4 to 75.0
Arnel 60 triacetate	2.0 to 2.3	33,000 to 38,000	74.0 to 75.0
Teflon fluorocarbon	1.7	50,000	100.0
Glass	6.0 to 7.3	195,000 to 237,500	65.0
Dynel modacrylic	3.0	50,000	100.0
Verel modacrylic	2.5 to 2.8	44,000 to 49,000	96.0 to 96.4

*Source - Reference 88.

+Compared with an unmercerized cotton control value of 2.8 gpd.

TABLE XV - FIBER TENACITIES*(Continued)

Material	Dry tenacity		Wet tenacity
	Grams per denier (gpd)	Pounds per square inch (psi)	Percent of dry tenacity
Nylon 6, regular	4.5 to 5.8	66,000 to 86,000	91.3 to 95.5
Nylon 6, high tenacity	6.8 to 8.6	99,000 to 125,500	79.4 to 87.2
Nylon 66, regular	4.6 to 5.9	67,000 to 86,000	87.0 to 88.0
Nylon 66, high tenacity	5.9 to 9.2	86,000 to 134,000	86.4 to 85.8
Darvan nytril	2.0	30,000	85.0
Polyethylene, low density	0.5 to 2.0	5,900 to 23,500	100.0
Polyethylene, high density	4.5 to 8.0	55,000 to 98,000	100.0
Polypropylene	4.0 to 7.0	46,000 to 81,500	100.0
Polyvinyl alcohol	4.5 to 6.0	91,000 to 122,000	80.0 to 85.0
Dacron polyester, regular	4.4 to 5.0	78,000 to 88,000	100.0
Dacron polyester, high tenacity	6.3 to 7.8	111,000 to 138,000	100.0
Fortrel polyester	4.0 to 4.3	71,000 to 76,000	100.0
Kodel polyester	2.5 to 3.0	39,000 to 47,000	100.0
Vycron polyester	5.6 to 6.3	97,500 to 110,000	. . .
Saran	1.1 to 2.3	24,000 to 50,000	100.0
Lycra spandex	0.6 to 0.8	9,000	19.0 to 25.0
Vyrene spandex	0.5 to 0.6	9,000	100.0
Steel	3.5	512,500	100.0
Vinyon	0.7 to 2.4	12,000 to 43,000	100.0
Viscose rayon, regular	1.5 to 2.4	28,000 to 47,000	46.6 to 58.3

*Source - Reference 88.

TABLE XV - FIBER TENACITIES* (Continued)

Material	Dry tenacity		Wet tenacity
	Grams per denier (gpd)	Pounds per square inch (psi)	Percent of dry tenacity
Viscose rayon, intermediate tenacity	2.4 to 3.2	45,000 to 62,000	50.0 to 59.3
Viscose rayon, high tenacity	3.0 to 5.0	56,000 to 97,000	63.3 to 72.0
Cuprammonium rayon	1.7 to 2.3	33,000 to 45,000	53.0 to 61.0
Fortisan saponified acetate	6.0 to 7.0	117,000 to 136,000	85.0
Fiber 40 (Avril) rayon	5.0	96,000	70.0
XL (Avron) rayon	4.1	80,000	73.1
Corval rayon	2.0 to 2.2	37,000 to 43,000	59.1 to 60.0
Zantrel rayon	3.8 to 4.0	73,500 to 77,000	74.0 to 75.0

*Source - Reference 88.

(2) Effects of Sterilization and Vacuum

The state of the art relating to the effects of biological sterilization and vacuum soaking on silk, nylon, Dacron, and Nomex material is adequately described in Reference 87. Major conclusions of the reference are discussed below.

Silk was immediately eliminated, and nylon was so seriously degraded by thermal sterilization that further testing was not considered. If the thermal sterilization could be mitigated, nylon probably would withstand the chemical sterilization without serious degradation. Du Pont reports that nylon has been subjected to ethylene oxide and to Freon 12, separately, at temperatures higher than the 104 F called for in Reference 86 without serious degradation. Therefore, the combination probably would not be seriously harmful. The nylon, after thermal cycling, was markedly stiffer and less flexible. No adhesion of the nylon to itself or to the stainless steel plates was observed (in contrast to the preliminary tests where adhesion of unscoured materials was observed). No adhesion was observed with either Dacron or Nomex. Thus, long-time, packed storage at elevated temperature with or without vacuum should not be a serious concern for fabric structures of nylon, Dacron, or Nomex. Dacron is a promising candidate material for a sterilizable retardation system. Average strength losses of all dacron material configurations resulting from both sterilization and vacuum exposures did not exceed 20 percent. Nomex is also a promising candidate material for the Mars entry retardation system. Average strength losses of all Nomex material configurations resulting from both sterilization and vacuum exposures did not exceed 5 percent.

Depending on the specific material and the temperature-vacuum envelope, some stiffening and heat setting of folds and wrinkles

could occur with possible adverse effects on deployment. Negligible effects due to folding and compacting were observed.

(3) Effects of Temperature and Sustained Loadings

Figures 49 and 50 present typical strength relationships for nylon, Dacron, and Nomex under various conditions. These curves indicate that optimum strength-to-weight characteristics for undegraded materials at room temperature are obtained with nylon, Dacron, and Nomex, respectively. Figure 50, however, indicates that these yarns appear in the same order when listed by their sensitivity to initial elevated temperature values and sustained loads applied at room temperature. Thus, after exposure to a preload temperature of 350 F, for example, Dacron is superior to scoured nylon after a loading time of 5 hr and Nomex is superior to Dacron after a loading time of 100 hr. These effects become more pronounced with exposure to higher preload temperatures, with Dacron having almost twice the tenacity of scoured nylon after exposure to 425 F and a relatively short 1-hr loading. Nomex, on the other hand, remains usable after exposure to preload temperatures up to 580 F and a continuous loading time of 200 hr.

Figure 51 indicates the relative performance of nylon, Dacron, and Nomex when subjected to a sustained load at an elevated temperature. At a temperature of about 400 F, nylon, Dacron, and Nomex, respectively, exhibit the best initial properties. Above 400 F, Nomex is the only one of the three that will withstand a sustained load.

Somewhat less temperature sensitivity was observed with unscoured nylon as opposed to scoured nylon, which resulted - apparently - from the protection of the manufacturing oils. No difference between scoured and unscoured Dacron is indicated in Reference 86.

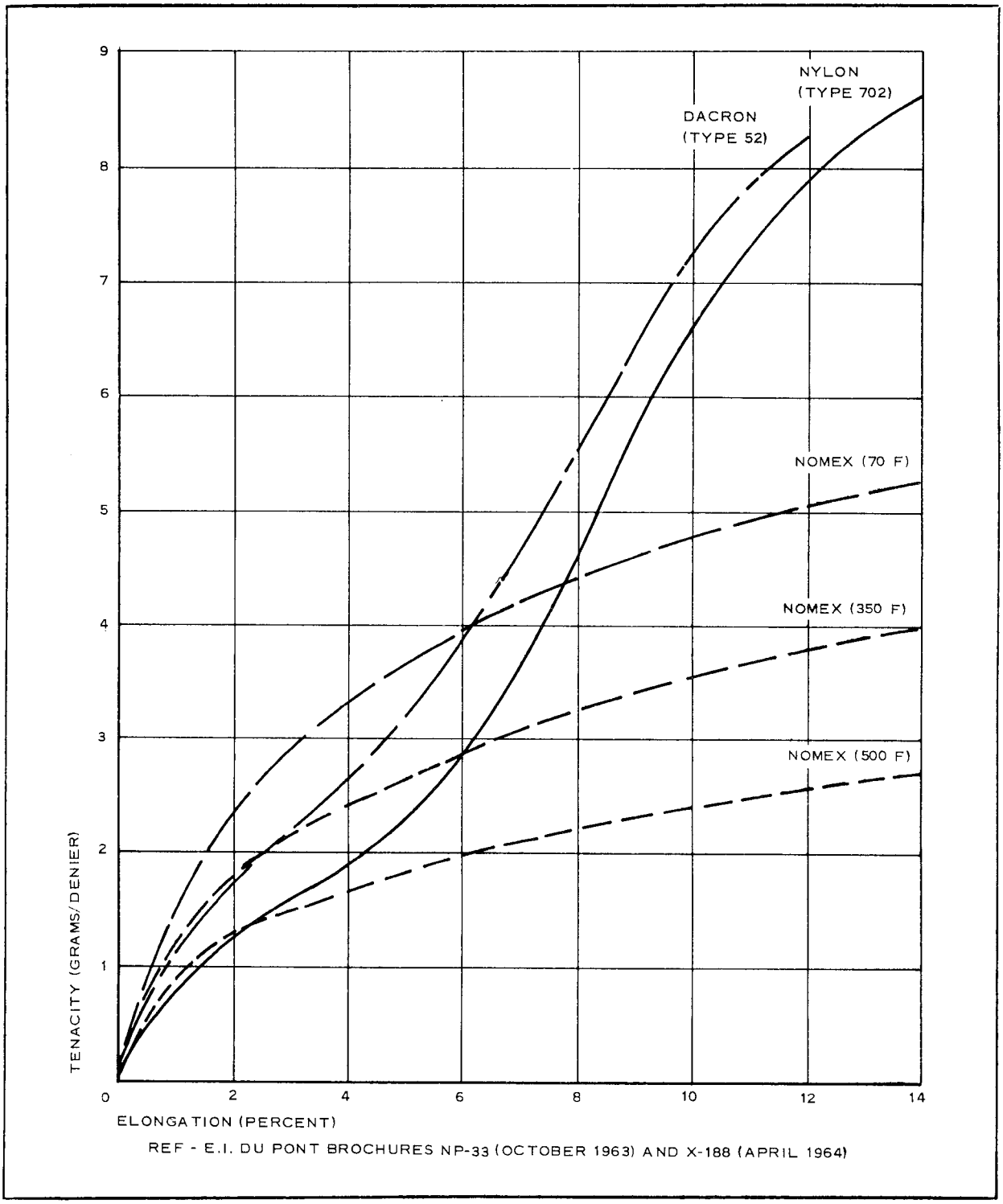

Figure 49 - Typical Stress-Strain Curves for Dacron, Nylon, and Nomex

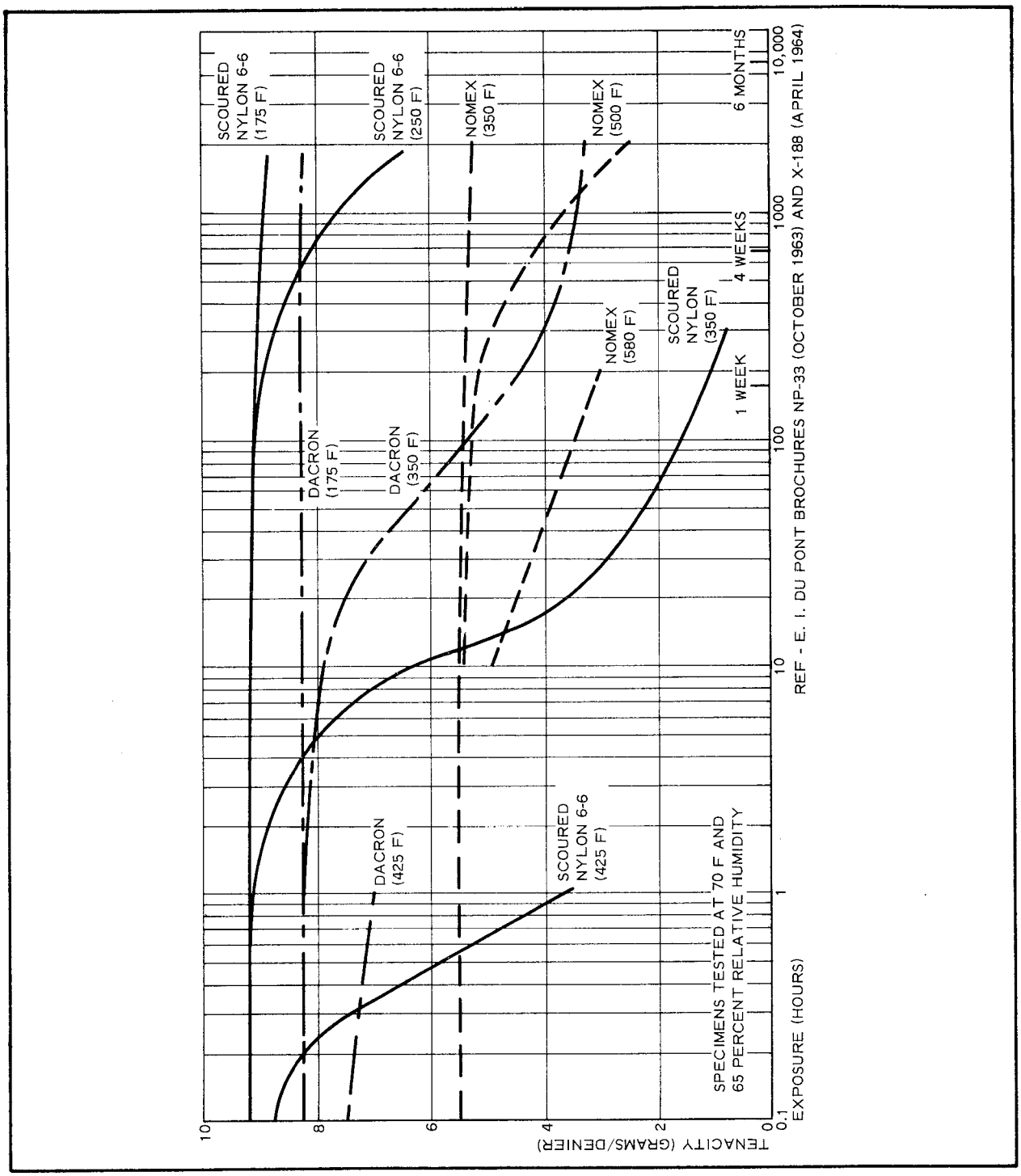

Figure 50 - Strength Retained by Nylon, Dacron, and Nomex Yarns after Exposure to Hot, Dry Air

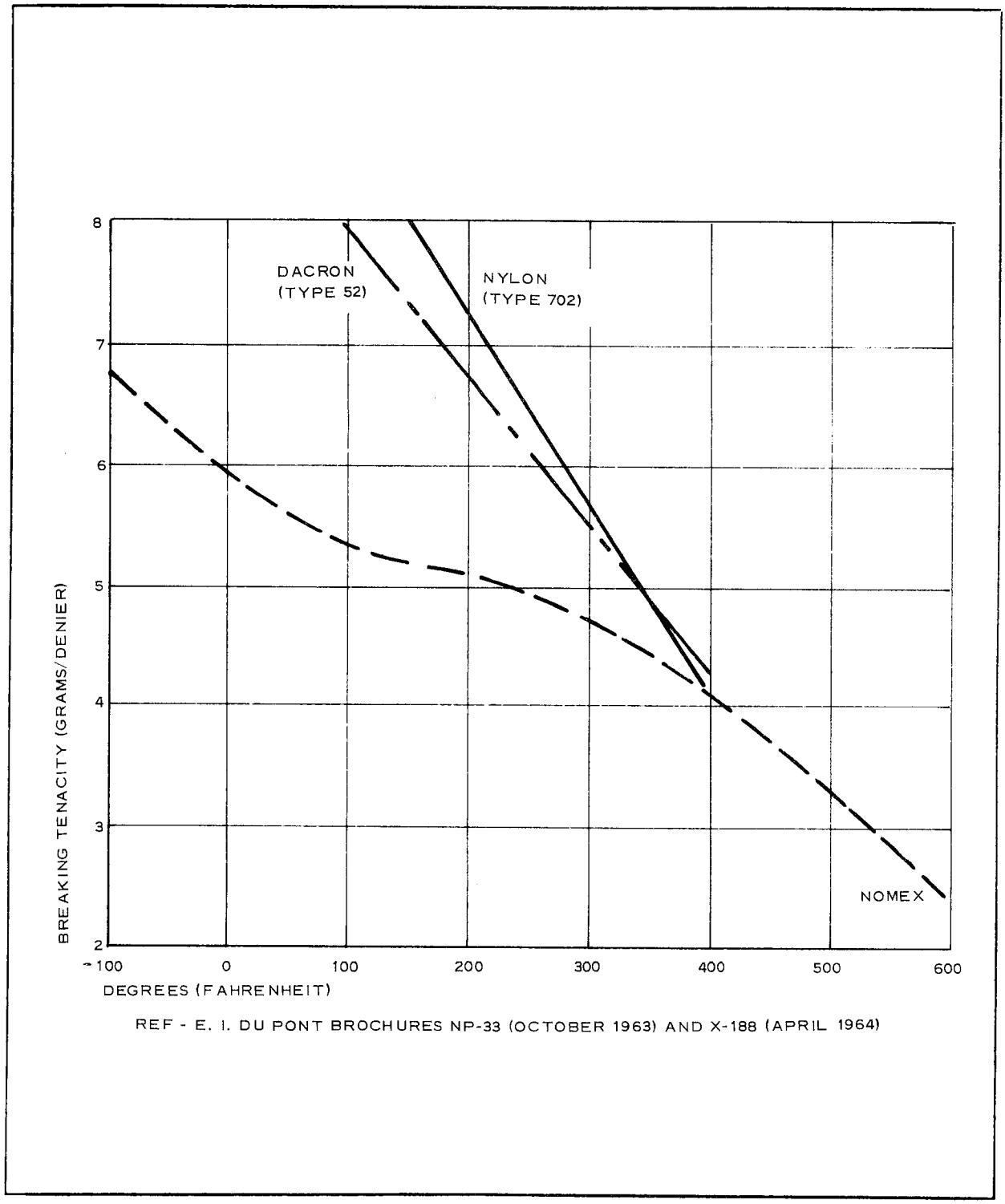

Figure 51 - Breaking Tenacity at Various Temperatures

(4) Stiffness

At room temperatures, nylon is more flexible than Dacron, and both are more flexible than Nomex for elongations below approximately 6 percent (see Figure 49). When stressed to break, however, Nomex is the most flexible, with Dacron and nylon both being approximately 50 percent stiffer.

(5) Shrinkage

The heat shrinkage of virgin fiber is presented in Figure 52. Dacron reaches about 25 percent shrinkage at about 440 F; nylon reaches 16 percent at the same temperature and Nomex only 4-1/2 percent at 600 F. These shrinkages occur in about 30 sec from the time the yarn reaches temperature. While nylon will start shrinking from temperatures above 75 F, Dacron does not start until temperatures above 140 F are obtained. The crossover is at 4 percent shrinkage at 225 F. A heat-setting process obviously must be called out in the procurement of nylon and Dacron before patterns are cut.

(6) Radiation Resistance

Nylon, Dacron, and Nomex are all degraded in tensile strength and elongation by irradiation with ultraviolet. Their responses, maximum and minimum, are not necessarily to the same wavelengths (see Figures 53 through 55). Nylon is least affected by 369 mμ and most degraded by 244 mμ; Dacron least by 369 mμ and most by 314 mμ; Nomex least by 314 mμ and most by 369 mμ. Nomex has the best long-range resistances. Bar graphs (see Figure 56) show how ultraviolet radiation and elevated temperatures affect Nomex.

Gamma radiation results are presented for Nomex in Figure 57. Radiation resistance of Nomex, Dacron, and nylon 6-6 is presented in Table XVI with respect to various radiation sources.

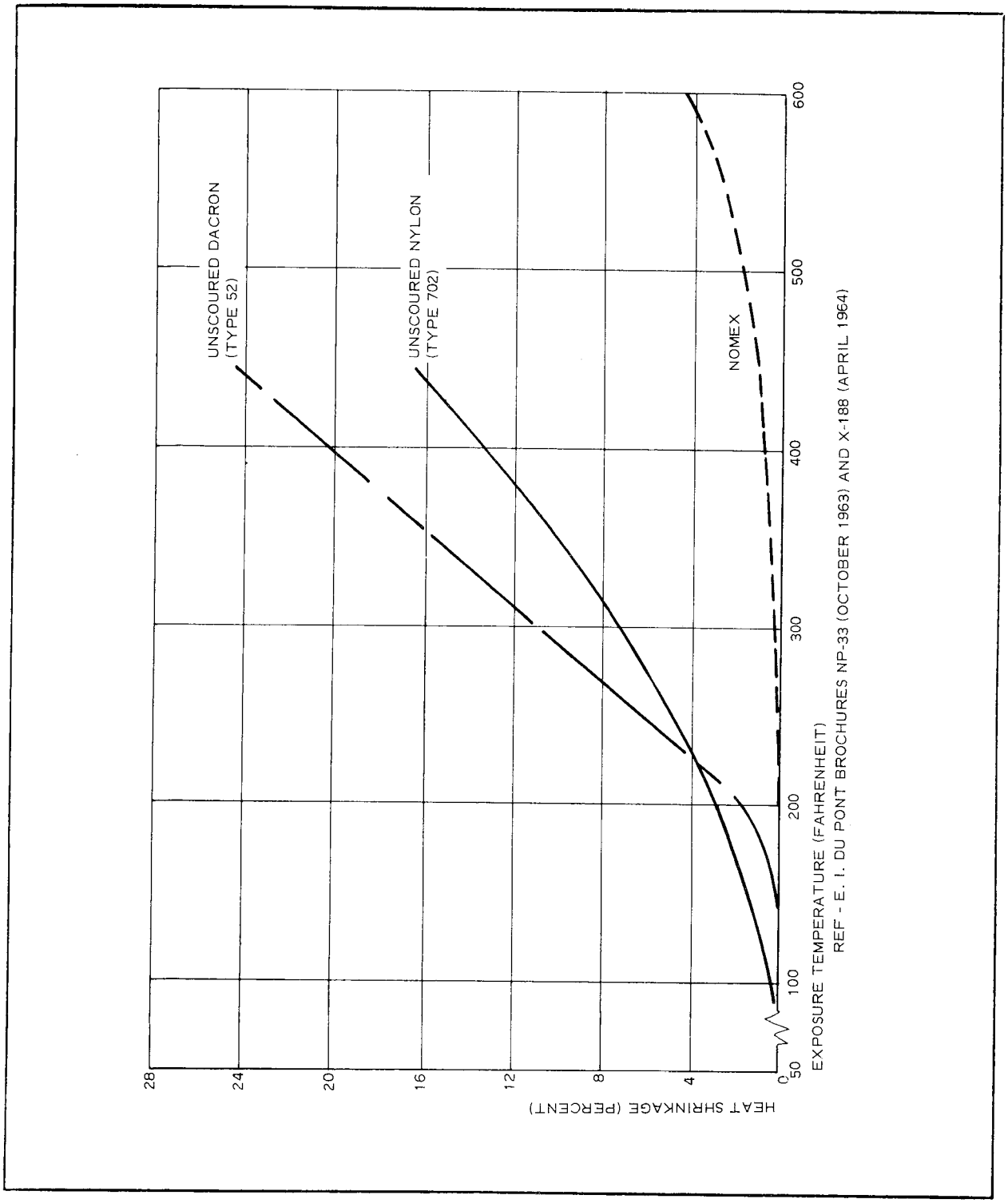

Figure 52 - Shrinkage of Nylon, Dacron, and Nomex Exposed to Hot, Dry Air

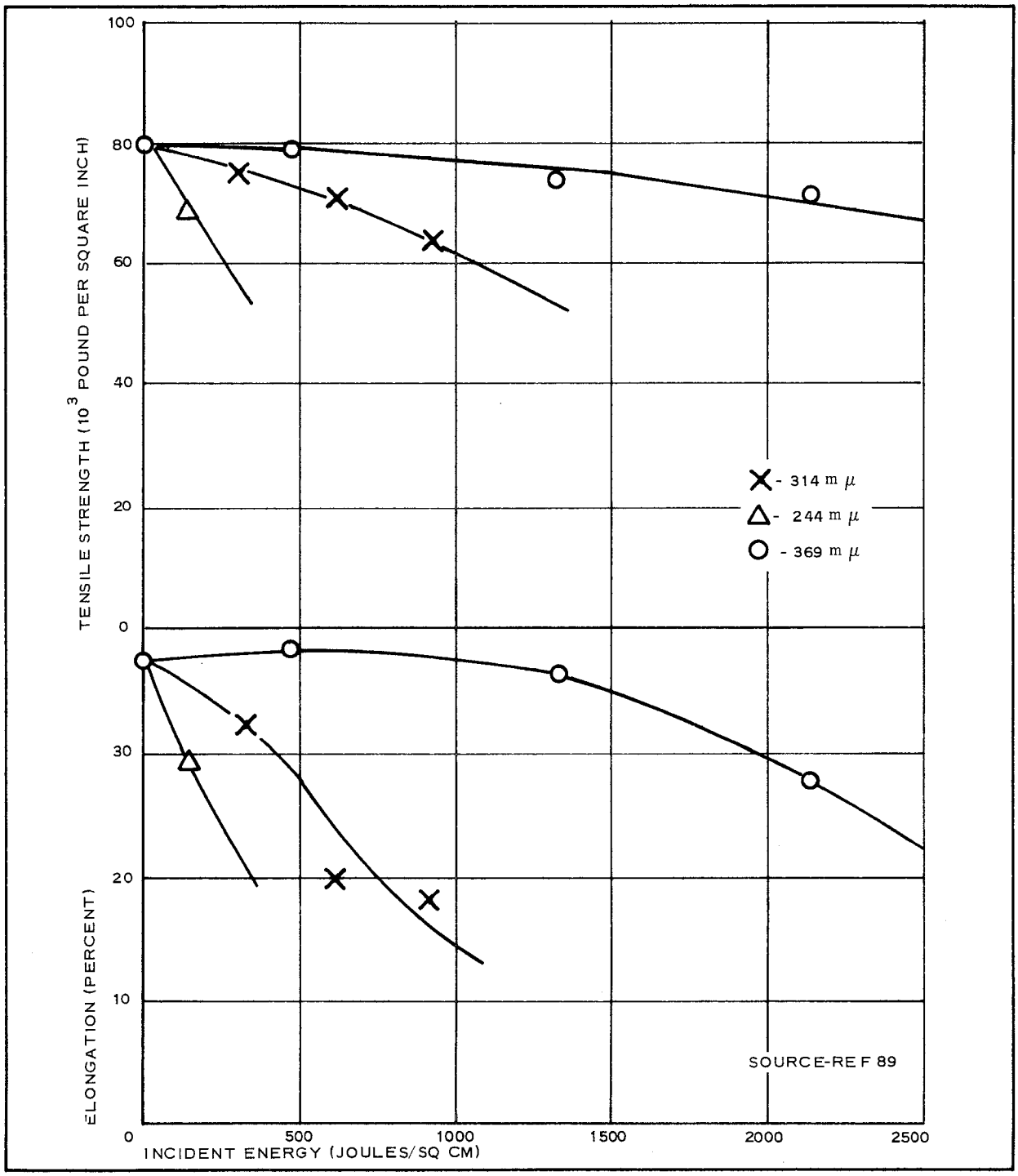

Figure 53 - Variation of Tensile Strength and Elongation of Nylon Fibers Irradiated in Nitrogen at 244 mμ, 314 mμ, and 369 mμ

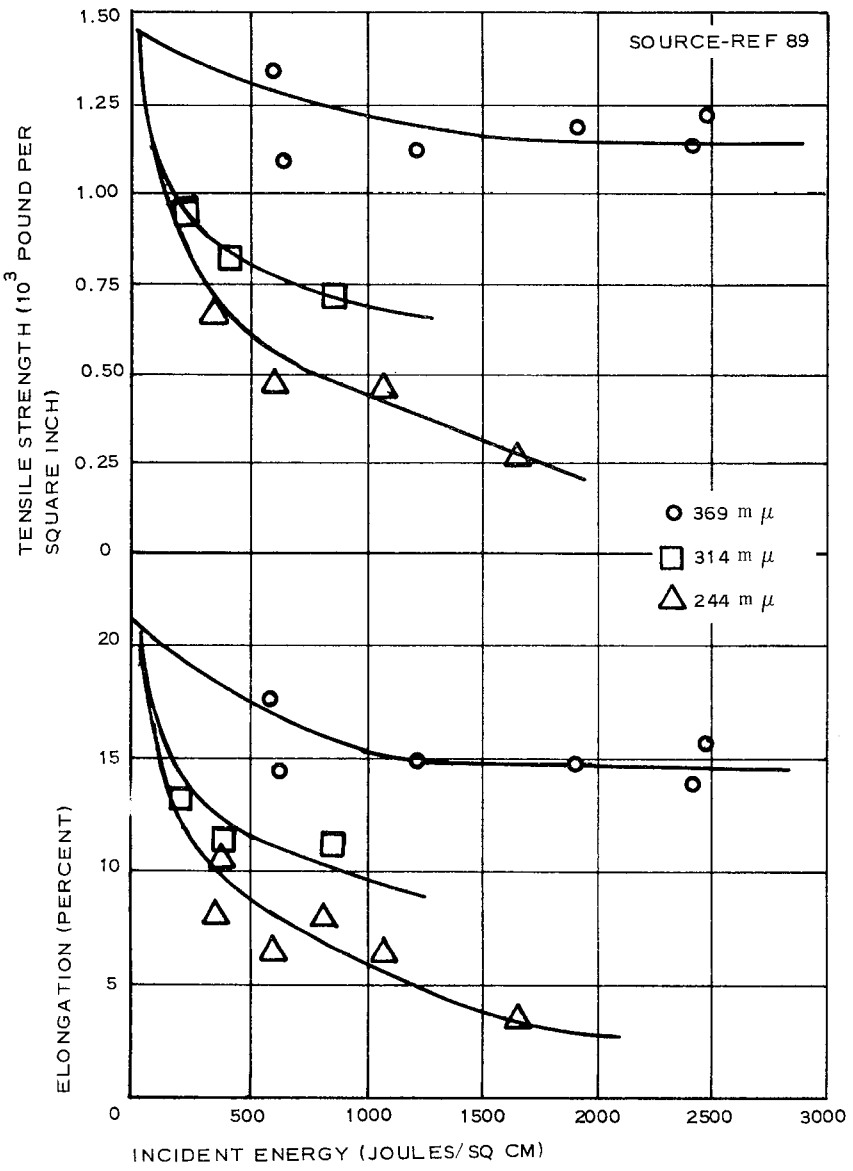

Figure 54 - Variation of Tensile Properties with Incident Energy for Dacron Irradiated in Nitrogen with A-H6 Lamp

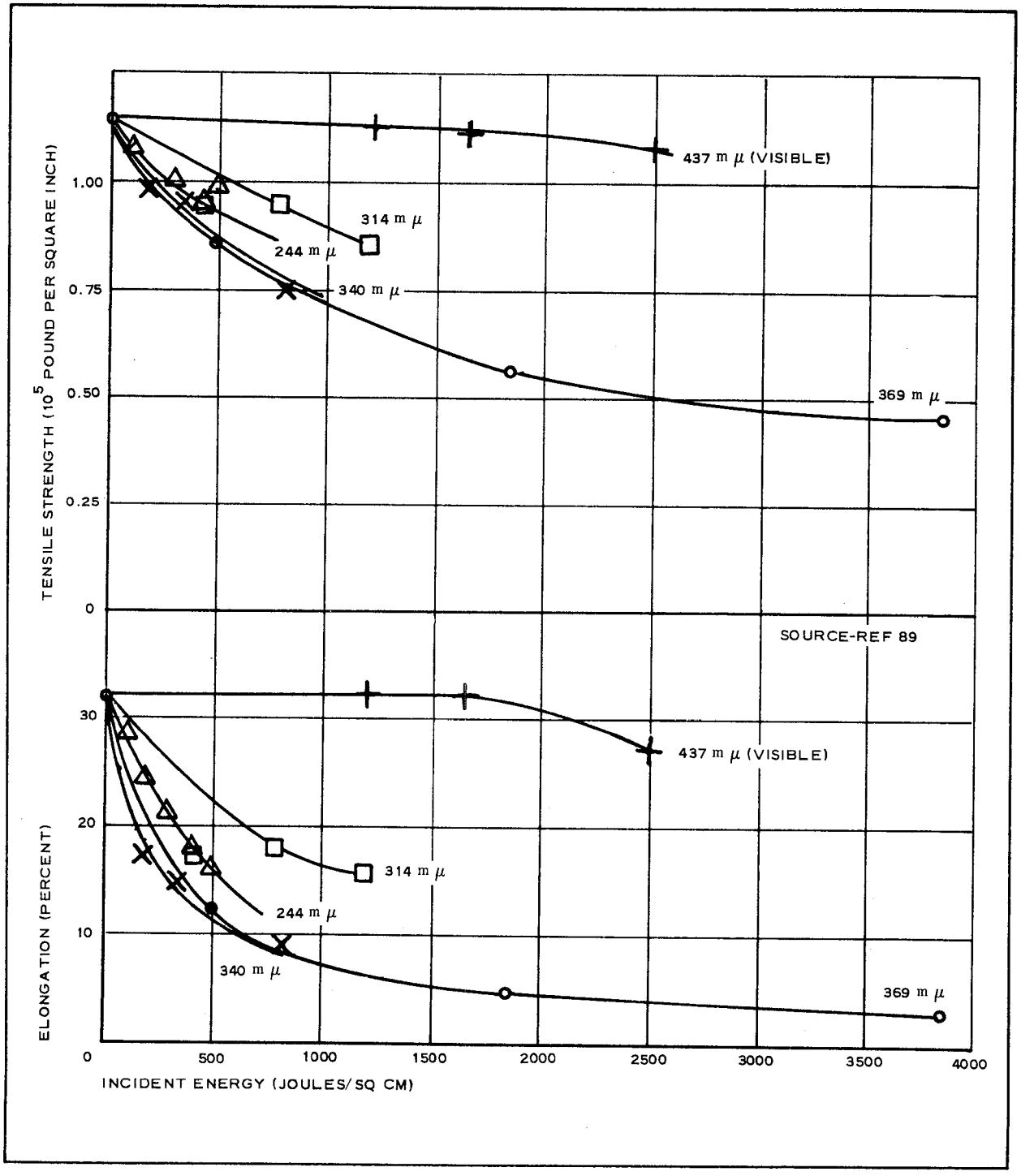

Figure 55 - Variation of Tensile Strength and Ultimate Elongation of Nomex Irradiated in Nitrogen with Ultraviolet Light and with Visible Light (437 mμ)

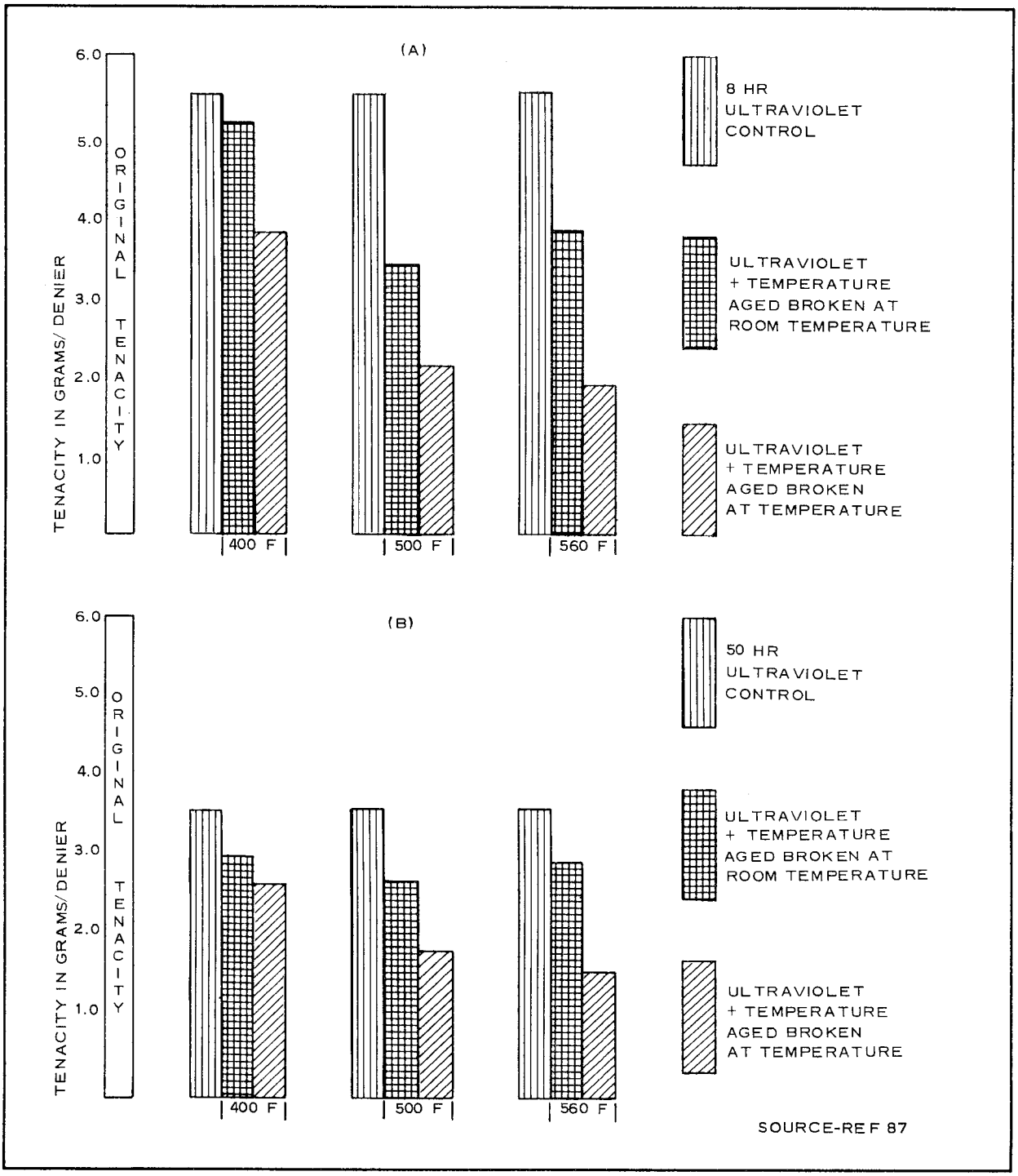

Figure 56 - Degradation of Nomex after Exposure to Ultraviolet Radiation and Elevated Temperatures

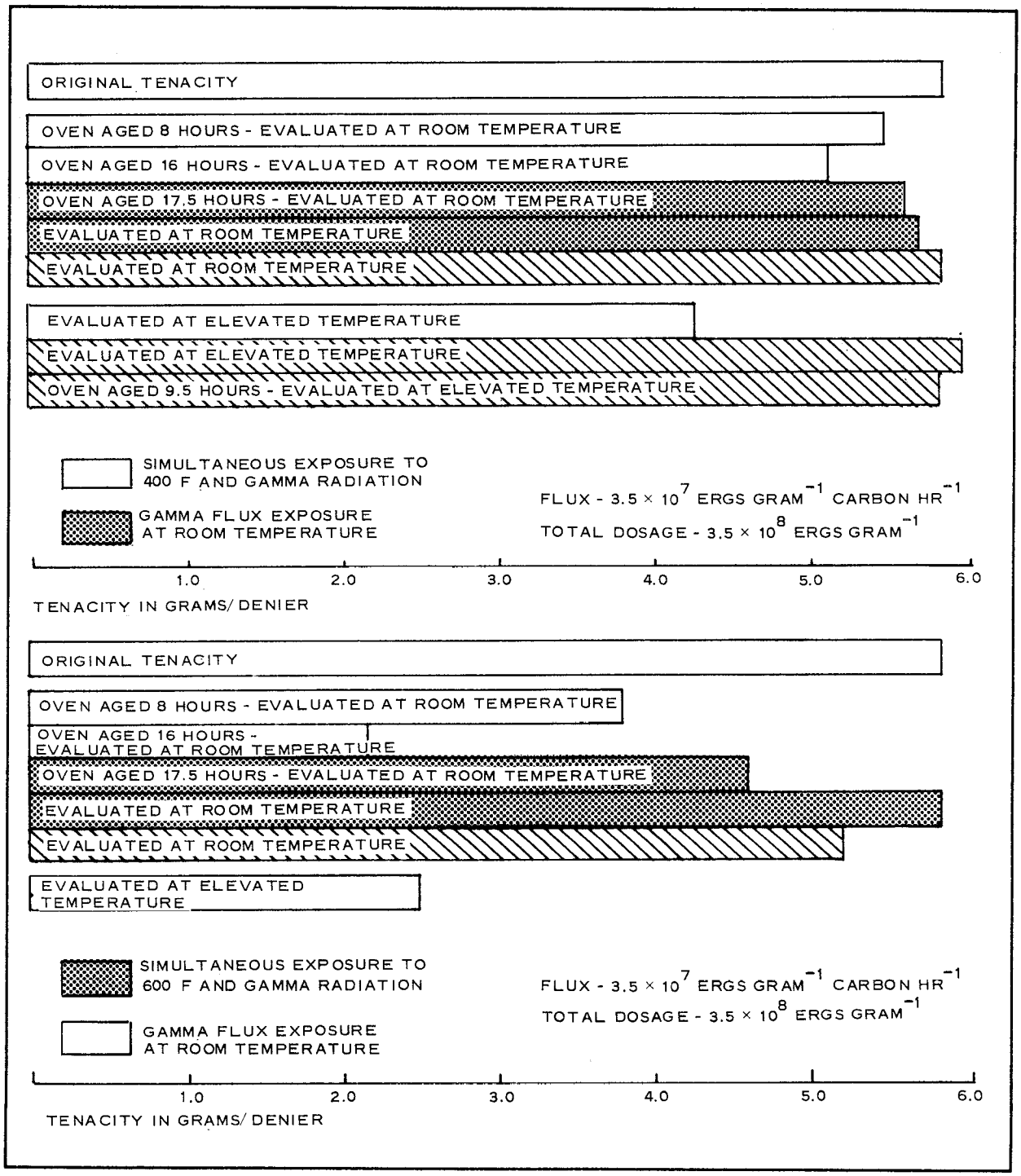

Figure 57 - Effects of Gamma Radiation on Nomex at 400 F (Top) and at 600 F (Bottom)

TABLE XVI - RADIATION RESISTANCE: EFFECT OF EXPOSURE ON YARN STRENGTH*

Dosage	Tenacity retained (percent)		
	Nomex	Dacron	66 Nylon
β - Van de Graaf			
200 mega reps	81	57	29
600 mega reps	76	29	0
X-rays (50 kv)			
50 hr	85	22	. . .
100 hr	73	0	. . .
250 hr	49	0	. . .
Brookhaven pile (50 C)			
200 mega reps	70	45	32
1000 mega reps	55	Radioactive	Crumbled
2000 mega reps	45	Radioactive	Crumbled

*Source - Reference 87.

(7) Weathering

The effects of outdoor exposure on a candidate decelerator material is an important consideration for determining both preoperative and postoperative requirements. Prior to operations, for example, exposure effects may indicate the sensitivity of the fabric to various types of stowage and handling. This, in turn, dictates the type and duration of the preoperative environment and indicates the general acceptability of fabric for various applications. In addition, the ability of decelerator materials to withstand the outdoor environment following operations may be critical in the success of the mission. For example, degradation of the fabric due to weathering may be critical if, following a test, the decelerator is not immediately located.

Figure 58 indicates the relative resistance of nylon and Nomex fabrics to a weathering environment. No generally clear superiority to weathering is exhibited by either, with nylon 330 being the least affected and nylon 300 being the most affected.

(8) Yarn-to-Fabric Strength Correlation

No simple and universal ratio exists between yarn and fabric material strengths and/or elongations. Fabric strength will invariably be less than the sum of its yarns, and fabric elongation will be greater. Many factors are involved including thread count in warp and fill; basic elongation characteristics of material; tension maintained during weaving (always greater in warp than in fill); rate of loading; uniaxial or biaxial stressing; yarn twist; and type of weave (basket, plain, flat duck, drill, twill, satin, herringbone, rip-stop, and others). Obvious weaving considerations are the mechanical effect of warp and fill threads on each other and the zig-zag geometry pattern mutually enforced, contrasted with an individually tested filament that would naturally be straight.

c. Filament Materials

Fabrics of woven metal strands show promise for future application. Fabrics of stainless steel and superalloy metals are obtainable (at considerable expense) and have temperature resistance and strength characteristics that are suitable for use in temperature environments up to 1800 F, provided that oxidation-prevention and thermal-insulating coatings are used. Figures 59 through 62 present strength data for various superalloy metal wires. To obtain comparative and meaningful data, the tests were performed under the same laboratory conditions. Test results (see Figures 60 and 62), for example, were conducted at a crosshead speed (rate of specimen elongation) of 2.0 in. per minute. Each specimen was exposed for one minute to the indicated pretest temperature level to ensure that the proper

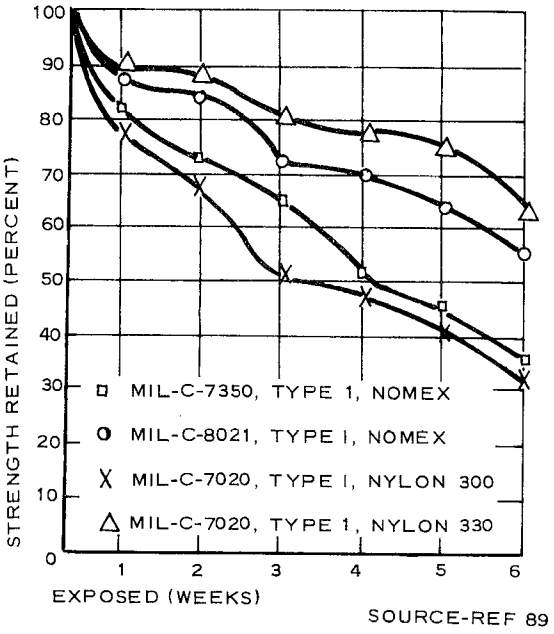

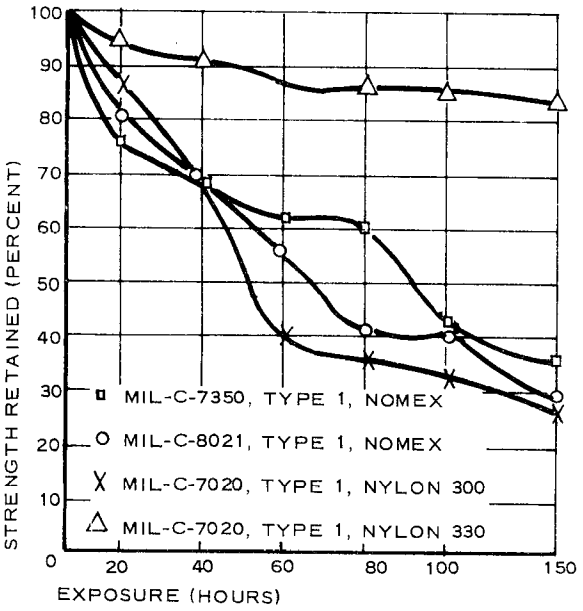

Figure 58 - Comparisons of Nylon and Nomex after Outdoor Exposure (Top) and after Accelerated Weathering (Bottom)

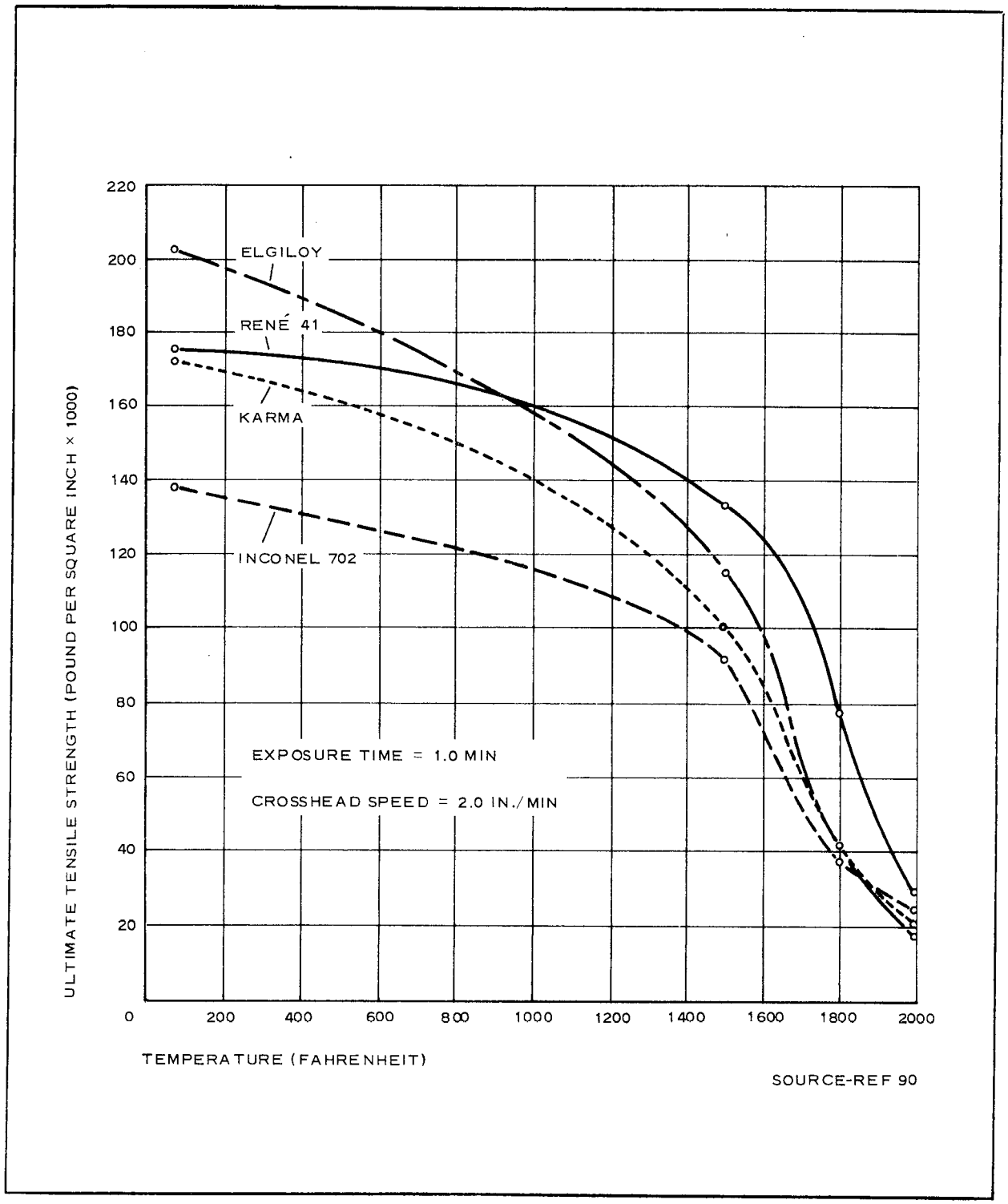

Figure 59 - High-Temperature Tensile Strength of 1.0-Mil Superalloy Wires

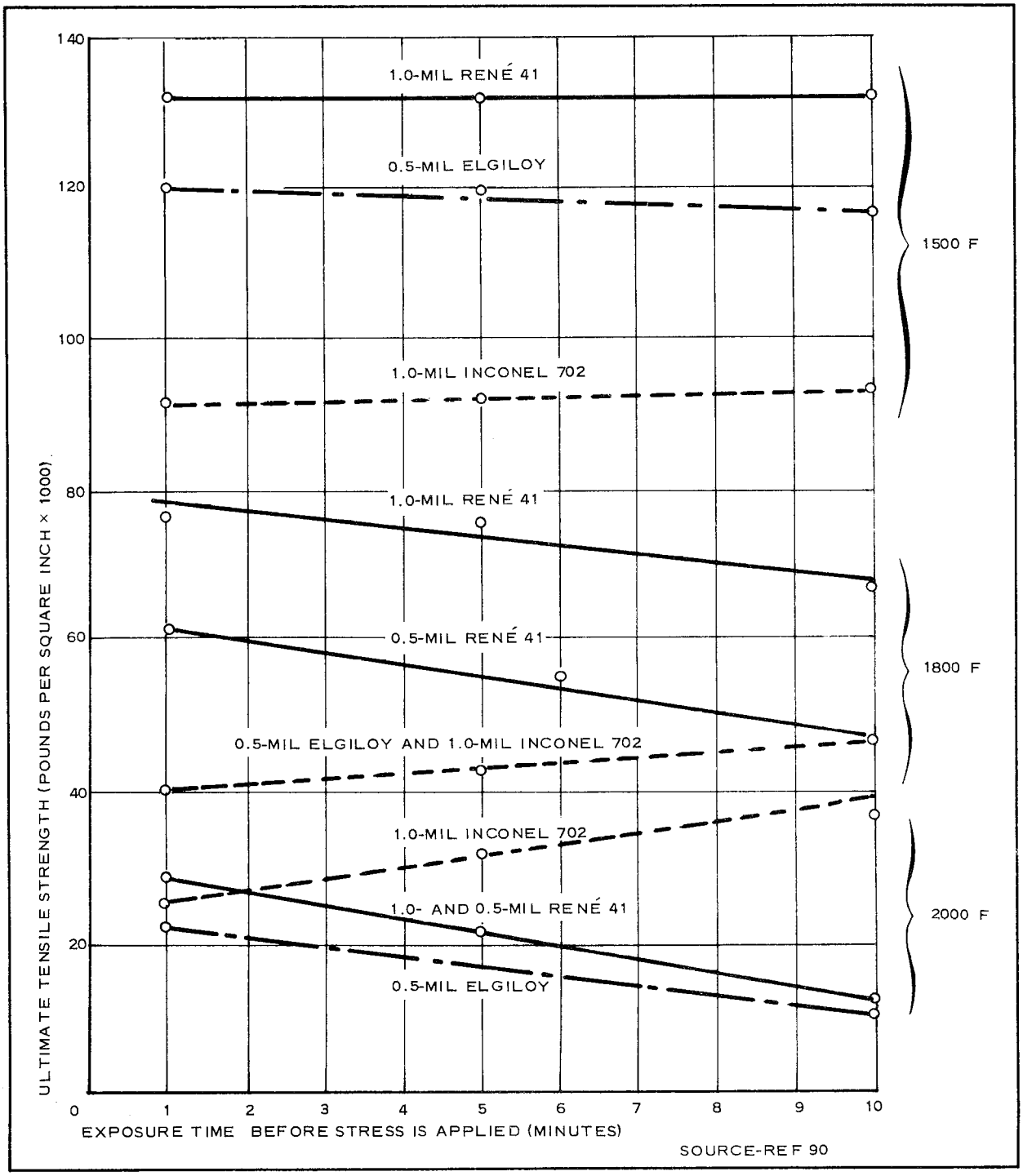

Figure 60 - High-Temperature Tensile Strength of 0.5- and 1.0-Mil Wires as a Function of Exposure Time

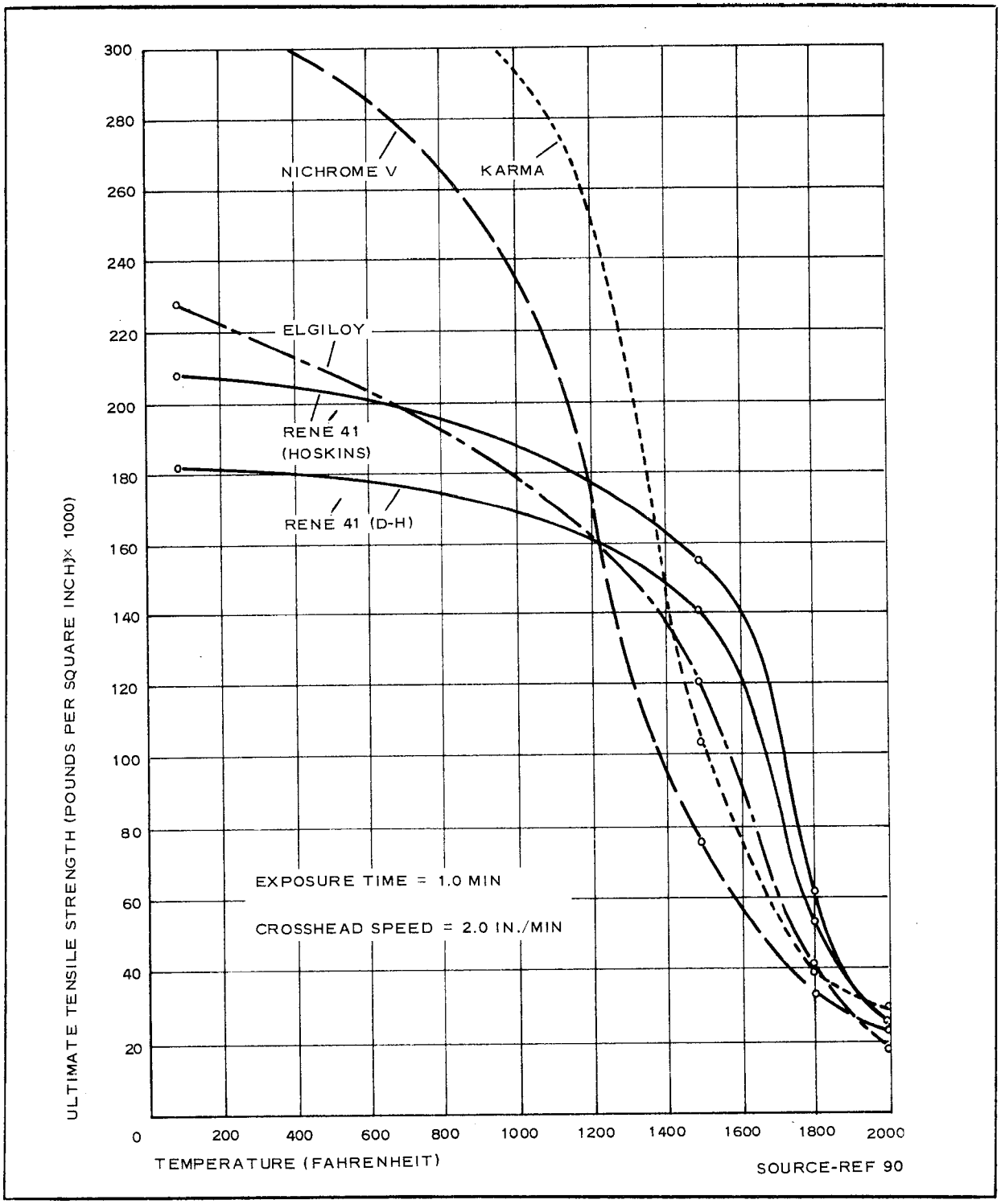

Figure 61 - High-Temperature Tensile Strength of 0.5-Mil Superalloy Wires

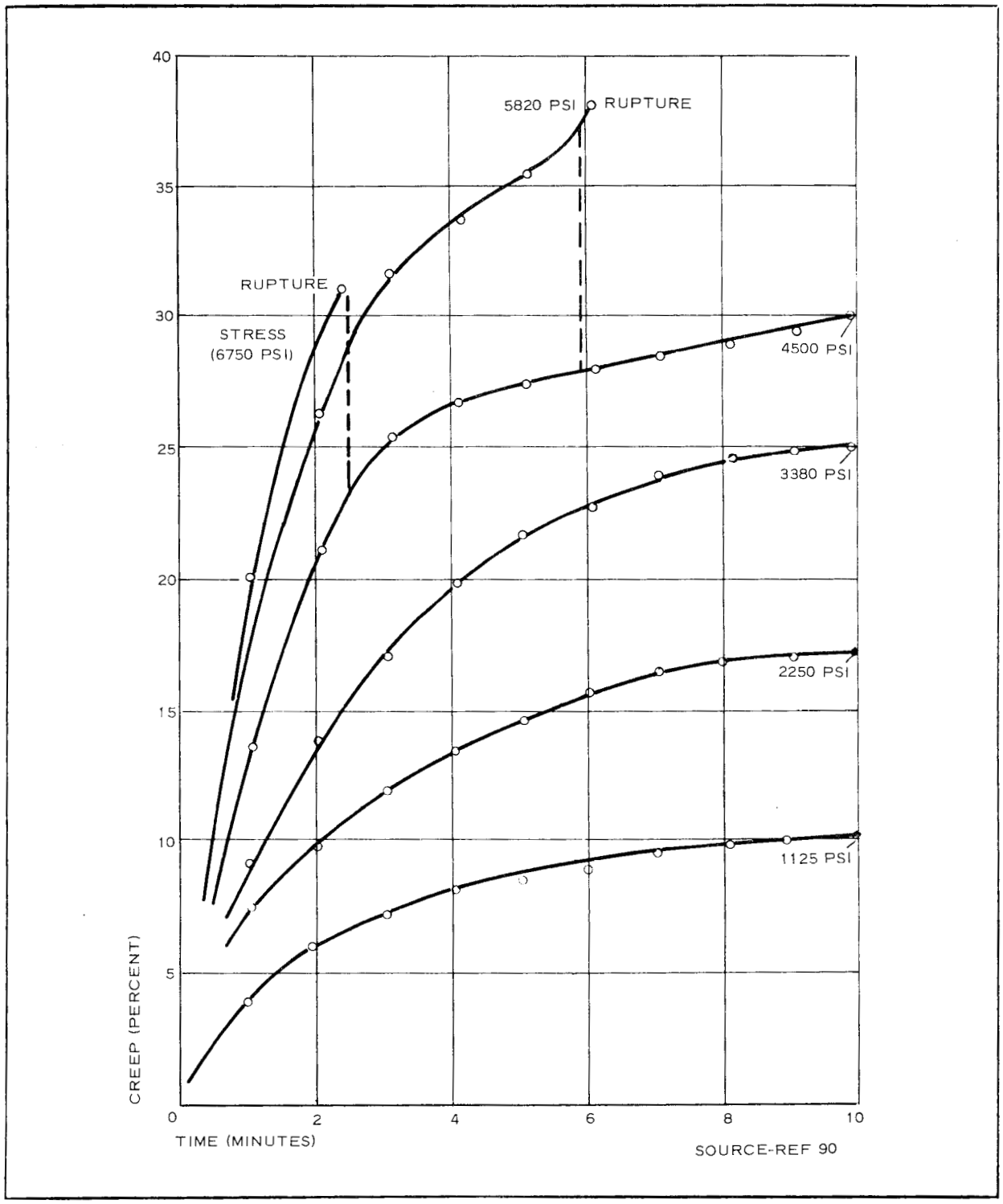

Figure 62 - Creep of 0.5-Mil René 41 Wire at 2000 F (Linear Plot)

value had been obtained. Wires of refractory metals (tungsten, molybdenum, tantalum) have the temperature-resistance characteristics needed for temperature environments in the upper ranges if (1) rapid oxidation of the metals at high temperatures and (2) producing and weaving fine filaments are overcome. Figure 63 shows a strength-to-weight ratio comparison of refractory and superalloy metal wires.

Available fiberglass yarns as a material for woven fabrics have serious deficiencies in flexibility and abrasion resistance. However, the high strength, modulus of elasticity, and temperature-resistance characteristics of fiberglass make it a potential material for use in a temperature-environment range of 600 to 1000 F, if the flexibility and interfilament abrasion deficiencies can be overcome in the development of new fibers.

Other materials with good potential as fibers or filaments for woven fabrics are boron filaments and carbon or graphite filaments. Since these materials are in the research and development phases, no specific data are available. Preliminary information on boron filaments shows a high modulus-to-density ratio, good temperature-resistance characteristics, and good strength characteristics. Carbon and graphite cloths have good temperature resistance but need improvement in strength-to-weight ratio and abrasion resistance. Figure 64 shows the strength-retention characteristics of graphite, carbon, and partially carbonized materials at lower temperatures.

d. Woven Fabric Materials

(1) General

Available woven fabric materials that have been or are applicable for deployable decelerator construction are listed below in order of increasing strength and temperature resistance:

1. Nylon

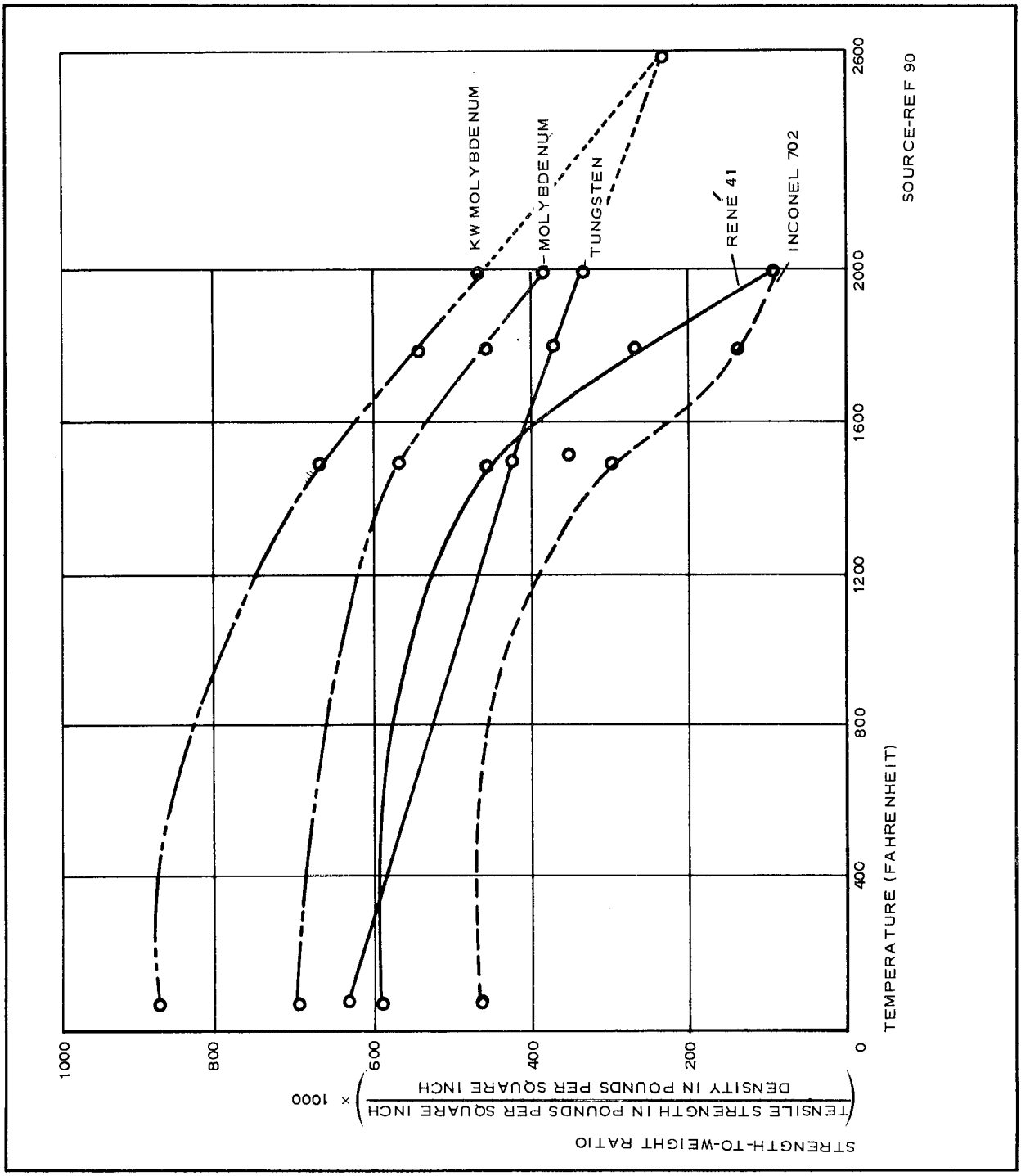

Figure 63 - Strength-to-Weight Ratio of 1.0-Mil Superalloy and Refractory Metal Wires

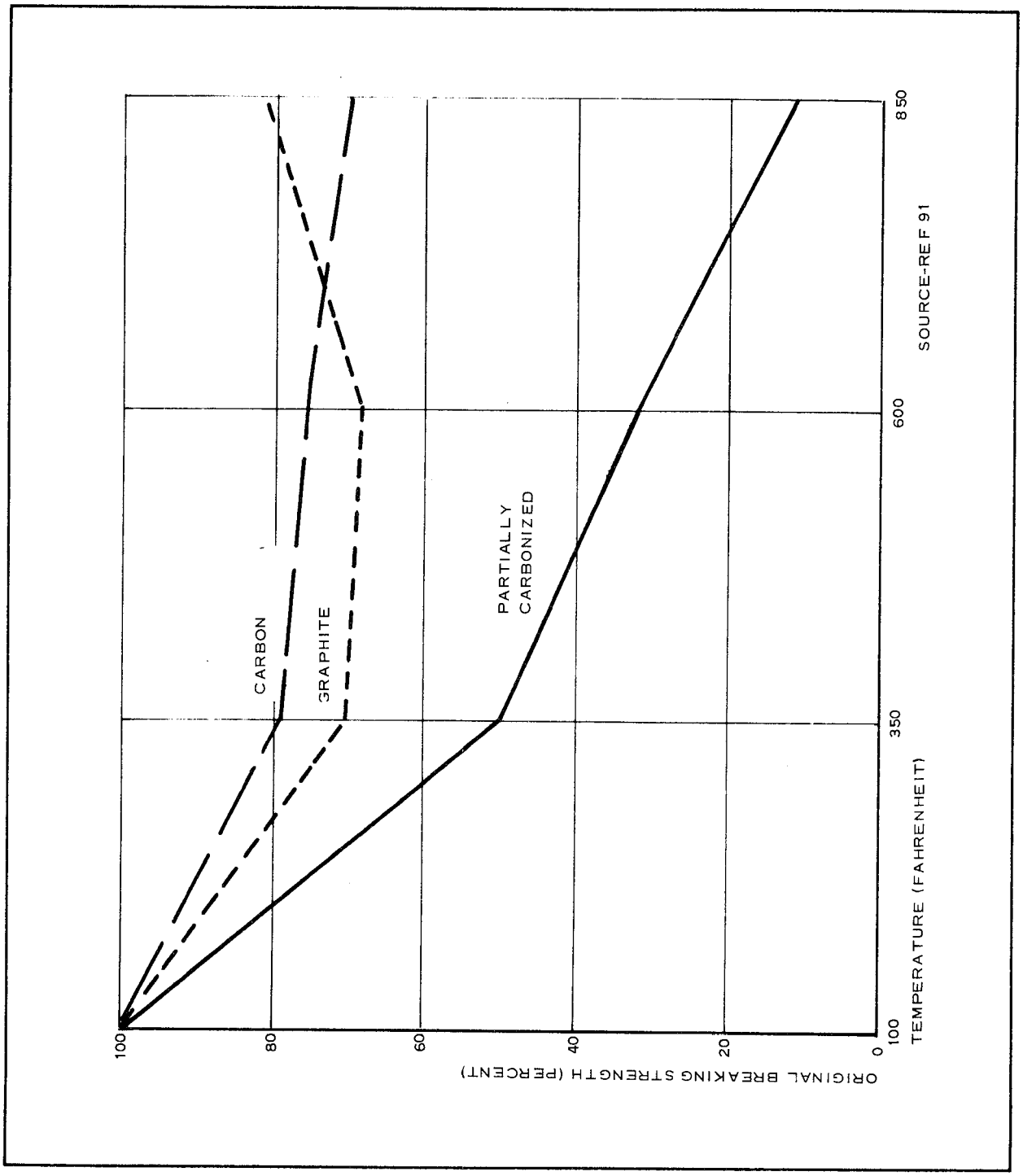

Figure 64 - Comparison of Strength-Retention Characteristics of Partially Carbonized, Carbon, and Graphite Fabrics

2. Dacron
3. Nomex
4. Fiberglass
5. Superalloys (René 41, Elgiloy, Inconel 702)

Most present applications are filled by woven fabrics of nylon, Dacron, or Nomex with or without coatings. Plastic film is suitable only for low-load, low-temperature applications. Although fiberglass has high basic strength, modulus, and temperature resistance, it is notoriously vulnerable to folding damage and interfilament abrasion. Fiberglass has been used very successfully in rigid applications but has been disappointing in flexible-fabric applications.

Fabrics of woven superalloy metal filaments and refractory metal filaments show much promise for future application but are at present in the early stages of development and are extremely expensive. The major expense involved is due to the high cost of drawing the metal wire down to the proper filament size. Evaluation costs also may be high because they cannot be directly related among themselves (see Items 1 through 5, above). However, when woven into cloth, each type will still have qualitative performance relative to each other, as do the filaments.

(2) Operational Temperature Ranges

Potential decelerator materials are available for operation from 300 to 1500 F (see Figure 65). The substrate material recommended from 300 to 600 F is Nomex (Du Pont's high-temperature polyamide) coupled with silicone or fluoroelastomers. Between 1000 to 1500 F, substrates of stainless steel or René 41 woven cloth coated with a high-temperature coating, such as CS-105 (Goodyear Aerospace), can be used.

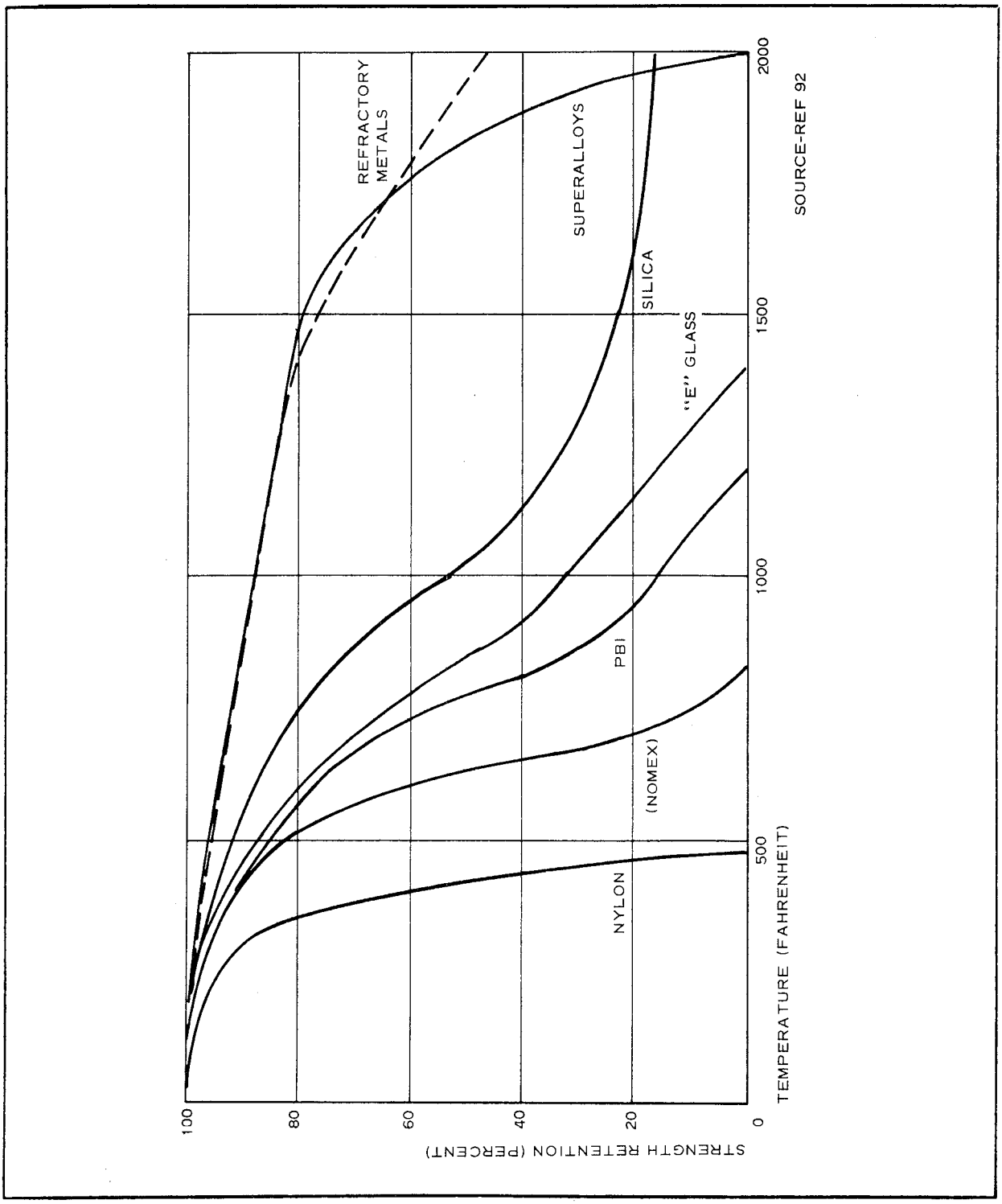

Figure 65 - Strength Retention vs Temperature for Present and Future Fibers

In other operational temperature ranges, proved materials are not now available. One of the most obvious areas for development of suitable materials lies between 600 to 1000 F. At temperatures above 600 F, the strength of Nomex drops rapidly; below 1000 F, the penalty in strength-to-weight ratio paid in the use of stainless-steel cloth is too severe.

A potential material to fill this void is fiberglass (see Figure 65). However, because of its self-destructive nature under flexing of pulsating loads, fiberglass does not lend itself to this application. Efforts have been underway for some time to minimize the abrasive nature of fiberglass, with moderate success. One approach to this problem has been to impregnate the yarns with elastomers to prevent adjacent filaments in the yarn from rubbing one another. Another approach has been the development of Beta glass fiber by Owens-Corning. The Beta fiber is an extremely fine filament. Both of these methods have resulted in some improvement in the performance of fiberglass in flexible applications; however, this work must be continued to realize the full potential of fiberglass.

Another possibility of filling the substrate-material void from 600 to 1000 F is to extend the capability of Nomex. Obviously, the most practical way to extend the capability of Nomex is to protect the substrate so its temperature never exceeds 600 F. One way to do this is to coat the substrate with ablative material; the thickness required and the associated rigidity of thermal insulators as they are now known make their use prohibitive. Relatively speaking, the development of low-temperature ablators has lagged the development of high-temperature ablators considerably. To obtain ablative materials that will satisfy the requirements for use on decelerators is a definite problem area that warrants considerable research and development.

Superalloy metal fabrics such as woven stainless steel and Rene 41 cloths provide substrate material capability to 1800 F. Goodyear Aerospace was instrumental in the first weaving of Rene 41 wire into a cloth having an end count of 200 × 200 and in weaving seven-strand 0.0016-in. Rene 41 wire into a cloth having a count of 100 × 100. However, there is room for improvement in woven metal cloths of stainless steel and Rene 41. Higher-strength, more flexible cloths are needed. Higher strength can be achieved by tighter packing of the metal filaments during the weaving operation, and increased flexibility can be obtained by using smaller diameter filaments. The feasibility of fabricating such cloths with textile stranding and weaving equipment has been demonstrated (see Reference 27). The resulting prototype cloths were highly flexible, high-strength cloths having a "hand" comparable to a textile. These cloths were woven on a prototype basis. Additional effort will be required to establish production methods and to improve the fabrics further.

e. Fabric Coatings

Coatings are applied for one or both of two primary reasons: (1) reduction of fabric porosity and (2) protection of the basic fabric from high temperatures of aerodynamic heating or other heat load. No rigid line of demarcation exists between coatings that are solely for gas tightness and those that are for heat protection. The urethane and silicone rubbers have higher temperature resistance than neoprenes; however, any coating with a low thermal conductivity can render a limited heat protection. The formation of an insulating char is sometimes a usable mechanism. For transients, an aluminum metalizing can be adequate, but when temperature requirements are high and of fairly long duration, coating performance can become quite sophisticated. Heat protection can be afforded by combining mechanical and chemical reactions to the temperature through char formation, sublimation, and ablation.

Coating materials are available that perform satisfactorily up to 1500 F. Up to 600 F, fluoroelastomers perform quite well for short periods of time. Up to 1000 F, silicones are available. Beyond this point and up to 1500 F, CS-105, high-temperature flexible coating is recommended. This coating consists of a silicone binder with a glass frit filler and has been used up to 1500 F.

The CS-105 coating acts and feels like a silicone elastomer at room temperature. As the temperature is raised, a thermal decomposition of the elastomer and fusing of the glass frit occur. The weight of decomposition is a time-temperature phenomenon that progresses slowly at 800 F and increases as the temperature rises. The glass frit does not fuse until 1100 to 1200 F has been reached. Hence, there is a range of temperatures (approximately 800 to 1100 F) where the elastomer is decomposing and the glass frit does not fuse. This represents a transition phase during which the coating is most susceptible to damage and the gas permeability increases. When the coating is subjected to a heat flux of such a magnitude, it must traverse the critical temperature range in a relatively short time. The glass frit fuses before the silicone elastomer decomposes excessively, provides a carrier for the silicone residue, and forms an adequate gas barrier.

Elastomer coating materials that are applicable for reducing porosity in decelerator structure fabrics are listed and described in Table XVII. Each material is evaluated in terms of its performance in a variety of environmental conditions so the limitations of the material are readily apparent.

Some typical coatings described by trade number and name that have been used or have been investigated for possible use in decelerators are shown in Table XVIII, along with typical thermal properties of these materials. Neoprene, DC-131, and Viton have been used satisfactorily on flight-tested decelerators in the low-to-medium temperature regime - that is, up to about Mach 2 and at altitudes above

70,000 ft. The remainder of the listed coatings are potential candidates to extend the operating capability of the state-of-the-art fabrics. In many applications, it may be appropriate to use ablative coating materials, which - because of the short deceleration times characteristic of deployable decelerators - need to function only over a limited time period.

The approach used to increase the temperature capability of the coating between the thermal degradation temperature of the elastomer and the desired operational temperature is to load the elastomer with a low-melting point inorganic material. As the temperature rises, a thermal decomposition of the elastomer occurs, and the inorganic material changes to a very viscous fluid. The viscous fluid is to have a high-surface tension that will hold the residue of the elastomer in suspension and maintain a continuous film. Upon cooling, the material is to solidify and form a solid gas barrier that has a certain amount of flexibility, although much less than the original unfired coating.

f. Joining Methods

The construction of foldable, packageable structures involves the classic problem of building compound shapes from plane material. Aerospace decelerators are assembled by sewing a multitude of individually patterned pieces of a plane fabric material. These pieces are seamed together, usually by sewing with threads of material similar to the fabric filaments. Ballute gore patterns, for example, are cut on the bias from "square" cloth - that is, cloth that has equal or nearly equal strength and elongation in warp and fill. Gores are alternated right and left bias to balance out differences in elongation in the warp and fill directions. So far, Ballutes and parachutes are of single-ply construction.

Joining methods include sewing, cementing, and - in the case of metal fabrics - spot welding. With plastic film material, cementing

TABLE XVII - RELATIVE GENERAL PROPERTIES OF ELASTOMERS*

Elastomer types	Tensile	Tear	Abrasion	Impact (fatigue)	Flame	Heat (F)	Cold (stiff)	Cold (brittle) (F)	Ozone	Radiation	Gas retention	Resistance - oil, weather, chemical	Unsuitable for	Specific gravity
Natural rubber	AB+	B	AB	AB	D	CD+ +250	B	B -80	D	BC	B	Highly resilient, low hysteresis, general	Contact with oils, ozone, strong oxidizing agents.	0.93
Styrene butadiene rubber (Buna S or GRS)	B	BC	AB	AB	D	C +275	BC	B -80 to -90	D	BC	B	General purpose rubber, not so resilient as natural, better resistance to aging.	Contact with oil, ozone, strong oxidizing agents.	0.94
Isobutylene isoprene rubber (Butyl or GR-1)	C	B	B	C	D	BC +300	C	BC -50 to -80	AB	D	A	Weather, heat, ozone, chemical, and solvent resistant, low air permeability.	Contact with oils.	0.92
Chloroprene rubber (Neoprene or GR-M)	B	B	AB	B	B	C +300 F	C	BC -45 to -70	AB	CD	AB	Weather resistant, fair oil resistance.	Temperature extremes, contact with aromatic oils and most fuels, long exposure to low temperatures	1.24
Polyurethane elastomers (Adiprene, Chemigum SL, CX-1046)	A	A	A	B	CD	C +250	C	A -30 to -95	A	B	A (R.T.)	Superior abrasion resistance, sunlight and ozone resistance, good oil resistance.	Contact with steam or hot water	1.05 to 1.17
Nitrile butadiene rubber (Buna N)	BC	BC	AC	C	D	B +275	BC	BC -80 to -90	D	BC	B	Medium to good oil resistance, fair fuel resistance	Contact with ozone, strong oxidizing agents.	0.99
Silicone rubbers	D	CD	CD	D	C	A +550	A	A -200	A	D	B	Resistant to temperature extremes, fair oil resistance, properties constant from 60 F to 500 F.	Contact with high pressure steam, aromatic oils, fuels, abrasion.	1.25
Chlorosulfonated polyethylene (Hypalon)	BC	BC	AB	BC	B	BC +325	C	B -70 to -80	A	BC	AB	Weather, heat, ozone, and moderate oil resistance, good color possibilities.	Aromatic oils and most fuels.	1.10
Fluorinated elastomers (Fluorel, Kel-F, Viton)	BC	BC	B	BD	A	A +450	D	BC +10 to -40	A	BC	A	Resistant to oxidizing acids, fuels containing up to 30 percent aromatics, ozone, weahter; excellent oil resistance.	Contact with diester lubricants, uses where material must be easily flexed at temperatures below 0 F.	1.40 to 1.85
Organic polysulfide rubbers (Thiokol, GR-P)	D	D	D	D	D	C +200 to +275	C	B -60 to -80	A	BC	A	Excellent oil resistance, good resistance to aromatic fuels, excellent weather and ozone resistance.	Resistance to compression set particularly at temperatures above 100 F, uses where mercaptan odor would be objectionable, contact with oxidizing acids.	1.25 to

*Source - Reference 93.

+A = exceptional, outstanding, or excellent; B = good; C = fair; D = poor.

157-A 157 157-B

TABLE XVIII - ELASTOMERIC COATINGS

Coating	Vendor	Specific gravity	Specific heat	Thermal conductivity	Emissivity	Remarks
Neoprene 1137-C	Goodyear	1.30	0.35 Btu/lb-deg F	0.14 Btu/hr-ft-deg F		Low temperature coating
DC-131	Dow-Corning	0.94	0.3-0.35 Btu/lb-deg F	0.167 at room temperature Btu/hr-ft-deg F		
Viton	Du Pont	1.85 to 1.90	0.395 Btu/lb-deg F	0.117 at 300 F Btu/hr-ft-deg F		
CS-105	Goodyear				0.92 at 1000 F	High temperature coating
D-65	Dyna-Therm	1.1	0.25 (68 to 150 F) Btu/lb-deg F	0.053 at 150 F Btu/hr-ft-deg F		Ablator
RTV-88	General Electric	1.48	0.35 Btu/lb-deg F	0.18 at 200 F Btu/hr-ft-deg F		
RTV-560	General Electric	1.42		0.19 at 315 F Btu/hr-ft-deg F		Ablator
AVCOAT II	AVCO	1.0	0.43 (65 to 240 F) Btu/lb-deg F	0.10 at 250 F Btu/hr-ft-deg F		Ablator
DC-325	Dow-Corning	0.87	0.32 (77 to 200 F) Btu/lb-deg F	0.08 at 200 F Btu/hr-ft-deg F	0.90 at 70 F	Ablator

is almost invariably involved - either a heat-sealing or solvent-sealing cementing or adhesive application. With soft fabrics, sewing is usual but cementing is sometimes practical, especially with an elastomer-coated cloth, and frequently results in higher joint efficiencies. Combinations of cementing and sewing have been used. Cementing has been for secondary purposes, such as sealing holes made by sewing or preventing the slippage of stitching. As earlier mentioned, joining of metal cloth has been by multiple staggered row spot welding. The Air Force has reported sewing such fabric successfully with wire thread (see Reference 94).

The development of the optimum seam for a specific application is a matter of design and test development. Factors involved are the cloth and its basic strength to be developed; the coating, if any; with an orthogonal or biased seam, etc. Variations possible include number of parallel rows of stitches, number of stitches per inch, type of stitch, presence or absence of reinforcing tapes or webs, types of seam, possible overlay of elastomeric coating, etc. The final bulkiness of the seam is a consideration with its consequent influence on packageability and deployment.

Seams are invariably a problem area. Seaming represents a sizable part of construction cost and contributes significantly to the variation in quality of the finished article. The seam adds bulk and weight, reduces flexibility, adds distortions when the structure is loaded, and almost never can be designed to develop 100 percent material strength. Seam design and material selection go hand in hand. While cementing can generally develop a structurally more efficient joint, it also is more adversely affected by elevated temperature.

g. Material Selection and Qualification

Materials selected for use in a particular decelerator structure are the result of analyzing both design factors and fabrication technology. Design factors such as static and dynamic loading, thermal loading,

maximum size and weight of structure, and aerodynamic drag requirements dictate the requirements for strength and temperature resistance. The material selected must meet these requirements after fabric strength-to-weight ratio, thickness, porosity, flexibility, and coatings have been considered. The selection of material usually will involve determination of the fiber or filament material and size, weave, seam construction, production sequence, and other production techniques. Different materials and fabrication techniques may be required for the components of the structure.

h. Current Development in Materials

Anticipated future materials are conventionally woven fabrics from exotic, high temperature-resistant fibers. Developments to be expected include entirely new fibers, improvements in properties of existing fibers, and development of finer filamentation and tighter weaving of the newer materials, such as the superalloys.

Glass fabrics, as mentioned earlier, require vastly improved interfilament abrasion resistance. Since the glasses have been subject to considerable research and development, much improvement in this basic characteristic is difficult to foresee. Possibly a surface coating, compatible with other requirements, may yet make possible the wide use of foldable, flexible glass fabrics.

The development of extremely thin surface coatings for oxidation prevention in refractory metal cloths is expected, enabling exploitation of these materials at high temperatures.

Other new fiber materials currently undergoing development are alumina/calcia, silicon carbide, boron, carbonized and graphitized yarns, and quartz. Development of these and other materials will yield some usable filaments.

The superalloys, such as René 41 and other proprietary formulations, are very much in a research and development phase. Wire

cloth of filaments are fine as 0.5 mil has been woven at considerable expense. Problems include drawing a much finer filament and weaving very dense fabrics without excessive filament breakage.

The technology of "whiskers" has been of scientific interest for some time. Whiskers are pure substances formed from single crystals. Therefore, they are free from impurities and grain boundary defects and represent the theoretical ultimate in strength characteristics. They also have stress levels far in excess of their standard material counterparts. Materials approaching the extreme stress levels of whiskers are not soon to be expected.

Elastomeric coatings of fabrics can be expected to improve. The urethanes and silicone rubbers are very promising at elevated temperatures. New combination coatings such as the CS-105 or Dyna-Therm D-65 coatings, which protect for a limited time by chemical and/or mechanical responses to temperature, can be expected.

Fine metal filamentation by electroforming, plastic metalizing, vapor deposition, and cold-drawing is being investigated experimentally (see Reference 90) and appears promising.

i. Future Development in Materials

Woven cloths of René 41 provide a substrate-material capability to 1800 F. However, to obtain a capability beyond this point, efforts must be directed toward the weaving of cloths of the refractory metals. Until recently, this has appeared to be a very difficult problem; however, developmental work in weaving metal fabrics using textile methods and equipment provides a sound basis from which this work can be carried on. Many of the problems encountered and the solutions evolved under Contract AF33(616)-7854 (see Reference 93) are applicable to the weaving of refractory metal fabrics.

One problem encountered with refractories involves their rapid oxidation at elevated temperatures. Rapid oxidation becomes especially

critical when the basic structural element is a filament with a diameter of 0.5 mil. To overcome this problem, oxidation-resistant coatings are required. Although considerable effort is being expended in this area, it is being directed primarily toward the protection of sheet stock, castings, and the like. Some of the coatings developed for gross parts can be adapted to the protection of filaments, but specific research for the protection of fine refractory metal filaments is needed. Processing and fabrication techniques for treated or coated refractory metal cloths also must be established.

Another possibility for extending the substrate-material temperature resistance capability above 1800 F lies in the use of carbon or graphite cloths. Recent efforts show marked improvements in fabrics woven from these materials; however, considerable research and development are required to improve the strength-to-weight ratio, abrasion resistance, and handling capabilities of these materials. Unfortunately, most of the research and development effort expended on these materials is directed toward their use in rigid laminations. Such effort does not tend to solve the peculiar problems attendant on their use as a flexible material.

Basic materials for use in the substrates at temperatures above 1800 F are available. The primary problem in the use of these materials involves working and fabricating them into basic structural elements from which decelerators can be fabricated.

Coating materials present another problem. There are no flexible coating materials that have temperature-resistance capabilities above 1500 F. As previously stated, CS-105 coating is operational to 1500 F within certain limits. Under Contract AF33(616)-7853, efforts to improve this coating and extend its capability were undertaken. It was found that some of the coatings developed had superior characteristics over very limited ranges, but that CS-105 was superior overall.

Research is being conducted under an Air Force contract to extend the capability of CS-105 to 2000 F and to examine other concepts for high-temperature coatings. This area of investigation requires considerable future effort, since the development of satisfactory flexible, high-temperature, impermeable coatings lags the development of substrate materials that can be used in the same temperature range.

Although cemented seams in decelerator structures can be very efficient, especially with elastomer-coated fabrics, no cements are available that have acceptable creep and strength characteristics beyond 180 to 200 F. The development of high-temperature cements with the proper bonding characteristics would provide increased latitude in design and fabrication of structures.

SECTION III - DESIGN DISCUSSION

1. SYSTEM DESIGNS AND LOGISTICS SEQUENCING METHODS

Exclusive of obtaining design criteria to define design requirements for specific high-speed recovery applications, all previous first-stage recovery systems have the following sequencing methods in common:

1. Automatic initiation
2. Deployment preparation, which consists of automatic canister opening; canister opening consists of sequencing disconnects (latches, cutters, pin-pullers), which void the canister exit of all restrictions
3. Automatic deployment initiation (utilizing either a thruster, mortar, or drogue-gun system)
4. Automatic decelerator inflation
5. Automatic decelerator release in preparation for final-stage system deployment

Figure 66 shows a typical deployment sequence. These components are interconnected and energized either electrically or mechanically.

Experience has proved that the use of ordnance devices such as thrusters, drogue guns, mortars, and ballistic disconnects was the best method to obtain adequate system operation. The pyrotechnic devices have met the following requirements:

1. Lightweight
2. Function in a high-g environment

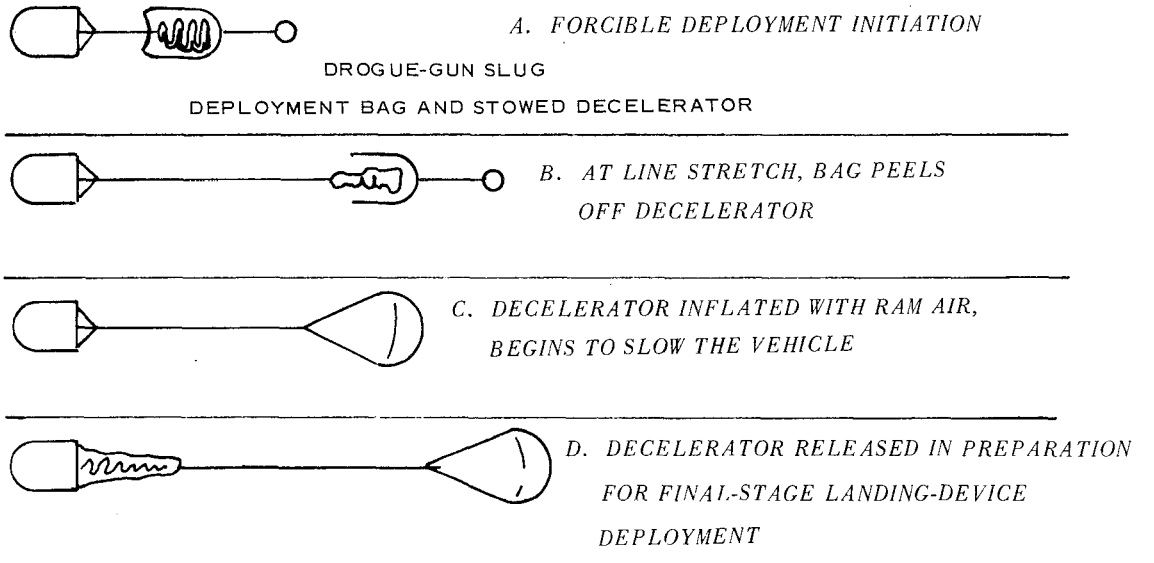

Figure 66 - Typical Recovery-System Deployment Sequence

3. Function positively and forcibly

4. Function in extremely short periods of time

Basic problems with pyrotechnics are their sensitivity to heat and their dependence on small variation in power supply electrical current requirements. The major problem is the stringent minimum weight and stowage space requirements. Additional standardization of component design also would aid in easing system design problems.

Table XIX summarizes the type of hardware, function, and method of operation.

The inflation mechanisms described in Table XIX are required when self-inflation is not feasible. For example, closed pressure vessels such as spheres or flared skirts require some type of inflation device at any deployment altitude; even ram-air-inflated devices such as parachutes and Ballutes may require supplemental inflation devices at extremely high altitudes (above 200,000 ft).

2. DESIGN PROCEDURES AND CRITERIA

a. General

The available decelerator-system design criteria, which are a measurement of the state of the art, are clearly dependent on available performance and design parametric data.

b. Preliminary Design Procedure for Supersonic Decelerator

Figure 67, taken from Reference 27, shows the significant parameters that are evaluated to obtain a preliminary design.

The major design effort consists of an operational computer trajectory study, an aerothermal parametric analysis, and a structures and weight study to meet these aerothermal performance requirements. Examples of key design parameters that must be evaluated and how they are interdependent on each other follow.

TABLE XIX - SEQUENCING HARDWARE

Item no.	Function	Type of hardware	Method of operation to obtain electric signal
1	System initiation	"Q" sensor	Measures a given pressure difference between static and total head.
		Barometric sensor	Measures a given pressure difference between static and sea level atmosphere.
		"G" sensor	Measures a given amount of strain in a cantelever deflected under the inertial loads.
		Timer	Mechanical or electrical clock.
		Telemetry	Telemetry signal from external source.
2	Deployment preparation	Release mechanics such as explosive bolts, cutters, pin pullers, latches, clamps, etc., and arming devices	Pyrotechnic charge provides energy to sever bolts or retaining straps, or to unlatch canister doors, or to arm subsequent sequencing devices.
3	Forcible deployment of the decelerator	Mortar	Pyrotechnic charge burns and provides high pressure gas to fill a blast bag beneath the stowed decelerator. The decelerator is displaced and ejected out and aft of the canister.
		Drogue gun	Pyrotechnic charge burns inside the gun and ejects a slug aft. The slug is bridled to the decelerator, and the kinetic energy of the slug pulls the decelerator from its canister.
		Thruster	Pyrotechnic charge burns inside the thruster ejecting the thruster cylinder, canister, and decelerator aft.
4	Decelerator inflation	Nitrogen bottle	High pressure nitrogen gas is released by a pyrotechnic valve inflating the decelerator.
		Gas generator	Pyrotechnic charge burns and provides high pressure gas to fill the decelerator.
		Sublimating powder	Solid powder sublimates, upon experiencing the extremely low static pressures at high altitude, and gases are generated to inflate the decelerator.
		Vaporizing liquids	Liquids such as alcohol vaporize, which provides the gases to inflate the decelerator.

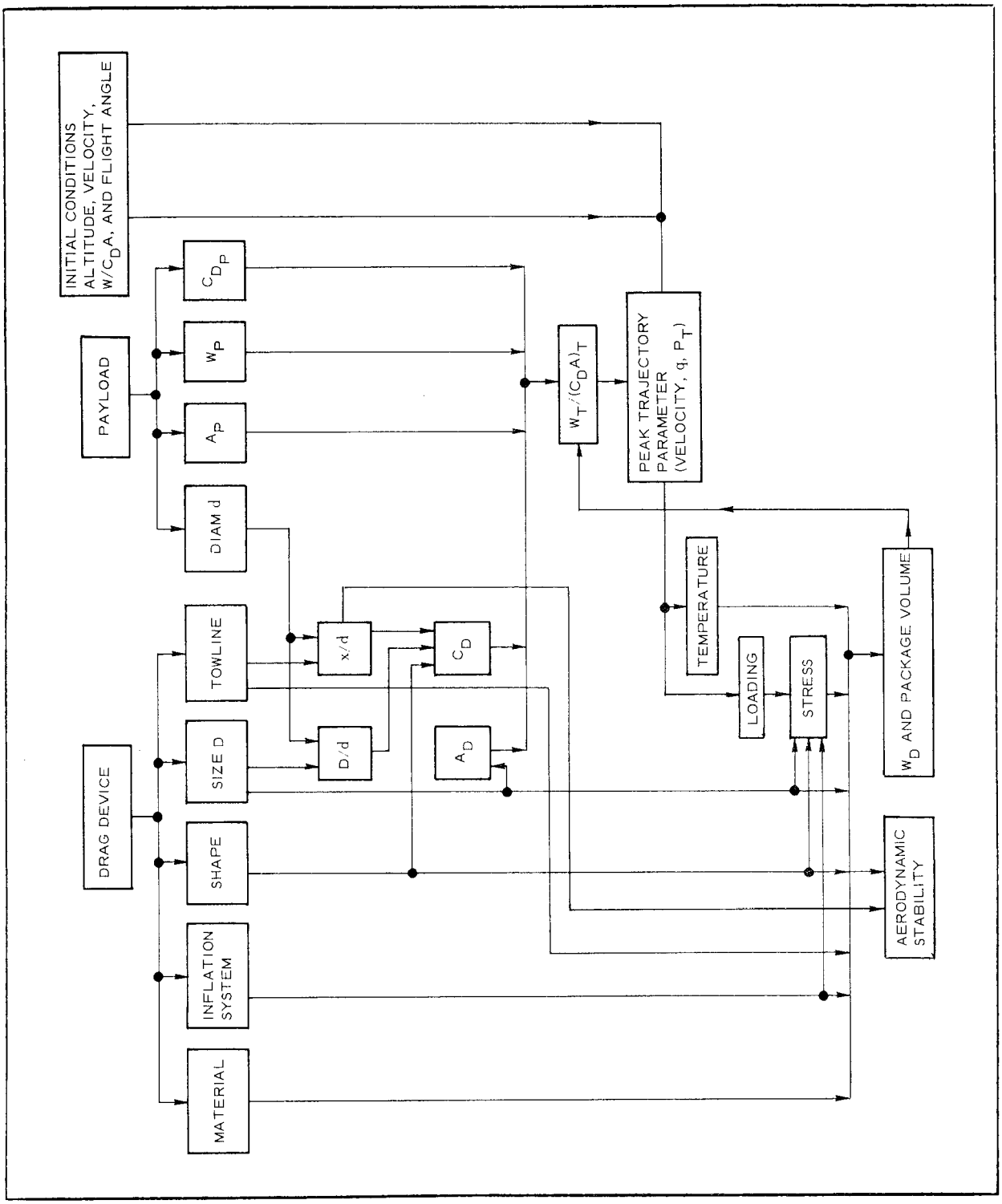

Figure 67 - Parameters Affecting Design of Towed Drag Devices

1. The descent initial conditions (altitude, velocity, W/C_DA, flight angle)
2. The ballistic coefficient after decelerator deployment (W/C_DA)
3. The drag area, which is influenced by the size and drag coefficient (efficiency)
4. The drag coefficient (C_D), which is influenced by x/d (towline length divided by the payload diameter), D/d (decelerator diameter divided by the payload diameter), and the decelerator nose shape

The problems of accurately forecasting drag due to the forebody wake flow around the towed decelerator and the importance of the towed parameters x/d and D/d have been discussed in detail. Because of this, and until such time as more basic research is conducted, experimental tests, if for no other reason, are required to obtain a given amount of steady-state drag for a given high-speed application. The following factors affect the structural and weight design:

1. The peak loading condition, which is influenced by all performance parameters
2. The peak stress condition, which is influenced by the loading, size, and shape of the decelerator
3. The stress-to-weight ratio, which is influenced by the aerodynamic-heating temperatures and the type of materials selected
4. The weight of the decelerator, which is influenced by the design parameters plus the miscellaneous hardware weights such as the inflation system, if required

c. Available Design Data for Dynamic Deployment Loads

It is evident that the decelerator must be designed to support all adverse loading conditions that occur during its period of operation. In most applications, this load is the opening-shock load that occurs during deployment. As was indicated in the discussion of Table XI, the available dynamic shock-load data from supersonic demonstrations are extremely limited. However, despite this limitation, these data show that a satisfactory design is a compromise between (1) short decelerator-inflation times that minimize fabric-flutter loads during inflation at the expense of higher shock load levels and (2) long decelerator inflation times that minimize shock load levels at the expense of longer-duration fabric-flutter loading.

As is shown in Reference 1, subsonic-flight-regime parachute design and test experience have proved that the peak opening-shock load can be related to dynamic pressure. In this case, it is called the "canopy loading" and is the product of dynamic pressure and opening-shock factor. This opening-shock factor varies with type of canopy, altitude of deployment, and weight of the payload. However, even in this well-known area of subsonic parachute applications, shock-factor data are limited to "infinite-mass" conditions, where for all practical purposes the payload does not slow down during parachute opening.

In summary, to fill these voids, it is recommended that a design evaluation consider the following procedures to determine the peak design loads:

1. Utilize subsonic opening-shock factors as partial evidence to forecast supersonic deployment loads.
2. Obtain transient-load experimental data from tests similar to new applications.

3. Evaluate inflated-decelerator steady-state loads along the required trajectory.

As Table XI shows, available documented dynamic-load data are limited to deployments below Mach 4.

Even though a procedure is set up to determine the peak design load, better experimental information is still needed for a more accurate definition of peak loads.

SECTION IV - DATA CONFIDENCE

1. GENERAL

Confidence in previous test data to be used for any reason is mandatory. In lieu of the user finding complete data for subsequent utilization in a new design application, the following evaluation procedures that have been used in the past will aid in increasing the level of confidence that specific aerodynamic data are valid. Some of the problems of similarity and model design also will be discussed.

2. SIMILARITY CRITERIA

The prime requirement for any trailing drag device that depends on dynamic pressure for inflation is that it opens or inflates and remains open and maintains its geometric shape over the full range of operational conditions. Unfortunately, the opening tendency of a parachute depends on a complex of variables that cannot be completely reproduced in the wind tunnel. Although scale is the main factor, Reynolds number alone does not appear to be an adequate criteria of similarity. Based on very limited free-flight data, it is believed that successful operation of a small scale model in the wind tunnel gives no assurance that the full scale model will also open and remain open at the same Reynolds number. For this reason, scaling effects must be determined from wind tunnel testing to ascertain the effect of various parameters on the successful operation of the full scale configuration in free flight.

Apart from differences in relative flexibility of structure, surface roughness, and effective porosity, it is also believed that the behavior of the model is different from full scale because of the strong effect of small differences in local flow along the canopy of a parachute. Combined

canopy pulsing and longitudinal vibration have been encountered in both wind tunnel and free flight but may be magnified in the wind tunnel.

Inflatable decelerators that are dependent on self-contained pressure systems or are ram-air inflated do not have the same inflation problems as parachutes that are dependent on the magnitude and stability of the dynamic pressure of the surrounding fluid. Absent from these configurations are the problems of local flow perturbations, which can cause squidding or violent fluttering.

3. FLEXIBILITY AND STRENGTH

Small scale wind tunnel models are likely to be relatively less flexible than the full scale prototypes unless special precautions are taken in detail design. As a minimum for approximation of aeroelastic similarity, the unit strengths of the textile used should be at the same ratio to applied loads as to those of the full scale decelerator. Therefore, it is necessary either to establish full scale loading criteria or to define clearly the full scale loading criteria represented by the models. The strength of materials to be used in the models will depend on the dynamic pressure range of the wind tunnel as well as that on a scale of the model.

The scaled-down, wind-tunnel inflated models will not likely have fabric texture, thickness, cell structure, and smoothness in proportion to the full scale device. The wind tunnel models will probably retain a stiffer or relatively more solid shape. No analysis of the effects of relative solidity of shape appears to be available, but it is estimated that this effect would be quite small.

4. SURFACE TEXTURE

Surface roughness, pores, and crimp ridges of textiles usually cannot be scaled down to small model dimensions and so may influence aerodynamic properties resulting from skin friction and boundary layer considerations. Within limits, the models can be assembled with scaled seams

and proportionately finer threads, but narrow hems and seams generally tend to be relatively coarse and rough. Surface texture and roughness affect the nature of the boundary layer and location of boundary layer transition. Depending on known differences between wind tunnel model and full scale device surface conditions, a drag correction for relative grain size may have to be made in conjunction with the Reynolds number drag corrections. This correction would be similar to that applied to missile models.

5. DYNAMICS

Unstable model configurations are difficult to measure not only because of their effect on the tunnel balance system but also because they tend to disintegrate in a very short run time. Means of effectively damping model vibrations without otherwise affecting performance are greatly to be desired. Another restriction that has yet to be evaluated from a dynamics point of view is the infinite payload mass condition usually associated with wind tunnel testing versus the finite conditions of flight.

The above discussion is mainly concerned with the correlation between wind tunnel data and free flight data. Equally important is to be able to correlate between theory, wind tunnel, and flight. Theoretical verification has again been greatly neglected.

Until statistical type flight data are accumulated and better means of recording and reducing flight data are available, engineering judgment must be employed. An example of relying on one system for obtaining final results is shown in Figure 68. Here, curve "A" represents the drag coefficient data obtained by radar tracking and curve "B" the drag coefficient data obtained by telemetry. The data shown in this figure were reduced from the results of two Ballute flight tests. In the case of curve "A," small errors in displacement measurements were magnified in the different integration processes for determining the velocities and acceleration. Errors are further magnified when these calculated velocities

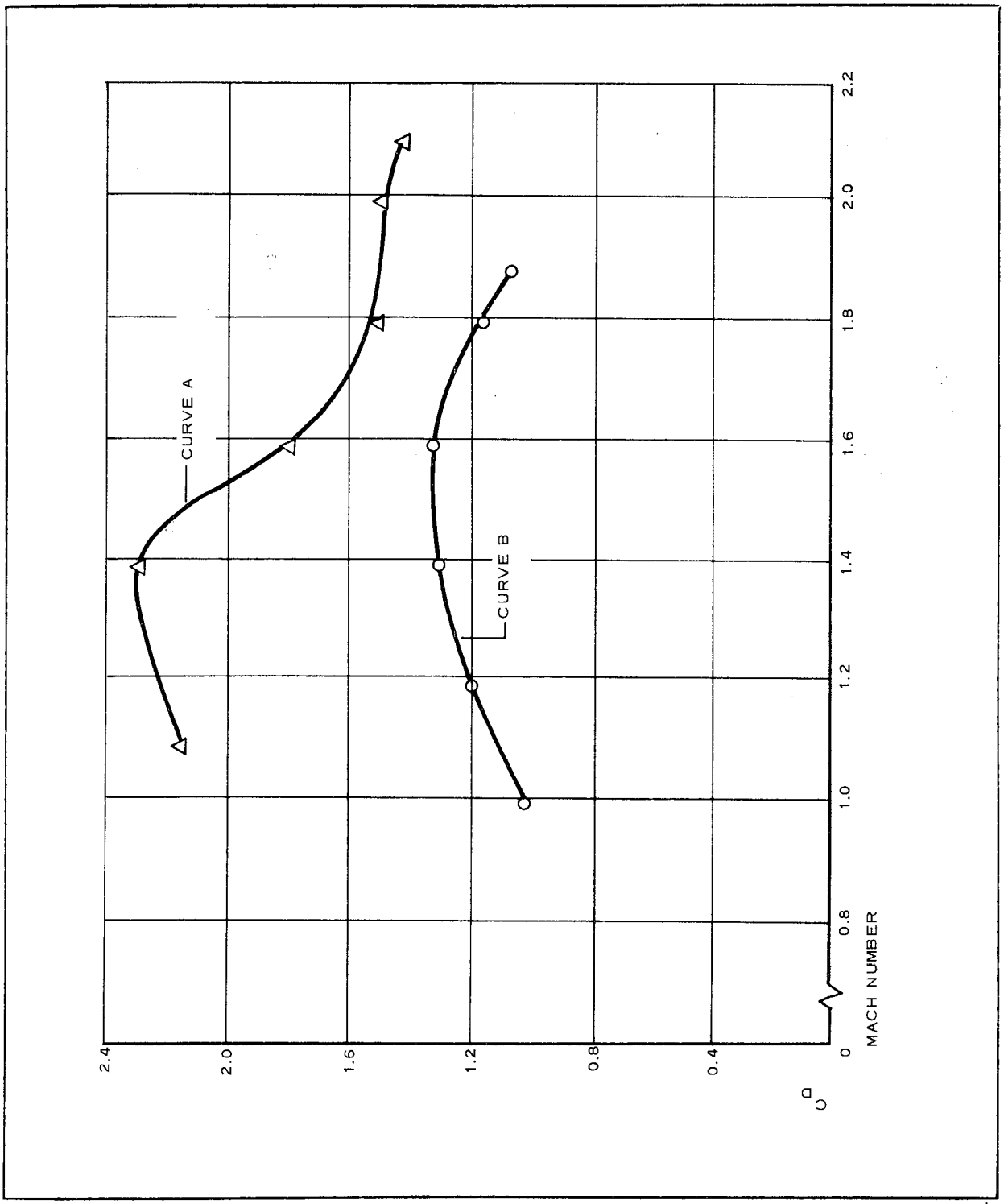

Figure 68 - Ballute C_D vs Mach Number (Flight Test Data)

(which must be squared to obtain the dynamic pressure) and acceleration values are used to calculate drag coefficient. Curve B data are believed valid since the drag results in wind tunnel tests of basic similar cone models showed similar drag coefficient values. This example is not shown to indicate that radar tracking is a poor method of obtaining drag coefficient results but only to point out the need for careful data reduction procedures.

SECTION V - PRESENT HIGH-SPEED RECOVERY TECHNIQUES, PROBLEM AREAS, AND VOIDS

1. GENERAL

The discussion up to this point has dealt with the available data in the different categories of aerodynamics, thermodynamics, and structural design. The intent of this section is to discuss and to correlate this data in light of present-day requirements for supersonic decelerators, thus pointing out the basic problem areas and voids in the existing technology. These general flight spectrum requirements and associated general aerothermal loading levels resulting are shown in Figures 1 and 2.

2. PERFORMANCE LIMITS

A review of Tables I through X reveals that common research objective to find decelerator system configurations that will meet a broad recovery flight spectrum (see Figure 1); namely, recovery of heavier payloads from higher speeds (and/or higher aerothermal loadings) and altitudes.

Towed nonporous textile decelerators up to five feet in diameter have been successfully flight tested up to deployment speeds of nearly Mach 4. In this case, a successful test means that the decelerator performed in a stable manner and produced high drag without structural failure. The implication of the high drag-producing flights without failure is as follows:

1. Models were fully inflated.
2. Models did not experience any significant cycle breathing (buzzing) after deployment and inflation.
3. Temperatures encountered were less than 600 F design condition limit (of coated textile fabrics).

Prior to these flight test demonstrations, metal cloth nonporous blunt body models were successfully tested in wind tunnels up to Mach 10 and textile models up to Mach 6. These tests indicate that satisfactory aerodynamic performance can be obtained. Since wind tunnel reservoir air is cooled and dried, these past wind tunnel tests do not demonstrate the decelerator's capability to withstand thermal environments anticipated above Mach 3 for more than a few seconds. Track tests have been accomplished using approximately four-foot models with deployments at Mach 1.4 and q's up to 2400 psf. This Mach 3 value, as a limit, is mentioned since equilibrium stagnation temperatures that would be encountered if the system is allowed to travel at that speed for any length of time is above the structural limit of textiles. Hence, a textile decelerator system for deployment above Mach 3 must be designed either to slow the payload down quickly to prevent overheating or to provide the fabric structure with additional protective devices so the basic fabric does not exceed the allowable 600 F limit. In the above mentioned flight test, the former condition existed where the decelerator was of sufficient size to slow the payload and itself down to Mach 3 in a few seconds to avoid the excessive heat.

Successful supersonic performance of porous decelerators - namely, parachutes - has been limited. While small wind tunnel models (less than one foot in diameter) did develop drag up to Mach 6 and four- to six-foot wind tunnel and flight models developed drag up to and between Mach 3 and 4, model coning instability and canopy inflation instability were encountered when operating above Mach 2.5. Evidence that this deterioration in aerodynamic performance during increasing Mach-number tests of the better-performing geometric openness parachutes was as follows:

1. Transonic steady-state drag coefficient (C_{D_o}) was between 0.4 and 0.5.
2. Above Mach 2.5, the drag coefficient (C_{D_o}) was between 0.2 and 0.35.

Section II detailed the possible reasons for this performance variation. In summary, parachutes were extremely sensitive to the changeable wake of the towing forebody. Based on this survey data, the better-performing models were the Parasonic and the reefed ribbon configurations. These data were limited to wind tunnel results only. In this case, better performance is defined as minimizing coning instability and canopy breathing and also obtaining a more fully and more constant inflated shape. The combined effect of providing a known (calibrated) amount of choking plus the isotensoid membrane design shape is believed to be the reason for the improved performance. The Parasonic canopy crown was coated to obtain the proper porosity. Thus, coating also has extended the thermal environment capability by one order of magnitude.

The other configuration that performed up to Mach 3 with a minimum of canopy breathing and coning instability was a reefed ribbon configuration (either the hemisflo or the conical ribbon type). The combined effect of lowering the geometric porosity more than 1/2 of that of the previous ribbon parachutes, plus the reef shape being a stable conical configuration, was believed to be the reason for the improved performance. It is important to note that the Mach 3 condition was the highest speed tested and in this case not necessarily the performance limit.

In summary, the survey found considerable experimental aerodynamic steady-state drag results that did indicate the aerodynamic capability of deployable decelerators performing satisfactory in the supersonic and hypersonic speed ranges. However, to say that the state of the art is such that there is adequate performance in design information available to design a lightweight system for future application is not the case. Even in the Mach 1 to 5 speed range, the more easily obtained steady-state drag information is fragmentary. For example, there is no one configuration or even a class of configurations that has been tested over a complete range of Mach numbers and Reynolds numbers. Above Mach 5, with few exceptions, the available drag data are a complete void. In

addition to lack of data, a basic phenomenon not yet completely understood is how the forebody wake flow affects the towed decelerator that must operate in that wake. When this flow is more fully understood in the wake, not only will the design have better forecast aerodynamic performance but also will have better forecast thermodynamic performance. Other areas that the survey showed as problem areas and voids are as follows:

1. Extreme shortage of cyclic steady-state data
2. Extreme shortage of transient deployment data
3. Extreme shortage of dynamic stability data

Because of the dynamic time dependent properties of the forebody wake acting on the towed decelerator in this wake, current acceptable dynamic and static stability coefficients do not appear adequate to describe the motion of a decelerator (see Section II, Item d).

3. STRUCTURES AND MATERIALS

The vast majority of supersonic decelerators that have been tested have been made of woven nylon or Nomex (high temperature nylon) fabrics. The selection of these fabrics was due to previous usage, cost, and because these fabrics had the physical properties that best matched the operational requirements. These requirements were lightweight, packageability, severe dynamic transient deployment loadings, and high level steady state inflation loading (under hostile temperature environment). Because textile materials - namely, Nomex - have a temperature resistance structural limit of slightly higher than 600 F and because flight temperature requirements are increasing considerably beyond 600 F, additional research and development material investigations have been and are being conducted.

Two basic methods of attack are being used. One method, which will hopefully aid in solving the immediate needs for higher operational

temperatures, is to protect the basic substrate (Nomex) with silicon or fluoro-elastomer coatings plus providing a coating additive that would increase the operating temperature limit to about 1000 F. The other method is to develop new coated material fabrics such as fiberglass, stainless steel, and superalloys. The apparent potential of the materials is as follows:

1. Fiberglass operating range - 600 to 1000 F
2. Stainless steel and René 41 - above 1100 to 1800 F
3. Refractory metals - above 1800 F
4. Carbon or graphite - above 1800 F

The most advanced of these newer materials are stainless steel and René 41. René 41 decelerators have been fabricated and tested in the wind tunnel at Mach 10 and at temperatures up to 1500 F.

Increasing temperatures above the present-day textile design limits will present the following major problem areas:

1. Higher heat resistant material has a high modulus that results in less flexibility and creates weaving problems plus lower foldability and lower dynamic structural loading capability.
2. The abrasive characteristics of fiberglass yarns cause self-destruction on the flexing and pulsating loads.
3. Refractory metals experience rapid oxidization at high temperatures and hence oxidization resistance coatings are required.
4. There is a near void in the development of low temperature - 600 to 1200 F - ablators (coatings).

In addition to the proper selection of the basic decelerator fabric, the

operational requirement for providing a lightweight decelerator can be achieved with the proper structural design. As new materials are developed, design parameters will have to be re-evaluated as to the overall shape and size, the selection of structural seams, attachments, fittings, and inflation methods.

4. PROBLEM AREAS AND VOIDS

There is very little experimental or analytical aerodynamic, thermodynamic, or structural data available in the supersonic and hypersonic speed ranges. There is a general lack of analytical methods to describe basic phenomena, including lack of aerodynamic data over a range of Reynolds number; a complete lack of quantitative experimental dynamic-stability data; and a basic lack of understanding of forebody wake flow when influenced by a towed decelerator. Specific problem areas are described below:

1. The aerodynamic and thermodynamic performance of promising decelerator configurations has not been investigated from the transonic regime to the hypersonic regime. Analytical techniques have not been verified experimentally in the areas listed below:
   a. Drag correlation, Mach number, and Reynolds number

      Shock and boundary layer interaction
   b. The effects of geometry and size
2. Performance and load density flow
   a. Applicable similarity parameters have not been established
   b. The effectiveness of free-stream Reynolds number, Knudsen number, etc., has not been determined
3. The formation and development of the wake have not been thoroughly investigated

Decelerator performance in compressible turbulent wakes has not been determined, the effects of Mach number and free-stream Reynolds number have not been determined, and payload signatures need to be defined. The effects of payload geometry, boundary layer, and separation on the correlation parameters have not been defined. Complete effects of D/d and x/d on performance are lacking. The effects of the decelerator itself on the wake interaction have not been studied completely, and the local flow thermal properties have not been completely defined.

4. The stability of various fundamental decelerator shapes is not known
   a. Static stability and dynamic stability derivatives need to be determined
   b. The stability of towed body systems needs to be studied
   c. Quantitative stability standards need to be established
   d. Inflation and breathing stability have not been adequately described
5. Heat transfer characteristics in complex decelerator shapes are an unknown
6. Methods of determining heat transfer in textile decelerators need to be investigated
   a. Low temperature ablative material for application to textile decelerators from 600 to 1500 F is missing
   b. Various methods of cooling and evaluating the relative merits of each have not been investigated
7. Lack of experimental data of resistance to abrasion from high-speed flutter
8. Lack of experimental data of resistance to shock loading

9. Lack of high temperature cements
10. Lack of high temperature coatings
11. Gaps in available materials between Nomex and superalloys
12. Lack of methods of fine wire drawing and weaving

The results when obtained to satisfy these voids (both experimental and analytical) need then to be correlated with free-flight results.

SECTION VI - CONCLUSIONS

1. GENERAL

The state-of-the-art survey considering the operational performance limits demonstrated by tests indicated the following conclusions:

1. Towed nonporous textile decelerators up to 5-ft in diameter have been successfully flight tested up to deployment speeds of nearly Mach 4; 10-in. diameter metal fabric models have been wind tunnel tested successfully up to Mach 10.

2. Four- to six-foot wind tunnel and flight parachute textile models developed drag up to Mach 4, although some instability was encountered above Mach 2.5.

The state-of-the-art survey of the individual disciplines affecting these operational performance limits described major problem areas, which are given in Items 2 and 3, below.

2. AERODYNAMICS

The state-of-the-art survey discussed these problems pertaining to aerodynamics:

1. There is a general lack of drag data above Mach 5 and incomplete data below Mach 5.

2. The basic wake flow phenomenon is not completely understood.

3. There is a complete lack of dynamic stability data.

3. STRUCTURES AND MATERIALS

The state-of-the-art survey described these problems pertaining to structures and materials:

1. Textile material models have a proved structural resistance to a temperature limit of 600 F.

2. Metal fabric models have been tested in the wind tunnel up to 1500 F.

3. Proved materials are available for future model developments from 300 to 600 F (textiles) and from 1000 to 1500 F (superalloys). There is a complete void for suitable proved materials between 600 to 1000 F and above 1500 F.

LIST OF SYMBOLS

Aerodynamic

$A(S)$ = reference frontal area

A_i = parachute canopy open inlet area

A_e = parachute canopy open exit area

A/A^* = cross-sectional area of stream tube divided by critical choked flow (nozzle) area

S = reference surface area

S_o = parachute canopy total enclosed surface area

D = decelerator reference diameter

d = forebody reference diameter

D_c = parachute constructed diameter

D_P = parachute inflated diameter

D_o = parachute nominal diameter based on S_o

C_D = drag coefficient, F/qA

C_{D_c} = parachute drag coefficient based on D_c

C_{D_f} = drag coefficient resulting from pressure drag on the body foward of the body base

C_{D_o} = parachute drag coefficient based on D_o

C_{D_P} = parachute drag coefficient based on D_P

F = drag force

L = lift force, normal to wind

ℓ = representative body length

N = normal force

M = moment

M_∞ = free-stream Mach-number

q = dynamic pressure

$q(q_\infty)$ = free-stream dynamic pressure

C_A = axial force coefficient

C_L = lift coefficient, L/qA

C_N = normal force coefficient, N/qA

C_M = moment coefficient, $M/qA\ell$

$C_P(C_{P_L})$ = pressure coefficient, $C_P = p_L - p_\infty/q_\infty$

p = pressure

p_L = local pressure

p_∞ = free-stream static pressure

C_{P_B} = base pressure coefficient

C_{P_o} = surface pressure coefficient

$C_{M_\alpha} = \partial C_M / \partial \alpha$

$C_{M_{\dot\alpha}} = \partial C_M / \partial \dot\alpha$

$C_{M_q} = \partial C_M / \partial (2V/q'd)$

$C_{N_\alpha} = \partial C_N / \partial \alpha$

$C_{N_{\dot{\alpha}}} = \partial C_N / \partial \dot{\alpha}$

$C_{N_q} = \partial C_N / \partial (2V/q'd)$

q' = pitch rate

R = body nose radius

r_b = body base radius

u = velocity in x direction

V = velocity

x = tow-line length between forebody and trailing afterbody

X_{cp} = longitudinal distance from apex to center of pressure

cp = center of pressure

FR = fineness ratio, body length divided by body diameter

Re = Reynolds number $\rho \ell V/\mu$

λ_S = mean free path behind shock wave

$\rho(\rho_\infty)$ = free-stream air density

ρ_S = density behind shock wave

α = angle of attack

$\dot{\alpha}$ = $d\alpha/dt$

θ = pitch angle

$\dot{\theta}$ = $d\theta/dt$

θ_ℓ = momentum thickness

θ_s = cone semiapex angle, flare angle

μ = fluid dynamic viscosity

σ = wake thickness

Thermodynamic

A = orifice status cross-sectional area

A^* = orifice throat area

C_f = local friction coefficient

c^* = characteristic orifice velocity

c = specific heat of material

c_p = specific heat of air at constant pressure

D = decelerater diameter

D_t = orifice throat diameter

$G(S)$ = local form factor

g = gravitational constant

h = heat-transfer coefficient

h_{aw} = adiabatic wall enthalpy

h_{cw} = cold wall enthalpy

h_w = wall enthalpy

k = thermal conductivity

P = pressure

P_t = total pressure

P' = local pressure

P_∞ = free-stream static pressure

$\dot{q}$ = heat flux rate

$\dot{q}_C$ = heat flux at $S/R_o = 1$ without forebody

$\dot{q}_o$ = heat flux at stagnation point without forebody

$\dot{q}_w$ = wall heat flux

$\dot{q}_{cw}$ = cold wall heat flux

R_o = decelerator nose radius

r' = local radial coordinate

r_e = radius of roof element

S = surface distance with meridional direction from the stagnation point

S' = local surface distance from the decelerator equator

T = local temperature

T_C = temperature at $S/R_o = 1$ without forebody

T_o = temperature at the stagnation point

T_w = material temperature

T_{aw} = adiabatic wall temperature

u' = local velocity

y = depth

Pr = Prandtl number

α = thermal diffusivity

δ = thickness

ε = emissivity

ρ = density of material

ρ' = local air density

μ = viscosity

μ_o = viscosity at total temperature

σ = dimensionless factor accounting for density and viscosity in boundary layer

τ = time

Structures and Design

A = forebody or decelerator reference area

A_f = surface area of decelerator

A_P = payload reference area

A_D = decelerator reference area

c = factor related to chute suspension line confluence angle

C_D = drag coefficient

$(C_DA)_T$ = total drag area of forebody and decelerator

D = decelerator diameter

D_P = parachute inflated diameter

d = forebody diameter

e = factor related to the strength loss from abrasion

E = modulus of elasticity

F_o = peak decelerator design load

f_f = design stress

h = number of meridian webs

J = safety factor

K = reacting load distribution factor

$K_c(K_m)$ = meridian cable or web strength-to-weight ratio

K_f = decelerator envelope fabric strength-to-weight ratio

K^2 = shape paramcter

k = factor rclated to strength loss from fatigue

L = length of each meridian

L_S = chute suspension line length

ℓ_S = shell length in meridian direction

m_p = nose-cap mass

m_R = mass of ring

m_{SH} = mass of shell

N_ϕ = meridian shell resultant

N_o = N_ϕ evaluated at $R = R_b$

o = factor related to strength due to strength loss in material from water and water vapor absorption

P = pressure

ΔP_R = pressure differential across decelerator envelope fabric

P_T = total pressure

p = pressure acting on the shell

q = dynamic pressure

R = decelerator radius

R_b = shell radius at the base

R_T = radial distance to point of tangency of nose cap and shell

T = meridian design tension load

t = thickness

u = factor for strength at connecting points

W = weight

$W_B(W_D)$ = decelerator weight

W_c = decelerator fabric coating weight

W_f = decelerator fabric weight

W_m = decelerator meridian weight

W_T = total weight of forebody and decelerator

W_P = payload (forebody) weight

Z = number of chute suspension lines

D. F. = total fabric design factor, the product of safety factor, dynamic loading, seam efficiency, temperature, etc.

D. F.' = median design factor

erf(K) = error function

C. F. = unit coating weight

β = angle between axis and tangent to surface

λ = chute geometric porosity

ρ = material density

ρ' = applied load distribution factor

σ_a = allowable stress

ϕ = angle between flow and normal to surface

LIST OF REFERENCES

1. Chernowitz, G.; and DeWeese, J. H.: Performance of and Design Criteria for Deployable Aerodynamic Decelerators. Second major revision of the USAF parachute handbook, ASD-TR-61-579, AD-429971, December 1963.

2. Foster, A. D.: A Compilation of Longitudinal Aerodynamic Characteristics Including Pressure Information for Sharp and Blunt-Nose Having Flat and Modified Bases. Sandia Corporation, SC-R-64-1311, January 1965.

3. Nichols, J. O.; and Nierengarten, E. A.: Aerodynamic Characteristics of Blunt Bodies. JPL-TR-32-677, N-116-287, November 1964.

4. Penland, J. A.: A Study of the Stability and Location of the Center of Pressure on Sharp, Right Circular Cones at Hypersonic Speeds. NASA TN D-2283, May 1964.

5. Penland, J. A.: Aerodynamic Force Characteristics of a Series of Lifting Cone and Cone-Cylinder Configurations at a Mach Number of 6.83 and Angles of Attack Up to 130 Degrees. NASA TN D-840, June 1961.

6. Aerodynamic Characteristics of Spherically Blunted Cones at Mach Numbers from 0.5 to 5.0. George C. Marshall Space Flight Center, MTP-Aero-61-38, May 1961.

7. Maas, W. L.: Experimental Determination of Pitching Moment and Damping Coefficients of a Cone in Low Density, Hypersonic Flow. University of California, Institute of Engineering Research, TR HE-150-190, Series 20, Issue No. 135, AD-266787, October 1961.

8. North American Aviation, Missile Division: External Drag Manual. NAA/MD 59-453, 1960, p 5-10.

9. Rainey, R. W.: Working Charts for Rapid Prediction of Force and Pressure Coefficients on Arbitrary Bodies of Revolution by Use of Newtonian Concepts. NASA TN D-176, December 1959.

10. Hoerner, S. F.: Fluid-Dynamic Drag. Published by author, 1958.

11. Tobak, M.; and Wehrend, W. R.: Stability Derivatives of Cones at Supersonic Speeds. NACA TN 3788, September 1956.

12. Gendtner, W. J.: Sharp and Blunted Cone Force Coefficients and Centers of Pressure from Wind Tunnel Tests at Mach Numbers from 0.50 to 4.06. Convair Report ZA-7-017, June 1955.

13. Young, G. B. W.; and Siska, C. P.: "Supersonic Flow Around Cones at Large Yaw." Journal of Aeronautical Sciences, Vol 19, p 111, 1952.

14. Stone, A. H.: "On Supersonic Flow Past a Slightly Yawing Cone." Journal of Mathematics and Physics, Vol 30, 1952.

15. Van Dyke, M. D.: A Study of Second Order Supersonic Flow Theory. NACA Report 1081 (formerly NACA TN 220), 1952.

16. Ferri, A.: Supersonic Flow Around Circular Cones at Angles of Attack. NACA Report No. 1045, 1951.

17. Van Dyke, M. D.: "First-Order and Second-Order Theory of Supersonic Flow Past Bodies of Revolution." Journal of Aeronautical Sciences, Vol 18, March 1951.

18. Staff of the Computing Section, Center of Analysis (under direction of Zdenek Kopal): Tables of Supersonic Flow Around Cones at Large Yaw. Technical Report No. 5, Massachusetts Institute of Technology, 1949.

19. Rantzsche, W.; and Wendt, H.: Cones in Supersonic Flow. RAND T-8, January 1948.

20. Stone, A. H.: "On Supersonic Flow Past a Slightly Yawing Cone." Journal of Mathematics and Physics, Vol 27, 1948.

21. Staff of the Computing Section, Center of Analysis (under direction of Zdenek Kopal): Tables of Supersonic Flow Around Yawing Cones, Technical Report No. 3, Massachusetts Institute of Technology, 1947.

22. Staff of Computing Section, Center of Analysis (under direction of Zdenek Kopal): Tables of Supersonic Flow Around Cones. Technical Report No. 1, Massachusetts Institute of Technology, 1947.

23. Heinrich, H. G.; Hess, R. S.; and Stumbris, G.: Drag Characteristics of Plates, Cones, and Spheres in the Wake of a Cylindrical Body at Transonic Speeds. RTD-TDR-63-4023, AD-457055, and X65-13630, January 1965.

24. Heinrich, H. G.; and Hess, R. S.: Drag Characteristics of Plates, Cones, Spheres, and Hemispheres in the Wake of a Forebody at Transonic and Supersonic Speeds. RTD-TDR-63-4242, December 1964.

25. Heinrich, H. G.; and Hess, R. S.: Drag Characteristics of Several Two-Body Systems at Transonic and Supersonic Speeds. RTD-TDR-63-4226, December 1964.

26. Charczenko, N.: Aerodynamic Characteristics of Towed Spheres, Conical Rings, and Cones Used as Decclerators at Mach Numbers from 1.57 to 4.65. NASA TN D-1789, N63-15308, April 1963.

27. Alexander, W. C.: Investigation to Determine the Feasibility of Using Inflatable Balloon-Type Drag Devices for Recovery Applications in the Transonic, Supersonic and Hypersonic Flight Regime. Part II, Mach 4 to Mach 10 Feasibility Investigation, ASD-TDR-62-702, December 1962.

28. Charczenko, N.; and McShera, J. T., Jr.: Aerodynamic Characteristics of Towed Cones Used as Decelerators at Mach Numbers from 1.57 to 4.65. NASA TN D-994, December 1961.

29. Wegener, P. P.; and Ashkenas, H.: Wind Tunnel Measurements of Sphere Drag at Supersonic Speeds and Low Reynolds Numbers. JPL-TR-34-160, N63-18848, June 1961.

30. Masson, D. J.: Measurements of Sphere Drag from Hypersonic Continuum to Free-Molecule Flow. Rand Report RM2678, November 1960.

31. Hodges, A. J.: "The Drag Coefficient of Very High Velocity Spheres." Journal of Aeronautical Sciences, Vol 24, 1957.

32. May, A.; and Witt, W. R., Jr.: Free Flight Determinations of the Drag Coefficient of Spheres. NAVORD Report 2352, August 1952.

33. Van Dyke, M. D.; Young, G. W.; and Sisha, C.: "Proper Use of the M.I.T Tables for Supersonic Flow Past Inclined Cones." Journal of Aeronautical Sciences, Vol 18, 1951.

34. Charters, A. C.; and Thomas, R. N.: "The Aerodynamic Performance of Small Spheres from Subsonic to High Supersonic Velocities." Journal of Aeronautical Sciences, Vol 12, 1945.

35. McShera, J. T., Jr.: Aerodynamic Drag and Stability Characteristics of Towed Inflatable Decelerators at Supersonic Speeds. NASA TN D-1601, March 1963.

36. Nebiker, F. R. and Karaffa, N. T.: Feasibility Study of an Inflatable Type Stabilization and Deceleration System for High-Altitude and High Speed Recovery. ASD-TR-60-182, November 1961.

37. McShera, J. T.; and Keyes, J. W.: Wind Tunnel Investigation of a Balloon as a Towed Decelerator at Mach Numbers from 1.47 to 2.50. NASA TN D-919, N62-71493, August 1961.

38. Uselton, J. C.; and Hahn, J. S.: Drag Characteristics of Three Ballute

Decelerators in the Wake of the ALARR Payload at Mach Numbers 2 to 4. AEDC-TR-65-218, Arnold Engineering Development Center, October 1965.

39. Unpublished data of tests at AEDC wind tunnel, August 1965.

40. Deitring, J. S.; and Hilliard, E. E.: Wind Tunnel Investigation of Flexible Aerodynamic Decelerator Characteristics at Mach Numbers 1.5 to 6. AEDC-TR-65-110, June 1965.

41. Unpublished AEDC Ballute wind tunnel tests conducted December 1964.

42. Unpublished Holloman AFB Ballute sled test conducted November 1964.

43. GER-11665S3: Aerodynamic Deployable Decelerator Performance Evaluation Program. Flight Test Report (TB-2), FDL/RTD/USAF, February 1965.

44. GER-11665S2: Aerodynamic Deployable Decelerator Performance Evaluation Program. Flight Test Report (TB-1B), FDL/RTD/USAF, February 1965.

45. GER-11665S1: Aerodynamic Deployable Decelerator Performance Evaluation Program. Flight Test Report (TB-1A),FDL/RTD/USAF, February 1965.

46. Knapp, H.: Gemini Ballute Structural Test at Mach Numbers 0.55 and 1.92. AEDC-TDR-64-131, June 1964.

47. Unpublished data of tests at AEDC wind tunnel, April 1964.

48. Bell, D. R.: Pressure Measurements on the Rigid Model of a Balloon Decelerator in the Wake of a Simulated Missile Payload at Mach Numbers 1.5 to 6. AEDC-TDR-64-65, April 1964.

49. GER-11538 (Altgelt, R.): Gemini Ballute System Development - Final Report. January 1965.

50. Deitering, J. S.: Performance of Flexible Aerodynamic Decelerators at Mach Numbers from 1.5 to 6. AEDC-TDR-63-119, July 1963.

51. Ashby, G. C.; and Cary, A. M.: A Parametric Study of the Aerodynamic Characteristics of Nose-Cylinder-Flare Bodies at a Mach Number of 6.0. NASA TN D-2854, June 1965.

52. Champney, W. B.; Athans, J. B.; and Mayerson, C. D.: A Study of Hypersonic Aerodynamic Drag Devices. WADC-TR-59-324, December 1960.

53. Deep, R. A.; and Henderson, J. H.: Study of Aerodynamic Characteristics of Cone-Cylinder-Conical Frustum Bodies by Linearized Theory of Supersonic Flow. Ordnance Missile Laboratory, Report 6R2P, June 1955.

54. Nickel, W. E.; and Sims, L. W.: Study of an Exploratory Free-Flight Investigation of Deployable Aerodynamic Decelerations Operating at High Altitudes and at High Mach Numbers. FDL-TDR-64-35, Vol 1, July 1964.

55. Lowry, J. F.: Aerodynamic Characteristics of Various Types of Full Scale Parachutes at Mach Numbers from 1.8 to 3.0. AEDC-TDR-64-120, June 1964.

56. Petersen, P. E.: Study of Parachute Performance and Design Parameters for High Dynamic Pressure Operation. FDL-TDR-64-66, May 1964.

57. Deitering, J. S.: Wind Tunnel Investigation of Flexible Parachute Model Characteristics at Mach Numbers 1.5 to 5. AEDC-TDR-63-263, January 1964.

58. Deitering, J. S.: Performance of Flexible Parachute Models at Mach Numbers from 1.5 to 4. AEDC-TDR-62-234, December 1962.

59. Maynard, J. D.: Aerodynamic Characteristics of Parachutes at Mach Numbers from 1.6 to 3. NASA TN D-752, May 1961.

60. Johnson, C. T.: Investigation of the Characteristics of 6-Foot Drogue Stabilization Ribbon Parachutes at High Altitudes and Low Supersonic Speeds. NASA TM X-448, November 1960.

61. Nichols, J. H.: Wind Tunnel Investigation of Stabilization Parachutes for the B-58 Crew Escape Capsule. AEDC-TN-59-107, September 1959.

62. Reichenau, D. E. A.: Aerodynamic Performance of Various Hyperflo and Hemisflo Parachutes at Mach Numbers from 1.8 to 3.0. AEDC-TR-65-57, March 1965.

63. Sims, L. W.: Analytical and Experimental Investigation of Supersonic Parachute Phenomena, ASD-TDR-62-844. Chicago, Ill., Cook Technological Center, February 1963 (CONFIDENTIAL).

64. Deitering, J. S.: Investigation of Flexible Parachute Model Characteristics at Mach Numbers 1.5 to 6. AEDC-TDR-62-185, X63-13449, October 1962.

65. Guy, L. D.: "Tension Shell Structures for Low Density Entry Vehicles." Presented at AIAA Second Annual Meeting, July 1965.

66. Anderson, M. S.; Robinson, J. C.; Bush, H. G.; and Frelich, R. W.: A Tension Shell Structure for Application to Entry Vehicles. NASA TN D-2675.

67. Unpublished towed tension shell wind tunnel data behind X-15 model conducted March 1965.

68. Study of a Drag Brake Satellite Recovery System. AVCO-Everett Research Laboratory, ASD-TR-61-348, Vol 1, 2, 3, and 4, January 1962.

69. Baer, A. L.; Lindsey, E. E.; and Rippey, J. O.: Pressure Distribution Tests on Five AVCO Modulated Drag Brake Configurations at Supersonic and Hypersonic Speeds. AEDC-TN-61-4, February 1961.

70. MacNeal, R. H.: Mechanics of a Coned Rotating Net. Astro Research Corporation, Report No. ARC-R-177, February 1965.

71. Kyser, A. C.: The Rotornet, a High-Performance Hypersonic Decelerator for Planetary Entry. Astro Research Corporation, Report No. ARC-R-176, February 1965.

72. Knacke, T. W.; Paulson, K. R.; and Schurr, G. G.: Study of Soft Recovery. Technical Report AFOSR-104, N62-13153, March 1961.

73. Reichenau, D. E. A.: Investigation of Various Full-Scale Parachutes at Mach Number 3.0. AEDC-TR-65-241, December 1965.

74. Wehrend, W. R.: An Experimental Evaluation of Aerodynamic Damping Moments of Cones with Different Centers of Rotation. NASA TN D-1768, March 1963.

75. Mayo, E. E.; Lamb, R. H.; and Romere, P. O.: Newtonian Aerodynamics for Blunted Raked-off Circular Cones and Raked-off Elliptical Cones. NASA TN D-2624, May 1965.

76. Lichtenstein, J. H.; Fisher, L. R.; Sher, S. H.; and Lawrence, G. F.: Some Static, Oscillatory, and Free-Body Tests of Blunt Bodies of Revolution at Low Subsonic Speeds. NASA Memo 2-22-59L, April 1959.

77. Marte, J. E.; and Weaver, R. W.: Low Subsonic Dynamic Stability Investigation of Several Planetary Entry Configurations in a Vertical Wind Tunnel (Part 1). Jet Propulsion Laboratory, Technical Report No. 32-743, May 1965.

78. Schlichfing, H.: Boundary Layer Theory, translated by J. Kesten. McGraw Hill, New York, N. Y., 1955.

79. Sims, L. W.: The Effects of Design Parameters and Local Flow Fields on the Performance of Hyperflo Supersonic Parachutes and High Dynamic Pressure Parachute Concepts. AFFDL-TR-65-150, Vol 1, September 1965.

80. GER-12687: Wakes, Their Structure and Influence Upon Aerodynamic Decelerators. Akron, Ohio, Goodyear Aerospace Corporation, May 1966.

81. Crawford, D. M.: Investigation of the Flow Over a Spiked Nose Hemisphere Cylinder at a Mach Number of 6.8. NASA TN D-118, December 1959.

82. Nebiker, F. R.: Aerodynamic Deployable Decelerator Performance Evaluation Program. AFFDL-TR-65-27, May 1965.

83. GER-11820 (Nerem, R. M.): Supersonic Wake Phenomena with Application to Ballute-Type Decelerators. November 1964.

84. GER-11824 (Nerem, R. M.): An Approximate Method for Including the Effect of the Inviscid Wake on the Pressure Distribution on a Ballute-Type Decelerator. November 1964.

85. Zeiberg, S. L.: "Transition Correlation for Hypersonic Wakes," AIAA Journal, Vol 2, No. 3, March 1964, 564, 565.

86. Candidate Materials for High-Temperature Fabrics. WADC-TR-59-155, September 1959.

87. Anderson, A. R.: Effect of Biological Sterilization and Vacuum on Certain Parachute Retardation System Components. Jet Propulsion Laboratory, Final Report No. 4324, August 1963.

88. Kaswell, E. R.: Wellington Sear Handbook of Industrial Textiles, 1963.

89. Symposium on Fibrous Materials. ASD-TDR-62-964, January 1963.

90. Metal Filaments for High-Temperature Fabrics. ASD-TR-62-180, February 1962.

91. Characterization of Graphite and Carbon-Based Fibrous Materials Exposed to Varying Environments. AFML-TR-65-59, June 1965.

92. Air Force Materials Symposium. AFML-TR-65-29, June 1965.

93. New and Improved Materials for Expandable Structures - Part 1. ASD-TDR-62-542, June 1962.

94. Flexible Fibrous Structural Materials. AFML-TR-65-118, April 1965.

I - NASA REPORTS

MacNeal, R. H.: Mechanics of a Coned Rotating Net. NASA CR-248, July 1965.

Kyan, A. C.: The Rotonet: A High-Performance Hypersonic Decelerator for Planetary Entry. NASA CR-247.

Afterbody Pressures on Boat-tailed Bodies of Revolution Having Turbulent Boundary Layers at Mach 6. NASA TN D-2761.

Study of the Stabilization and Drag at Mach Numbers from 4.5 to 13.5 of a Conical Venus Entry Body. NASA TN D-2877.

Smetana, F. O.: Investigations of the Permeability of Parachute Fabrics. N65-15016, NASA-CR-60137.

McShera, J. T., Jr.: The Use of a Supersonic Wind Tunnel as a Means of Investigating Decelerator Configuration. X65-10857, NASA-TM-X-54543

Charczenko, N.: Wind Tunnel Investigation of Drag and Stability of Parachutes at Supersonic Speeds. NASA-TM-X-991, August 1964.

Rakich, J. V.: Numerical Calculation of Supersonic Flows of a Perfect Gas Over Bodies of Revolution at Small Angles of Yaw. NASA TN-D-2390, July 1964

Bertram, M. H.: Correlation Graphs for Supersonic Flow around Right Circular Cones at Zero Yaw in Air as a Perfect Gas. NASA TN D-2339, June 1964.

Arrington, J. P. and Maddalon, D. V.: Aerodynamic Characteristics of Several Lifting and Nonlifting Configurations at Hypersonic Speeds in Air and Helium (U). NASA TM-X-918, June 1964 (CONFIDENTIAL)

Penland, J. A.: A Study of the Stability and Location of the Center of Pressure on Sharp, Right Circular Cones at Hypersonic Speeds. NASA TN D-2283, May 1964

Yoshikawa, K. K. and Wick, B. H.: Aerodynamic and Rocket Braking of Blunt Non-lifting Vehicles Entering the Earth's Atmosphere at Very High Speeds, NASA TN D-2239, April 1964

Burk, S. M., Jr.: Low-Speed Free-Flight Stability and Drag Characteristics of Radially Vented Parachutes. NASA TN D-2271, March 1964

Harris, J. E.: A Basic Study of Spherically Blunted Cones Including Force and Moment Coefficient Correlation and Air-Helium Simulation Studies, (M.S., Thesis), NASA CR-56254, X65-12565, March 1964

Keyes, J. W.: Longitudinal Aerodynamic Characteristics of Blunted Cones at Mach Numbers of 3.5, 4.2 and 6.0. NASA TN D-2201, February 1964

Nichols, J. and Nierengarten, E.: Static Aerodynamic Characteristics of Blunted Cones and Round-Shouldered Cylinders Suitable for Planetary Entry Vehicles at a Mach Number Range 1.65 to 9.00. NASA CR-58666, N64-29212, February 1964

Smedal, H. A., Capt. USN(MC), and Creer, B. Y.: Physiological Effects of Acceleration Observed during a Centrifuge Study of Pilot Performance, NASA TN D-345, December 1963

Barton, R. L. and Kilgore, R. A.: The Aerodynamic Damping and Oscillatory Stability in Pitch of Two High-Drag Bodies of Revolution at Transonic Speeds. NASA TM X-906, X64-10091, November 1963

Wehrend, W. R., Jr.: A Wind Tunnel Investigation of the Effect of Changes in Base Contour on the Damping in Pitch of Blunted Cone. NASA TN D-2062, November 1963

Brooks, C. W., Jr. and Trescot, C. D., Jr.: Transonic Investigations of the Effects of Nose Bluntness, Fineness Ratio, Cone Angle, and Base Shape on the Static Aerodynamic Characteristics of Short, Blunt Cones at Angles of Attack to 180 Degrees. NASA TN D-1926, August 1963

Terry, J. E. and Miller, R. J.: Aerodynamic Characteristics of a Truncated-Cone Lifting Re-entry Body at Mach Numbers from 10 to 21. NASA TM X-786, August 1963 (CONFIDENTIAL)

Chapman, G. T. and Jackson, C. T., Jr.: Measurement of Heat Transfer to Bodies of Revolution in Free Flight by Use of a Catcher Calorimeter. NASA TN D-1890, July 1963

Chapman, A. J.: An Experimental Evaluation of Three Types of Thermal Protection Materials at Moderate Heating Rates and High Total Heat Loads. NASA TN D-1814, July 1963

Schippell, H. R.: Trailblazer I Re-entry-Body Wind-Tunnel Tests at a Mach Number of 6.7 with Theoretical Aerodynamics and a Limited Dynamic Analysis. NASA TN D-1936, July 1963

McShera, J. T., Jr. and Wassum, D. L.: Stability and Control Characteristics of a Low-Lift-Drag-Ratio Re-entry Vehicle at Mach Numbers from 2.30 to 4.65. NASA TM X-891, July 1963, (CONFIDENTIAL)

Reid, R. and Middleton, D. B.: A Trajectory Analysis of a Variable-Drag Payload Ejected from a Vehicle in a Low Earth Orbit. NASA TN D-1938, July 1963

Shaw, D. S.; Fuller, D. E.; and Babb, C. D.: Effects of Nose Bluntness, Fineness Ratio, Cone Angle, and Model Base on the Static Aerodynamic Characteristics of Blunt Bodies at Mach Numbers of 1.57, 1.80 and 2.16 and Angles of Attack up to 160 Degrees. NASA TN D-1781, May 1963

Charczenko, N.: Aerodynamic Characteristics of Towed Spheres, Conical Rings, and Cones Used as Decelerators at Mach Numbers from 1.57 to 4.65. NASA TN D-1789, N63-15308, April 1963

McShera, J. T., Jr.: Aerodynamic Drag and Stability Characteristics of Towed Inflatable Decelerators at Supersonic Speeds. NASA TN D-1601, March 1963

Wehrend, W. R., Jr.: An Experimental Evaluation of Aerodynamic Damping Moments of Cones with Different Centers of Rotation. NASA TN D-1768, March 1963

Grimwood, J. M.: Project Mercury - A Chronology. NASA SP-4001, 1963

Fuller, D. E. and Babb, O. D.: Static Stability Investigation of Proposed Project Fire Space-Vehicle and Re-entry-Package Configurations at Mach Numbers from 1.47 to 4.63. NASA N63-10178, NASA TN D-1497, November 1962

Tobak, M.: Analytical Study of the Tumbling Motions of Vehicles Entering Planetary Atmospheres. NASA TN D-1549, October 1962

Coltrane, L. C.: Stability Investigation of a Blunted Cone and a Blunted Ogive with a Flared Cylinder Afterbody at Mach Numbers from 0.30 to 2.85. NASA TN D-1506, October 1962 (Supersedes NASA TM X-199)

Gamse, B. and Yaggy, P. F.: Wind Tunnel Tests of a Series of 18-Foot-Diameter Parachutes with Extendable Flaps. NASA TN D-1334, August 1962

Sanger, M. B., Jr.: Drag Characteristics and Dynamic Stability in Descent of a Rotary Parachute Tested in a Vertical Tunnel. NASA TN D-1388, August 1962

Seiff, A.: Secondary Flow Fields Embedded in Hypersonic Shock Layers. TN D-1304, NASA, May 1962

Peterson, V. L.: Motions of a Short 10 Degree Blunted Cone Entering a Martian Atmosphere at Arbitrary Angles of Attack and Arbitrary Pitching Rates. NASA TN D-1326, May 1962

Hillje, E. R. and Pearson, A. O.: Transonic Static and Dynamic Longitudinal Stability Characteristics of a Low-Fineness-Ratio, Blunted-Cylinder Re-entry Body having a Converging-Cone Afterbody. NASA TM X-672, X62-10101, May 1962 (CONFIDENTIAL)

Lazzeroni, F. A.: Experimental Investigation of a Disk-Shaped Re-entry Configuration at Transonic and Low Supersonic Speeds. NASA TM X-652, X62-10098, May 1962 (CONFIDENTIAL)

Hillje, E. R. and Kilgore, R. A.: Transonic Dynamic Longitudinal Stability Characteristics of Six Ballistic Re-entry Configurations Designed for Supersonic Impact. NASA TM X-673, X62-10021, March 1962 (CONFIDENTIAL)

Holtzclaw, R. W.: Static Stability and Control Characteristics of a Half-Cone Entry Configuration at Mach Numbers from 2.2 to 0.7. NASA TM X-649, March 1962

Penland, J. A.: A Study of the Aerodynamic Characteristics of a Fixed Geometry Paraglider Configuration and Three Canopies with Simulated Variable Canopy Inflation at a Mach Number of 6.6. NASA TN D-1022, March 1962

Hillje, E. R. and Kilgore, R. A.: Transonic Dynamic Longitudinal Stability Characteristics of Six Ballistic Re-entry Configurations Designed for Supersonic Impact. X62-10021, NASA TM X-673, March 1962 (CONFIDENTIAL)

Thompson, R. F. and Jones, E. M.: Recovery Operations. N62-10236, February 1962

Thompson, R. F. and Cheatham, D. C.: Considerations for Spacecraft Recovery from Lunar Missions. N-107-051, January 1962

Wells, W. R. and Armstrong, W. O.: Tables of Aerodynamic Coefficients Obtained from Developed Newtonian Expressions for Complete and Partial Conic and Spheric Bodies at Combined Angles of Attack and Sideslip with Some Comparisons with Hypersonic Experimental Data. NASA TR R-127, 1962

Goodwin, G. and Howe, J. T.: Recent Developments in Mass, Momentum, and Energy Transfer at Hypervelocities. NASA University Conference on the Science and Technology of Space Exploration, NASA SP-11, Vol 2, 1962, pp 291-301

Treon, S. L.: Static Aerodynamic Characteristics of Short Blunt Cones with Various Nose and Base Cone Angles at Mach Numbers from 0.6 to 5.5 and Angles of Attack to 180 Degrees. NASA TN D-1327, 1962

Smith, W. G. and Peterson, W. P.: Free-Flight Measurements of Drag and Stability of a Blunt-Nosed Cylinder with a Flared Afterbody in Air and Carbon Dioxide. NASA TM X-642, December 1961

Stivers, L. S., Jr. and Levy, L. L, Jr.: Longitudinal Force and Moment Data at Mach Numbers from 0.60 to 1.40 for a Family of Elliptic Cones with Various Semi-apex Angles. NASA TN D-1149, December 1961

Charczenko, N. and McShera, J. T., Jr.: Aerodynamic Characteristics of Towed Cones Used as Decelerators at Mach Numbers from 1.57 to 4.65. NASA TN D-994, December 1961

Dickey, R. R.: Forces and Moments on Sphere-Cone Bodies in Newtonian Flow. NASA TN D-1203, December 1961

McShera, J. T. and Keyes, J. W.: Wind Tunnel Investigation of a Balloon as a Towed Decelerator at Mach Number from 1.47 to 2.50. NASA TN D-919, N62-71493, August 1961

Penland, J. A.: Aerodynamic Force Characteristics of a Series of Lifting Cone and Cone-Cylinder Configurations at a Mach Number of 6.83 and Angles of Attack up to 130 Degrees. NASA TN D-840, June 1961

Henderson, A. Jr. and Braswell, D. O.: Charts for Conical and Two-Dimensional Oblique-Shock Flow Parameters in Helium at Mach Numbers from about 1 to 100. NASA TN D-819, June 1961

Aerodynamic Characteristics of Spherically Blunted Cones at Mach Numbers from 0.5 to 5.0. George C. Marshall Flight Center, Report MTP-AERO-61-38, May 1961

Maynard, J. D.: Aerodynamic Characteristics of Parachutes at Mach Numbers from 1.6 to 3. NASA TN D-752, May 1961

Crier, N. T. and Sands, N.: Regime of Frozen Boundary Layers in Stagnation Region of Blunt Re-entry Bodies. NASA TN D-865, May 1961

McDearmon, R. W. and Lawson, W. A.: Investigation of the Normal-Force, Axial-Force, and Pitching Moment Characteristics of Blunt Low-Fineness-Ratio Bodies of Revolution at a Mach Number of 3.55. NASA TM X-467, N63-13911, April 1961

Czarnecki, K. R. and Jackson, M. W.: Effects of Cone Angle, Mach Number, and Nose Blunting on Transition at Supersonic Speeds. NASA TN D-634, January 1961

Stoney, W. E., Jr.: Collection of Zero-Lift Drag Data on Bodies of Revolution from Free-Flight Investigations. NASA TR R-100 (supersedes NACA TN 4201), 1961

Margolis, K.: Theoretical Evaluation of the Pressures, Forces, and Moments at Hypersonic Speeds Acting on Arbitrary Bodies of Revolution Undergoing Separate and Combined Angle-of-Attack and Pitching Motions. NASA TN D-652, 1961

Armstrong, W. O.: Hypersonic Aerodynamic Characteristics of Several Series of Lifting Bodies Applicable to Re-entry Vehicle Design. NASA TM X-536, 1961

Fletcher, H. S. and Wolhart, W. D.: Damping in Pitch and Static Stability of Supersonic Impact Nose Cones, Short Blunt Subsonic Impact Nose Cones, and Manned Re-entry Capsules at Mach Numbers from 1.93 to 3.05. NASA TM X-347, November 1960

Briggs, B. R.: The Numerical Calculation of Flow Past Conical Bodies Supporting Elliptic Conical Shock Waves at Finite Angles of Incidence. NASA TN D-340, November 1960

Johnson, C. T.: Investigation of the Characteristics of 6-Foot Drogue-Stabilization Ribbon Parachutes at High Altitudes and Low Supersonic Speeds. NASA TM X-448, November 1960

Smith, F. M.: A Wind-Tunnel Investigation of the Aerodynamic Characteristics of Bodies of Revolution at Mach Numbers of 2.37, 2.98 and 3.90 at Angles of Attack to 90 Degrees. NASA TM X-311, August 1960

Grant, F. C.: Analysis of Low-Acceleration Lifting Entry from Escape Speed. NASA TN D-249, June 1960

Wehrend, W. R., Jr. and Reese, D. E., Jr.: Wind Tunnel Tests of the Static and Dynamic Stability Characteristics of Four Ballistic Re-entry Bodies. NASA TM X-369, 1960

Rainey, R. W.: Working Charts for Rapid Prediction of Force and Pressure Coefficients on Arbitrary Bodies of Revolution by Use of Newtonian Concepts. NASA TN D-176, December 1959

Crawford, D. H.: Investigation of the Flow over a Spiked-Nose Hemisphere-Cylinder at a Mach Number of 6.8. NASA TN D-118, December 1959

Lockwood, V. E. and McKinney, L. W.: Lift and Drag Characteristics at Subsonic Speeds and at a High Mach Number of 1.9 of a Lifting Circular Cylinder with a Fineness Ratio of 10. NASA TN D-170, December 1959

Grant, F. C.: Importance of the Variation of Drag with Lift in Minimization of Satellite Entry Acceleration. NASA TN D-120, October 1959

Trout, O. F., Jr.: Experimental Investigation of Several Copper and Beryllium Hemisphere Models in Air at Stagnation Temperature of 2000 F to 3600 F. NASA TM X-55, September 1959

Henderson, A., Jr. and Johnston, P. J.: Fluid-Dynamic Properties of Some Simple Sharp and Blunt-Nosed Shapes at Mach Numbers from 16 to 24 In. Helium Flow. NASA Memo 5-8-59L, June 1959

Sommer, S. C. and Tobak, M.: Study of the Oscillatory Motion of Manned Vehicles Entering the Earth's Atmosphere. NASA Memo 3-2-59A, April 1959

Kehlet, A. B. and Patterson, H. G.: Free-Flight Test of a Technique for Inflating an NASA 12-Foot Diameter Sphere at High Altitudes. NASA Memo 2-5-59L, January 1959

Chapman, D. R.: An Approximate Analytical Method for Studying Entry into Planetary Atmospheres. NASA TR R-11, 1959

Letko, W.: Experimental Investigation at a Mach Number of 3.11 of the Lift, Drag and Pitching-Moment Characteristics of a Number of Blunt, Low-Fineness-Ratio Bodies. NASA Memo 1-18-59L, 1959

Turner, K. L. and Shaw, D. S.: Wind-Tunnel Investigation at Mach Numbers from 1.60 to 4.50 of the Static-Stability Characteristics of Two Non-Lifting Vehicles Suitable for Re-entry. NASA Memo 3-2-59L, 1959

Rainey, R. W.: Working Charts for Rapid Prediction of Force and Pressure Coefficients on Arbitrary Bodies of Revolution by Use of Newtonian Concepts. NASA TN D-176, December 1959

Fletcher, H. W. and Wolhart, W. D.: Damping in Pitch and Static Stability of a Group of Blunt-Nose and Cone-Cylinder-Flare Models at a Mach Number of 6.83. NASA Memo 5-6-59L, 1959

Fisher, L. R.: Equations and Charts for Determining the Hypersonic Stability Derivatives of Combinations of Cone Frustums Computed by Newtonian Impact Theory. NASA TN D-149, 1959

Chapman, D. R.: Deceleration during Entry in Planetary Atmospheres. N-65794, November 1958

Fisher, L. R.; Keith, A. L., Jr.; and DiCamillo, J. R.: Aerodynamic Characteristics of Some Families of Blunt Bodies at Transonic Speeds. NASA Memo 10-28-58L, November 1958

Coltrane, L. C.: Stability Investigation of a Blunt Cone and a Blunt Cylinder with a Square Base at Mach Numbers from 0.64 to 2.14. NACA RM L58G24, September 1958

Tobak, M. and Allen: Dynamic Stability of Vehicles Traversing Ascending or Descending Paths through the Atmosphere. NACA TN 4275, July 1958

Speegle, K. C.; Charvin, L. T.; and Heberlig, J. C.: Heat Transfer for Mach Numbers up to 2.2 and Pressure Distributions for Mach Numbers up to 4.7 from Flight Investigation of a Flat-Face-Cone and a Hemisphere-Cone. NACA RM L58B18, May 1958

Kehlet, A. B.: Some Effects of Reynolds Number on the Stability of a Series of Flared-Body and Blunted-Cone Models at Mach Numbers from 1.62 to 6.86. NACA RM L57J29, January 1958

Eggers, A. J., Jr.: Recovery Dynamics - Possibility of Non-destructive Landing. N-60624, 1958

Beckwith, I. E. and Gallagher, V. V.: Heat Transfer and Recovery Temperatures on a Sphere with Laminar, Transitional, and Turbulent Boundary Layers at Mach Numbers of 2.00 and 4.15. NACA TN 4125, December 1957

Allen, H. Julian: Motion of a Ballistic Missile Angularly Misaligned with the Flight Path upon Entering the Atmosphere and its Effect upon Aerodynamic Heating, Aerodynamic Loads, and Miss Distance. NACA TN 4048, October 1957

Reller, J. O., Jr.: Heat Transfer to Blunt Nose Shapes with Laminar Boundary Layers at High Supersonic Speeds. NACA RM A57F03A, N62-64403, August 1957

Centolonzi, F. T.: Characteristics of a 40-Degree Cone for Measuring Mach Numbers, Total Pressure, and Flow Angles at Supersonic Speeds. NACA TN 3967, May 1957

Carter, H. S. and Bressette, W. F.: Heat-Transfer and Pressure Distribution on Six Blunt Noses at a Mach Number of 2. NACA RM L57C18, April 1957

Eggers, A. J., Jr.: Re-entry and Recovery of a High-Drag Satellite Initially in Circular Orbit about the Earth. N-59811, February 1957

Penland, J. A.: Aerodynamic Characteristics of a Circular Cylinder at Mach Number 6.86 and Angles of Attack up to 90 Degrees. NACA TN 3861 (supersedes RM L54A14), January 1957

Love, E. S.: Base Pressure at Supersonic Speeds on Two-Dimensional Airfoils and on Bodies of Revolution with and without Fins having Turbulent Boundary Layers. NACA TN 3819, January 1957

Kaplan, C.: Flow of a Compressible Fluid Past a Sphere. NACA TN 762

Seiff, A.; Sommer, S. C.; and Canning, T. N.: Some Experiments at High Supersonic Speeds on the Aerodynamic and Boundary-Layer Transition Characteristics of High Drag Bodies of Revolution. NACA RM A56I05, 1957

Tobak, M. and Wehrend, W. R.: Stability Derivatives of Cones at Supersonic Speeds. NACA TN 3788, September 1956

Leiss, A.: Free-Flight Investigation of Effects of Simulated Sonic Turbojet Exhaust on the Drag of Twin-Jet Boattail Bodies at Transonic Speeds. NACA RM L56D30, N62-63881, July 1956

Bromm, A. F., Jr. and Goodwin, J. M.: Investigation at Supersonic Speeds of the Variation with Reynolds Number and Mach Number of the Total, Base and Skin-Friction Drag of Seven Boattail Bodies of Revolution Designed for Minimum Wave Drag. NACA TN 3708 (supersedes RM L53I29b), June 1956

Jorgensen, L. H. and Perkins, E. W.: Investigation of Some Wake Vortex Characteristics of an Inclined Ogive-Cylinder Body at Mach Number 1.98. NACA, August 1955

Reller, J. O., Jr. and Hamaker, F. M.: An Experimental Investigation of Base Pressure Characteristics of Non-lifting Bodies of Revolution at Mach Numbers from 2.73 to 4.98. NACA TN 3393, March 1955

Chapman, D. R.: An Analysis of the Corridor and Guidance Requirements for Supercircular Entry into Planetary Atmospheres. NASA TR R-55

Stine, H. A. and Wanlass, K.: Theoretical and Experimental Investigation of Aerodynamic-Heating and Isothermal Heat-Transfer Parameters on a Hemispherical Nose with Laminar Boundary Layer at Supersonic Mach Numbers. NACA TN 3344, December 1954

Sacks, A. H.: Aerodynamic Forces, Moments, and Stability Derivatives for Slender Wings and Bodies of General Cross Section. NACA TN 3283, 1954

Messing, W. E.; Rabb, L.; and Disher, J. H.: Preliminary Drag and Heat Transfer Data Obtained from Air-Launched Cone-Cylinder Test Vehicle over Mach Number Range from 1.5 to 5.18. NACA RM E53I04, November 1953

Grisby, C. E. and Ogburn, E. L.: Investigation of Reynolds Number Effects for a Series of Cone-Cylinder Bodies at Mach Numbers 1.62, 1.93 and 2.41. NACA RM L53H22, October 1953

Hearth, D. P. and Gordon, G. C.: Investigation at Supersonic Speeds of an Inlet Employing Conical Flow Separation from a Probe Ahead of a Blunt Body. NACA RB E52K18, 19 January 1953

Robins, A. W.: Preliminary Investigation of the Effects of Several Seeker-Nose Configurations on the Longitudinal Characteristics of a Canard-Type Missile at a Mach Number of 1.60. NACA RM L53I18, 1953

Equations, Tables and Charts for Compressible Flow. NACA Report 1135, 1953

Pilano, R. O.: Preliminary Free-Flight Investigation of the Zero-Lift Drag Penalties of Several Missile Nose Shapes for Infrared Seeking Devices. NACA RM L52F23, 9 December 1952

Ehret, D. M.: Accuracy of Approximate Methods for Predicting Pressures or Pointed Non-lifting Bodies of Revolution in Supersonic Flow. NACA TN 2764, August 1952

Dennis, D. H. and Cunningham, B. E.: Forces and Moments on Pointed and Blunt-Nosed Bodies of Revolution at Mach Numbers from 2.75 to 5.00. NACA RM A52F22, August 1952

Eggers, A. J., Jr. and Savin, R. C.: Approximate Methods for Calculating the Flow about Non-lifting Bodies of Revolution at High Supersonic Airspeeds. NACA TN 2579, December 1951

Ferri, A.: Supersonic Flow around Circular Cones at Angles of Attack. NACA Report No. 1045, 1951

Ferri, A.: The Method of Characteristics for the Determination of Supersonic Flow over Bodies of Revolution at Small Angles of Attack. NACA Report 1044, 1951

Hart, R. G.: Flight Investigation of the Drag of Round-Nosed Bodies of Revolution at Mach Numbers from 0.6 to 1.5 using Rocket-Propelled Test Vehicles. NACA RM L51E25, 1951

Herberle, J. W.; Wood, G. P. and Gooderum, P. B.: Data on Shape and Location of Detached Shock Waves on Cones and Spheres. NACA TN 2000, January 1950

Ferri, A.: Supersonic Flow around Circular Cones at Angles of Attack. NACA TN 2236, 1950

Chapman, D. R.: An Analysis of Base Pressure at Supersonic Speeds, and Comparison with Experiment. NACA TN 2137, 1950

Alexander, S. R.: Flight Investigation at Low Supersonic Speeds to Determine the Effectiveness of Cones and a Wedge in Reducing the Drag of Round-Nose Bodies and Airfoils. NACA RM L8L07a, March 1949

Ferri, A.: The Methods of Characteristics for the Determination of Supersonic Flow-Over Bodies of Revolution at Small Angles of Attack. NACA TN 1809, 1949

Mirels, H.: Theoretical Wave Drag and Lift of Thin Supersonic Ring Airfoils. NACA TN 1768, 1948

II - WRIGHT FIELD DOCUMENTS

Nebiker, F. R.: Aerodynamic Deployable Decelerator Performance Evaluation Program. AFFDL-TR-65-27, May 1965

Heinrich, H. G.; Hess, R. S.; and Stumbris, G.: Drag Characteristics of Plates, Cones and Spheres in the Wake of a Cylindrical Body at Transonic Speeds. RTD-TDR-63-4023, AD-457055, X65-13630, January 1965

Giemza, C. J. and Hunter, W. B.: Structural Heat Shield for Re-entry and Hypersonic Lift Vehicles/High Temperature Composite Structure. ML-TDR-64-267, Part 1, Vol I, AD-459376, X65-14059, January 1965

Heinrich, H. G. and Hess, R. S.: Drag Characteristics of Several Two-Body Systems at Transonic and Supersonic Speeds. RTD-TDR-63-4226, December 1964

Heinrich, H. G.; Hess, R. S.; and Stumbris, G.: Drag Coefficients of Several Bodies of Revolution at Transonic and Supersonic Velocity. ASD-TDR-63-663, AD-608303, N65-12138, September 1964

Haak, E. L. and Niccum, R. J.: Pressure Distribution Measurements of Conventional Ribbon Parachutes in Supersonic Flow. ASD-TDR-63-662, AD-608305, September 1964

Brockman, H.: Development of Nomex Mesh Materials. ML-TDR-64-208, AD-607890, September 1964

Myers, E. C.: Proceedings, Symposium on Parachute Technology and Evaluation. Vol II, FTC-TDR-64-12

Myers, E. C.: Proceedings, Symposium on Parachute Technology and Evaluation. Vol I, FTC-TDR-64-12, September 1964

RTC-TDR-64-12: Symposium on Parachute Technology and Evaluation - Proceedings. Edited by Earl C. Meyers, Calif., Air Force Flight Test Center, Air Force Systems Command, Edwards Air Force Base, 12 September 1964

Nickel, W. E. and Sims, L. W.: Study an Exploratory Free-Flight Investigation of Deployable Aerodynamic Decelerations Operating at High Altitudes and at High Mach Numbers. FDL-TDR-64-35, Vol I, July 1964

Petersen, P. E.: Study of Parachute Performance and Design Parameters for High Dynamic Pressure Operation. FDL-TDR-64-66, May 1964

Chernowitz, G. and DeWeese, J. H.: Performance of and Design Criteria for Deployable Aerodynamic Decelerators. (Second major revision of the USAF Parachute Handbook), ASD-TR-61-579, AD-429971, December 1963

Kaman Aircraft Corporation: Investigation of Stored Energy Rotors for Recovery. ASD-TDR-63-745, December 1963

Dolbin, B. J.; Newell, F. D.; and Schelhorn, A. E.: Development and Flight Calibration of a Variable-Drag Device on a Variable Stability T-33 Airplane. ASD-TDR-62-910, AD-425705, N64-13627, November 1963

ASD-TDR-63-453: Flight Vehicle Structural Design Criteria, Recovery Phase. September 1963

Freeston, W. D., Jr. and Cardella, J. W.: New and Improved Materials for Expandable Structures, Phase 1 - Weaving of Stranded Metal Yarns. ASD-TDR-62-542, September 1963

Epting, J. L., Jr.: Silicone Finished Glass Fiber Tapes and Webbings for Decelerators. ASD-TDR-63-808, AD-422524, September 1963

Foerster, A. F.; et al: Analytical and Experimental Investigation of Coated Metal Fabric Expandable Structures for Aerospace Applications. ASD-TDR-63-542, August 1963

ASD-TDR-63-329: Proceedings of Retardation and Recovery Symposium. Ohio Flight Accessories Lab., Aeronautical Systems Division, Air Force Systems Command, May 1963

Hartofilis, S. A.: Pressure Measurement at Mach 19 for a Winged Re-entry Configuration: Part of an Investigation of Hypersonic Flow Separation and Control Characteristics. ASD-TDR-63-319, May 1963

Cosken, R. J. and Chu, C. C.: Investigation of the High Speed Impact Behavior of Fibrous Materials, Part III, Impact Characteristics of Parachute Materials. WADD-TR-60-511, May 1963

Proceedings of Retardation and Recovery Symposium. (Dayton, November 13-14, 1962 Final Report), ASD-TDR-63-329, AD-408772, May 1963

ASD-TR-63-69: Design and Instrumentation Testing for a Hypersonic Parachute Free-Flight Test Capability. May 1963

Gran, W. M.; Musil, J. L.; and Fratamico, J. A.: Design and Instrumentation Testing for a Hypersonic Parachute Free-Flight Test Capability (Phases II and III). ASD-TR-63-64, May 1963

Neff, R. J.: Development of HT-1 Materials for Personnel Parachute Packs and Harnesses. ASD-TDR-63-312, April 1963

Neff, R. J.: Development of HT-1 Materials for Decelerators. ASD-TDR-63-248, March 1963

Sims, L. W.: Analytical and Experimental Investigation of Supersonic Parachute Phenomena. ASD-TDR-62-844, Chicago, Ill., Cook Technological Center, February 1963 (CONFIDENTIAL)

ASD-TDR-62-542: New and Improved Materials for Expandable Structures. Part IV - Phase III, Re-entry Coatings, October 1963; Part V - Phase IV, High Temperature Protective Study, February 1963

Walcott, W. B.: Study of Parachute Scale Effects. ASD-TDR-62-1023, N63-13009, January 1963

Hung, F. C.: Flight Vehicle Structural Design Criteria, Recovery Phase. ASD-TDR-63-453, AD-423012

Alexander, W. C.: Investigation to Determine the Feasibility of Using Inflatable Balloon-Type Drag Devices for Recovery Applications in the Transonic, Supersonic and Hypersonic Flight Regime. Part II, Mach 4 to Mach 10 Feasibility Investigation, ASD-TDR-62-702, December 1962

Abbott, D. E.; Holt, M.; and Nielsen, J. N.: Investigation of Hypersonic Flow Separation and its Effects on Aerodynamic Control Characteristics, ASD-TDR-62-963, November 1962

Ligon, W. M.: Research and Development on High Altitude, High Speed Crew Escape Systems Testing Concept. Vol I - Subsystem and Simulation Investigation, ASD-TDR-62-471, Vol I, Dallas, Tex., Vought Astronautics, November 1962

Huang, R. S.: Research and Development on High Altitude, High Speed Crew Escape Systems Testing Concepts. Vol II - Test Vehicle Investigation, ASD-TDR-62-471, Vol II, Dallas, Tex., Vought Astronautics, November 1962

Meyer, R. A.: A Study of the Load Bearing Behavior and Other Characteristics Influencing Vibration or Flutter in Decelerator Ribbons. ASD-TDR-62-988, November 1962

Aebischer, A. C.: Investigation to Determine the Feasibility of Using Inflatable Balloon-Type Drag Devices for Recovery Applications in the Transonic, Supersonic and Hypersonic Flight Regimes - Part 1, Functional and Performance Demonstration. ASD-TDR-62-702, September 1962

Heinrich, H. G. and Haak, E. L.: Stability and Drag of Parachutes with Varying Effective Porosity. ASD-TDR-62-100, September 1962

Lubinsky, T. P.: Track Tests of Canopy Escape Capsule. ASD-TDR-62-404, August 1962

Epstein, A. and Hamilton, A. F.: Study of Design Parameters for Structure Subject to Aerodynamic Heating. ASD-TR-61-95, August 1962

Cobb, E. S., Jr.: High Strength, Glass Fiber Webbings, Tapes and Ribbons for High Temperature Pressure Packaged Decelerators. ASD-TDR-62-518, July 1962

Dawn, F. S. and Ross, J. H.: Investigation of Polybenzimidazole Fibers at High Temperature. ASD-TDR-62-435, July 1962

Chew, F. E.; Oling, L.; and Clutz, H. A.: Investigation of Stabilization and Control Systems for Application to Aerospace Vehicle Escape Capsules. ASD-TDR-62-243, June 1962

Investigation of Landing Point Control of Re-entry Vehicles Utilizing Variable Area Aerodynamic Decelerators Incorporating Lift. ASD-TDR-62-287, June 1962

Berndt, R. J.: Supersonic Parachute Research. ASD-TDR-62-236, May 1962

Heinrich, H. G. and Haak, E. L.: Stability and Drag of Parachutes with Varying Effective Porosity. ASD-TDR-62-100, April 1962

Knacke, T. W. and Dimmick, D. T.: Design Analysis of Final Recovery Parachutes B-70 Encapsulated Seat and the USD-5 Drone. ASD-TDR-62-75, April 1962

Tyndall, R. R.: Analytical and Empirical Investigation of a Completely Flexible Rotor Blade. ASD Technical Memorandum ASRMPT-TM-628, March 1962

ASD-TR-61-100: Feasibility Study of Hypersonic Parachute Free Flight Test Capability - Phase I. Chicago, Ill., Cook Research Labs., Phase I, March 1962

Johnson, D. E.; Newton, E. H.; Benton, E. R.; Ashman, L. E. and Knapton, D. A.: Metal Filaments for High-Temperature Fabrics. ASD-TR-62-180, February 1962

Coskren, R. J. and Chu, C. C.: Investigation of the High Speed Impact Behavior of Fibrous Materials, Part II - Impact Characteristics of Parachute Materials. ASD-TR-60-511, February 1962

The Problem of Descent to the Surface of the Earth and Planets. Air Force Systems Command, Wright-Patterson AFB, Foreign Technology Division, N63-18435, February 1962

Glasser, P. E. and Merra, S.: Thermal Radiation Effects on Decelerator Materials. ASD-TDR-62-185, February 1962

ASD-TR-62-180: Metal Filament for High Temperature Fabrics. February 1962

Dawn, F. S. and Ross, J. H.: Investigation of the Thermal Behavior of Graphite and Carbon-Based Fibrous Materials. ASD-TDR-62-782

Heinrich, H. G. and Haak, E. L.: The Drag of Cones, Plates and Hemispheres in the Wake of a Forebody in Subsonic Flow. ASD-TR-61-587, December 1961

Milhoan, F. M.; Vorachek, J. J.; and D'Allura, J.: Investigation of Escape Capsule Systems for Multi-Place Aircraft. Parts I and II, WADD-TR-57-329, December 1961

Study of a Drag Brake Satellite Recovery System. AVCO-Everett Research Lab., ASD-TR-61-348, November 1961

Broderick, M. A. and Turner, R. D.: Design Criteria and Techniques for Deployment and Inflation of Aerodynamic Drag Devices. ASD-TR-61-188, November 1961

Wells, J. A.: Design Study of the Capsule Escape Vehicle Parachute Recovery System Hardware. ASD-TR-61-178, Vol I, October 1961

Coplan, M. J. and Freeston, W. D., Jr.: High Speed Flow and Aerodynamic Heating Behavior of Porous Fibrous Structures. N-106-882, October 1961

Nielsen, J. N.; Burnell, J. A.; and Sacks, A. H.: Investigation of Flexible Rotor Systems, Results of Phases I and II. ASD-TR-61-660 September 1961

Petersen, P. E.: Study of Parachute Performance at Low Supersonic Deployment Speeds: Effects of Changing Scale and Clustering. ASD-TR-61-186, July 1961

Champney, W. B.; Athans, J. B.; and Mayerson, C. D.: A Study of Hypersonic Aerodynamic Drag Devices - Final Technical Report. WADC-TR-59-324, Part II, Buffalo, N. Y., Cornell Aeronautical Labs., Inc., June 1961

Heinrich, H. G. and Haak, E. L.: The Drag of Cones, Plates and Hemispheres in the Wake of a Forebody in Subsonic Flow. ASD-TR-61-587, December 1961

Milhoan, F. M.; Vorachek, J. J.; and D'Allura, J.: Investigation of Escape Capsule Systems for Multi-Place Aircraft. Parts I and II. WADD-TR-57-329, December 1961

Study of a Drag Brake Satellite Recovery System. AVCO-Everett Research Lab., ASD-TR-61-348, November 1961

Broderick, M. A. and Turner, R. D.: Design Criteria and Techniques for Deployment and Inflation of Aerodynamic Drag Devices. ASD-TR-61-188, November 1961

Wells, J. A.: Design Study of the Capsule Escape Vehicle Parachute Recovery System Hardware. ASD-TR-61-178, Vol I, October 1961

Coplan, M. J. and Freeston, W. D., Jr.: High Speed Flow and Aerodynamic Heating Behavior of Porous Fibrous Structures. N-106-882, October 1961

Nielsen, J. N.; Burnell, J. A.; and Sacks, A. H.: Investigation of Flexible Rotor Systems, Results of Phases I and II. ASD-TR-61-660 September 1961

Petersen, P. E.: Study of Parachute Performance at Low Supersonic Deployment Speeds: Effects of Changing Scale and Clustering. ASD-TR-61-186, July 1961

Champney, W. B.; Athans, J. B.; and Mayerson, C. D.: A Study of Hypersonic Aerodynamic Drag Devices - Final Technical Report. WADC-TR-59-324, Part II, Buffalo, N. Y., Cornell Aeronautical Labs., Inc., June 1961

Engstrom, B. A.: Performance of Trailing Aerodynamic Decelerators at High Dynamic Pressures. Phase IV, WADD-TR-58-284, Part IV, June 1961

Gross, R. S. and Riffle, A. B.: Performance Evluation of the Vortex Ring Parachute Canopy. ASD-TR-61-410, June 1961

Nebiker, F. R. and Karaffa, N. T.: Feasibility Study of an Inflatable Type Stabilization and Deceleration System for High-Altitude and High-Speed Recovery. ASD-TR-60-182, August 1961

Abbott, N. J.: Some Effects of Compression and Heat on Decelerator Materials. WADD-TR-60-588, June 1961

Engstrom, B. A. and Lang, R. P.: Performance of Trailing Aerodynamic Decelerators at High Dynamic Pressures. Part 4, WADD-TR-58-284, Junc 1961

Petersen, P. E.: Study of Parachute Performance at Low Supersonic Deployment Speeds; Effects of Changing Scale and Clustering. ASD-TR-61-186, May 1961

McGrath, J. C.: Fibrous Materials for Decelerators and Structures. ASD-TN-61-59, May 1961

Engstrom, B. A.: Performance of Trailing Aerodynamic Decelerators at High Dynamic Pressures. Phases V and VI, WADD TR-58-284, Part V, May 1961

Ruprecht, F. A. and Prima, C. D.: A Study of Design and Materials for Low Cost Aerial Delivery Parachutes. Technical Report II, Cook Research Labs., Contract AF33(616)-6009, Parachute Section, Crew Equipment Branch, ASD, April 1961

Rockhold, V. G.; Onspaugh, C. M.; and March, W. L.: Study to Determine Aerodynamic Characteristics on Hypersonic Re-entry Configurations. Part I - Experimental Phase, Vol 2 - Experimental Report - Mach Numbers 5, WADD-TR-61-56, March 1961, (CONFIDENTIAL)

Engholm, G.; Lis, S. J.; and Bambenek, R. A.: Instantaneous Local Temperatures of Aerodynamic Decelerators. Part II Thermal Properties, WADD-TR-60-670, February 1961

Cheatham, R. G.; Shank, M. E.; and Backer, S.: Textile Fibers in High Temperature Applications. TR-60-327, February 1961

Engholm, G., et al.: Instantaneous Local Temperatures of Aerodynamic Decelerators. Part I, WADD-TR-60-670, February 1961

Study of a Drag Brake Satellite Recovery System. Results of Phase I, WADD-TR-60-775, January 1961, AD254673

Engholm, G.; Baschiere, R. J.; and Bambenek, R. A.: Instantaneous Local Temperatures of Aerodynamic Decelerators. Part I Methods of Predicting, WADD-TR-60-670, December 1960

Little, C. O., Jr.: Thermal and Gamma Radiation Behavior of a New High Temperature Organic Fiber. WADD-TN-60-299, December 1960

Engstrom, B. A.: Performance of Trailing Aerodynamic Decelerators at High Dynamic Pressures. Phase III, WADD-TR-58-284, Part III, December 1960

Heinrich, H. G.: Some Research Efforts Related to Problems of Aerodynamic Deceleration. WADD-TN-276, November 1960

Coats, J. D.: Static and Dynamic Testing of Conical Trailing Decelerators for the Pershing Re-entry Vehicle. AEDC-TD-60-188, October 1960

Serbin, J. and Becker, H.: The Design and Evaluation of Heat Stabilized Tapes and Webs. WADD-TR-60-252, AD249409, October 1960

Walcok, W. S.: Deterioration of Textile Materials by Ultraviolet Light. WADD-TR-60-510, AD249237, October 1960

Mileaf, H. (ed): Handbook of Fibrous Materials. AD249782, WADD-TR-60-584, October 1960

Mileaf, H.: Handbook, Part 1 of Fibrous Materials. WADD-TR-60-584, October 1960

Chu, C. C.; et al.: Investigation of the High Speed Impact Behavior of Fibrous Materials. Part I, Design and Apparatus, WADD-TR-60-511, AD-247493, September 1960

Jailer, R. W.; Freilich, G.; and Norden, M. L.: Analysis of Heavy Duty Parachute Reliability. American Power Jet Co., WADD-TR-60-200, AD-246490, June 1960

Copland, M. J.; Powers, D. H., Jr.; Barish, G.; and Valko, E. I.: Possible Application of Organic Fibers in High Temperature Environment. WADD-TR-60-9, June 1960

Lambertson, W. A.; et al.: Continuous Filament Ceramic Fibers. WADD-TR-60-244, June 1960

Brandt, H. H. and Linden, L.: Effects of Picks per Inch and Finishing Procedures on the Properties of 1.1-ounce Nylon Ripstop Parachute Fabric. Textile Series Report No. 113, Quartermaster Research and Engineering Command, AD-241246, June 1960

Hankey, W. L.; Neumann, R. D.; and Flinn, E. H.: Design Procedures for Computing Aerodynamic Heating at Hypersonic Speeds. WADC-TR-59-610, June 1960

Champney, W. B. and Engel, B.: A Study of Hypersonic Aerodynamic Drag Devices. Interim Technical Report (unclassified title). WADC TR-59-324, April 1960 (CONFIDENTIAL)

Seshadri, C. V.; et al.: Air Flow Characteristics of Parachute Fibers at Simulated High Altitudes. WADC-TR-59-374, March 1960

Williams, R. B. and Benjamin, R. J.: Analysis of Webbing Impact Data and Determination of Optimum Instrumentation to be Used in Conjunction with the Impacting of Webbing. WADC-TR-59-694, Impact Behavior of Textile Materials, Final Report, March 1960

Engstrom, B. A.: Performance of Trailing Aerodynamic Decelerators at High Dynamic Pressures. Phase II, WADD-TR-58-284, Part II, March 1960

Schoeck, P. A.; et al.: Experimental Studies for Determining Heat Transfer on the Ribbons of FIST-Type Parachutes. WADC-TN-59-345, February 1960

Hayes, J. E.; Rose, P. H.; and VanderVelde, W. E.: Analytical Study of a Drag Brake Control System for Hypersonic Vehicles. WADD-TR-60-267, January 1960

Engstrom, B. A.: Performance of Trailing Aerodynamic Decelerators at High Dynamic Pressures. Part II - Phase II Test Results, WADD-TR-58-284, January 1960

Heinrich, H. G.: Analytical and Experimental Consideration of the Velocity Distribution in the Wake of a Body of Revolution. WADD Technical Report 60-257, December 1959

Controlled Burn-Through of Re-entry Drag Chutes. Submitted to WADC on 7 December 1959 by Materials Technology, Inc.

Heinrich, H. G.; and Scipio, L. A.: Performance Characteristics of Extended Skirt Parachute. WADC-TR-59-562, October 1959

Marshall, F. J.: Optimum Re-entry into the Earth's Atmosphere by use of a Variable Control Force. The University of Chicago Institute for System Research, WADC-TR-59-515, October 1959

Cornish, R. H.; et al.: Mass Transfer Cooling of Parachute Materials. WADC-TR-58-684, AD229441, September 1959

Ruprecht, F. A.; et al.: A Study of Design and Materials for Development of Low Cost Aerial Delivery Parachutes. WADC-TR-59-385, AD237460, September 1959

Johnson, D. E.; et al.: Candidate Materials for High Temperature Fabrics. WADC-TR-59-155, AD232975, September 1959

Tyndall, R. R.: Preliminary Qualitative Evaluation of a Stored Energy Recovery System. WADC-TN-59-267, July 1959

Newquist, E. A.; Cassidy, M. D.; Lindblom, C. W.; and Sullivan, P. J.: Development of an Ejectable Nose Escape Capsule. WADC-TR-59-493, June 1959

Heinrich, H. G. and Ibrahim, S. K.: Application of the Water Surface Wave Analogy in Visualizing the Wave Pattern of a Number of Primary and Secondary Body Combinations in Supersonic Flow. WADC-TR-59-457, September 1959

Chu, C. C.; et al.: Development of Improved Nylon Webbings. WADC-TR-58-509, AD211911, April 1959

Heinrich, H. G.: Pressure Distribution in Transonic Flow of Ribbon and Guide Surface Parachutes. WADC-TN-59-32, February 1959

Little, C. O., Jr.: Amount of Deterioration Present in Parachutes Manufactured over 15 Years Ago, WADC-TN-59-30, February 1959

Ciffren, A. and Swenson, W. A.: Study and Development of Parachutes and Systems for In-Flight Landing Deceleration of Aircraft. Part II, Development and Test Evaluation of the Ring Slot Parachute, WADC-TR-57-566, AD155707, January 1959

Drag Parachute Retracting System. WADC-TR-57-57, January 1959

Engstrom, B. A. and Meyer, R. A.: Performance of Trailing Aerodynamic Decelerators at High Dynamic Pressures. Part III - Wind Tunnel Testing of Rigid and Flexible Parachute Models, WADC-TR-58-284, 1959

Meyer, R. A.: Wind Tunnel Investigation of Conventional Types of Parachute Canopies in Supersonic Flow. WADC-TR-58-532 AD202856, December 1958

Landis, M. B. and Frame, F. W. III: Development of Coreless Type Brands for use in Personnel Parachute Suspension Lines. WADC-TR-58-410, December 1958

Meyer, R. A.: Wind Tunnel Investigation of Conventional Types of Parachute Canopies in Supersonic Flow. WADC-TR-58-532, Chicago, Ill., Cook Research Labs., December 1958

Gimalowski, E. A.: Development of a Final Stage Recovery System for a 10,000 Pound Weight. WADC-TR-59-109, December 1958

Wilder, S. H.: Model Parachute Test in Vertical Wind Tunnel at Wright Air Development Center. WADC-TR-58-279, AD204424, September 1958

Theoretical Parachute Investigations. Progress Reports, WADC Contract AF33(615)-3955, September 1958

Little, E. F.: An Evaluation of Fungicidal Treatments in Cotton Cargo Parachute Webbings Stored at College, Alaska. WADC-TR-56-384, Part II, AD-155857, August 1958

Eirich, F. R. and Saad, I.: Improvement of Thermal Stability of Textile Fibers. Progress Report No. 8, Annual Summary, Contract N140(132)5775B, Polytechnic Institute of Brooklyn for U.S. Navy Supply Research and Development Facility, AD213554, July 1957 - 30 June 1958

Engstrom, B. A.: Performance of Trailing-Aerodynamic Decelerators at High Dynamic Pressures. Part I, Development of Test Method and Test Equipment, WADD-TR-58-284, June 1958

Foote, J. R. and Giever, J. B.: Study of Parachute Opening. Part II, WADC TR-56-253, June 1958

Rosenlof, K. D.: Drag Coefficient of FIST Ribbon Parachutes - Reefed and Fully Inflated. AFFTC-TR-58-5, AD131459, May 1958

Chu, C. C.; et al.: Development of High Tenacity Heat Stable Dacron Parachute Items. WADC-TR-57-765, AD155511, May 1958

Klein, W. C., et al.: Research Program for the Development of a Design Procedure to Engineer Parachute Fabrics. WADC-TR-58-65, AD 155517, May 1958

Aickinger, G. E.: Symposium on Missile and Drone Recovery. WADC-TR-58-125, AD151099, March 1958

Krizik, J. G.; et al.: Design Data on Biaxial Forces Developed in Parachute Fabrics. WADC-TR-57-443, AD142208, December 1957

Ruoff, A. L.; et al.: Aerodynamic Heating of Parachutes. WADC-TR-57-157, AD142261, December 1957

Hartnett, J. P.; et al.: Values of the Emissivity and Absorptivity of Parachute Fabrics. WADC-TN-57-443, AD151072, December 1957

Klein, W. G.; et al.: Development of Design Data on the Mechanics of Air Flow through Parachute Fabrics. WADC-TR-56-576, AD131055, September 1957

Eckert, E. R. G.; et al.: Transient Temperatures of Parachutes during Descent. WADC-TN-57-320, August 1957

Eckert, E. R. G.; Hartnett, J. P.; and Turnocliff: Transient Temperatures of Parachutes during Descent and Generalized Trajectories for Free Falling Bodies of High Drag. WADC-TN-57-320

Ruoff, Sin, and Frank: Aerodynamic Heating of Parachutes. WADC-TR-57-157

Downing, J. R.; et al.: Recovery Systems for Missiles and Target Aircraft. Part III - High Subsonic and Transonic Trackborne Parachute Tests, WADC Technical Report 5853, Cook Research Lab., December 1956

Downing, J. R.; Harkins, H. V.; McClow, J. H., Jr.; and Petersen, P. E.: Recovery Systems for Missiles and Target Aircraft, High Subsonic and Transonic Track Borne Parachute Tests AF TR-5853, Part III, December 1956

United States Air Force Parachute Handbook. WADC-TR-55-265, AD118036, December 1956

Cates, D. M.: A Study of the Effects of Chemicals on the Properties of Parachute Fabrics. WADC-TR-55-340, Supplement 1, AD110524, November 1956

Cates, D. M.: A Study of the Effects of Chemicals on the Strengths of Nylon and Dacron Parachute Fabrics. WADC-TR-56-288, AD110558, November 1956

Bomb Stabilization by Parachute. WADC-TR-54-4, AD110584, November 1956

Foote, J. R. and Giever, J. B.: Study of Parachute Opening. Phase I, WADC-TR-56-253, September 1956

Pounder, E.: Parachute Inflation Process Wind-Tunnel Study. WADC-TR-56-391, AD97180, September 1956

Templeton, J. G.: A Study of the Effects of Chemicals on the Properties of Parachute Fabrics. WADC-TR-55-340, AD97243, September 1956

Coskrew, R. J. and Constantine, T. T.: Development of High Tenacity-Heat Stable Dacron Yarns. WADC-TR-55-297, AD97242, September 1956

Kaswell, E. R. and Coplan, M. J.: Development of Dacron Parachute Fabrics. WADC-TR-55-135, AD97241, September 1956

Ferri, A. and Pallone, A.: Note on the Flow on the Rear Part of Blunt Bodies in Hypersonic Flow. WADC-TN-56-294, July 1956

Wiant, H. W.; and Fredette, R. O: A Study of High Drag Configurations as First Stage Decelerators. WADC-TN-56-320, July 1956

Pounder, Edwin: Parachute Inflation Process Wind Tunnel Study. Part I, Infinite Mass Case, WADC-TN-56-326, AD97182, July 1956

Wiant, H. W. and Fredette, R. O.: A Study of High Drag Configurations as First Stage Decelerators. WADC-TN-56-320, July 1956

Thomson, G.; et al.: Research and Development of Abrasion Resistant Treatments for Dacron Webbings. WADC-TR-55-313, AD97103, July 1956

Miller, C. R.: A Study of Parachute Seam Design Criteria. Part II, Investigation of the Strength of Nylon Webbing Joints. WADC-TR-56-313, AD110406, June 1956

Thomson, G.; et al.: Research and Development of Abrasion Resistant Treatments for Nylon Webbings. WADC-TR-56-151, AD103961, June 1956

Coplan, M. J. and Block, M. G.: A Study of Parachute Seam Design Criteria. Part I, Investigation of the Strength of Nylon and Rayon Cloth Seams, WADC-TR-56-313, AD110407, June 1956

Neff, R. J.: The Development of Current Nylon Webbings Utilizing 840 Denier Yarns in Lieu of Now-Specified 210 Denier Yarns. WADC-TR-55-494, AD-102826, May 1956

Bickford, H. J.; et al.: The Development of High Strength Nylon Parachute Fabrics. WADC-TR-55-465, AD101948, May 1956

Sublette, R. A.: The Effect of Five Synthetic Lubricants on USAF Fabrics. WADC-TR-55-379, AD100696, May 1956

Bickford, H. J.; et al.: Development of Dacron Parachute Materials. WADC-TR-55-432, February 1956

McCarthy, J.: Handbook of Parachute Textile Materials and Properties. WADC-TR-55-264, AD89171, February 1956

McCrath, J. and Johnson, R. H.: The Effects of Gamma Radiation on Textile Materials. WADC-TR-56-15, AD92044, February 1956

Krzywoblocki, M. Z.: Aerodynamic Studies: The Forces Acting on an Air Vehicle, A Review of the Literature. WADC-TN-56-360

Lavrakas, V. and Katz, A.: The Effect of Surface Finish on Friction and Fusion of Parachute Cloth and Line. WADC-TR-54-323, Part 2, December 1955

Block, L. C.: Aerodynamic Heating of Parachute Ribbons. WADC-TR-54-572, November 1955

Lavrakas, V. and Katz, A.: The Effect of Surface Finishes on Friction and Fusion of Parachute Cloth and Line. WADC-TR-54-323, Part 1, AD91873, October 1955

Topping, A. D.; Marketos, J. D.; and Costakos, N. C.: A Study of Canopy Shapes and Stresses for Parachutes in Steady Descent. WADC-TR-55-294, Goodyear Aircraft Corporation, October 1955

Sweeney, J. W.: Evaluation of Antistatic Agents on Nylon Parachute Cloth. WADC-TR-54-513, September 1955

Lavrakas, V.: The Effect of Fabric Structure on the Frictional Fusion of Parachute Materials. WADC-TR-54-570, AD90859, August 1955

X-7A Supersonic Ramjet Test Vehicle Parachute Recovery System Section Two - Recovery Systems. WADC-TR-55-162, June 1955

Loptien, C. W. and Goodwin, M. D.: Wind Tunnel Tests of Full Scale G. P. 2000 and 3000 Pound Bombs Stabilized with Parachutes. WADC-TN-55-167, May 1955

Nurse, J. W., Jr., First Lt., USAF: A Study of the Effect of Temperature on Parachute Textile Materials. WADC-TR-54-117, 1955

Bickford, H. J.; Kuehl, D. K.; and Rusk, T. L.: Study of the Control of Permeability of Nylon Parachute Cloth at High and Low Differential Pressures. WADC-TR-54-468, March 1955

Brown, C. D.: A Study of the Laws of the Flow of Fluids through Fabrics. WADC-TR-54-199, January 1955

Graham, C. R.: 56-Ft Nominal Diameter Parachute with 10 Percent Extended Skirt. Technical Note FTL 54-17, August 1954

McGrath, J. C.: Symposium on Parachute Textiles. WADC-TR-54-49, AD-4978, July 1954

Kiker, J. W.: B-47 Approach Control Parachute. WADC-TN-54-18, July 1954

Muse, J. W., Jr.: A Study of the Effect of Temperature on Parachute Textile Materials. WADC-TR-54-117, AD55667, July 1954

Eckert, E. R. G.: Survey on Heat Transfer at High Speeds. WADC-TR-54-70, April 1954

Daniels, L. E., Capt. USAF: Effects of the Upstream Influence of a Shock Wave at Separated Boundary Layer. WADC-TR-54-31, January 1954

Berndt, R. J.: Force Distribution in a Parachute Harness. TMR WCLE-53-292, November 1953

Bickford, H. J.: Development of 0.9-Oz. Nylon Parachute Cloth. WADC-TR-53-351, AD26850, September 1953

Ewing, E. G.: A Study to Establish a Parachute Research and Development Program. Vol III, Summary and Analysis of Existing Knowledge, WADC-TR-53-78, AD110453, August 1953

Ewing, E. G.: A Study to Establish a Parachute Research and Development Program. Vol II, Summary and Analysis of Existing Knowledge, WADC-TR-53-78, AD110452, August 1953

A Study to Establish a Parachute Research and Development Program. Vol I, Bibliography and Collection of Extracts, WADC-TR-53-78, August 1953

Coplan, M. J. and Singer, E.: A Study of the Effect of Temperature on Textile Materials. WADC-TR-53-21, Part 2, July 1953

Coplan, M. J.: A Study of the Effect of Temperature on Textile Materials. WADC-TR 53-21, Part 1, May 1953

Yoshihara, H.: On the Flow Over a Cone-Cylinder Body at Mach Number One. WADC-TR-52-295, 1952

Erdmann, S.: Drag Coefficients for Cones and Spheres at Supersonic Speed. Central Air Documents Office, Wright-Patterson AFB, (Trans.) F-TS-4687-RE, February 1948

III - AEDC DOCUMENTS

Deitering, J. S. and Hilliard, E. E.: Wind Tunnel Investigation of Flexible Aerodynamic Decelerator Characteristics at Mach Numbers 1.5 to 6. AEDC-TR-65-110, June 1965

Dunkin, O. L. and Trimmer, L. L.: Hypersonic Aerodynamic Characteristics of Two Elliptic Half-Cones at M Equals 8 and Angles of Attack to 90 Degrees. 1 November 1963 - 1 October 1964, AEDC-TR-65-46, AD458753

Little, H. R.: Aerodynamic Force Tests of the Asset Re-entry Configuration in Tunnel F. X65-12386, January 1965

Jenke, L. M. and Lucas, E. J.: Supersonic Wind Tunnel Tests of a Parachute Test Sled. AEDC-TDR-64-203, AD448066, X65-10485, October 1964

Knapp, H.: Gemini Ballute Structural Test at Mach Numbers 0.55 and 1.92. AEDC-TDR-64-131, June 1964

Lowry, J. F.: Aerodynamic Characteristics of Various Types of Full Scale Parachutes at Mach Numbers from 1.8 to 3.0. AEDC-TDR-64-120, June 1964

Bell, D. R.: Pressure Measurements on the Rigid Model of a Balloon Decelerator in the Wake of a Simulated Missile Payload at Mach Numbers 1.5 to 6. AEDC-TDR-64-65, April 1964

Deitering, J. S.: Wind Tunnel Investigation of Flexible Parachute Model Characteristics at Mach Numbers 1.5 to 5. AEDC-TDR-63-263, January 1964

Clark, E. L.: Hypersonic Stability and Performance Characteristics of a Family of Modified Conoids (U). AEDC-TDR-64-20, January 1964 (CONFIDENTIAL)

Riddle, C. D. and White, W. E.: An Investigation of the Deployment Characteristics and Drag Effectiveness of the Gemini Personnel Decelerator at Subsonic and Supersonic Speeds. Phase II, AEDC-TDR-63-255, N64-12073, December 1963

Nichols, J. H. and Sibley, G. O.: An Investigation of the Deployment Characteristics and Drag Effectiveness of the Gemini Personnel Decelerator at Subsonic and Supersonic Speeds. AEDC-TDR-63-182, X63-14731, August 1963

Deitering, J. S.: Performance of Flexible Aerodynamic Decelerators at Mach Numbers from 1.5 to 6. AEDC-TDR-63-119, July 1963

Galigher, L. L.: Wind Tunnel Tests of the Kaman KRC-6M Rotochute at Supersonic Speeds. AEDC-TDR-63-128, X63-14209, July 1963

Deitering, J. S.: Performance of Flexible Parachute Models at Mach Numbers from 1.5 to 4. AEDC-TDR-62-234, December 1962

The Drag of Spheres in Rarefied Hypervelocity Flow. AEDC-TDR-62-205, December 1962

Deitering, J. S.: Investigation of Flexible Parachute Model Characteristics at Mach Numbers 1.5 to 6. AEDC-TDR-62-185, X63-13449, October 1962 (CONFIDENTIAL)

Brillhart, R. E., Jr. and Donaldson, J. C.: Force Tests of AVCO Re-entry Configurations at Mach Numbers 2, 5, and 8. AEDC-TDR-62-92, N62-12390, May 1962

Edenfield, E. E.: Force Tests of Two ASD Blunt Lifting Bodies at Mach Number 19 (U). AEDC-TDR-62-103, N-110,059, May 1962 (CONFIDENTIAL)

Kayser, L. D.: Pressure Distribution, Heat Transfer, and Drag Tests on the Goodyear Ballute at Mach 10. AEDC-TDR-62-39, March 1962

Griffith, B. J. and Wolmy, W.: Sharp and Blunt Cone Force Tests at M of Approximately 17 and Various Reynolds Numbers. AEDC-TDR-62-67, March 1962

Wolmy, W.: Blunt Cone Force Tests at M = 20. AEDC-TDR-62-43, March 1962

Jones, J. H. and Deitering, J. S.: Force and Pressure Tests on a Blunt Cone at Mach Number 8. AEDC-TDR-63-22, February 1962

Ward, L. K. and Urban, R. H.: Dynamic Stability Tests of Three Re-entry Configurations at Mach 8. AEDC-TDR-62-11, January 1962

Morgan, L. A.: Wind Tunnel Investigation of Flexible Parachute Models at Supersonic Speeds. AEDC-TN-61-176, January 1962

Jones, J. H. and Deitering, J. S.: Force and Pressure Tests on a Blunt Cone at Mach Numbers from 2 to 5. AEDC-TN-61-164, December 1961

Baer, A. L.: Pressure Distributions on a Hemisphere Cylinder at Supersonic and Hypersonic Mach Numbers. AEDC-TN-61-96, N63-82291, August 1961

Herron, R. D. and Binion, T. W., Jr.: Tests of the Kaman KRC-6M Rotochute at Transonic Speeds. AEDC-TN-61-60, N-96964, May 1961

Ward, L. K.: Dynamic Tests on the AVCO Deployable Aerodynamic Decelerator at Supersonic and Hypersonic Speeds. AEDC-TN-61-30, AD252765, N-98246, March 1961

Donaldson, J. C.: Static Stability Tests on the AVCO Deployable Aerodynamic Decelerator at Supersonic and Hypersonic Speeds. AEDC-TN-60-209, AD246-279, N-94179, November 1960

Coats, J. D.: Static and Dynamic Testing of Conical Trailing Decelerators for the Pershing Re-entry Vehicle. AEDC-TN-60-188, October 1960

Spring, D. J.: An Investigation of the Static Stability and Axial-Force Characteristics of the AVCO Satellite Drag Brake System at Transonic Speeds. AEDC-TN-60-139, AD240367, July 1960

Palko, R. L.: Aerodynamic Heating Tests at Mach Number 5 of Nylon Parachute Material Protected with Various Subliming Compounds. AEDC-TN-59-41, AD214595, May 1959

IV - OTHER MILITARY DOCUMENTS

Gazley, C., Jr.: Deceleration and Mass Change of an Ablating Body during High-Velocity Motion in the Atmosphere. Contract AF-49/638/-700, AD-610287, N65-21100, January 1965

Persh, J.: Advanced Re-entry Programs. Vol III-Summary, AD-355931, X65-13792, December 1964 (SECRET)

Persh, J.: Advanced Re-entry Programs. Vol II-Materials and Systems Studies, AF-04/694/-486, X65-13791, December 1964 (SECRET)

Braun, W. F.: Growth of the Turbulent Inner Wake behind Large Spheres at Supersonic Velocities. BRL-MR-1597, AD-453850, N65-15557, September 1964

Moulin, L.: Optimization of Recovery Trajectories for Space Vehicles, Final Scientific Report. AFOSR-64-2481, AD-609573, N65-19305, September 1964

Reid, W. P.: Stability of a Towed Object. Mathematics Report M-52, NOLTR-64-116, AD-447154, N64-30595, October 1964

Zarin, N. A.: Wind Tunnel Tests of Rectangular Finned Variable Gap Tangent Ogive-Cylinder Model at Mach Numbers 1.75 to 4.50. BRL-Memo-1583, AD-451304, N65-11438, August 1964

Moulin, L.: A Possible Compromise between Rocket and Atmospheric Braking, VKI-TN-17: AD-602391, NS4-25796, June 1964

Caldwell, D. M.: Recovery of Lunar Vehicles - Geometric Constraints on Trajectories. FTC-TDR-63-39, February 1964

Gordon, H. C. and Hattendorf, G. A.: Flight Qualification of Ribless Guide Surface Drag Parachute to Produce Low Lift to Drag Ratios. FTC-TDR-63-42, AD-429956, X64-12660, February 1964

Preston, C. R., Jr.: Space Rendezvous, Rescue and Recovery, Comp. (An abstract compilation. A report bibliography), N-110-911, AD-410085, August 1963

Jenkins, B. Z.: Real Gas Flow Field Properties around Blunt Cones. Vol I, Army Missile Command RF-TR-63-18, August 1963

Spring, D. J.: The Static Stability and Drag of Three Blunt-Cone Re-entry Bodies at Mach Numbers 15 and 18 (U). AMC-RF-TR-63-17, July 1963 (CONFIDENTIAL).

Persh, J.: Advanced Re-entry Programs. Vol I, Semi-annual report, AD-337406, X65-10872, July 1963

Lehn, J. R.: Anti-submarine Warfare Laboratory Research and Development Program for Airborne Towed Vehicles. AD-296131, NADC-AW-6229, X65-12494, January 1963

Reiss, M.: Measuring the Coefficient of Drag of an Accelerometer - Instrumented Sphere in a Shock Tube. NOLTR-62-162, N62-17007, August 1962

Ehni, F. P.; and Haldeman, W. F.: Study of Soft Recovery from Two-stage Vehicles. Part II: Vertical Descent Trajectories Including Aerodynamic Heating, N62-13823, May 1962

Freed, A.: Newtonian Drag Coefficients and Weights for Blunted Cone Spheres at Small Angles of Attack. MIT, Lincoln Lab., AFESD TDR 62-81 (Report No. 220-5), March 1962

Schwiderski, E. W.: Singularities in Supersonic Flows past Bodies of Revolution. N62-11837, February 1962

Schurr, G. G.: Study of Soft Recovery from Two-Stage Vehicles. AFOSR-DRA-62-2 N62-11959, January 1962

NavWeps Report 1488 (Vol 3): Handbook of Supersonic Aerodynamics. Section 8, Bodies of Revolution, October 1961

Faucher, G. A.; Procunier, R. W.; and Stark, C. N.: Flight Information and Experimental Results of Inflatable Falling Sphere System for Measuring Upper Air Density. USAF, Geophysics Research Directorate, GRD Research Notes No. 63, AFCRL 685, AD-265172, August 1961

Hayes, J. E.; and Vander Velde, W. E.: A Satellite Landing Control System Utilizing Drag Modulation. AD-603134, N64-85802, August 1961

Bixler, D. N.; and Gates, D. F.: Force and Moment Measurements of Models of the ARGMA Configuration in the NOL 4-In. Hypersonic Shock Tunnel No. 3. NOLTR 61-96, N-106-467, August 1961

Knacke, T. W.; Paulson, K. R.; and Schurr, G. G.: Study of Soft Recovery. Technical Report, AFOSR-104, N62-13153, March 1961

Haak, E. L.; Heinrich, H. G.; Ibrahim, S. K.; Niccum, R. J.; and Riabokin, T.: Theoretical Parachute Investigations Progress Report. AD-605143, N65-80441, 1961

Masson, D. J.; Morris, D. N.; and Bloxsom, D. E.: Measurements of Sphere Drag from Hypersonic Continuum to Free-Molecule Flow. USAF, Project Rand Research Memorandum TM-2678, The Rand Corporation, 3 November 1960

Berger, S. A.: Hypersonic Flow over Cones. AFOSR TN 60-1214, September 1960

Downing, Dr. J. R.; Hawkins, Dr. H. V.; McClow, P. W., Jr.; and Petersen, P. E.: Recovery Systems for Missiles and Target Aircraft. AF Technical Report 5853

Trajectory Study of Parachute Test Vehicles. AD-243876, AFFTC TR 60-37, N-93096, July 1960

Beeding, E. L., Jr.: Daisy Decelerator Tests. Run number 520-707, N64-81247, July 1960

Sims, J. L.: Supersonic Flow around Right Circular Cones - Tables for Zero Angle of Attack. ABMA Report DA-TR-11-60

Sims, J. L.: Supersonic Flow around Right Circular Cones - Tables for Small Angle of Attack. ABMA Report DA-TR-19-60, April 1960

Musil, J. L.: Requirements and Considerations for Testing Hypersonic Retardation Devices for Re-entry Vehicle Recovery. AFFTC TR 59-4, March 1959

Freeman, H. F.; and Rosenberg, C.: High Altitude and High Airspeed Tests of Standard Parachute Canopies. AFFTC-TR-58-32, AD-152286, October 1958

Kahl, G. D.: Supersonic Drag and Base Pressure of a 70-Degree Cone Cylinder. BRL Memo Report 1178, N-68696, November 1958

Aerodynamic Heating of Parachutes. SN-52823

Recovery Systems for Missiles and Target Aircraft. SN-45004

Felix, A. R.: Force Tests of a Related Family of Twenty Nose Cones for a Range of Mach Numbers from 0.47 to 1.93. ABMA Report DA-TN-42-58, July 1958

Marks, A. S.: Normal Force, Pitching Moment, and Center of Pressure of Several Spherically Blunted Cones at Mach Numbers of 1.50, 2.10 and 4.04. US AOMC-ARGMA-OML Report 6R8F, April 1958

Katz, J. R.: Pressure and Wave Drag Coefficients for Hemispheres, Hemisphere-Cones, and Hemisphere-Ogives. Naval Ordnance Test Station, NavOrd Report 5849, March 1958

Lehnert, R.; and Schermerhorn, V. L.: Wake Investigation on Sharp and Blunt Nose Cones at Supersonic Speeds. NavOrd Report 5668, U.S. Naval Ordnance Lab., January 1958

Re-entry Studies. Vol 1, Army Ballistic Missile Agency, X63-82211, November 1958.

Recovery Systems for Missiles and Target Aircraft. AF Technical Report 5853, Part I, March 1954, Part III, December 1956

May, A.: Supersonic Drag of Spheres at Low Reynolds Numbersin Free Flight. NavOrd Report 4392, Aeroballistic Research Report 356, N-49669, December 1956

Sabin, C. M.: The Effects of Reynolds Number, Mach Number, Spin Rate, and Other Variables on the Aerodynamics of Spheres at Subsonic and Transonic Velocities. Memorandum Report No. 1044, Ballistic Research Lab., November 1956

Martin, G. E.: Aerodynamic Phenomena for Bodies of Revolution in Supersonic Motion. NAFI TP-7, N-53536, September 1956

Liccini, L. L.: Hypersonic Tunnel No. 4 Results IX: The Development of a Water-Cooled Strain-Gage Balance (Including Sting Effects) and its Application to a Study of Normal Force and Pitching Moments of a Cone and Cone-Cylinder at Mach Numbers 5 to 8. NavOrd Report 4334, U.S. Naval Ordnance Lab., August 1956

Deep, R. A.; and Henderson, J. H.: Study of Aerodynamic Characteristics of Cone-Cylinder-Conical Frustum Bodies by Linearized Theory of Supersonic Flow. Ordnance Missile Lab., Report 6R2P, 8 June 1955

Downing, Dr. J. R.; McClow, J. H. Jr.; Hawkins, Dr. H. V.; and Fredette, R. O.: Recovery Systems for Missiles and Target Aircraft, Subsonic Free Flight Validation Test Phase. AF TR 5853 Part II, March 1955

Dickinson, E. R.: Some Aerodynamic Effects of Head Shape Variation at Mach Number 2.44. BRL Memo Report 838, N-35758, October 1954

Buford, W. E.: Magnus Effect in the Case of Rotating Cylinders and Shell. BRLM 821, July 1954

Stimler, F. S.; and Ross, R. S.: Drop Tests of 16,000 Sq In., Model Parachutes. Vol VIII, AF TR 5867, May 1954

Downing, J. R.; Areson, D. L.; and McClow, J. H., Jr.: Recovery Systems for Missiles and Target Aircraft. Subsonic Sled Test Phase, AF TR 5853, Part I, March 1954

Buford, W. E.; and Shatunoft, S.: The Effects of Fineness Ratio and Mach Number on the Normal Force and Center of Pressure of Conical and Ogival Head Bodies. BRL Memo Report No. 760, February 1954

Schmidt, L. E.: The Dynamic Properties of Pure Cones and Cone Cylinders. BRL-MR-759, January 1954

Cone Static Stability Investigation at Mach Numbers 1.56 through 4.24. NavOrd Report 3584, AD-28203, 7 December 1953

Shantz, I.: Cone Static Stability Investigation at Mach Numbers 1.56 through 4.24. NavOrd Report 3584, December 1953

Lenert, R.: Base Pressure of Spheres at Supersonic Speeds. NavOrd Report 2774, February 1953

Heinrich, H. G.: Experimental Parameters in Parachute Opening Shock Theory. Shock and Vibration Bulletin No. 19. Research and Development Board, Dept. of Defense, AD-9513, February 1953

Murphy, C. H.; and Schmidt, L. E.: The Effect of Varying Length on the Aerodynamic Characteristics of Bodies of Revolution in Supersonic Flight. BRL Report 876, 1953

May, A.; and Witt, W. R., Jr.: Free Flight Determinations of the Drag Coefficient of Spheres. NavOrd Report 2352, August 1952

Beastall, D.; and Turner, J.: The Effect of a Spike Protruding in Front of a Bluff Body at Supersonic Speeds. ARC R and M 3007, January 1952

Weinig, F. S.: On the Dynamics of the Opening Shock of a Parachute. USAF Office of Aeronautical Research. TR 6, 1951

Heinrich, H. G.: Aerodynamics, Performance and Design of Personnel Guide Parachute. Memorandum Report No. WCEE-672-145-A-9-1, November 1951

Hoerner, S.: Drag Characteristics of Parachutes. USAF AFTR 6201, ATI-92530, October 1950

Test and Evaluation of 24-Ft Hemispherical Baseball Parachute. Report No. 5028-49-2, U.S. Naval Parachute Experimental Unit, Naval Air Station, El Centro, Calif.

Test and Evaluation of Hemispherical Baseball Retarding Parachutes. Report No. 5018-49-4, U.S. Naval Parachute Experimental Unit, Naval Air Station, El Centro, Calif.

USAF Handbook ATI No. 35532, April 1947 (revised March 1951)

Clippinger, R. F.; Giese, J. H.; and Carter, W. C.: Tables of Supersonic Flows about Cone Cylinders. Part I: Surface Data, Report No. 729, Ballistic Research Labs., July 1950

Buhler, W. C.: Parachute Airfoil Type, Performance of. Memorandum Report No. MCREXE-672-19T, January 1949

Knacke, T.; and Hegele, A.: Model Parachutes, Comparison Tests of Various Types. Memorandum Report MCREXE-672-12B, January 1949

Buhler, W. C.: Porosity, Effect of, on Parachute Opening. MCREXE-672-2A, December 1948

Knacke, T.: FIST Type Parachute, Design, Use and Construction of. Memorandum Report No. MCREXE-672-19LL, June 1948

Heinrich, H. G.: Parachutes, Guide Surface. Memorandum Report No. MCREXE-672-25F, ATI No. 28935, February 1948

Buford, W.: Comparison of the Theoretical Aerodynamic Characteristics of a Series of Cones with the Results Found by Supersonic Wind Tunnel Experiments. SSWTL Memorandum to Director, BRL 23, 1948

Weinig, F. S.: Parachutes with Canopies Composed of Self-Supporting Ribbons. USAF Translation of German Report F-TR-2148-ND, ATI 25818, October 1947

Knacke, T.: Reefing Methods, Parachute. TSEPE 672-25D, October 1947

Harris, P.: Separation of Shock Wave from the Nose of a 40-Degree Cone. BRL 651, 1947

Eckert, E.: Calculation of the Temperature which a Parachute Canopy Attains at High Altitude. AMC TR F-TR-2133-WD, December 1946

Kane, E. D.: Sphere Drag Data at Supersonic Speeds and Low Reynolds Number. BRL 514 TN 4125, January 1945

Von Karman, T.: Note on Analysis of the Opening Shock of Parachutes at Various Altitudes. Army Air Corps Scientific Advisory Group, 1945

Henn: Descent Characteristics of Parachutes. USAF Translation of German Report ZWB/WM/6202, October 1944

Hallenbeck, G. A.: The Mgnitude and Duration of Parachute Opening Shocks at Various Altitudes and Air Speeds. AF MR ENG 49-696-66, 1944

Heinrich, H. G.: Investigation of the Stability of Parachutes in the Development of a Stable Parachute Manufactured of Permeable Material. USAF Translation of German Report No. 300, MTI 42978, March 1943

Duncan, W. J.: The Cause of the Spontaneous Opening and Closing of Parachutes. ARC RM No. 2119, 1943

Heinrich, H. G.; and Gerhard, R.: Wind Tunnel Tests of Parachutes. USAF Translation of German Report FGZ 192, ATI 23380, March 1942

Doetsch, H.: Three-Component Measurements of Parachute Canopies of Different Shapes. USAF Translation of German Report FB 229, February 1935

Miller, Lt. A. P.: The David Taylor Model Basin. Dept. of the Navy

Whicker, E.; and Lum, F.: Stability, Strength, and Opening Characteristics of Parachutes in Water. David Taylor Model Basin, Dept. of the Navy

V - CONTRACTORS' REPORTS AND DOCUMENTS

Keck, J. C.: Research in Re-entry Physics, Final Technical Summary Report, AVCO-Everett Research Lab., DA-19-020-AMC-0210, AD-357619, X65-15161, March 1965

Graham, J. J.: Inflatable Flare Stabilization Device for ALARR - Design and Development, GER-11511, Goodyear Aerospace Corporation, Akron, Ohio, February 1965

Results of incomplete unpublished GAC In-House drop test program

Results of unpublished Snakeye II (NOTS funded) analytical and test study program

Barsh, M. K.; Barton, C. J.; Keville, J. F.; Tomkinson, S. L.: Semi-Rigid Structures for Re-entry Applications - Seventh Interim Engineering Progress Report. Space General Corp., SGC-335-23, IR-7-943B/VII, X65-12481, December 1964

Klett, R. D.: Drag Coefficients and Heating Ratios for Right Circular Cylinders in Free-Molecular and Continuum Flow from Mach 10 to 30. Sandia Corp., SC-RR-64-2141, N65-24226, December 1964

GAC Memorandum, ARD-7538, dated December 30 1964, entitled Estimate of Ballute Weight

GAP-1997, S/3: Proposal for Improved Data-Recorder Recovery System, Goodyear Aerospace Corporation, Akron, Ohio, 15 December 1964

Ahart, A. P.: Stress Analysis - Gemini Ballute System GA526, GER-11936, Goodyear Aerospace Corporation, Akron, Ohio, in press

Investigation of Recovery Tecniques Applicable to the Terminal Portion of the Sleigh Ride MK-12 R/V Descent Trajectory (unclassified title), Goodyear Aerospace Corporation, GER-11826, November 1964 (SECRET).

Nerem, R. M.: An Approximate Method for Including the Effect of the Inviscid Wake on the Pressure Distribution on a Ballute Type Decelerator, GER-11824, Goodyear Aerospace Corporation, Akron, Ohio, November 1964

Nerem, R. M.: Supersonic Wake Phenomena with Application to Ballute-Type Decelerators, GER-11820, Goodyear Aerospace Corporation, Akron, Ohio, November 1964

GER-11806: Aerodynamic Deployable Decelerator Performance Evaluation Program, Parachute Test Items LP-3 and LP-4, Goodyear Aerospace Corporation, Akron, Ohio, 30 November 1964

GAP-2974: Proposal for Aerodynamic Deployable Decelerator Performance Evaluation Program - Phase III, Goodyear Aerospace Corporation, Akron, Ohio, 23 November 1964

GER-11672, S/1: Aerodynamic Deployable Decelerator Performance Evaluation Program (ADDPEP), Goodyear Aerospace Corporation, Akron, Ohio, October 1964

GAP-2849: Proposal for Recovery System for the Martin-Marietta Corporation. Goodyear Aerospace Corporation, Akron, Ohio, 9 September 1964

Schneider, J.; Schuster, L.; Visich, M., Jr.: Additional Aerodynamic Characteristics of a Canted-Cone Re-entry Body at Hypersonic Velocities. General Applied Science Labs., Inc., TR-465, AD-352910, X65-11495, July 1964 (SECRET).

Oberg, A. J.: An Engineering Design Study and Test Program for the Paravulcoon Recovery System Monthly Progress Letter Number VIII. Minneapolis-Honeywell Regulator Co., N64-82087, March 1964.

GAP-2485: NASA High-Speed Deceleration System Proposal, Vol 1. Goodyear Aerospace Corporation, Akron, Ohio, 6 February 1964

GAP-2456: Proposal for Aerodynamic Deployable Decelerator Performance Evaluation Program - Phase II. Goodyear Aerospace Corporation, Akron, Ohio, 5 February 1964

Ellett, D. M.: Pressure Distributions on Sphere Cones. Sandia Corp., N65-14813, January 1964

Cloud, J. B.; and Lindell, L. K.: Research on Method for Production of Thermatic Structural and/or Heat Shielding Materials. Phase II - Process Development and Trial Production. IR-8-117/11, AD-440279, 1964

Nerem, R.: Hypersonic Aerodynamic Heating, GER-11482, Goodyear Aerospace Corporation, Akron, Ohio, 31 January 1964

GER-11138, S/7: ADDPEP Monthly Progress Report No. 8. Goodyear Aerospace Corporation, Akron, Ohio, January 1964

GER-11415: Analysis and Design of Hyperflo Test Item SP-5 (ADDPEP). Goodyear Aerospace Corporation, Akron, Ohio 15 January 1964 (CONFIDENTIAL).

GER-11138, S/6: Aerodynamic Deployable Decelerator Performance Evaluation Program - Monthly Progress Report No. 7. Goodyear Aerospace Corporation, Akron, Ohio, 8 December 1963

GER-11319: Preliminary Design Report of an Inflatable Stabilization Skirt, Goodyear Aerospace Corp., Akron, Ohio, November 1963 (CONFIDENTIAL).

GER-11279: Analysis and Design of Ballute Test Item B-1 (ADDPEP). Goodyear Aerospace Corporation, Akron, Ohio, 10 October 1963

Gebhardt, J. E. and Sheeter, H. H.: Series II Test Program on Full-Scale Gemini Astronaut Ballute in AEDC Supersonic Propulsion Wind Tunnel, GER-11276, Goodyear Aerospace Corporation, Akron, Ohio, October 1963

Drawing 530A002-001: Vehicle Assembly - Capability C. Contract AF-33(657)-10955, 11 October 1963

Gross, F. R.: Orbital Recovery with Expandable Pressurized Drag Bodies, GER-11124, Goodyear Aerospace Corporation, Akron, Ohio, 1 July 1963

GER-10772: Parametric Study of Orbital Recovery with Expandable Drag Bodies. Goodyear Aerospace Corporation, 1962

Reding, J. P.: Separated Flow Effects on the Static Stability of Cone-Cylinder Flare Bodies. Lockheed Missile and Space Co., LMSC-802336, X63-15817, 1962 (CONFIDENTIAL).

Space Vehicle Recovery Control System Concepts. Raytheon Co., Equipment Div., N63-17967, 1962

GER-10923: Nova Booster Recovery System Study. Goodyear Aerospace Corporation, Akron, Ohio, 21 December 1962

Francis, W. L. and White, C. O.: Study of Hypersonic Flow Fields and Aerodynamic Forces on Sharp Cones at Angle of Attack in Low-Density Flow. Reentry Systems Program, Aeronutronic, AD-400946, N65-80443, November 1962

McCauley, W. D.: Low Density Hypersonic Similarity of Cones and Slightly Blunted Sphere Cones. General Electric Co., Missile and Space Vehicle Dept., Vol V, X63-11325 (SECRET).

GAP-1706: Proposal for Aerodynamic Deployable Decelerator Performance Evaluation Program - Phase I. Goodyear Aerospace Corporation, Akron, Ohio, 24 October 1962.

Aebischer, A. C.: Free-Flight Drop Testing of the Apollo Earth Landing System, Goodyear Aerospace Corporation, Akron, Ohio, GAP-1622, 20 August 1962

N-114,601: General Electric Co., R62SD63

Briggs, J. L.; and Marshall, L. A.: Prediction of Aerodynamic Coefficients (U). August 1962 (CONFIDENTIAL).

Aebischer, A. C.: Ballute Stabilization and Deceleration System for Emergency Recovery of a Gemini Astronaut. Goodyear Aerospace Corporation, Akron, Ohio, enclosure to GAC Letter X49-F9982, 19 August 1962

Weber, H. E. and Pugmire, T. K.: Missile and Space Vehicle Dept., General Electric Co., ARC Research Studies, X62-10635, August 1962 (CONFIDENTIAL).

Kattner, W. T.: A Bibliography of Bibliographies Relating to Re-entry Problems. General Dynamics/Fort Worth, ERR-FW-153, AD284,363, N-110,755, July 1962

Houtz, N. E.: The Application of Isotensoid Membranes to the Design of Inflatable Drag Bodies. Goodyear Aerospace Corporation, GER-10770, 31 July 1962

Aebischer, A. C.: Development of an Expandable Structure for High Effective Area Rocket Nozzles. Goodyear Aerospace Corporation, Akron, Ohio, GAP-1444, 13 July 1962

Karaffa, N. T.: High-Density Disk Samples, Deployment and Ballute Recovery, Description. Goodyear Aerospace Corporation, Akron, Ohio, GER-10753, 15 June 1962

GER-10729: An Approximate Method for Establishing Recovery System Design Criteria. Goodyear Aerospace Corporation, Akron, Ohio, 8 June 1962

Experimental Investigation of the Aerodynamic Characteristics of 40 Degree Half-Angle Cones with Varying Degrees of Bluntness at Mach Number 9. Aeronutronic, A Division of Ford Motor Company, AERON-U-1638, April 1962

Nebiker, F. R.: Research and Development of an Expandable Structure Type Deceleration and Stabilization for use in the Mach 10 Flight Regime. Goodyear Aerospace Corporation, GER-10668, 20 April 1962

Aebischer, A. C.: Design Test Harness and Field Test Stellar Guidance System. Goodyear Aerospace Corporation, Akron, Ohio, GAP-1378, 3 April 1962

Hritzay, D.; and Wiant, R.: Wire Cloth Structure for a Radiating Re-entry Vehicle, AVCO-Everett Research Lab., N62-11813, March 1962

Optimum Staging for Arbitrary Boost Trajectories. DODCO TR-117, March 1962

GER-10614: A General Six-Degrees-of-Freedom Trajectory Model for an IBM-1410 Digital Computer. Goodyear Aerospace Corporation, Akron, Ohio, 20 March 1962

Aebischer, A. C.: Deceleration and Stabilization System for Sandia Corporation Sand-Lo Program. Goodyear Aerospace Corporation, Akron, Ohio, GAP-1323, 20 March 1962

Etherton, B. D.; Burns, F. T.; Nooman, L. C.: Escape Capsule Stabilization Parachute System Development. General Dynamics/Fort Worth, X63-14521, February 1962

GAP-1258: Proposal for the Development of Structural Design Criteria for Recovery of Aerospace Vehicles and Boosters. Goodyear Aerospace Corporation, Akron, Ohio, 16 January 1962

Deployable Aerodynamic Decelerators: A Literature Survey, Compiled by Literature Research Group. Aerospace Library, Aerospace Corporation, TDR-930(2701-01) TN-2, November 1961

GER-10465: Stress Analysis of the Trailing Drag Body Wind Tunnel Models for the Langley Unitary Plan Wind Tunnel, Second Series of Tests. Goodyear Aerospace Corporation, Report, 2 November 1961

AAD-408: Four-Degrees-of-Freedom Equations of Motion for Re-Entry Vehicles. 18 October 1961

Karaffa, N. T.: Raytheon Decay Missile Inflatable Decelerator. Goodyear Aerospace Corporation, Akron, Ohio, GER-10417, 26 September 1961 (SECRET).

GAP-1040: Proposal for Recovery of Missile or Satellite-Borne Radioactive Components. Goodyear Aerospace Corporation, Akron, Ohio, 20 September 1961

GER-10412: A Fabrication and Material Report on Expandable Structure Reentry Drag Cones for the Douglas Aircraft Company, Inc. Goodyear Aerospace Corporation, Akron, Ohio, 20 September 1961

GAP-9992: Proposal for Design and Fabrication of Pershing G and C Unit Recovery System. Goodyear Aerospace Corporation, Akron, Ohio, 16 August 1961

Gebhardt, J. E.: Design and Fabrication of Pershing Missile Recovery System. Goodyear Aerospace Corporation, Akron, Ohio, 12 June 1961

GAP-9848: Piggyback Ballute Orbit Decay Recovery Program. Goodyear Aerospace Corporation, Akron, Ohio, 12 June 1961

Beltram, A. A.: Aerodynamics of Cones and Protuberances. Lockheed Missiles and Space Division Lockheed Aircraft Corporation, Special Bibliography 3-30-61-1-SB-51-28, May 1961

Kuly, P. W.: Pre Test Report, Transonic and Supersonic Wind Tunnel Tests of Drag Bodies for the Project 726 8 Percent Scale Model Re-entry Vehicle at NASA. Langley Field, N-97325, May 1961, ER 11801

Fredette, R. O.: Parachute Research Above Critical Aerodynamic Velocities. Unpublished report of Cook Research Lab., May 1961

GAP-9794: Proposal for Development and Fabrication of Inertial Guidance Test Container and Recovery System. Goodyear Aerospace Corporation, Akron, Ohio, 15 May 1961

GER-10241: Reliability at Goodyear Aircraft Corporation. Goodyear Aerospace Corporation, Akron, Ohio, 15 April 1961

ARD-876: Preliminary Investigation of Metal Fabric Re-Entry Drag Bodies. Goodyear Aerospace Corporation, 22 February 1961

Nebiker, F. R.: An Inflatable Balloon-Type Deceleration and Stabilization System for Recovery of Space Vehicles. Goodyear Aerospace Corporation, Akron, Ohio, GER-9774, Rev. A, 23 January 1961

An Inflatable Balloon - Type Deceleration and Stabilization System for Recovery of Space Vehicles. GER-9774, Rev. A, Goodyear Aerospace Corporation, January 1961

GER-10239: Study of Inflatable Balloon Type Drag Devices for Mach 10 Flight Regime. Goodyear Aerospace Corporation, Akron, Ohio, 1961

Ewing, E. G.: Ringsail Parachute Characteristics. Radioplane Report No. PTM-323-A, January 1961

GAP-9517: Inflatable Balloon-Type Drag Devices for Mach 10 Regime. Goodyear Aerospace Corporation, Akron, Ohio, 13 December 1960, Rev. A

Supersonic Tests Conducted at the Cook Technological Center Wind Tunnel on Parachute Type Decelerator Models. Cook Research Lab., October 1960, Unpublished report.

GAP-9270: Proposal for Saturn Booster Recovery System. Goodyear Aerospace Corporation, Akron, Ohio, 9 September 1960

Booster Recovery Study. Aerojet-General Corporation, Report No. 1816, July 1960

GER-9827: Astronautics Handbook. Goodyear Aerospace Corporation, Akron, Ohio, 13 June 1960

Stimler, F.; and Ross, R.: Drop Tests of 16,000-Sq-In Model Parachutes. AFTR-5867, Vol 8, April 1960

GER-8978: Monthly Progress Reports on AF33(616)-6010 Drag Balloon Study Program. Goodyear Aerospace Corporation, Akron, Ohio, Rev. A through S, 6 August 1958 to 15 April 1960

Storer, E. M.: Zero-Lift Forebody Drag Coefficients for Various Sphere Cone Configurations at Mach Numbers of 3.5 to 25. General Electric Co., Missile and Space Vehicle Dept., N63-81739, (Aerodynamics Data Memo No. 1:19), March 1960

Landberg, S. R.: Densities of the Upper Atmosphere Derived from Discoverer Satellites. Lockheed Missiles and Space Division, Sunnyvale, Calif., March 1960

Kane, M. T.: Test Results of the First Two Supersonic Parachute Test Vehicle Firings. Sandia Corporation Report SCTM 329-59(51), 15 October 1959

GAP-6938S7: Proposed Balloon Stabilization and Deceleration System for Manned Orbital Re-entry Vehicles. (Proj. Mercury). Goodyear Aircraft Corporation, Akron, Ohio, CN-76547, 29 September 1959.

AAD-214: Drag and Pressure Distribution Coefficients of Spheres, Spike Spheres, and Spheres in the Wake of Various Bodies at Mach Numbers of 1.5, 2.0 and 2.5 and Dynamic Stability of Tethered Spheres and Balloons. Goodyear Aerospace Corporation, September 1959

Detra, R. W.; Kantrowitz, A. R.; Riddell, F. R.; and Rose, P. H.: Drag Brake for Manned Satellite Recovery. AVCO Corp., CN-72149, Preprinted from Astronautics, July 1959

Detra, R. W.; Riddell, F. R.; and Rose, P. H.: Controlled Recovery of Non-Lifting Satellites. Research Report 54, AVCO Research Laboratories, A Division of AVCO Corporation, May 1959

Drag Re-entry Body Study. (Illustrated brochure). Convair, ZP-268, CN-79561, April 1959

Sandgren, F. B.; Belfiglio, R. A.; and Romick, D. C.: "Recoverable Boosters are Studied to Cut Manned Space Flight Cost," Missiles and Rockets. April 1959

ER 10384: Dyna-Soar Escape System Report. Baltimore, Md., The Martin Company, March 1959, AF No. 59RDZ-25, Project WS4646, Contract No. AF33(600)-3770

59ADZ-6696: Dyna-Soar Escape Subsystem, Performance Specification. MSF No. 20, Baltimore, Md., The Martin Company, March 1959, Project US464L, Contract No. AF33(600)-3770

Heiser, G. D.: Results from Wind Tunnel Tests of the GE-Mark 2 Nose Cone Data Capsule with Modifications Designed to Improve the Aerodynamic Stability. General Electric Company, R59SD334, CN-71135, March 1959

Detra, R. W. and Riddell, F. R.: Returning Alive from Space. AVCO Research Lab., CN-71841, 1959

GER-9003: Interim Technical Report on Balloon-Type Stabilization and Deceleration for High-Altitude and High-Speed Recovery. Goodyear Aerospace Corporation, Akron, Ohio, 1 October 1958

GER-8844: Proposal for Study of Inflatable Structure Materials for Space Application. Goodyear Aerospace Corporation, 26 May 1958

0-1,850,000 Ft, Table of Dynamic Pressures at a Mach Number of One for Altitudes from 0-150,000 Ft. Goodyear Aerospace Corporation Memorandum DAD 428, Rev. A, April 1958

Wilcox, B.: The Calculation of Filling Time and Transient Loads for a Parachute Canopy during Deployment and Opening. Report No. SC-4141 (TR), Sandia Corporation (subsidiary of Western Electric Company), February 1958

Proposal for a Recovery System for NASA Manned Satellite Capsule. Cook Research Lab., CN-68108, P-1605A, 1958

Linnell, D.: Vertical Re-entry of Very Lightweight Bodies into the Earth's Atmosphere. Research Note 9, Convair Scientific Research Lab., A Division of General Dynamics Corporation, October 1957

Schilling, D. L.: A Method for Determining Parachute Opening Shock Forces. Report No. 12543, Lockheed Aircraft, August 1957

Dole, S. H.: The Atmosphere of Venus. Rand Paper P-978, Rand Corporation, October 1956

GER-8265: Supplementary Aerodynamic Analysis of Cockpit Capsule Concept for Multiplace Aircraft Escape Study. Goodyear Aerospace Corporation, Akron, Ohio, July, Contract AF33(616)-5017

Gendtner, W. J.: Sharp and Blunted Cone Force Coefficients and Centers of Pressure from Wind Tunnel Tests at Mach Numbers from 0.50 to 4.06. Convair Report ZA-7-017, June 1955

Ciffrin, A.: Aerodynamic Appraisal of the Rotofoil. Radioplane Report No. 633, March 1952

GER-4552: Ejectable Seat Capsule Final Report, Task I. Goodyear Aerospace Corporation, Akron, Ohio, December 1951, Contract NOa(s)-51-292-C

Report R-65: Handbook for the Design of Guided Missile Recovery Systems (U), Task II, Project Recovery. Radioplane Company, Van Nuys, Calif., March 1951 (CONFIDENTIAL).

Rantzsche, W.; and Wendt, H.: Cones in Supersonic Flow. RAND T-8, January 1948

VI - UNIVERSITY TECHNICAL REPORTS

McConnell, D. G.: An Investigation of Transient Melting Ablation at the Surface of a Decelerating Spherical Body. Case Institute of Technology, Cleveland, Ohio, N65-16341, 1964

Nichols, J. O.; and Nierengarten, E. A.: Aerodynamic Characteristics of Blunt Bodies. JPL-TR-83-677, N-116-287, November 1964

Law, E. H.: The Longitudinal Equations of Motion of an Airborne Towed Vehicle Incorporating an Approximation of Cable Drag and Inertia Effects. Princeton University, Princeton, N. J., Report 687, AD-602734, N65-10904, May 1964

Eichhorn, R.; and Small, S.: Experiments on the Lift and Drag of Spheres Suspended in a Poiseuille Flow. Princeton University, Princeton, N. J., Technical Report PR-106-P, AD-434449, N64-19636, February 1964

Glauz, W. D.: Aerodynamic Forces on Oscillating Cones and Ogive Bodies in Supersonic Flow. Purdue University (Thesis - Ph. D.) CN-116-592, January 1964

Jaffe, P.: Hypersonic Ballistic Range Results of Two Planetary Study Configurations in Air and Carbon Dioxide/Nitrogen Mixtures. JPL Technical Report No. 32-543, Pasadena, Calif., Jet Propulsion Lab., University of Calif., January 1964

Kawmura, R.; Sawada, T.; and Seki, K.: Study of Row of Circular Cylinders in Supersonic and Hypersonic Flow. III - Drag of Row of Parallel Circular Cylinders in Supersonic Flow, University of Tokyo, Aeronautical Research Institute, Bulletin, Vol 3, A64-14916, December 1963

Harlum, P.: A Table of Mars Atmosphere and Uncertainty in the CGS System. Pasadena, Calif., Jet Propulsion Lab., California Institute of Technology, July 1963

Dayman, B.; et al.: The Influence of Shape on Aerodynamic Damping of Oscillatory Motion during Mars Atmosphere Entry and Measurement of Pitch Damping at Large Oscillation Amplitudes. JPL Technical Report No. 32-380, Pasadena, Calif., Jet Propulsion Laboratory, University of California, February 1963

Maslach, G. J.; and Schaaf, S. A.: Cylinder Drag in the Transition from Continuum to Free Molecule Flow. University of California, Physics of Fluids, Vol 6, A63-14883, March 1963

Mackworth, J. C.: Aerodynamic Instability of Non-lifting Bodies Towed Beneath an Aircraft. Toronto University, Institute of Aerophysics, Canada, UTIA-TN-65, N63-14844, January 1963

A General Study of Processes for the Realization of Design Configurations in Materials. Interim Technical Progress Report No. 2, Cornell Aeronautical Laboratory, N63-18026, April 1962

Vijuk, R. M.: A Study of Automatic Brake Control Systems. Report No. 2, Pennsylvania State University, N64-81699, April 1962

Aroesty, J.: Sphere Drag in a Low Density Supersonic Flow. Institute of Engineering Research, University of California (submitted in partial satisfaction of the requirements for the degree of Ph. D. in engineering science), HE-150-192, N-107-475, January 1962

Maas, W. L.: Experimental Determination of Pitching Moment and Damping Coefficients of a Cone in Low Density, Hypersonic Flow. University of California, Institute of Engineering Research, TR HE-150-190, Series 20, Issue No. 135, AD-266787, 9 October 1961

Haak, E. L.: Stability and Drag Parachutes with Varying Effective Porosity. Lecture, University of Minnesota, Summer Course, 17-28 July 1961

Wegener, P. P. and Ashkenas, H.: Wind Tunnel Measurements of Sphere Drag at Supersonic Speeds and Low Reynolds Numbers. JPL-TR-34-160, N63-18848, June 1961

Ruger, C. J.: Approximate Solutions for Aerodynamics Heating of Re-entry Vehicles. Polytechnic Institute of Brooklyn, PIBAL Report No. 729, AD-268826, November 1961

Heinrich, H. G.: "Snatch Force," Chapter V of Aerodynamic Deceleration. Minneapolis, Minn., University of Minnesota Center for Continuation Study in Cooperation with the Department of Aeronautics and Engineering Mechanics, July 1961

Heinrich, H. G.; and Monson, D. J.: "Stress Analysis of Parachutes." Chapter VI of Aerodynamic Deceleration, Minneapolis, Minn., University of Minnesota Center of Continuation Study in Cooperation with the Department of Aeronautics and Engineering Mechanics, July 1961

Heinrich, H. G.; et al.: Theoretical Parachute Investigations. Progress Reports, Contract AF33(616)-6372, University of Minnesota, January 1960 through January 1961

Sreekanth, A. K.: Drag Measurements on Circular Cylinders and Spheres in the Transition Regime at a Mach Number of 2, Institute of Aerophysics, University of Toronto, Aeronautical Research Laboratory, UTIA Report 74, ARL-53, N-98428, April 1961

Wegener, P. P.: A New Method to Measure Sphere Drag in Rarefied Supersonic Gas Flows and Some Results. JPL-TR-34-44, N-81857

Heinrich and Riobokin: Analytical and Experimental Considerations of the Velocity Distribution in the Wake of a Body of Revolution. Department of Aeronautical Engineering, University of Minnesota, December 1959

Maslach, G. J.; and Talbot, L.: Low-Density Aerodynamic Characteristics of a Cone at Angle of Attack. University of California, Technical Report HE-150-172, October 1959

MIT-DSR No. 5-7426: Textile Division, Mechanical Engineering Department, MIT, August 1957, AD-139272, Materials and Parachutes and Retardation Devices. Notes on Special Summer Program, MIT, 20-31 July 1959

Miele, A.; and Cappellari, J. O.: Effect of Drag Modulation on the Maximum Deceleration Encountered by a Re-entering Ballistic Missile. Purdue University School of Aeronautical Engineering, N-73265, June 1959

Hammitt, A. G.; and Murphy, K. R. A.: Approximate Solutions for Supersonic Flow Over Wedges and Cones. Princeton University, Forrestal Research Center Report No. 449, April 1959

Bobrovnikoff, N. T.: Natural Environment of the Planet Mars. Ohio State University Research Foundation, TN 847-1, AD-242177, February 1959

Shaw, J. H.; and Bobrovnikoff, N. T.: Natural Environment of the Planet Venus. Ohio State University Research Foundation, TN 847-2, AD-242176, February 1959

Kendall, J. M., Jr.: Experiments on Supersonic Blunt-Body Flows. JPL-CIT Progress Report No. 20-372, February 1959

Materials for Parachute and Retardation Devices. MIT, Lecture Notes, Summer Sessions, 1959

Heinrich, H. G.: Dynamic Problems of Retardation Devices. Lecture Notes, Parachute Course, University of Minnesota, 1959

Munson, A. G.: A Preliminary Experimental Investigation of the Flow Over Simple Bodies of Revolution at M = 18.4 in Helium. GALCIT Memorandum No. 35 (Contract No. DA-04-495-Ord-19), December 1956

Machell, R. M.; and O'Bryant, W. T.: An Experimental Investigation of the Flow Over Blunt-Nosed Cones at a Mach Number of 5.8. GALCIT Memorandum No. 32 (Contract No. DA-04-495-Ord-19), June 1956

Moore, R. G.: "Radar Reflectivity of Metallized Parachutes." Paper presented at Parachute Engineering Short Course at Purdue University, June 1956

Ashley, H.: Dynamic Stability of a Body Moving through the Air. MIT Parachute Technology Notes, June 1955

Oliver, R. E.: An Experimental Investigation of Flow Over Simple Blunt Bodies at a Nominal Mach Number of 5.8. Guggenheim Aeronautical Laboratory, California Institute of Technology, Wind Tunnel Memorandum No. 26, June 1955

Wedderspoon, J. R.; and Young, A. D.: Note on the Results of Some Profile Drag Calculations for a Particular Body of Revolution at Supersonic Speeds. College of Aeronautics, Cranfield, England, Report 81, N-34521, July 1954.

Marson, G. B.; Keates, R. E.; and Socha, W.: An Experimental Investigation of the Pressure Distribution on Five Bodies of Revolution at Mach Numbers of 2.45 and 3.19. College of Aeronautics, Cranfield, England, Report 79, April 1954

Ipsen, D. C.: Cone Drag in a Rarefied Gas Flow. University of California Engineering Projects, Report HE-150-114, August 1953

Foote, J. R.; and Scherberg, M. G.: Dynamics of the Opening Parachute. Ohio State University Engineering Experimental Station Bulletin, September 1952, 149: 131-143

Sherman, F. S.; and Kane, E. D.: Supplementary Data on Sphere Drag Tests. University of California Engineering Projects Report HE-150-71, February 1950

Kane, E. D.: Drag Forces on Spheres in Low Density Supersonic Gas Flow. University of California Engineering Projects, Report HE-150-65, February 1950

Hodges, A. J.: The Drag Coefficient of Very High Velocity Spheres. New Mexico School of Mines, Research and Development Division, October 1949

Staff of the Computing Section, Center of Analysis (under direction of Zdenek Kopal): Tables of Supersonic Flow around Cones of Large Yaw, Technical Report No. 5, MIT, 1949

Staff of Computing Section, Center of Analysis (under direction of Zdenek Kopal): Tables of Supersonic Flow around Cones, Technical Report No. 1, MIT, 1947

Staff of the Computing Section, Center of Analysis (under direction of Zdenek Kopal): Tables of Supersonic Flow around Yawing Cones, Technical Report No. 3, MIT, 1947

Kniper, G. P.: The Atmospheres of the Earth and Planets. University of Chicago Press, 1947

Stewart, H. J.: Theoretical Lift and Drag of Cones at Supersonic Speeds. JPL Memorandum 4-14, N63-83866, November 1946

Reagan, J. F.; and Stimler, F. J.: The Development of an Analytical Method for Investigating Parachute Stability. Guggenheim Airship Institute Report DGAI 134, October 1945

Harleman, D.: AF Technical Report 5985, Part 4, Studies on the Validity of the Hydraulic Analogy to Supersonic Flow, Massachusetts Institute of Technology, Cambridge, Mass.

Von Karman, T.: The Problem of Resistance in Compressible Fluids. GALCIT Pub. No. 75, 1936.

VII - SYMPOSIUMS AND PAPERS

Lyons, W. C.: "Hypersonic Drag Stability and Wake Data for Cones and Spheres." AIAA Journal, November 1964, pp 1948-1956

Barzda, J. J.: "Rotors for Recovery." In American Institute of Aeronautics and Astronautics, Entry Technology Conference, (Technical Papers, AIAA Publication CP-9, New York, American Institute of Aeronautics and Astronautics), A64-26656, October 1964

Roberts, L.: "Entry Into Planetary Atmospheres." Astronautics and Aeronautics, October 1964

Topping, A. D.: "Shear Deflections and Buckling Characteristics of Inflated Members." Journal of Aircraft, Vol 1, September-October 1964

Kendall, R. T.: "The Paracone - A Replacement for the Parachute." In Joint Parachute Test Facility Proceedings, Symposium on Parachute Technology and Evaluation, Vol I, X65-10845, September 1964

Nebiker, F. R.: "Expandable Drag Devices for Mach 10 Flight Regime." In Joint Parachute Test Facility Proceedings, Symposium on Parachute Technology and Evaluation, Vol I, X65-10841, September 1964

Cobb, D. B.: "Parachute Test Work at the Royal Aircraft Establishment." In Joint Parachute Test Facility Proceedings. Symposium on Parachute Technology and Evaluation, Vol I, X65-10852, September 1964

Ross, J. H.: "Unique Flexible Fibrous Materials for Decelerators." In Joint Parachute Test Facility Proceedings. Symposium on Parachute Technology and Evaluation, Vol II, X65-10827, September 1964

Babish, C. A.; and Nickel, W. E.: "The Cree Vehicle - A Free Flight Aerodynamic Decelerator Testing System." In Joint Parachute Test Facility Proceedings, Symposium on Parachute Technology and Evaluation, Vol I, X65-10859, September 1964

Gray, J. H.: "Attenuation of Deployment and Opening Forces of Certain Aerodynamic Decelerators." In Joint Parachute Test Facility Proceedings, Symposium on Parachute Technology and Evaluation, Vol II, X65-10832, September 1964

Blow, C. M.: "The Development and Testing of Elastomeric Materials for Fluid Sealing Applications." British Hydromechanics Research Association, International Conference on Fluid Sealing, Second, Cranfield, England, April 1964, Aircraft Engineering, Vol 36, A64-24812, July 1964.

Gross, R. J.; and Reiss, G. W.: "The Asset Recovery System." In Aerospace Corporation, Trans. of the Ninth Symposium on Ballistic Missile and Space Technology, Vol II, X65-13610, July 1964

Fink, M. R.: "Hypersonic Dynamic Stability of Sharp and Blunt Slender Cones." In Aerospace Corporation, Trans. of the Ninth Symposium on Ballistic Missile and Space Technology, Vol II, X65-13609, July 1964

Houtz, N. E.: "Optimization of Inflatable Drag Devices by Isotensoid Design." AIAA Paper 64-437, A64-20102, July 1964

Fox, N. L.; and Blaylock, R. F.: "Aerodynamic Effects of Atmospheric Composition." AIAA Paper 64-481, American Institute of Aeronautics and Astronautics, June 1964

Krah, J. W.: "High Temperature Telemetry Antennas for Asset." In Ohio State University and USAF Research and Technology Division, Symposium on Electro-Magnetic Windows Proceedings, Vol 4, A65-11382, 2-4 June 1964

Dastin, S. J.; and Rosenberg, P.: "Reinforced Plastics for Project Fire Reentry Vehicle." Prepared for Presentation at Society of Plastics Engineers Regional Technology Conference, X64-12048, May 1964

Cobb, D. B.: "Parachute Test Work at the Royal Aircraft Establishment." Symposium on Parachute Technology, El Centro, Calif., April 1964

Brady, J. J.; and Levensteins, Z. J.: "Hypersonic Drag, Stability, and Wake Data for Cones and Spheres." AIAA Paper 64-44, A64-12931, January 1964

Jackson, B. G.: "Aerodynamic Drag and Stability." In Manned Spacecraft - Engineering Design and Operation. Edited by P. E. Purser, M. A. Faget, and N. F. Smith, Fairchild Publications, Inc., A65-12535, 1964

Finch, T. W.: "Aerodynamic Braking Trajectories for Planetary Orbit Attainment." AIAA Paper 64-478, N64-24165, 1964

Nerem, R. M.; and Stickford, G. H.: "Shock Layer Radiation during Hypervelocity Re-entry." In American Institute of Aeronautics and Astronautics, Entry Technology Conference (AIAA Publication CP-9, New York, American Institute of Aeronautics and Astronautics, 1964), A64-26664

Wasserman, L.; and Slattery, J. C.: "Upper and Lower Bounds on the Drag Coefficient of a Sphere in a Power-Model Fluid." American Institute of Chemical Engineers, Annual Meeting, 56th Symposium on Non-Newtonian Fluid Mechanics - I, Paper 40B, A63-25855, December 1963.

French, K. E.: "Inflation of a Parachute." AIAA Journal, November 1963

Barzda, J. J.: "Results of the Kaman KRC-6M Rotochute Tests at Supersonic Speeds." American Helicopter Society Journal, Vol 8, A64-10791, October 1963

Gross, F. R.: "Orbital Recovery with Expandable Pressurized Drag Bodies." Society of Automotive Engineers, National Aeronautic and Space Engineering and Manufacturing Meeting, Paper 756A, A63-24096, September 1963

Petersen, N. V. (ed.): "Advanced in the Astronautical Sciences." Vol 16, Part 1, Space Rendezvous, Rescue, and Recovery. USAF and American Astronautical Society, Space Rendezvous, Rescue and Recovery Symposium, A63-24744, September 1963

Moss, B.: "Lifting and Non-lifting Decelerators for Boosters and Satellite Recovery." In Space Rendezvous, Rescue, and Recovery Proceedings of the American Astronautical Society, Symposium, Air Force Flight Test Center, Edwards AFB, Advances in the Astronautical Sciences, Vol 16, Part 2, A64-27828, September 1963

Gonor, A. L.: "On Three-Dimensional Bodies of Minimum Drag at High Supersonic Speed." Journal of Applied Mathematics and Mechanics, Vol 27, No. 1, Translation, A63-19259, July 1963

Simon, W. E.; and Walter, L. A.: "Approximation for Supersonic Flow Over Cones." AIAA Journal, Vol I (Martin Marietta Corporation), July 1963

Heinrich, H. G.: "A Supersonic Parachute Based on the Inlet Diffuser Concept." Presented at the 22nd Meeting of the Flight Mechanics Panel, Torino, Italy, N64-16209, AGARD-445, April 1963

Chow, W. L.: "Conical Flarings in Uniform Supersonic Flow at Zero Angle of Attack." AIAA Journal, Vol 1, A63-15969, April 1963

Nebiker, F. R.: "Expandable Balloon-Type Drag Devices for Mach 10 Flight Regime." Society of Automotive Engineers - American Society of Naval Engineers, National Aeronautical Meeting, A63-14457, April 1963

Bulakh, B. M.: "On the Nonsymmetric Hypersonic Flow around a Circular Cone." Journal of Applied Mathematics and Mechanics, Vol 26, Translation, March 1963

Schaaf, S. A.; and Maslach, G. J.: "Cylinder Drag in the Transition from Continuum to Free Molecule Flow." Physics of Fluids, Vol 6, A63-14883, March 1963

Martin, W. A.: "Mach 3 Technology and the Recoverable Booster." Institute of the Aerospace Sciences Annual Meeting 31st, IAS Paper 63-7, A63-11437, January 1963

Sims, L. W.: Evolution of the Hyperflo Parachute. In AF Systems Command Trans. of the 8th Symposium on Ballistic Missile and Space Technology, Vol 2, N64-15261, 1963

Brendel, J.: The Mark VB Recovery System (U). Air Force Systems Command, Los Anglees, Calif., Space Systems Division, Trans. of the 8th Symposium on Ballistic Missile and Space Technology, Vol 7, 1963 (See X64-13261) (SECRET).

Spalding, D. B.: "A New Analytical Expression for the Drag of a Flat Plate Valid for Both the Turbulent and Laminar Regimes." International Journal of Heat and Mass Transfer, Vol 5, December 1962, A63-11124

Gunkel, R. J.; Bond, P.; and Bergonz, F. H.: "Recovery System Concepts for a Reusable Chemical Booster." American Rocket Society, Annual Meeting, 17th and Space Flight Exposition, Paper 2718-62, A63-12764, November 1962

Solt, G. A., Jr.: "Aerodynamic Decelerator - Their Use and Future." Proceedings of Retardation and Recovery Symposium (ASD), N63-23327, November 1962

Oberg, A. J.; Sopczak, S. S.; and Sutton, M. A.: "Paravulcoon Recovery and Landing System." In Aeronautics Systems Division Proceedings of Retardation and Recovery Symposium, N63-23324, November 1962

Buckner, J. K.: "Application of Axisymmetric Flow Analysis to Inflation Stability of Supersonic Flexible Parachute." In Aeronautics Systems Division Proceedings of Retardation and Recovery Symposium, N63-23318, November 1962

Knacke, T. W.: "Systems Considerations." In Aeronautics Systems Division Proceedings of Retardation and Recovery Symposium, N63-23325, November 1962

Rose, P. H.: "Heating Problem for Supersatellite Re-entry." In Aeronautics Systems Division Proceedings of Retardation and Recovery Symposium,N63-23315, November 1962

Ross, J. H.: "High Temperature Fibrous Materials for Decelcrators." In Aeronautics Systems Division Proceedings of Retardation and Recovery Symposium, N63-23320, November 1962

Babish, C. A.; and Berndt, R. J.: "Supersonic Parachute Research." In Aeronautics Systems Division Proceedings of Retardation and Recovery Symposium N63-23317, November 1962

McMullen, J. C.; and Smith, A. M.: "Martian Entry Capsule - Design Considerations for Terminal Deceleration." USAF, Office of Scientific Research and General Electric Co., Space Sciences Laboratory, Dynamics of Manned Lifting Planetary Entry, Symposium 3rd, Proceedings, A63-23666, October 1962

Hoshizaki, H.: "Heat Transfer in Planetary Atmospheres at Super-Satellite Speeds." American Rocket Society Journal, October 1962

Bogdonoff, S. M.; and Vas, I. E.: "Some Experiments on Hypersonic Separated Flows." American Rocket Society Journal, October 1962

Ginter, R. L.; and Cerreta, L. M.: "Insulation-Radiation Temperature Control of Inflatable Hypersonic Vehicles." Paper 595G, SAE, October 1962

Cobb, E. S.: High Strength Glass Fiber Tapes and Webbings for High Temperature Pressure Packed Decelerator Applications. Collection of Papers presented at Symposium on Fibrous Matter, X63-12491, October 1962

Harris, J. T.: "High Temperature Metallic Fabric for Re-entry Applications, Society of Automotive Engineers." National Aerospace Engineering and Manufacturing Meeting, Paper 5904, A63-12409, October 1962

St. Germain, A. R.; and Zick, L. P.: "Circumferential Stresses in Pressure Vessel Shells of Revolution." Report from Trans. of the ASME, Journal of Eng. for Ind. presented at the Petro. Mech. Eng. Conference, N64-20675, September, 1962, ASME Paper 62-PET-4

Stocker, P. M.; and Mauger, F. F.: "Supersonic Flow Past Cones of General Cross-Section." Journal Fluid Mech., Vol 13, Part 3 (Armament Research and Development Establishment, War Office), July 1962

Edsall, R. H.: "Calculation of Flow Fields about Blunt Bodies of Revolution Traveling at Escape Velocity." New York American Rocket Society, presented at the ARS Lunar Missions Meeting, ARS Paper 2492-62, N62-14463, July 1962

Brooks, W. B.; and Reis, F. E.: "Drag on a Right Circular Cylinder in Rarefied Flow at Low Speed-Ratios." In Office of Naval Research Proceedings of the 3rd Intern. Symposium on Rarefied Gas Dynamics, N63-21603, June 1962.

Aroesty, J.: "Sphere Drag in a Low-Density Supersonic Flow." In Office of Naval Res. Proceedings of the 3rd Intern. Symposium on Rarefied Gas Dynamics, N63-21601, June 1962

Ashkenas, H.: "Low-Density Sphere Drag with Equilibrium and Nonequilibrium Wall Temperature." Intern. Symposium on Rarefied Gas Dynamics, Proceedings of 3rd Intern. Symposium held in Paris, June 1962

Aroesty, J.: "Sphere Drag in a Low Density Supersonic Flow." In Office of Naval Res. Proceedings of the 3rd Intern. Symposium on Rarefied Gas Dynamics, N63-21601, June 1962

Ashkenas, H.: "Low-Density Sphere Drag with Equilibrium and Nonequilibrium Wall Temperature." JPL Institute of Technology. In Office of Naval Res. Proceedings of the 3rd Intern. Symposium on Rarefied Gas Dynamics, June 1962, N63-21602

Bloxsom, D. E.; and Rhodes, B. V.: "Experimental Effect of Bluntness and Gas Rarefaction on Drag Coefficients and Stagnation Heat Transfer on Axisymmetric Shapes in Hypersonic Flow." Institute of the Aerospace Sciences, National Summer Meeting, A63-11218, June 1962

Traugott, S. C.: "Some Features of Supersonic and Hypersonic Flow About Blunted Cones." Journal of Aero. Science, Vol 29, April 1962

Wood, C. J.: "Hypersonic Flow over Spiked Cones." Journal Fluid Mech., Vol 12, Part 4, April 1962

Pritchard, E. B.: "Aerodynamic Control of Deceleration and Range for the Lunar Mission." Preprint Paper 513D for Presentation at the SAE National Aeronautics Meeting, N62-12501, April 1962

Meyer, J. B.; and Mayo, B. R.: "Emergency and Routine Space Vehicle Recovery." Institute of Radio Engineers, Intern. Convention, IRE Intern. Convention Record, A63-12527, March 1962

Burke, A. F.; and Curtis, J. H.: "Blunt-Cone Pressure Distributions at Hypersonic Mach Numbers." Journal Aerospace Science, Vol 29, February 1962

Lees, L.; and Hromas, L.: "Turbulent Diffusion in the Wake of a Blunt-Nosed Body at Hypersonic Speeds." IAS Paper No. 62-71, January 1962

Lorsch, H. G.: "Heat Transfer to Porous Nose Caps and Leading Edges of Hypersonic Vehicles and Re-entry Aids." In Advances in the Astronautical Sciences, Vol XI, edited by H. Jacobs, American Astronautical Society, Annual Meeting, 8th Proceeding, A64-11472, January 1962

Walts, F. M.: "Re-entry/Recovery Design Considerations of a Lunar Return Data Vehicle." Presented at the AAS 8th Annual National Meeting, AAS 62-40, N-108-097, January 1962

Edsal, R. H.: "Calculation of Flow Fields about Blunt Bodies of Revolution Traveling at Escape Velocity." New York American Rocket Society, N62-14463, 1962

Slattery, R. E.; and Clay, W. G.: "Width of the Turbulent Trail behind a Hypervelocity Sphere." Physics of Fluids, Vol 4, No. 10, October 1961

Hamilton, J. S.: "Large Booster Recovery Techniques." Presented at ARS Space Flight Report to the Nation, N-105-706, October 1961

Hastings, S. M.; and Pasiuk, L.: "The Aerodynamic Heating of Blunt, Axisymmetric, Re-entry Type Bodies with Laminar Boundary Layer at Zero and at Large Angles of Yaw in Supersonic and Hypersonic Air Streams." Intern Heat Transfer Conference, A63-25589, August 1961

A63-11342: "A Simple Method of Sphere Drag Measurement in Rarefied Supersonic Gas Flows." Peter P. Wegener and Harry Askhenas, California Institute of Technology, Jet Propulsion Laboratory, Pasadena, Calif., International Symposium on Rarefied Gas Dynamics, 2nd, Proceedings, Berkeley, Calif., 3-6 August 1960, In Rarefied Gas Dynamics, New York, Academic Press, Inc., 1961

Dukes, W. H.: "Requirements for High Temperature Materials for Hypersonic Re-entry Vehicles." In High Temperature Materials. Part 2, Metallurgical Society Conferences, A63-25216, April 1961

Lysdale, C. A.: "Launch-Vehicle Recovery Techniques," presented at IAS 29th Annual Meeting, IAS Paper No. 61-51, N-92279, January 1961

Lysdale, C. A.: "Booster Recovery Concepts," presented at ASS 7th Annual Meeting, ASS Preprint 61-21, N95446, January 1961

Luidens, R. W.: "Atmospheric Braking for Space Missions." For presentation at 1961 AFBMD/Aerospace Corporation Symposium, NASA CC-E-1270, 1961

Maynard, J. D.: "Aerodynamics of Decelerators at Supersonic Speeds." Symposium of Recovery of Space Vehicles sponsored by the Los Angeles Section of the Institute of the Aero. Sci., September 1960

Maynard, J. D.: "Aerodynamics of Decelerators at Supersonic Speeds." NASA/Langley Research Center (for presentation at the Symposium on Recovery of Space Vehicles in Los Angeles, Calif. from August 31 to September 1 1960)

Skhlovskii, I. S.; and Kurt, V. G.: "Determination of Atmospheric Density as a Height of 430 km by Means of the Diffusion of Sodium Vapors." ARS Journal, Vol 30, No. 7, July 1960

Strong, J. R.; and Moores, C. B.: "Some Observations of the Atmospheres of Venus and the Earth during the Stratola IV Balloon Flight." Paper given at the American Geophysical Union Meeting, Washington, D.C., April 1960

Connors, J. F.; and Lovell, J. C.: "Some Observations on Supersonic Stabilization and Deceleration Devices." Presented at the IAS 28th Annual Meeting, CN-80512, January 1960

Koh, J. C. Y.: "Measured Pressure Distribution and Local Heat Transfer Rates for Flow Over Concave Hemispheres," presented at ARS Semi-Annual Meeting. ARS-1146-60, N-85481, 1960

Connors, J. F.; and Lovell, J. C.: "Source Observations on Supersonic Stabilization and Deceleration Devices." IAS Paper No. 60-19, 1960

Shipps, R. P.: "On the Methods and Economics of Recovering Boosters for Orbital Vehicles." IAS Paper No. 60-29, 1960

King-Hele, D. G.: "Density of the Upper Atmosphere from Analysis of Satellite Orbits." Further Results, Nature, Vol 184, October 24 1959

Phillips, R. L.; and Cohen, C. B.: "Use of Drag Modulation to Reduce Deceleration Loads during Atmospheric Entry," ARD Journal, June 1959

Parvin, R. H.: "The Earth and Inertial Space. Part II-Shape of the Earth." Aerospace Engineering, Vol 18, No. 5, May 1959

Pritchard, E. B.: "The Stability of Several Missile Nose Configurations in Hypersonic Flow." Institute of the Aero. Sci., 1959 1st Award Papers, IAS Student Branch Paper Competition

VanDyke, M. D.: "The Supersonic Blunt Body Problem - Review and Extension." VAS, Vol 25, No. 8, August 1958

Thale, J.: "Recovery from a Satellite Orbit," presented at ARS Semi-Annual Meeting. ARS 650-58, N-61896, June 1958

Romick, D. C.; Belfiglio, R. A.; and Sandgren, F. B.: "Recoverable Boosters are Studied to Cut Manned Space Flight Cost." Missiles and Rockets, April 1958

Herman, R.: "Problems of Hypersonic Flight at the Re-entry of Satellite Vehicles." Proceedings of the 9th Annual Congress of the IAF, Amsterdam, 1958

Charwat, A. F.: "The Stability of Bodies of Revolution at Very High Mach Numbers." Jet Propulsion, V 27, No. 8, Part 1, N-68775, August 1957

Ehricke, K. A.; and Pence, H.: "Re-entry of Spherical Bodies into the Atmosphere at Very High Speeds." Presented at ARS Spring Meeting, ARS 428-57, N-60902, April 1957

Hodges, A. J.: "The Drag Coefficient of Very High Velocity Spheres." Journal of the Aero. Sci., Vol 24, 1957

Ipsen, D. C.: "Experiments on Cone Drag in a Rarefied Air Flow." Jet Propulsion, December 1956

Betram, M. H.: "Tip-Bluntness Effects on Cone Pressure at M = 6.85." Journal Aero. Sci., Vol 23, September 1956

Heinrich, H. G.: "Drag and Stability of Parachutes." Aeronautical Engineering Review, June 1956.

Krahn, E.: "Negative Magnus Force." Journal of the Aeronautics Sciences, Vol 23, No. 4, April 1956

Heinrich, H. G.: "Drag and Stability of Parachutes." IAS Engineering Review, Vol 15, Jan-June 1956

Roberts, R. C.; and Riley, J. D.: "A Guide to the Use of the MIT Cone Tables." Journal of Aeronautical Sciences, Vol 21, 1954

Foote, J. R.; and Scherberg, M. G.: "Dynamics of the Opening Parachute." Proceedings of the Second Midwestern Conference on Fluid Dynamics, Ohio State University, 1952

Van Dyke, M. D.: "First-Order and Second-Order Theory of Supersonic Flow Past Bodies of Revolution." Journal of Aeronautical Sciences, Vol 18, March 1951

Van Dyke, M. D.; Young, G. W.; and Sisha, C.: "Proper Use of the MIT Tables for Supersonic Flow Past Inclined Cones." Journal of Aeronautical Sciences, Vol 18, 1951

O'Hara, F.: "Notes on the Opening Behavior and the Opening Forces of Parachutes." The Journal of the Royal Aeronautical Society, November 1949

Charters, A. C.; and Thomas, R. N.: "The Aerodynamic Performance of Small Spheres from Subsonic to High Supersonic Velocities." Journal of Aeronautical Sciences, Vol 12, 1945

Hall, A. A.; and Hislop, G. S.: "Velocity and Temperature Distributions in the Turbulent Wake behind a Heated Body of Revolution." Proceedings of the Cambridge Philosophical Society, Vol 34, 1939

Goldstein, S.: "On the Velocity and Temperature Distribution in the Turbulent Wake behind a Heated Body of Revolution." Proceedings of the Cambridge Philosophical Society, Vol 34, 1938

Goldstein, S.: "On the Velocity and Temperature Distribution in the Turbulent Wake behind a Heated Body of Revolution." Proceedings of the Cambridge Philosophical Society, Vol 34, 1938

Swain, L. M.: "Turbulent Wake behind a Body of Revolution." Proceedings of the Royal Society of London, Series A, Vol 125, 1929

VIII - MISCELLANEOUS

Heinrich, H. G.: "Aerodynamic Principles of the Supersonic Guide Surface Parachute." Berlin, West Germany, Paper A64-27037, September 1964

Niehaus, G.: "On the Applicability of the Hydraulic Analogy to Investigations of Aerodynamic Deceleration Systems." Berlin, West Germany, Paper A64-26277, September 1964 (in German)

Buogiorno, C.; and Trella, M.: "Considerations on the Drag Coefficient for the San Marco Satellite." Roma, Universita, Scuola Dingegneria, Aerospaziale, Centro Ricerche Aerospaziali, No. 5, July 1964, A65-15359

Berry, C. J.; David, B. M.; and Rogers, E. W. E.: Experiments with Cones in Low-Density Flows at Mach Numbers Near 2. National Physical Laboratory, Teddington, Great Britain, NPL-Aero-1095, X65-12352, March 1964

Krasnov, N. F.: An Approximation of Aerodynamic Coefficients of Thin Bodies of Revolution Moving at Very Great Supersonic Speeds. Transl. into English from Tr., Vyssheye Tekhn. Uschilishche Iment, Baumana, Moscow, No. 32, FTD-MT-63-169, AD-605587, N65-14399, March 1964

Krasnov, N. F.: "Aerodynamics of Bodies of Revolution." Second Edition, In Russian, Book on Aerodynamics of Bodies of Revolution, A65-11430, 1964

Marsden, A. J.: "The Drag and Opening Characteristics of Parachutes of Several Designs when Towed Behind an Aircraft - Their Consistency and Comparison with Previous Data." London, Min. of Aviation, N65-21863, RAE-TN-Mech-Eng-390, October 1963

Brown, I. S. H.: "Properties of Rotating Parachutes." London, Min. of Aviation, RAE-TN-Mech-377, X64-10126, May 1963

Kell, C.: Free-Flight Measurements of Pressure Distribution at Transonic and Supersonic Speeds on Bodies of Revolution having Parabolic Afterbodies. Aeronautical Research Council, Great Brittain, ARC-R+M-3290, previously issued as RAE-Aero 2605, ARC-20433, N63-11902, 1962.

Smith, A. M.; and Peck, R. F.: "The Recovery of Flight Test Payloads." AGARD Report 397, 1962

Chuskin, P. I.; and Shlishnina, N. P.: Tables of Supersonic Flow about Blunted Cones. Academy of Sciences USSR (moscow), 1961, translated and edited by J. F. Springfield, Research and Advanced Development Division AVCO Corporation, Wilmington, Mass., September 1962

Boyd, E. A.: Aerodynamic Characteristics of a Hypersonic Parachute. College of Aeronautics, Great Brittain, Report 162, N-106-570, November 1961

Waters, M. H. L.; and Browning, A. C.: The Use of Parachutes at High Speed and High Altitude. Royal Aircraft Establishment Technical Note Mech. Eng. 340, N-106-710, August 1961

Waters, M. H. L.; and Browning, A. C.: The Use of Parachutes at High Speed and High Altitude. Technical Note No. Mech. Eng. 340, Royal Aircraft Establishment, AD-267692, August 1961

Timoshenko, S. P.; and Gere, J. M.: Theory of Elastic Stability. Second Edition, New York, McGraw-Hill Book Company, Inc., 1961

Roberts, B. G.: An Experimental Study of the Drag of Rigid Models Representing Two Parachute Designs at M = 1.40 and 2.0. Ministry of Aviation C.P. No. 565, London, 1961

Roberts, B. G.: An Experimental Study of the Drag of Rigid Models Representing Two Parachute Designs at M = 1.40 and 2.19. Royal Aircraft Establishment Tech. Note Aero 2734, N-98050, December 1960

Zandberger, P. J.; and Von Der Walle, F.: The Approximate Influence of Base-Drag on the Optimum Shape of Axisymmetric Configurations in Linearized Supersonic Flow. N63-80719, National Aeronautical Research Institute, Amsterdam, Netherlands, 1 February 1960

Baker, A.; and Swallow, J. E.: "Impact Testing of Textile Yarns. Part I, Experiments with a Falling Weight Method." Tech. Note Chem. 1355, Royal Aircraft Establishment, Great Brittain, AD-232617, November 1959

Cobb, D. B.: "The Techniques of Measuring the Force Exerted by a Parachute during Opening." TN Mech. Eng. 301, Royal Aircraft Establishment, October 1959

Urey, H. C.: "The Atmospheres of the Planets." Encyclopedia of Physics, Vol LII, Astrophysics III, The Solar System, Springer-Verlag, Berlin, 1959

Hoerner, S. F.: Fluid-Dynamic Drag. Published by author, 1958

Kreith, F.: Principles of Heat Transfer. International Textbook Company, Scranton, Pa., 1958

Brown, W. D.: Parachutes. Pitman, N. Y., First edition, 1957

Liepmann, H. W. and Roshko, A.: Elements of Gas Dynamics. John Wiley and Son, New York, 1957

Beastall, D.; and Turner, J.: The Effect of a Spike Protruding in Front of a Bluff Body at Supersonic Speeds. Aeronautical Research Council R and M 3007, Royal Aircraft Establishment Tech. Note Aero 2137 (supersedes RAE Tech. Note Aero 2137), 1957

Schlichting, H.: Boundary Layer Theory. McGraw-Hill, New York, 1955

Milne-Thompson, L. M.: Theoretical Hydrodynamics. Macmillan, N. Y., Third edition, 1955.

Krause, H. G. L.; Kaeppeler, H. J.; Koelle, H. H. and Kubler, M. E.: Determination of Maximum Skin Temperatures Due to Aerodynamic Heating for Unwinged Missiles Re-entering the Atmosphere (Report 6). Astronautisches Forschungsinstifuf Stuttgard, Stuttgart, Germany, July 1954

Ketschin; Kibel; and Rose: Theoretische Hydromechanik. Akademi Verlag, Berlin, 1954

de Vancouleurs, G.: Physics of the Planet Mars. Macmillan, N. Y., 1954

Shapiro, A. H.: The Dynamics and Thermodynamics of Compressible Fluid Flow. Vols I and II, The Ronald Press Company, New York, 1954

Pope, A.: Wind Tunnel Testing. Second edition, John Wiley and Sons, New York, 1954

Howarth, L. (ed.): Modern Developments in Fluid Dynamics, High Speed Flow. Vol II, Oxford at the Clarendon Press, 1953

Hoerner, S. F.: Aerodynamic Drag. Midland Park, N. J., published by author, 1951

O'Hara, F.: Notes on the Opening Behavior and Opening Forces of Parachutes. Royal Aeronautical Society Journal, Vol 53, London, November 1949

Leipman, H. W.; and Puckett, A. E.: Introduction to Aerodynamics of a Compressible Fluid. Galcit Aeronautical Series, Wiley, N. Y., 1947

Lighthill, J. H.: Supersonic Flow Past Bodies of Revolution. R and M No. 2003, British A. R. C., 1945

Ferrari, C.: Determination of the Pressure Exerted on Solid Bodies of Revolution with Pointed Noses Placed Obliquely in a Stream of Compressible Fluid at Supersonic Velocity. R. T. P. Translation No. 1105, British Ministry of Aircraft Production (from Atti R. Accad. Sci. Torino, Vol 72, pp 140-163, 1936

Lamb, H.: Hydrodynamics. Dover, N. Y., Sixth edition, 1932.

Jones, R. A.: On the Aerodynamic Characteristics of Parachutes. British ARC Report R and M No. 862, June 1923